

A new *Maldane* species and a new Maldaninae genus and species (Maldanidae, Annelida) from coastal waters of China

Yueyun Wang^{1,2,3}, Xinzheng Li^{1,3}

1 Institute of Oceanology, Chinese Academy of Sciences, Qingdao 266071, China **2** University of Chinese Academy of Sciences, Beijing 100049, China **3** Laboratory for Marine Biology and Biotechnology, Qingdao National Laboratory for Marine Science and Technology, Qingdao, Shandong, 266070, China

Corresponding author: Xinzheng Li (lixzh@qdio.ac.cn)

Academic editor: C. Glasby | Received 9 May 2016 | Accepted 16 June 2016 | Published 6 July 2016

<http://zoobank.org/BD740B8D-6E45-4DD2-BA57-55A9655CC6AA>

Citation: Wang Y, Li X (2016) A new *Maldane* species and a new Maldaninae genus and species (Maldanidae, Annelida) from coastal waters of China. ZooKeys 603: 1–16. doi: 10.3897/zookeys.603.9125

Abstract

Paramaldane, new genus, with type species *Paramaldane glandicineta* **sp. n.**, and *Maldane adunca* **sp. n.** (Maldanidae, Polychaeta) are described based on material from the coast of south China. The new genus *Paramaldane* is similar to *Maldane* Grube, 1860 and *Sabaco* Kinberg, 1867, but it clearly differs from all genera within the subfamily Maldaninae by a unique combination of characters: the cephalic plate is almost circular with low, entire and smooth cephalic rim, nuchal grooves small and crescentic, lacking a collar on chaetiger 1, short companion notochaetae, a collar-like glandular band on the anterior part of the sixth chaetiger, and a well-developed anal valve. *Paramaldane glandicineta* **sp. n.** is characterised by having a glandular band on the anterior part of the sixth chaetiger, an almost circular cephalic plate, an entire and smooth cephalic rim, and small crescentic nuchal grooves. *Maldane adunca* **sp. n.** is characterised by a low cephalic rim, nuchal grooves with a strongly curved anterior part and isolated from the cephalic rim. Finally, a taxonomic key to genera of Maldaninae and a comparative table to species of *Maldane* are provided.

Keywords

New species, new genus, *Maldane*, *Paramaldane*, Polychaeta, South China Sea, taxonomy

Introduction

The Maldanidae, also known as bamboo worms, is a tubicolous and common family found in hard or soft substrates from the intertidal region to the deep sea (Paterson et al. 2009; De Assis and Christoffersen 2011). Maldanid species have a long, cylindrical body, generally with one or both truncate ends; elongated median segments with prominent tori on the end of each chaetiger; a keel-shaped prostomium fused to the peristomium; and a pair of nuchal grooves located on each side of the prostomium (Fauchald 1977; Fauchald and Rouse 1997; De Assis and Christoffersen 2011).

Arwidsson (1906) split Maldanidae into subfamilies after the major and complete revision of the family, leaving *Maldane* and *Asychis* in the nominotypical subfamily as the Maldaninae. The subfamily Maldaninae is recognised by the presence of cephalic and anal plates, and having the anus dorsal to the plate (Fauchald 1977). Light (1991) reviewed the Maldaninae and considered characters of cephalic and anal plates, the types of notochaetae, and the presence of a collar on chaetiger 1 as important generic characters. This author made a major revision of Maldaninae, and recognized six genera: *Asychis* Kinberg, *Maldane* Grube, *Sabaco* Kinberg, *Bathyasychis* Detinova, *Chirimia* Light and *Metasychis* Light. Posteriorly, De Assis and Christoffersen (2011) analyzed the phylogenetic relationships within Maldanidae based on morphological characters.

During a sorting of the Maldanine specimens deposited in the Marine Biological Museum, Chinese Academy of Sciences (MBM) in the Institute of Oceanology, Chinese Academy of Sciences, Qingdao (IOCAS), some specimens of *Asychis*-like species were identified, which belonged to an unknown species. Based on these specimens, two new species are fully described and illustrated and a new genus of Maldaninae is proposed. A taxonomic key to genera of Maldaninae and a table comparing the morphology of all species of *Maldane* are provided.

Material and methods

The specimens were collected from the South China Sea from 1959 to 1962. They have been stored in 70% ethanol. Specimens were examined under Zeiss Stemi 2000-C stereomicroscopes, and compound microscopes. Drawings were prepared with the aid of 'AxioCam MRc 5' digital camera fitting on the stereomicroscopes. Line drawings are completed in the Adobe Photoshop CS6 using a graphics tablet. Notochaetae and neurochaetae were extracted carefully and observed under optical and scanning electron microscopes (SEM). All specimens are deposited in the Marine Biological Museum, Chinese Academy of Sciences (MBM). An identification key to the genera of Maldaninae modified from Light (1991) is provided below. Table 1 compares morphological characters for all known species of genus *Maldane*.

Table 1. Morphological comparison of species of *Maldane*. Unless otherwise indicated, character information is from Light (1991) and the original descriptions and illustrations. Unknown information marked with '?'.

Characters	<i>M. adunca</i> sp. n.	<i>M. arctica</i> Detinova, 1985	<i>M. californiensis</i> Green, 1991	<i>M. capensis</i> (Day, 1961)	<i>M. cristata</i> Treadwell, 1923	<i>M. cuculligera</i> Ehlers, 1887
Type locality	Southwest of Macao	Arctic	Southern California	South Africa	California	Gulf of Mexico
Collar on chaetiger 1	No	No	Yes, limited ventral side	No	No	Yes, limited ventral side
Pigmentation	absent	?	?	Head of living worm flecked with brown	Anterior segments with dark brown pigment	Nuchal groove with brown pigment spot?
Shape of nuchal grooves	Strongly curved anteriorly, J-shaped	Short, slightly curved	Slightly curved	J-shaped	Short and divergent anteriorly	slightly curved
Posterior cephalic rim	Low	Pocket-like	Pocket-like	Pocket-like	Pocket-like	Pocket-like
Dorsal glandular band on chaetiger 5	Absent	?	Absent	Absent	Sixth chaetiger with an anterior dorsal flange*	Dorsal glandular band
Prostomial palpode	Bluntly rounded	Spade-like	Rounded to semi-triangular	Broadly spatulate	Hemispherical	Bluntly rounded
Border of anal plate	Laterally notched	Laterally notched	Laterally notched	Laterally notched	Laterally notched	Laterally notched
Ventral part of anal rim	Smooth to slightly crenulate	Smooth	Slightly crenulate	Crenulate	Slightly crenate	Smooth to slightly crenulate
Characters	<i>M. decorata</i> Grube, 1877**	<i>M. glabra</i> Knox & Cameron, 1971	<i>M. glebfjex</i> Grube, 1860	<i>M. gorgonensis</i> Monro, 1933	<i>M. malinveni</i> McIntosh, 1885***	<i>M. marsupialis</i> Grube, 1878
Type locality	Congo	Port Phillip Bay, Australia	French	Gorgona Island, Colombia	Strait of Gibraltar	Philippines
Collar on chaetiger 1	No	Ventrally; inconspicuous	No	No	No	No
Pigmentation	?	?	No pigmentation	?	?	2 eye spots on peristomium
Shape of nuchal grooves	?	Faintly J-shaped	Short and arched	Boldly curved	?	Slightly curved
Posterior cephalic rim	?	Pocket-like	Pocket-like	Pocket-like	Low	Pocket-like
Dorsal glandular band on chaetiger 5	?	Absent	Absent	Absent	?	Absent
Prostomial palpode	?	Prow-like	Spade-like	Bluntly rounded	?	Spade-like
Border of anal plate	?	Laterally notched	Laterally notched	Complete, no notches	?	Complete, no notches
Ventral part of anal rim	?	Smooth	Crenulate	Smooth	?	Smooth

Characters	<i>M. meridionalis</i> (Chamberlin, 1919)	<i>M. monilata</i> Fauchald, 1972	<i>M. philippinensis</i> Treadwell, 1931	<i>M. pigmentata</i> (Imajima & Shiraki, 1982)	<i>M. sarsi</i> Malmgren, 1865	<i>M. theodori</i> Augener, 1926
Type locality	Between Galapagos Islands and Peru	Middle America Trench	Darvel Bay	Kashima Sea	Sweden	Queen Charlotte Sound, New Zealand
Collar on chaetiger 1	No	Yes	No	No	No	Yes
Pigmentation	Living worm with dark pigment areas on anterior body	Without distinct color patterns	?	Anterior body with brown spots	Anterior end with black- brown pigmentation, but smaller individuals may be missing	?
Shape of nuchal grooves	Short, curved	Short, curved	Short, curved	Short, curved in a semicircle	Short, slightly curved	J-shaped
Posterior cephalic rim	?	Pocket-like	Pocket-like	Low	Pocket-like	Pocket-like
Dorsal glandular band on chaetiger 5	Absent	Absent	?	Absent	Crescentic glandular band, but not always present	?
Prostomial palpode	Narrow and pointed	Broadly rounded	Spade-like	Broadly rounded	Spade-like	Broadly spatulate
Border of anal plate	?	Laterally notched	Laterally notched	Laterally notched	Laterally notched	Laterally notched
Ventral part of anal rim	?	Crenulated	Smooth	Smooth	Smooth to slightly crenulated	Crenulated

*from Imajima and Shiraki 1982.

***Maldane decorata* Grube, 1877 inadequate descriptions and no illustrations in original paper.

****Maldane malmgreni* McIntosh, 1885, inadequate descriptions in original paper.

Systematics

Family Maldanidae Malmgren, 1867

Subfamily Maldaninae Malmgren, 1867

Genus *Paramaldane* gen. n.

<http://zoobank.org/DE537EA3-4C8C-485F-9684-23D70FF5229E>

Type species. *Paramaldane glandicincta* sp. n.

Diagnosis. Body with 19 chaetigers. Cephalic plate circular. Prostomial palpode bluntly rounded, and confluent with cephalic rim. Cephalic rim low and entire with slight incisions. Cephalic keel short. First chaetiger without collar. Chaetiger 6 with a collar-like glandular band. Neurochaetae beginning to present on the second chaetiger. Notochaetae spirally fringed with short companion chaetae. Two preanal achaetigerous segment. Anus dorsal, with anal valve. Anal plate well-developed, but no anal cirri; with two lateral deep incisions on anal rim.

Etymology. The generic name is a combination of the prefix para- (meaning resembling) and the generic name *Maldane*. The new genus is related to *Maldane* in morphology. Gender: feminine.

Remarks. The new genus *Paramaldane* is superficially similar to *Maldane* Grube, 1860 and *Sabaco* Kinberg, 1867. The anal plate and notochaetae type of *Paramaldane* are closer to *Maldane*. The shape of prostomial palpode and nuchal grooves are closer to *Sabaco*. However, the new genus can be easily distinguished by the characters of the cephalic plate, which are considered to be of generic importance (Light 1991; Green 1994). The cephalic rim of *Maldane* and *Sabaco* is divided into two lateral lobes and a posterior lobe by deep lateral notches, but that of the *Paramaldane* is almost smooth. The prostomial palpode of *Maldane* is spade-like, but that of *Paramaldane* is bluntly rounded and confluent with cephalic rim. Both *Sabaco* and *Paramaldane* have small crescentic nuchal grooves that are isolated from cephalic rim, but *Sabaco* has a complete collar on the first chaetiger that is lacking in *Paramaldane*. Notochaetae of *Sabaco* have long companion chaetae, but companion notochaetae of *Paramaldane* are short. An identification key to the genera of Maldaninae modified from Light (1991) is provided below.

Paramaldane glandicincta sp. n.

<http://zoobank.org/B4BB3FC1-50B5-4A56-B9D5-83B84F894F63>

Figs 1–2

Type material examined. Holotype: MBM 008120, complete. Original label: South China Sea, Station 6175, mud sediment, 141 m, 28 January 1959. Paratypes: MBM 008130, 1 complete specimen, Southeast of Hainan Island, 18°30'N, 110°45'E. Original label: South China Sea, Station 6156, mud sediment, 100 m, 8 March 1960;

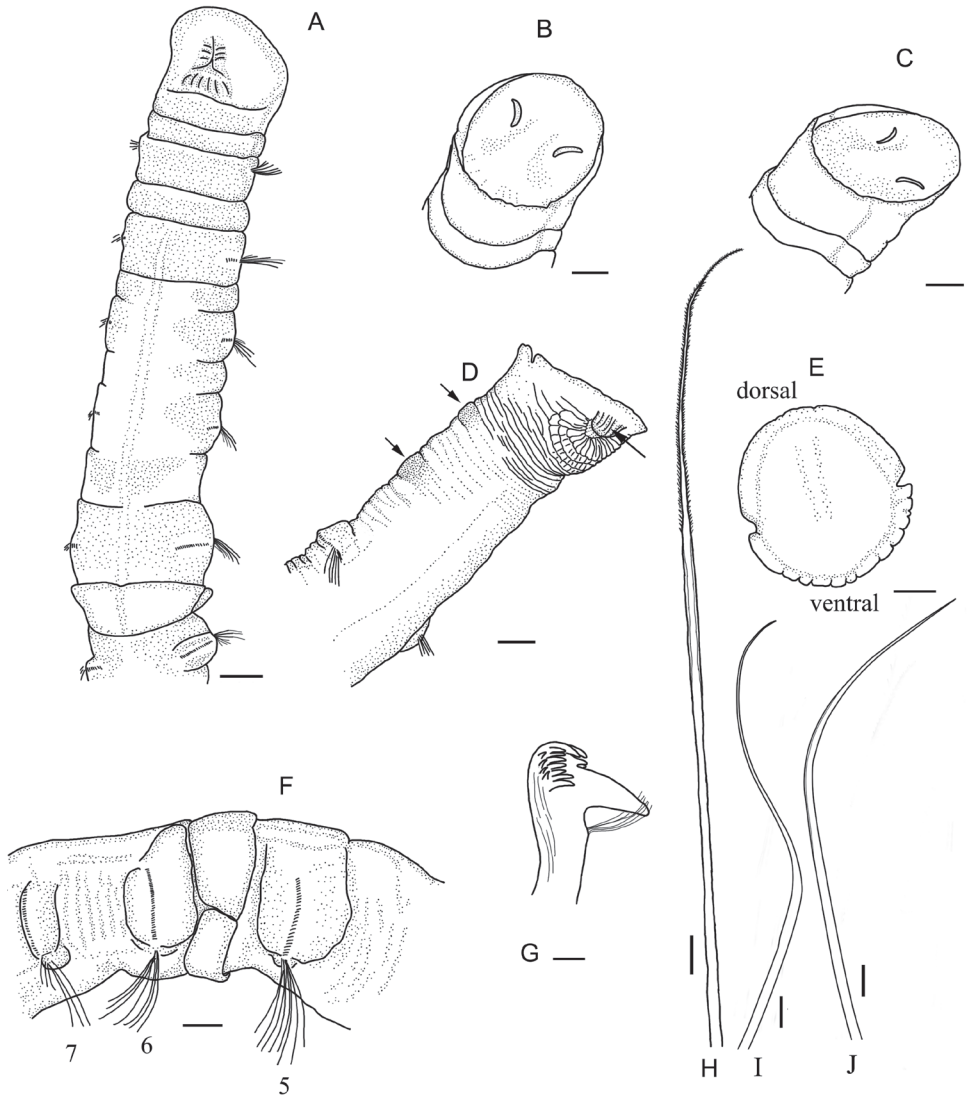


Figure 1. *Paramaldane glandicineta* sp. n. **A** ventral side of anterior body **B** dorsal view of cephalic plate **C** lateral view of cephalic plate **D** ventral view of pygidium, arrows show preanal achaetigerous segments and anal valve **E** frontal view of anal plate **F** lateral view of glandular band on sixth chaetiger, showing collar-like glandular band **G** lateral view of neurochaeta from chaetiger 5 **H** spirally-fringed notochaeta from chaetiger 10 **I** geniculate companion chaeta from chaetiger 10 **J** capillary companion chaeta from chaetiger 10. Scale bars: **A–F** = 0.5 mm, **G** = 10 μ m, **H** = 50 μ m, **I–J** = 200 μ m.

MBM 008214, two incomplete specimens, posterior part lost, Southeast of Hainan Island, 18°30'N, 110°30'E. Original label: South China Sea, Station 6143, mud sediment, 122.5 m, 22 April 1959.

Type locality. China, south of Hainan Island, 17°30'N, 110°00'E, 28 January 1959.

Diagnosis. Complete specimen with 19 chaetigers and two preanal achaetigerous segments. Cephalic plate rounded. Cephalic rim with two lateral creases, margin of the rim almost smooth. Anterior chaetigers biannulate. Sixth chaetiger with thick, collar-like glandular band. Rim of anal plate with deep lateral notches, ventral margin of anal rim crenulate, dorsal margin smooth.

Description. Holotype complete, 43 mm long, and 2.0 mm wide at the third chaetiger. Paratype of MBM 008130 complete, 74 mm long and 2.5 mm wide. Body cylindrical with 19 chaetigers, two preanal achaetigerous segments, and pygidium. First chaetiger without neurochaetae. Anterior part of the sixth chaetiger with thick glandular band forming a low collar and overlapping posterior part of the fifth chaetiger (Figs 1A, F; 2C–E).

Cephalic plate obliquely truncated, edge almost circular (Fig. 1B, C). Cephalic rim smooth (Fig. 1C), with a pair of shallow lateral creases (Fig. 1B). Deep furrow from lateral crease runs backward on peristomium to front edge of first chaetiger. Margin of posterior part of cephalic rim very weakly undulating (Fig. 1B, C). Anterior parts of rim completely smooth, and fused with prostomial palpode. Prostomial palpode indistinct, smoothly circular. Cephalic keel short and slightly arched. Nuchal grooves short, slightly curved, isolated from cephalic rim (Fig. 1B).

First four chaetigers completely biannulate, each comprising an achaetigerous and chaetigerous annulus. First six chaetigers short, following chaetigers elongated. Epidermal glands developed well on chaetigers 1–6. Glands only present on parapodial tori of following segments. Thick glandular band resembling a collar located on anterior part of sixth chaetiger, covering rear of fifth chaetiger, divided into dorsal and ventral parts by two lateral slits (Figs 1F, 2C). Dorsal margin of glandular band smooth (Fig. 2E). A small notch on ventral median line of ventral glandular band (Figs 1A, 2D).

Neurochaetae beginning to present on second chaetiger, with many small teeth on main fang (Figs 1G, 2H, I). Anterior chaetigers with simple capillary notochaetae. Middle and posterior chaetigers with long spirally-fringed notochaetae and short companion notochaetae (Fig. 2J). Long notochaetae with spinose spiral bands imbricated over main shaft (Figs 1H, 2M). Short companion chaetae two kinds: geniculate and capillary chaetae (Figs 1I, J, 2K). Geniculate companion chaetae with a long whip-like tip (Fig. 2K); transitional part smooth and thicker than shaft (Fig. 2L).

Two preanal achaetigerous segments marked by parapodial rudiments (Figs 1D, 2F, G). First achaetigerous segment longer than last one. Anus on dorsal side with a flaplike anal valve (Figs 1D, 2F). Pygidium forming a flat anal plate with a pair of deep lateral notches (Fig. 2F). Ventral part of the anal rim with 7–8 conspicuous crenulations (Fig. 1E). Dorsal rim smooth to slightly crenulated.

Etymology. The specific name *glandicincta* is a combination of *glans* and *cinctus* (meaning "belt", feminine form *cincta*), referring to the characteristic glandular belt on the six chaetiger.

Remarks. *Paramaldane glandicincta* sp. n. is characterised by a collar-like glandular band on the anterior margin of the sixth chaetiger.

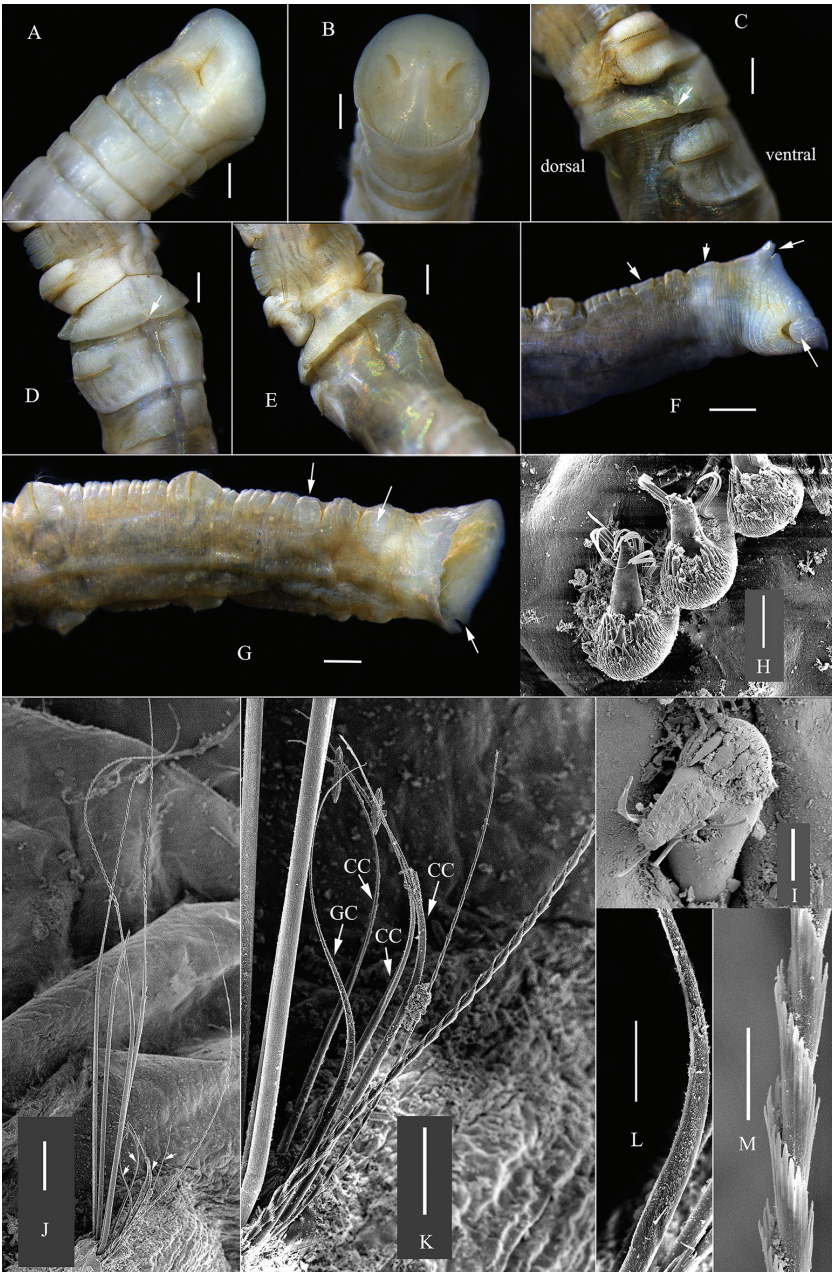


Figure 2. *Paramaldane glandicincta* sp. n. **A–G** holotype of MBM 008120 **A** ventral side of anterior end **B** cephalic plate **C** lateral view of glandular band, arrow shows lateral slit **D** ventral side of glandular band, arrow shows the midventral notch **E** dorsal side of glandular band **F–G** dorsal and ventral side of pygidium, arrows show preanal achaetigerous segments, anal valve and lateral notch on anal plate **H–M** chaetae from MBM 008214 **H–I** neurochaetae from 8th and 4th chaetigers respectively; **J** notochoetae from 8th chaetiger, arrows show companion chaetae **K** companion chaetae from 8th chaetiger **L** transitional part of geniculate capillary **M** spinose part of notochoetae. GC, geniculate companion chaeta. CC, capillary companion chaeta. Scale bars: **A–G** = 0.5 mm, **H–I** = 100 μ m, **J** = 1.0 mm, **K** = 500 μ m, **L** = 200 μ m, **M** = 100 μ m.

Genus *Maldane* Grube, 1860***Maldane adunca* sp. n.**

<http://zoobank.org/B3061C48-1D4E-4140-808D-771F70BADAB6>

Figs 3–5

Type material examined. Holotype: MBM 008111, complete. Original label: South China Sea, Station 6076, mud sediment, 39 m, 21 April 1959. Paratypes, same collecting data as holotype, MBM 240860–240861, nine specimens.

Other material examined: MBM 008125, 1 complete specimen, south of Macao, 21°30'N, 113°30'E, Station 6062, silt sediment, 35 m, 24 April 1959; MBM 006330, 10 complete specimens, northeast of Hainan Island, 20°00'N, 111°30'E, Station 6119, mud sediment, 70 m, 12 April 1959; MBM 201498, 1 anterior part, Beibu Gulf, Station 6209, mud sediment, 56.8 m, 6 July 1960; MBM 201496, 1 complete worm, Beibu Gulf, Station 7905, silt sediment, 29 m, 1 January 1962; MBM 201494, 1 complete worm, Beibu Gulf, Station 6200, mud sediment, 32.5 m, 13 July 1960.

Type locality. China, southwest of Macao, 21°00'N, 113°00'E, 21 April 1959.

Comparative material examined. *Maldane sarsi*. MBM 241068, 2 complete specimen, west of Point Barrow, 71°29.170'N, 161°58.899'W, Station C17, mud sediment, 45 m, 8 August 2008; MBM 008150, 2 complete specimen, north of Yantai, Shandong Province, 38°06'N, 121°31.98'E, Station 2009, mud sediment, 57.5 m, 18 October 1958; MBM 008062, 1 complete specimen, the Yellow Sea, 36°30'N, 124°00'E, Station 3022, mud sediment, 70 m, 21 January 1959; MBM 008228, 1 complete specimen, east of Zhoushan Islands, 29°45'N, 122°30'E, Station 4128, mud sediment, 54 m, 12 July 1959; MBM 008009, 1 complete specimen, the East China Sea, 28°30'N, 123°30'E, Station 4074, mud sediment, 77 m, 9 December 1959; MBM 201497, 1 complete specimen, west of Hainan Island, 18°35.36'N, 106°50.58'E, Station 7702, mud sediment, 55 m, 20 January 1962;

Diagnosis. Cephalic plate obliquely truncated, elliptical. Cephalic rim low and divided into lateral and dorsal lobes by lateral incisions. Lateral cephalic rim confluent with prostomial palpode. Prostomial palpode bluntly rounded. Nuchal grooves deep and strongly curved outward anteriorly, J-shaped. Anal plate almost truncate and rounded. Rim of anal plate low, with deep lateral incisions.

Description. Holotype about 65 mm in length, 1.5 mm in width. Largest specimens more than 70 mm in length, and 3.0 mm in width. Segments short on anterior and posterior body, longer on middle body (Figs 3A, 4D).

Body with 19 chaetigers, two preanal achaetigerous segments followed by a pygidium. Cephalic plate obliquely truncated, elliptical (Figs 3B, E, H, 4A). Prostomial palpode bluntly rounded, perfectly fused with cephalic rim. Cephalic rim lower and smooth, with two lateral notches. Cephalic keel remarkable, high and long, with posterior part widens (Figs 3B, E, 4A, B). Nuchal grooves short, anteriorly strongly curved outward, J-shaped (Figs 3B, E, H, 4A). Nuchal grooves isolated from cephalic rim. Mouth trilobed, and divided into upper and lower lips by a transverse fissure. Upper lip incised medially (Fig. 3G).

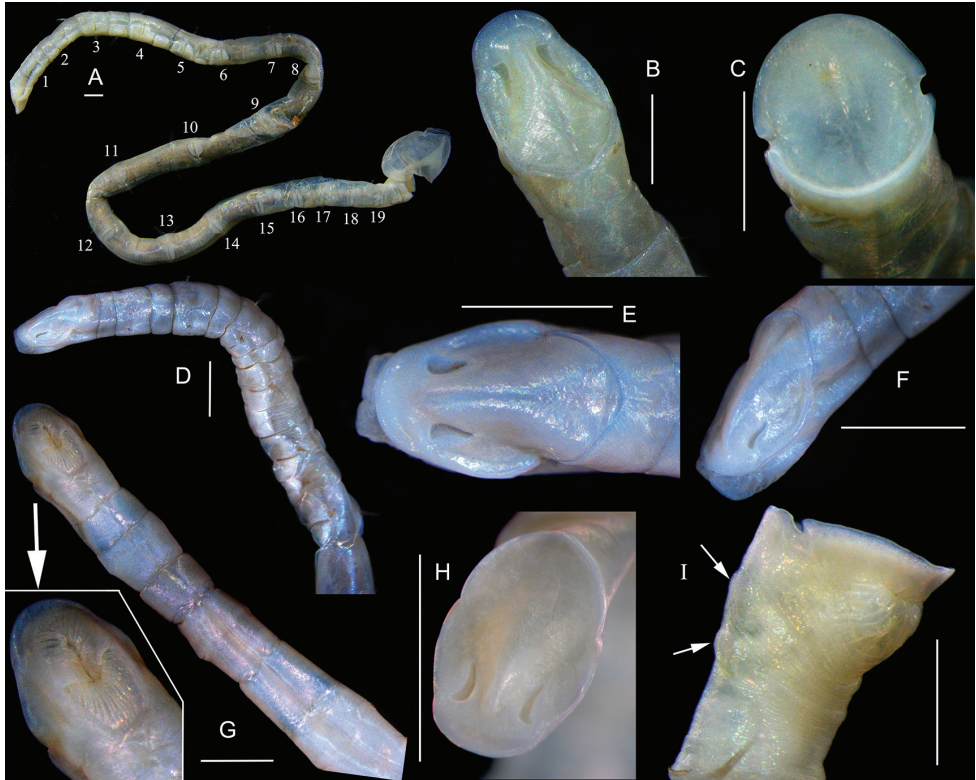


Figure 3. *Maldane adunca* sp. n. **A–C** paratype of MBM 240860 **A** complete body of MBM 240860 **B** dorsal view of cephalic plate **C** end view of anal plate **D–F**, paratype of MBM 240861 **D** anterior body showing glandular pads **E** dorsal view of cephalic plate **F** lateral view of cephalic plate **G–I** MBM 006330 **G** ventral view of anterior body **H** dorsal view of cephalic plate **I** pygidium, arrows shows pre-anal chaetigerous segments. Scale bars: 0.5 mm.

First five chaetigers biannulate (Figs 3A, D, 4D). First chaetiger without neurochaetae. Neurochaetae typical rostrate uncini similar on all chaetigers (Fig. 5A, B). Neurochaeta with several transversal rows of small teeth on main fang. Anterior chaetigers with capillary notochaetae. Middle and posterior chaetigers with spirally fringed notochaetae (Fig. 5D, H); spinose spiral bands closely imbricated over main shaft (Fig. 5C). Short companion chaetae geniculate (Fig. 5F, J, I), narrowly limbate (Fig. 5E) and bilimbate (Fig. 5G, J).

Two short and rudimentary preanal chaetigerous segments (Figs 3I, 4C), which deeply stained with methyl green. Anal pore with a less-developed anal valve (Fig. 3I). Anal mound well developed. Anal plate truncated, nearly rounded; median part of plate with a shallow furrow dorso-ventrally extended (Fig. 3C). Rim of anal plate low and incised laterally (Fig. 3C, I). Dorsal part of rim smooth. Ventral part of the rim smooth to weakly serrated.

Variation. Body wall of small individuals thin but thick in large ones. Body of small individuals smooth, semitransparent and lacking epidermal glands. Large individuals with glandular pads on parapodial tori and ventral side of chaetigers 3–5.

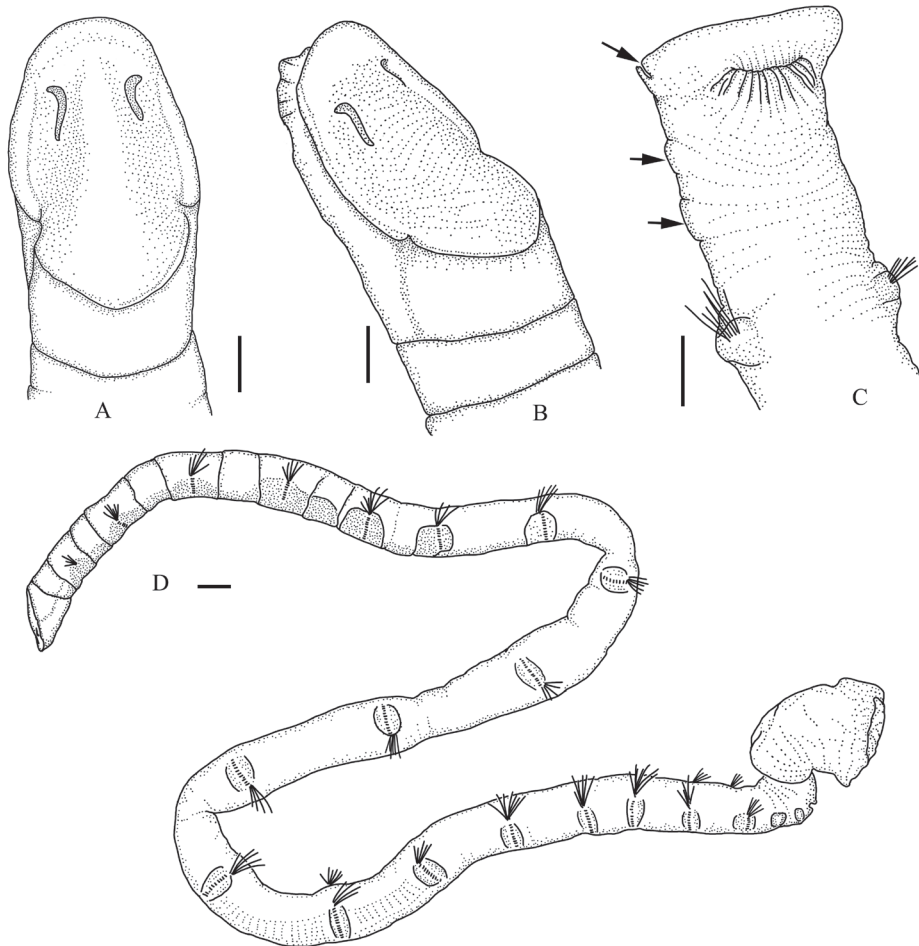


Figure 4. *Maldane adunca* sp. n. **A** dorsal view of cephalic plate **B** lateral view of cephalic plate **C** dorsal view of pygidium, arrows show pre-anal chaetigerous segments and lateral notch of rim of anal plate **D** complete body. Scale bars = 0.5mm.

Etymology. The specific epithet is the Latin adjective *adunca* (feminine, meaning hooked) and refers to the strongly curved nuchal grooves.

Remarks. *Maldane adunca* sp. n. is distinctive in the genus *Maldane* with its low cephalic rim and hook-like nuchal grooves. *Maldane adunca* sp. n. is close to *Maldane sarsi* Malmgren, 1865, a potential species-complex, which is thought to be a cosmopolitan species (Day 1967, Hartman 1961). However, the new species differs from the latter by possessing a low cephalic rim, strongly curved nuchal grooves which are isolated from the cephalic rim, and lacking crescentic glandular bands on the dorsal surface of the fifth chaetiger. In *M. sarsi*, the cephalic rim is well developed, its posterior part forms a deep pocket-like structure (Arwidsson 1906) and overlaps the posterior part of cephalic keel, cephalic keel is strongly arched, the nuchal grooves are narrow and slightly curved

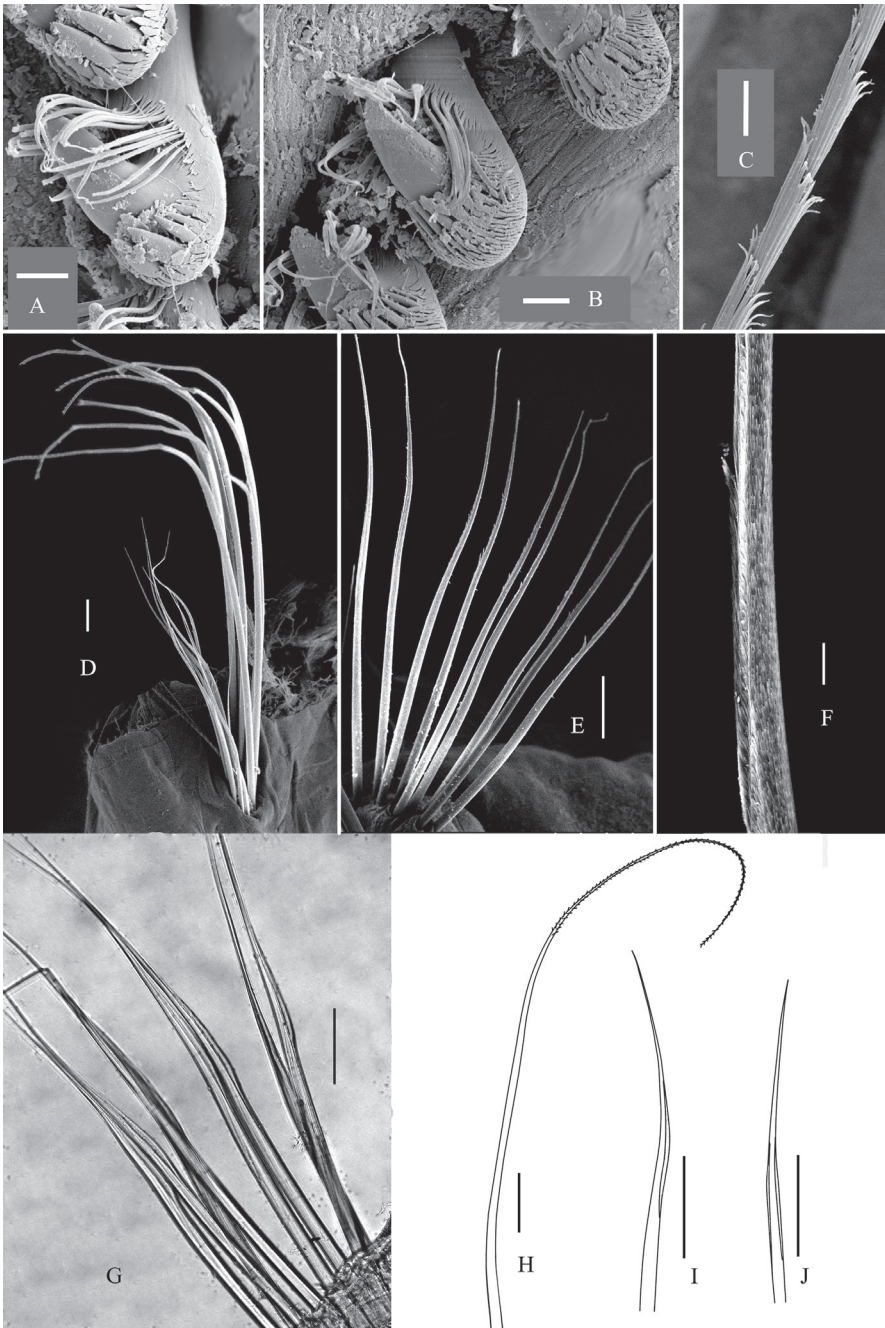


Figure 5. Chaetae of *Maldane adunca* sp. n. **A–B** neurochaetae from the 2nd and 17th chaetigers **C** spinose part of notochaetae **D** notochaetae from 16th chaetiger **E** short limbate companion chaetae from 18th chaetiger **F** transitional part of geniculate companion chaetae **G** companion chaetae from 14th chaetiger. H–J, notochaetae drawn from optical microscope **H** spirally-fringed notochaetae **I** geniculate companion chaetae **J** bilimbate companion chaetae. BC, bilimbate companion chaeta. GC, geniculate companion chaeta. Scal bars: **A–C** = 60 μ m, **D–E** = 0.5 mm, **F–G** = 50 μ m, **H–J** = 0.5 mm.

and connected with margin of cephalic rim, and the dorsal surface of the fifth chaetiger sometimes bears a crescentic glandular band (Green 1991, Fauvel 1953). *Maldane adunca* sp. n. is also closely related to *Maldane glebifex* Grube, 1860. The new species differs from the latter in the form of the anal rim and nuchal grooves. *Maldane glebifex* has a crenulated border to the anal plate while *M. adunca* sp. n. has a smooth to slightly crenulated anal rim. The nuchal grooves of *M. adunca* sp. n. are much more curved than that of *M. glebifex*. In terms of geographical distribution, *M. glebifex* is a Mediterranean/North Atlantic species (Fauvel 1927), and it is unlikely to occur in the South China Sea.

Light (1991) revised the subfamily Maldaninae and recognized 16 species of *Maldane*, of which *Maldane pellucida* Sars, 1869 was recognized later as *nomina nuda* (Oug et al. 2014). At present, *Maldane* includes 18 species: *M. adunca* sp. n., *M. arctica*, *M. californiensis*, *M. capensis*, *M. cristata*, *M. cuculligera*, *M. decorate*, *M. glabra*, *M. glebifex*, *M. gorgonensis*, *M. malmgreni*, *M. marsupialis*, *M. meridionalis*, *M. monilata*, *M. philippinensis*, *M. pigmentata*, *M. sarsi*, *M. theodori*. *Maldane sarsi* includes two subspecies: *M. sarsi antarctica* Arwidsson, 1911 and *M. sarsi borealis* Imajima, 1963 but their validity is doubtful. *Maldane sarsi antarctica* resembles the stem species. Color and gland pattern is main difference between the subspecies and its stem species according to Arwidsson (1911), but they are not robust taxonomic characters. Imajima (1963) collected only one specimen to erect *M. sarsi borealis*. This subspecies has 18 chaetigers, and anal plate of it incised ventrally. The chaetiger number is unusual in *Maldane* (usually, 19 chaetigers in *Maldane* species). Table 1 compares morphological characters for all known species of genus *Maldane*.

Key to the genera of Maldaninae

- 1 First two chaetigers without neurochaetae.....***Bathyasychis* Detinova, 1982**
- Only first chaetiger without neurochaetae..... **2**
- 2 Chaetiger 6 without collar-like glandular band **3**
- Chaetiger 6 with collae-like glandular band***Paramaldane* gen. n.**
- 3 Pygidium with anal valve **4**
- Pygidium without anal valve..... **5**
- 4 Nuchal grooves U-shaped; prostomial palpode mushroom-shaped
.....***Chirimia* Light, 1991**
- Nuchal grooves slightly curved to J-shaped; prostomial palpode spade-like...
.....***Maldane* Grube, 1860**
- 5 First chaetiger without a collar***Asychis* Kinberg, 1867**
- First chaetiger with a collar complete or limited to the ventral side **6**
- 6 Nuchal grooves J- or U-shaped; prostomial palpode mushroom-shaped; cephalic rim with crenulations or digitiform cirri; first chaetiger with a collar usually ventrally limited, sometimes complete ***Metasychis* Light, 1991**
- Nuchal grooves small, crescentic; prostomial palpode spadelike or indistinct; cephalic rim smooth without crenulations or digitiform cirri; the first chaetiger with a complete collar***Sabaco* Kinberg, 1867**

Acknowledgements

This study was financially supported by the Ocean Public Welfare Scientific Research Project (No. 201505004-1 and 201105012). We are grateful to Dr. José Eriberto De Assis of Federal University of Pernambuco for his comments and providing us with many papers. We are grateful to Dr. Geoff Read for his comments and suggestions improving the manuscript. We thank Dr Chris Glasby for his assistance in language. Thanks to all the managers of the MBMCAS for their help with specimens sorting.

References

- Arwidsson I (1907) Studien über die Skandinavischen und Arktischen Maldaniden nebst zusammenstellung der übrigen bisher bekannten Arten dieser Familie. Zoologische Jahrbucher 9(Suppl.): 1–308.
- Arwidsson I (1911) Die Maldaniden. Wissenschaftliche Ergebnisse der Schwedischen Südpolar Expedition 1901-1903 Stockholm Zoologie II, Band 6, Lieferung 6: 1–44.
- Augener H (1926) Papers from Dr. Th. Mortensen's Pacific Expedition 1914–16 – XXXIV Polychaeta III – Polychaeten von Neuseeland – II Sedentaria. Videnskabelige Meddelelser fra Dansk naturhistorisk Forening i Köbenhavn 81: 157–294.
- Chamberlin RV (1919) The Annelida Polychaeta. Museum of Comparative Zoölogy at Harvard College 48: 1–514.
- Day JH (1961) The polychaeta fauna of South Africa. Pt. 6. Sedentary species dredged off Cape coasts with a few new records from the shore. Journal of the Linnean Society London 44: 463–560. doi: 10.1111/j.1096-3642.1961.tb01623.x
- Day JH (1967) A monograph on the Polychaeta of southern Africa. Part 2. Sedentaria. British Museum of Natural History Publications 656: 459–878.
- De Assis JE, Christoffersen ML (2011) Phylogenetic relationships within Maldanidae (Capitellida: Annelida), based on morphological characters. Systematics and Biodiversity 9: 41–55. doi: 10.1080/14772000.2011.604358
- Detinova NN (1985) O taksonomicheskom znachennii stroenya parapodii u nekotorykh Maldanidae (Polychaeta). [On the taxonomic significance of the structure of parapodia in some Maldanidae (Polychaeta)]. Zoologicheskyy Zhurnal 64: 1487–1492. [In Russian with English summary]
- Ehlers E (1887) Report on the annelids of the dredging expedition of the US coast survey steamer 'Blake'. Memoirs of the Museum of Comparative Zoology, Harvard 15, 335 pp.
- Fauchald K (1972) Benthic polychaetous annelids from deep water off western Mexico and adjacent areas in the Eastern Pacific Ocean. Allan Hancock Monographs in Marine Biology 7: 1–575.
- Fauchald K (1977) The polychaete worms, definitions and keys to the orders, families and genera. Natural History Museum of Los Angeles County, Science Series 28: 1–188.
- Fauchald K, Rouse G (1997) Polychaete systematics: past and present. Zoologica Scripta 26(2): 71–138. doi: 10.1111/j.1463-6409.1997.tb00411.x

- Fauvel P (1927) Polychètes sédentaires. Addenda aux errantes, Archiannélides, Myzostomaires. Faune de France, Paris, 494 pp.
- Fauvel P (1932) Annelida Polychaeta of the Indian Museum, Calcutta. *Memoirs of the Indian Museum* 12: 1–262.
- Fauvel P (1953) The Fauna of India including Pakistan, Ceylon, Burma and Malaya. Annelida Polychaeta. Indian Press, Allahabad, 507 pp.
- Green KD (1991) *Maldane californiensis*, a new species (Polychaeta: Maldanidae) and a review of its relations. *Bulletin of Marine Science* 48(2): 214–226.
- Green KD (1994) The head of Maldanidae polychaetes of the subfamily Maldaninae. *Memoires du Museum National d'Histoire Naturelle* 162: 101–109.
- Grube AE (1860) Beschreibung neuer oder wenig bekannter Anneliden. *Archiv für naturgeschichte* 26: 71–118.
- Grube AE (1877) Anneliden - Ausbeute S.M.S. Gazelle. *Monatsbericht der Koniglich Preussischer Akademie der Wissenschaften zu Berlin*, 509–554.
- Grube AE (1878) Annulata Semperiana. Beiträge zur Kenntnis der Annelidenfauna der Philippinen nach den von Herrn Prof. Semper mitgebrachten Sammlungen. *Mem. Acad. Sci. St. Petersburg* 25: 1–300
- Hartman O (1961) Polychaetous annelids from California. *Allan Hancock Pacific Expeditions* 25: 1–226.
- Imajima M (1963) Polychaetous annelids collected off the west coast of Kamchatka II. Notes on species found in the collection of 1959. *Publications of the Seto Marine Biological Laboratory* 11(2): 345–372.
- Imajima M, Shiraki Y (1982) Maldanidae (Annelida: Polychaeta) from Japan. (Part 2). *Bulletin of the National Science Museum, series A (Zoology)* 8(2): 47–88
- Kinberg JH (1867) Annulata nova. Öfersigt af Kongliga Vetenskaps-Akademiens förhandlingar, Stockholm 23: 337–357.
- Knox GA, Cameron DB (1971) Port Phillip Bay Survey Part 2. Polychaeta. *Memoirs of the National Museum of Victoria* 32: 21–41.
- Light WHJ (1991) Systematic revision of the genera of the Polychaeta subfamily Maldaninae Arwidsson. *Ophelia Supplement* 5: 133–146.
- Malmgren AJ (1865) Nordiska Hafs-Annulater. Öfersigt af Königlich Vetenskaps-Akademiens Förhandlingar 22: 181–192.
- Malmgren AJ (1867) Annulata Polychaeta Spetsbergiae, Gröenlandiae, Islandiae et Scandinaviae hactenus cognita. *Ex Officina Frenckelliana, Helsingforslae*, 127 pp. doi: 10.5962/bhl.title.13358
- McIntosh WC (1885) Report on the Annelida Polychaeta collected by H.M.S. Challenger during the years 1873–76. *Challenger Report* 12: 1–554.
- Monro CCA (1933) The Polychaeta Sedentaria collected by Dr. C. Crossland at Colón, in the Panama Region, and the Galapagos Islands during the Expedition of the S.Y. 'St. George'. *Proceedings of the Zoological Society of London* 103(4): 1039–1092. doi: 10.1111/j.1096-3642.1933.tb01640.x
- Oug E, Bakken T, Kongsrud JA (2014) Original specimens and type localities of early described polychaete species (Annelida) from Norway, with particular attention to species described by OF Muller and M. Sars. *Memoirs of Museum Victoria* 71: 217–236.

- Paterson GL, Glover AG, Froján CB, Whitaker A, Budaeva N, Chimonides J, Doner S (2009) A census of abyssal polychaetes. *Deep Sea Research Part II: Topical Studies in Oceanography* 56(19): 1739–1746. doi: 10.1016/j.dsr2.2009.05.018
- Treadwell AL (1923) Polychaetous Annelids from Lower California with descriptions of new species. *American Museum Novitates* 74: 1–11.
- Treadwell AL (1931) Contributions to the biology of the Philippine Archipelago and adjacent regions. Four new species of polychaetous annelids collected by the United States fisheries steamer 'Albalross' during the Philippine Expedition of 1907-1910. *Bulletin of the United States National Museum* 100: 313–321.

Conflict of mitochondrial phylogeny and morphology-based classification in a pair of freshwater gastropods (Caenogastropoda, Truncatelloidea, Tateidae) from New Caledonia

Marlen Becker¹, Susan Zielske¹, Martin Haase¹

¹ *Vogelwarte, Zoologisches Institut und Museum, Ernst-Moritz-Arndt-Universität Greifswald, Soldmannstraße 23, D-17489 Greifswald, Germany*

Corresponding author: *Martin Haase* (martin.haase@uni-greifswald.de)

Academic editor: *F. Köhler* | Received 10 May 2016 | Accepted 17 June 2016 | Published 6 July 2016

<http://zoobank.org/5AAF1FA5-2A9D-4ABB-A581-F163D229B225>

Citation: Becker M, Zielske S, Haase M (2016) Conflict of mitochondrial phylogeny and morphology-based classification in a pair of freshwater gastropods (Caenogastropoda, Truncatelloidea, Tateidae) from New Caledonia. ZooKeys 603: 17–32. doi: 10.3897/zookeys.603.9144

Abstract

Morphological classification and mitochondrial phylogeny of a pair of morphologically defined species of New Caledonian freshwater gastropods, *Hemistomia cockerelli* and *H. fabrorum*, were incongruent. We asked whether these two nominal species can be unambiguously distinguished based on shell morphology or whether the taxonomic discrepancy inferred from these character types was reflected in the variation of shell morphology. Our investigations were based on phylogenetic analyses of a fragment of the mitochondrial cytochrome c oxidase subunit I, geometric morphometric analyses as well as micro computer tomography. The species presorted to morphospecies by eye overlapped in shell shape. However, statistically, all shells were correctly assigned, but not all of them significantly. Qualitatively, both nominal species can be unambiguously distinguished by the presence/absence of a prominent denticle within the shell. In the phylogenetic analyses, individuals from three populations clustered with the “wrong” morphospecies. In the absence of data from multiple loci, it was assumed for the single specimen from one of these populations that its misplacement was due to a recent hybridization event, based on its very shallow position in the tree. For the other two cases of misplacement neither introgression nor incomplete lineage sorting could be ruled out. Further investigations have to show whether the morphological overlap has a genetic basis or is due to phenotypic plasticity. In conclusion, despite their partly unresolved relationships *H. cockerelli* and *H. fabrorum* may be considered sister species, which are reliably diagnosable by the presence or absence of the denticle, but have not yet fully differentiated in all character complexes investigated.

Keywords

Geometric morphometrics, hybridization, incomplete lineage sorting, introgression, morphology, shape, South Pacific, taxonomy

Introduction

Conflict in phylogenetic signal between different characters, e.g. between different genes, between mitochondrial (mt) and nuclear (nc) DNA, or between genes and morphology, is commonly observed across a wide range of taxa (e.g., Wiens and Hollingsworth 2000; Shaw 2002; Pelser et al. 2010; Sauer and Hausdorf 2010; Debiasse et al. 2014; Sharma et al. 2015). This conflict may be due to a number of reasons including selection, convergent evolution, various forms of reticulate evolution, cryptic species, demography, inhomogeneous evolutionary rates, incomplete lineage sorting, and unresolved taxonomy (Felsenstein 1978; Maddison 1997; Funk and Omland 2003; Seehausen 2004; Arnold 2006; Mallet 2007; Nosil 2012). In a recent phylogenetic analysis of tateid gastropods from New Caledonia, Zielske and Haase (2015) discovered incongruent topologies of trees based on mitochondrial (COI, 16S rRNA) and nuclear (ITS2) gene sequences regarding a pair of nominal species, *Hemistomia cockerelli* (Haase and Bouchet 1998) and *H. fabrorum* (Haase and Bouchet 1998). Not only were the sets of sequence data in conflict, also classification based on shell morphology did not match the DNA data. Zielske and Haase (2015) assumed that introgression through hybridization may be responsible for these conflicts, however, postponed a more definite statement to a more comprehensive analysis involving more populations and more specimens per locality.

These investigations were initially the goal of the present account. Unfortunately, we could not consistently amplify ITS2 across the entire, enlarged data set. Therefore, we had to restrict this analysis to a comparison of COI-phylogeny and shell morphology. Typical *H. cockerelli* have a slender-conical shell whereas *H. fabrorum* is much broader. In addition, *H. cockerelli* is characterized by a prominent palatal denticle c. 1/3 whorl behind the outer lip (Figs 1, 2). Anatomically, these two species are very similar (Haase and Bouchet 1998). However, the variation within and among populations of each taxon is considerable and identification based on shell shape alone may be ambiguous. Both species occur in springs as well as small streams and have fairly broad, overlapping ranges. Occasionally, they are encountered in sympatry (Haase and Bouchet 1998, present paper: population 38). Hence, the question guiding our present analysis was whether these two nominal species can be unambiguously distinguished from each other based on shell morphology. In other words, we asked whether the conflict between shell-based classification and DNA-based phylogenies (Zielske and Haase 2015) is reflected in shell morphology and how this conflict may be biologically explained and interpreted taxonomically.

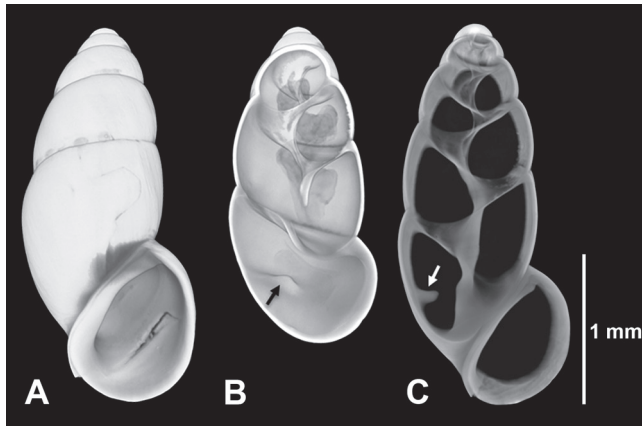


Figure 1. *Hemistomia cockerelli*, paratype. **A** Whole shell slightly tilted for better recognition of denticle exposed after digitally opening in **B** (arrow) **C** Longitudinal section in upright position showing denticle (arrow).

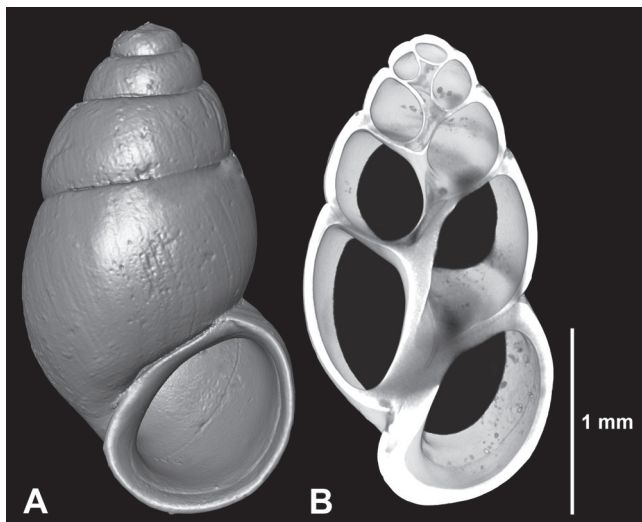


Figure 2. *Hemistomia fabrorum*, topotype. **A** Whole shell **B** Longitudinal section.

Material and methods

Material

Most specimens examined in this study were collected in 2012 at 22 localities in New Caledonia (Table 1, Fig. 3; Zielske and Haase 2015). Presorting of the collected animals to morphospecies was made by eye and in case of population 46 deviated from our previous paper. 37 paratypes (Haase and Bouchet 1998) of *H. cockerelli* included in morphometric analyses were borrowed from the Museum National d'Histoire Na-

Table 1. Material investigated. N_{gen}, number of genetically investigated specimens; N_{mor}, number of morphologically investigated specimens; Pop#, population number; Pt, paratypes.

Pop#	Species	Latitude Longitude	N _{mor}	N _{gen}
1A	<i>H. fabrorum</i>	22°08'59.0"S, 166°29'10.6"E	25	10
6B	<i>H. fabrorum</i>	21°48'08.0"S, 166°04'14.6"E	36	9
8	<i>H. fabrorum</i>	21°44'32.1"S, 166°05'20.6"E	4	0
9A	<i>H. cockerelli</i>	21°44'30.9"S, 166°05'57.9"E	3	2
10	<i>H. fabrorum</i>	21°42'55.4"S, 166°07'21.1"E	15	8
11	<i>H. cockerelli</i>	21°48'16.8"S, 166°00'00.8"E	26	7
13	<i>H. cockerelli</i>	21°47'30.8"S, 165°54'31.6"E	20	7
14	<i>H. cockerelli</i>	21°47'30.8"S, 165°54'38.7"E	11	8
15A	<i>H. cockerelli</i>	21°47'24.4"S, 165°54'51.2"E	6	1
16	<i>H. cockerelli</i>	21°47'24.4"S, 165°54'51.2"E	10	2
17	<i>H. cockerelli</i>	21°39'52.8"S, 165°43'10.3"E	11	2
18	<i>H. cockerelli</i>	21°39'40.6"S, 165°43'06.9"E	22	1
25B	<i>H. fabrorum</i>	21°34'15.7"S, 165°49'41.2"E	11	9
28	<i>H. fabrorum</i>	21°31'07.4"S, 165°48'20.0"E	11	10
30C	<i>H. cockerelli</i>	21°34'21.6"S, 165°41'02.5"E	9	1
31	<i>H. cockerelli</i>	21°33'33.5"S, 165°42'11.3"E	7	2
32	<i>H. cockerelli</i>	21°34'55.9"S, 165°40'16.7"E	6	0
36	<i>H. cockerelli</i>	21°38'22.1"S, 165°51'37.5"E	9	3
38B	<i>H. fabrorum</i>	21°38'09.3"S, 165°51'52.7"E	11	9
38C	<i>H. cockerelli</i>	21°38'09.3"S, 165°51'52.7"E	10	6
39	<i>H. fabrorum</i>	21°37'56.1"S, 165°51'54.4"E	6	2
41	<i>H. cockerelli</i>	21°38'12.3"S, 165°51'34.1"E	5	0
46	<i>H. fabrorum</i>	21°14'30.2"S, 165°16'30.8"E	13	9
Pt	<i>H. cockerelli</i>	21°49.2'S, 166°56.6'E	37	0

turelle Paris (MNHN-IM-2012-2694). Altogether 324 individuals from 24 sites were used for morphometric analyses. 108 thereof from 20 sites were used for phylogenetic analyses. The COI-sequence of a specimen from population 18 was taken from Ziel-ske and Haase (2015). Sequences were submitted to GenBank and received acces-sion numbers KT203603 - KT203710. Specimens included in the recent study are encoded as follows: "Population.Specimen Number", for instance "1A.01" represents specimen number one from population 1A.

Shell morphology

All 324 individuals were investigated for the presence/absence of a denticle 1/3 whorl behind the outer lip, which has been described as diagnostic for *H. cockerelli* (Haase and Bouchet 1998), under a dissecting microscope. For documentation, four speci-mens were selected for micro-computed X-ray tomography (μ CT) - one paratype of

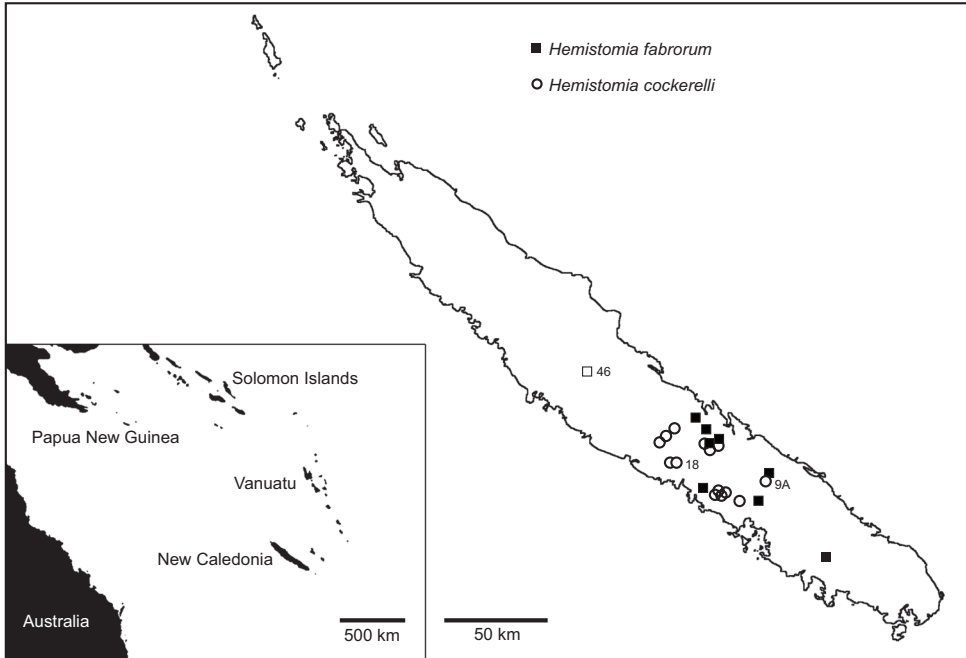


Figure 3. Map of New Caledonia showing sampling localities. Samples “misplaced” in phylogenetic analyses identified by population numbers.

H. cockerelli, one topotype of *H. fabrorum*, and one specimen each from morphologically intermediate populations 9A and 46 (see below). Scans were performed using an XRadia Micro XCT-200 (Carl Zeiss X-ray Microscopy Inc., Pleasanton, USA). The samples were placed in pipette tips glued on an insect pin. Each shell was scanned for 1 h at 40 kV and 8 W at four times magnification. Image stacks were processed and three dimensional surface models constructed using the 3D analysis software AMIRA v. 5.6.0 (FEI, Visualization Science Group).

For geometric morphometric investigations (Zelditch et al. 2012), shells were photographed at 30-times magnification using a Nikon SMZ 800 stereoscopic microscope (Nikon Corporation, Tokyo, Japan) equipped with a Nikon DS-2M camera and NIS-Elements AR v. 3.2 software (Nikon, Tokyo, Japan). Snails were placed onto a silicone surface for easier positioning, all orientated with the longitudinal axis (columella) parallel to the y-axis. Images were converted into tps format using TPSUTIL v. 1.58 (Rohlf 2013a). 17 landmarks (Fig. 4) were digitized for each individual with TPSDIG v. 2.17 (Rohlf 2013b). In order to check the repeatability of the procedure, it was repeated for ten specimens on two consecutive days. The comparison with Goodall’s F-test in TWO-GROUP v. 8 (a program of the IMP suite written by David Sheets: <http://www.canisius.edu/~sheets/morphsoft.html>) was not significant ($p = 0.59$) indicating that positioning the shells and placing the landmarks was highly repeatable (cf. Haase and Misof 2009).

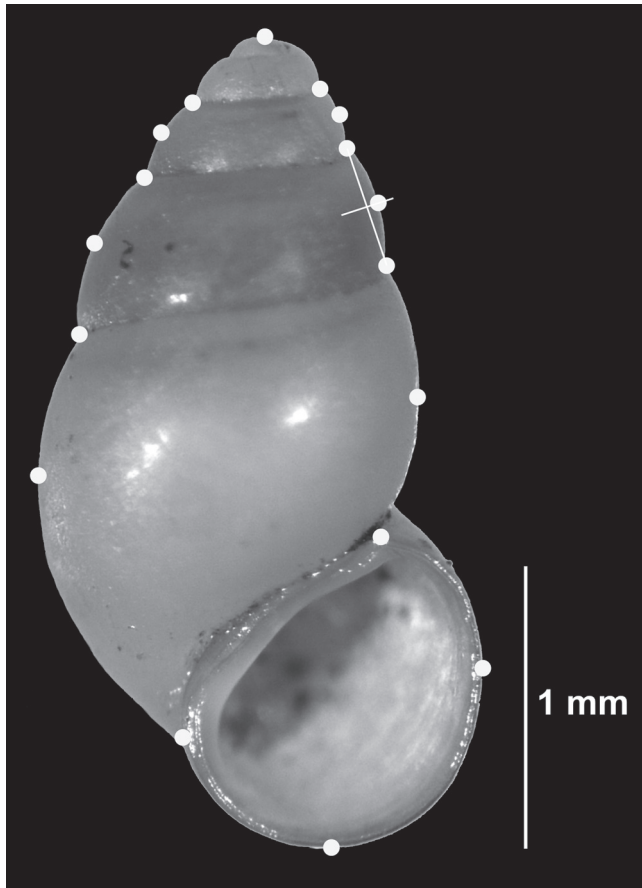


Figure 4. Seventeen landmarks placed on a shell of *Hemistomia fabrorum* from population 39.

In order to visualize the morphological variation, a principal component analysis (PCA) was performed using MORPHOJ v. 1.06a (Klingenberg 2011). COORDGEN v. 8 belonging to the IMP suite was used in order to generate input-data for further analyses with other IMP programs. Based on the PCA, we identified individuals with uncertain morphospecies allocation for further analyzes by canonical variates analysis (CVA) and assignment tests conducted with the IMP program CVAGEN v. 8. For this identification, equal frequency confidence ellipses with a probability of 95% were plotted on the PCA graph. Individuals localized in the intersection of both ellipses and its neighborhood were classified as uncertain and treated as “unknown specimens” in assignment tests including jackknife-assignment (Webster and Sheets 2010). The CVA axes determined by the two known groups were used to assign the unknown specimens to one of the known groups. A pair-wise comparison between the two morphospecies including all specimens previously assigned to either morphospecies with a p-value higher than 0.05 was performed with Goodall’s F-test in TWOGROUP v. 8.

DNA isolation and sequencing

DNA was isolated using Qiagen's DNeasy Blood & Tissue Kit (QIAGEN GmbH; Hilden, Germany) in compliance with the manufacturer's protocol except that we eluted only in 20 μl of AE-buffer. A fragment of the mitochondrial cytochrome c oxidase subunit I gene (COI) was amplified using the primers LCO1490 and HCO2198 (Folmer et al. 1994), the latter modified at position 12 (G \rightarrow A; Zielske et al. 2011). Polymerase chain reactions were performed in 12.5 μl containing 1.1 μl 10x BH4 buffer (BIOLINE GmbH; Luckenwalde, Germany), 4.4 mM MgCl, 0.3 μM of each primer, 0.2 mM dNTP, 0.5 μl BSA (1%), 0.25 U DNA-Polymerase (BIOLINE), 5–50 ng DNA and water. The PCR conditions were 95 °C for 5 min for denaturation and 40 cycles starting at 94 °C for 60 s, followed by annealing for 90 s with an initial touchdown from 55 to 46 °C with a drop of one degree per cycle, an extension step at 72 °C for 60 s, and 10 min final extension at 72 °C. Amplification products were purified using 4 μl PCR-product and 1 μl Exo-SAP [0.04 μl Exonuclease I (20.000 U/ml; New England BioLabs GmbH; Frankfurt/Main, Germany), 0.15 μl 10x Shrimp Alkaline Phosphatase Buffer (Promega; Madison, WI, USA), 0.81 μl ddH₂O] per sample. This mix was incubated at 37 °C for 15 min followed by 85 °C for another 15 min. Cycle sequencing was conducted using the Big Dye Terminator Ready Reaction Mix v3.1 (Applied Biosystems, (ABI); Carlsbad, CA, USA) and the PCR primers. The cycle sequencing products were purified using Agencourt's® CleanSEQ® Dye-Terminator Removal (Beckman Coulter; Beverly, MA, USA) before sequencing on an ABI 3130xl Genetic Analyzer.

Phylogenetic analyses

COI sequences were edited using the software DNA BASER v. 4.16 (DNA Baser Sequence Assembler v. 4.16 2014). After addition of two outgroup sequences of *H. nyo* and *H. andreae* (see Haase and Zielske 2015; Zielske and Haase 2015), the alignment was generated with Clustal W implemented in MEGA v. 6.06 (Tamura et al. 2013) and trimmed to a length of 658 bp. The alignment was screened for potential stop-codons with the software DAMBE v. 5.5.1 (Xia 2013) to check for potential editing errors and nuclear pseudogenes. jMODELTEST v. 2.1.4 (Darriba et al. 2012) identified HKY + I + Γ as best-fitting DNA substitution model according to the Bayesian information criterion. Three phylogenetic analyses were conducted, a maximum likelihood analysis (ML), a bio-neighbor-joining analysis (BNJ), and a neighbor-net analysis. ML was performed using Garli 2.01 (Zwickel 2006). Both optimal tree and bootstrap support were inferred from 500 replicates. The BNJ tree including 5000 bootstrap replicates was constructed in PAUP* v. 4.0b10 (Swofford 2002). Bootstrap support was considered significant if > 75. The neighbor-net was computed with the software SPLITSTREE v. 4.13 (Huson and Bryant 2006) based on the K3ST-model. The optimal model (see above) could not be applied because the program issued undefined distance values.

Results

Geometric morphometrics

The first two axes of the PCA comparing the morphospecies explained 76.2% of the total morphological variation. The nominal species were fairly well separated along axis 1, however, the 95% confidence ellipses were overlapping. Nineteen specimens within the area of overlap and its neighborhood as defined in Figure 5 were treated as specimens with unknown identity (“unknown”) in further analyses. The CVA defined the set of axes allowing for the greatest possible discrimination of the two groups and axis 1 was highly significant ($p < 0.001$). These axes were used to assign the unknown specimens. Eight of these specimens were classified as *H. cockerelli* and 11 as *H. fabrorum*. All assignments were correct with respect to the initial classification by eye, however, only nine significant. Twelve of the 305 shells with - according to the PCA - unambiguous identity were also assigned correctly but not significantly.

A jackknife test of assignment, a cross-validation procedure, was performed *a posteriori* to assess the robustness of the CV axes and comprised these 305 specimens. In 10,000 replicates, 10% of the specimens (31) were randomly selected as unknown data and assigned to one of the resulting groups of the following CVA analysis based on the remaining 274 shells. 99% of the assignments were correct and significant, 1% correct and not significant, and no shell was incorrectly assigned.

In a subsequent Goodall’s F test both morphospecies were highly significantly ($p < 0.001$) distinguished. This test included all specimens unambiguously ($p > 0.05$) assigned to one of the nominal species in the previous CVA-based tests.

Micro-CT

The μ CT-based three dimensional shell surface models revealed, as expected, presence and absence of the palatal denticle in the paratype of *H. cockerelli* and the topotype of *H. fabrorum*, respectively (Figs 1, 2). In the specimen from population 9A with shells unusually broad for *H. cockerelli*, the denticle was well developed, while it was entirely absent in the shell from population 46, a slender *H. fabrorum*, also confirming the initial classification.

Phylogenetic analyses

The phylogenetic tree reconstructions inferred very similar relationships. Figure 6 emphasizes the fully resolved BNJ topology, because it had higher bootstrap support than the ML tree except for the clade of population 46. In order to show the general congruence of both reconstructions, the ML topology is given in Figure 6B. The main differences between both optimal topologies were the different positions of the clade of population 46 and individual 6B.10. In the BNJ tree population 46 was nested

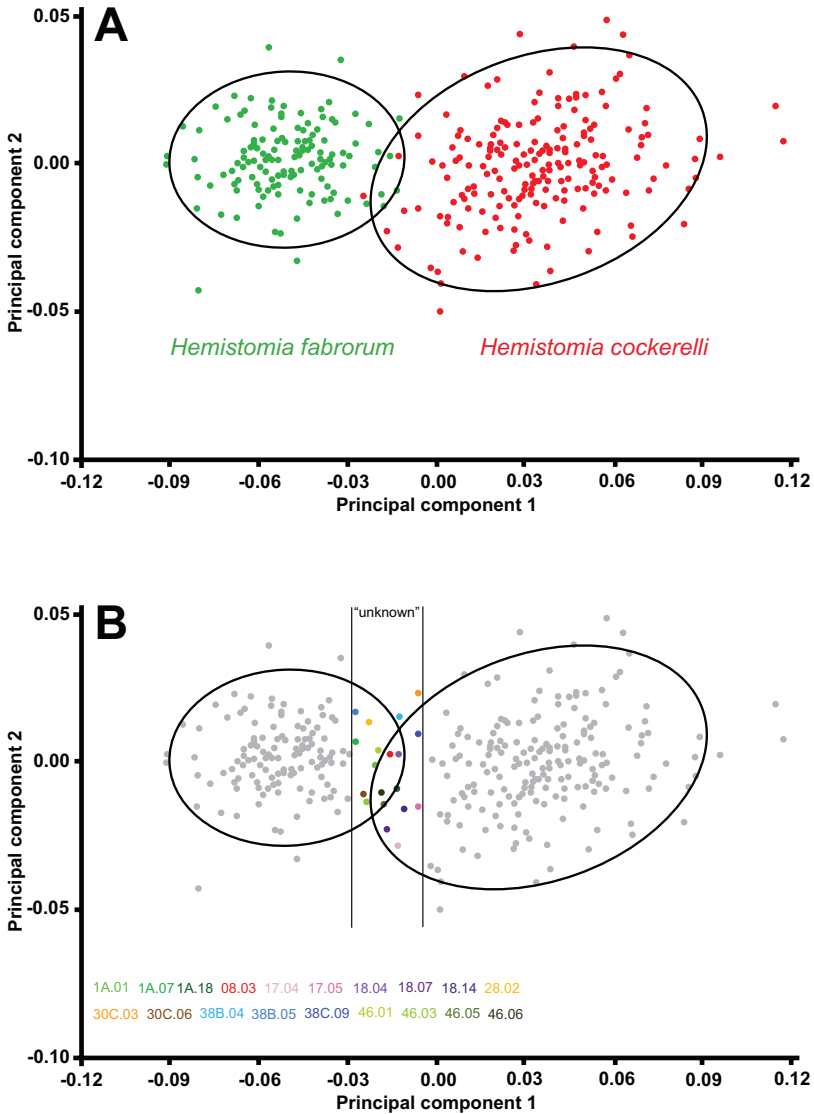


Figure 5. Landmark-based principal component analysis with 95% confidence ellipses. **A** Variation of visually determined *H. cockerelli* and *H. fabrorum* **B** Definition of specimens treated as “unknown” in assignment test.

among specimens allocated to *H. cockerelli* and 6B.10 sister species of a clade containing sequences from populations 25, 28, 38, and 39. In the ML tree, population 46 was sister group to nominal *H. cockerelli* and 6B.10 clustered with other individuals from population 6B. However, when unsupported nodes including those concerning both aforementioned lineages were collapsed, the topologies were practically identical. The

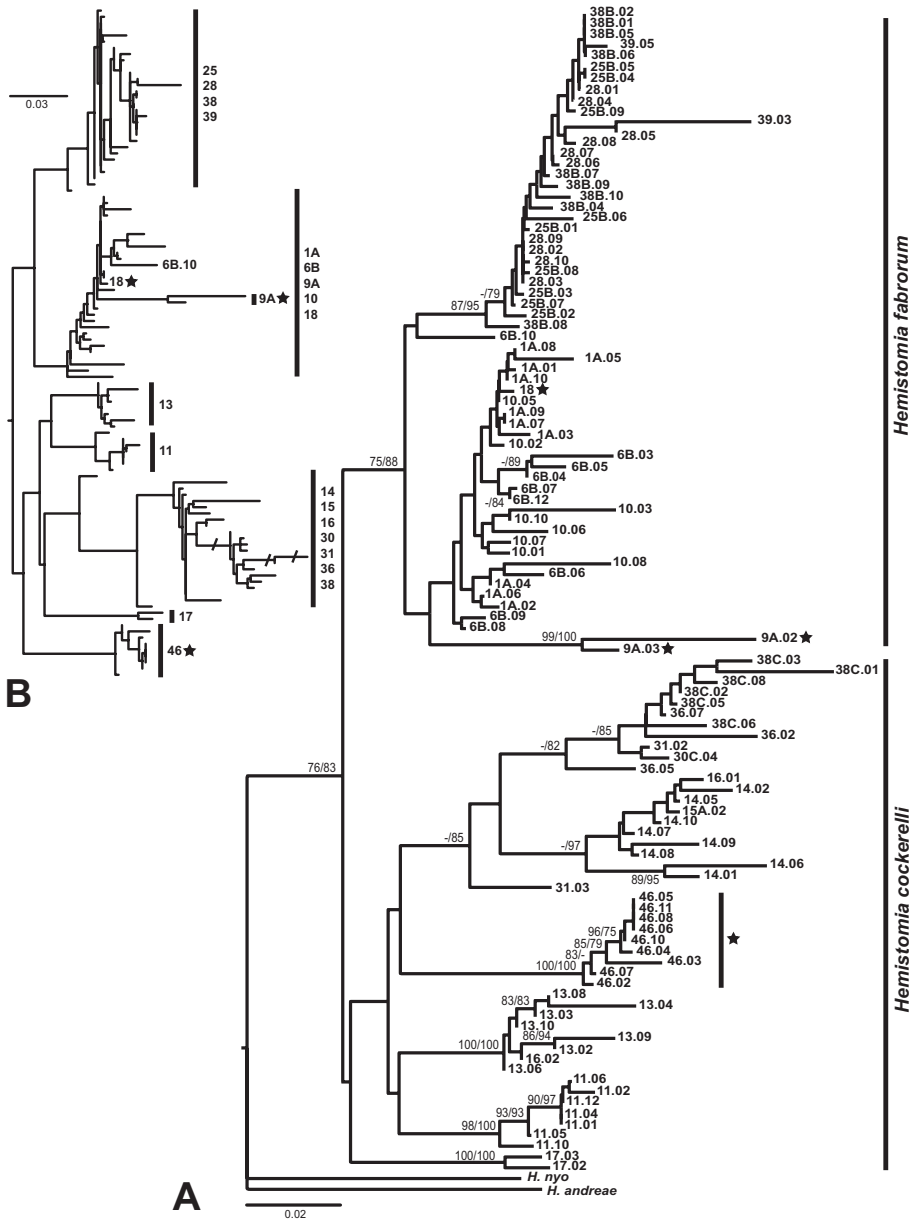


Figure 6. Phylogenetic reconstructions. **A** Bio-neighbor-joining tree based on COI fragment with bootstrap support values from both maximum likelihood and neighbor-joining analyses (ML/BNJ) **B** Maximum likelihood topology. Asterisks indicate “misplaced” individuals. In B only the “misplaced” individuals and one individual (6B.10), whose position differs considerably in both trees, are indicated. Otherwise, only the clade composition is given. Crossed branches are shortened by 50%. The outgroup was pruned from the tree. Scale bars: substitutions per site.

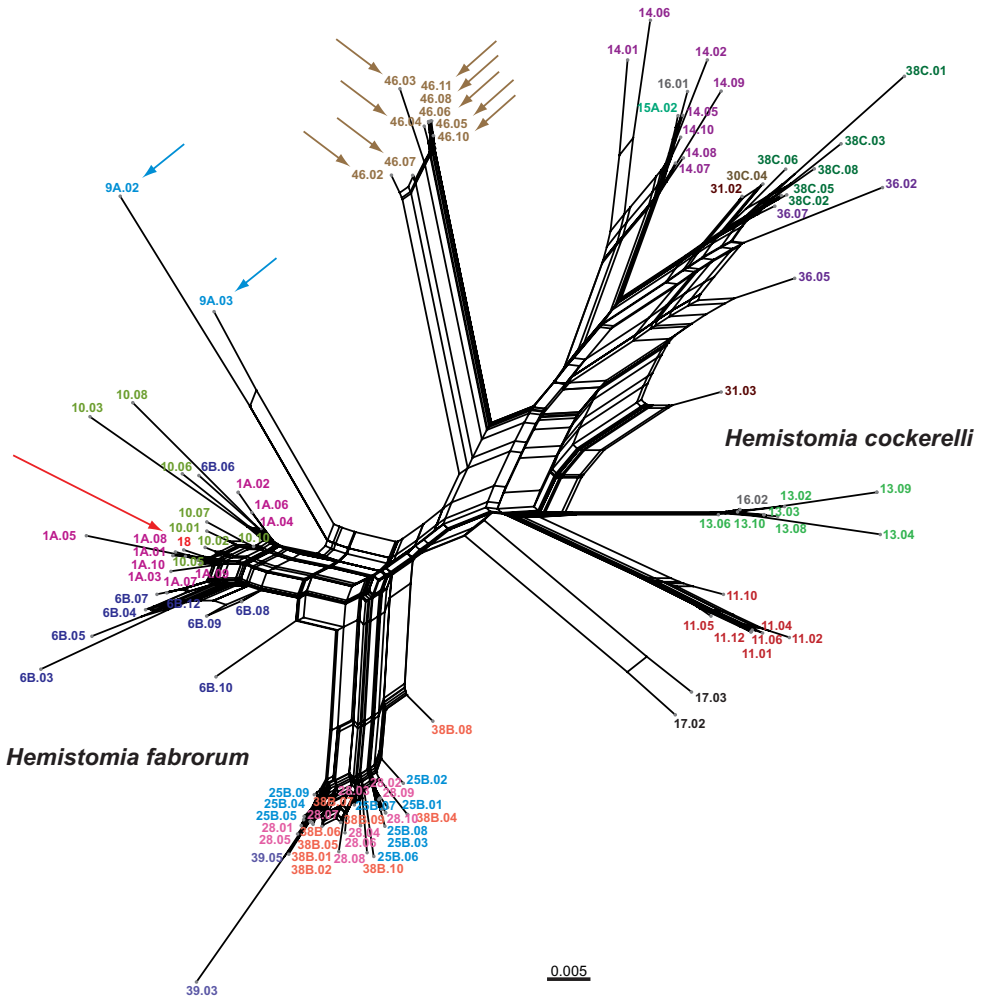


Figure 7. Neighbor-net illustrating conflict in phylogenetic signal of sequence data. Arrows indicate “misplaced” individuals. Scale bar: substitutions per site.

ingroup was well supported. It consisted of two main clades of which only the one containing the majority of specimens identified as *H. fabrorum* received significant bootstrap support. This *H. fabrorum*-clade included three specimens that were morphologically identified as *H. cockerelli*, one from population 18 nested with a short branch among individuals from populations 1A and 10, and the two snails from population 9A forming a well supported clade on a long branch. In turn, population 46, morphologically identified as *H. fabrorum*, clustered with specimens allocated to *H. cockerelli*. Within both morphospecies, not all populations were monophyletic. The neighbor-net revealed basically the same topology including the shallow position of the specimen from population 18 and the rather basal connections of the snails from populations 9A and 46, respectively (Fig. 7). The network also illustrated the conflict-

ing signal within the two major clades most likely due to lack of data and homoplasy, which explain e.g. the lack of bootstrap support for the *H. cockerelli*-clade in the tree reconstructions (Fig. 6).

Discussion

Conflict in phylogenetic/taxonomic signal between different characters is not uncommon among truncatelloidean gastropods, in particular in cases of recent events of speciation and young evolutionary radiations (e.g., Haase 2005; Haase et al. 2007; Zielske and Haase 2014a, b), but also among deeper lineages (Colgan et al. 2006; Wilke et al. 2006; Prié and Bichain 2009). Geometric morphometric analyses and μ CT-scans showed that the two nominal species *H. cockerelli* and *H. fabrorum* are distinguishable by their shell characteristics. The presorting to morphospecies was 100% in accordance with the final allocation of specimens based on the CVA despite a slight overlap of the variation in the PCA. However, less than 50% of the assignments of specimens with intermediate shape treated as “unknown” specimens were significantly correct. Thus, in face of this remaining ambiguity shell shape alone is not a perfect discriminator. However, both taxa can be unambiguously identified by the presence (*H. cockerelli*) or absence (*H. fabrorum*) of the shell denticle (Haase and Bouchet 1998). This denticle is either fully developed or absent. We did not observe intermediate states such as a smaller size. Across *Hemistomia*, this denticle exhibits a considerable variation in shape, size and position and is readily visible through the shell under a dissecting microscope. In several mainly larger species, it is lacking, though (Haase and Bouchet 1998). Also in the genetically “misplaced” specimens from populations 9A, 18 (both morphologically *H. cockerelli*) and 46 (morphologically *H. fabrorum*), the denticle was either present or absent.

As the number of individuals misplaced in the phylogenetic analyses was very low and in particular because ncDNA data were lacking, explanations for the incongruences have to remain largely speculative. However, at least for dubious shallow relationships the assumption of a recent event, which can only be introgression through hybridization, is very likely. The specimen identified as *H. cockerelli* from population 18 was nested among individuals allocated to *H. fabrorum* from three populations. Since all surrounding, more basal nodes belonged to *H. fabrorum*, this misplaced specimen most likely has inherited its mitochondria through introgression by hybridization of a female *H. fabrorum* with a male *H. cockerelli* in the not too distant past.

In contrast, the misplaced clades consisting of the two specimens from population 9A and the nine individuals of *H. fabrorum* from population 46, respectively, were connected to deeper, partly unsupported nodes. It is exactly this situation which makes the distinction of incomplete lineage sorting and hybridization difficult (Joly et al. 2009). Assuming hybridization as cause of the topological inconsistencies requires adhoc hypotheses, though. In order to coalesce prior to the completion of speciation a lineage “misplaced” through introgression would have a sole survivor and that only in

the species it introgressed into (Joly et al. 2009). Therefore, assuming incomplete lineage sorting as cause for the position of populations 9A and 46 is more parsimonious, although hybridization cannot be ruled out.

In conclusion, despite their partly unresolved relationship *H. cockerelli* and *H. fabrorum* may be considered sister species, which are reliably diagnosable by the presence or absence of the palatal denticle, but have not yet fully differentiated in all character complexes investigated. The range of *H. fabrorum* covers wide parts of southern New Caledonia and largely overlaps with that of *H. cockerelli*, which is found almost across the entire island (Haase and Bouchet 1998). In contrast to the majority of spring snails in New Caledonia and elsewhere, both species have fairly wide ranges with many island-like populations. This kind of structure has been shown to preserve genetic variation and delay lineage sorting as the effective population size remains large (Slatkin 1991; Thomaz et al. 1996). Most of the investigated *Hemistomia* populations occurred in close geographical proximity. Consequently, interactions between both species cannot be excluded. Interestingly, only in a single locality, 38, were both species found sympatrically. The fifteen individuals sequenced from there fell into the respective correct clades. This suggests that hybridization is probably occurring only rarely. However, three individuals from population 38 were among the 19 with ambiguous shell shape. These comprised also individuals of populations 18 and 46. However, it is impossible to tell whether ambiguities in shell shape had a genetic cause or were due to phenotypic plasticity, which obviously plays an important role in a related species from New Zealand, *Potamopyrgus antipodarum* (Gray, 1843) (Haase 2003; Kistner and Dybdahl 2013; and literature therein).

In order to unambiguously identify the causes of the genetic inconsistencies an even denser sampling design as well as using more genetic markers would be required. The potential role of phenotypic plasticity can only be assessed in common garden experiments. The ambiguous genetic signal also calls for caution for barcoding (Hebert et al. 2003) if this is conducted without morphological control (e.g. Goldstein and DeSalle 2010). Morphologically, *H. fabrorum* represents the derived conditions regarding the broader shell shape and the lack of a denticle considering that the closest relatives of the pair of species discussed in this account, *H. andreae* and *H. nyo*, are hardly distinguishable from *H. cockerelli* (Haase and Bouchet 1998; Haase and Zielske 2015).

Acknowledgements

We are indebted to Christine Pöllabauer and numerous local guides for their logistic support during field work in New Caledonia. We are grateful to Gabriele Uhl and Peter Michalik for assistance with μ CT and Jakob Krieger as well as Andy Sombke with Amira. We thank Christel Meibauer for her help in the lab. Frank Köhler, Tom Wilke, and three anonymous reviewers helped to improve earlier versions of the manuscript. Financial support was received from the Deutsche Forschungsgemeinschaft (HA4752/2-1).

References

- Arnold ML (2006) Evolution through genetic exchange. Oxford University Press, New York, 272 pp.
- Colgan DJ, Ponder WF, Da Costa P (2006) Mitochondrial DNA variation in an endemic aquatic snail genus, *Caldicochlea* (Hydrobiidae, Caenogastropoda), in Dalhousie Springs, an Australian arid zone spring complex. *Molluscan Research* 26: 8–18.
- Darriba D, Taboada GL, Doallo R, Posada D (2012) jModelTest 2: more models, new heuristics and parallel computing. *Nature Methods* 9: 772–772. doi: 10.1038/nmeth.2109
- Debiasse MB, Nelson BJ, Hellberg ME (2014) Evaluating summary statistics used to test for incomplete lineage sorting: mito-nuclear discordance in the reef sponge *Callispongia vaginalis*. *Molecular Ecology* 23: 225–238. doi: 10.1111/mec.12584
- Felsenstein J (1978) Cases in which parsimony or compatibility methods will be positively misleading. *Systematic Zoology* 27: 401–410. doi: 10.2307/2412923
- Folmer O, Black M, Hoeh W, Lutz R, Vrijenhoek R (1994) DNA primers for amplification of mitochondrial cytochrome oxidase c subunit I from diverse metazoan invertebrates. *Molecular Marine Biology and Biotechnology* 3: 294–299.
- Funk DJ, Omland KE (2003) Species-level paraphyly and polyphyly: frequency, causes, and consequences, with insights from animal mitochondrial DNA. *Annual Review of Ecology, Evolution, and Systematics* 34: 397–423. doi: 10.1146/annurev.ecolsys.34.011802.132421
- Goldstein PZ, DeSalle R (2010) Integrating DNA barcode data and taxonomic practices: Determination, discovery, and description. *BioEssays* 33: 135–147. doi: 10.1002/bies.201000036
- Haase M (2003) Clinal variation in shell morphology of the freshwater gastropod *Potamopyrgus antipodarum* along two hill-country streams in New Zealand. *Journal of the Royal Society of New Zealand* 33: 549–560. doi: 10.1080/03014223.2003.9517743
- Haase M (2005) Rapid and convergent evolution of parental care in hydrobiid gastropods from New Zealand. *Journal of Evolutionary Biology* 18: 1076–1086. doi: 10.1111/j.1420-9101.2005.00894.x
- Haase M, Bouchet P (1998) Radiation of crenobiontic gastropods on an ancient continental island: the *Hemistomia*-clade in New Caledonia (Gastropoda: Hydrobiidae). *Hydrobiologia* 367: 43–129. doi: 10.1023/A:1003219931171
- Haase M, Misof B (2009) Dynamic gastropods: stable shell polymorphism despite gene flow in the land snail *Arianta arbustorum*. *Journal of Zoological Systematics and Evolutionary Research* 47: 105–114. doi: 10.1111/j.1439-0469.2008.00488.x
- Haase M, Zielske S (2015) Five new and cryptic freshwater gastropod species from New Caledonia (Caenogastropoda, Truncatelloidea, Tateidae). *ZooKeys* 523: 63–87. doi: 10.3897/zookeys.523.6066
- Haase M, Mildner P, Wilke T (2007) Identifying species of *Bythinella* (Caenogastropoda, Rissooidea): a plea for an integrative approach. *Zootaxa* 1563: 1–16.
- Hebert PD, Ratnasingham S, de Waard JR (2003) Barcoding animal life: cytochrome c oxidase subunit I divergences among closely related species. *Proceedings of the Royal Society of London B* 270: 96–99. doi: 10.1098/rsbl.2003.0025

- Huson DH, Bryant D (2006) Application of phylogenetic networks in evolutionary studies. *Molecular Biology and Evolution* 23: 254–267. doi: 10.1093/molbev/msj030
- Joly S, McLenachan PA, Lockhart PJ (2009) A statistical approach for distinguishing hybridization and incomplete lineage sorting. *American Naturalist* 174: E54–E70. doi: 10.1086/600082
- Kistner EJ, Dybdahl MF (2013) Adaptive responses and invasion: the role of plasticity and evolution in snail shell morphology. *Ecology and Evolution* 3: 424–436. doi: 10.1002/ece3.471
- Klingenberg CP (2011) MorphoJ: an integrated software package for geometric morphometrics. *Molecular Ecology Resources* 11: 353–357.
- Maddison WP (1997) Gene trees in species trees. *Systematic Biology* 46: 523–536. doi: 10.1093/sysbio/46.3.523
- Mallet J (2007) Hybrid speciation. *Nature* 446: 279–283. doi: 10.1038/nature05706
- Nosil P (2012) Ecological speciation. Oxford University Press, New York, 280 pp. doi: 10.1093/acprof:osobl/9780199587100.001.0001
- Pelser PB, Kennedy AH, Tepe EJ, Shidler JB, Nordenstam B, Kadereit JW, Watson LE (2010) Patterns and causes of incongruence between plastid and nuclear Senecioneae (Asteraceae) phylogenies. *American Journal of Botany* 97: 856–873. doi: 10.3732/ajb.0900287
- Prié V, Bichain J-M (2009) Phylogenetic relationships and description of a new stygobite species of *Bythinella* (Mollusca, Gastropoda, Caenogastropoda, Amnicolidae) from southern France. *Zoosystema* 31: 987–1000. doi: 10.5252/z2009n4a12
- Rohlf FJ (2013a) tpsUtil, file utility program. version 1.58. Department of Ecology and Evolution, State University of New York at Stony Brook.
- Rohlf FJ (2013b) tpsDig, version 2.17. Department of Ecology and Evolution, State University of New York at Stony Brook.
- Sauer J, Hausdorf B (2010) Reconstructing the evolutionary history of the radiation of the land snail genus *Xerocrassa* on Crete based on mitochondrial sequences and AFLP markers. *BMC Evolutionary Biology* 10: 299. doi: 10.1186/1471-2148-10-299
- Seehausen O (2004) Hybridization and adaptive radiation. *Trends in Ecology & Evolution* 19: 198–207. doi: 10.1016/j.tree.2004.01.003
- Sharma PP, Fernández R, Esposito LA, González-Santillán E, Monod L (2015) Phylogenomic resolution of scorpions reveals multilevel discordance with morphological phylogenetic signal. *Proceedings of the Royal Society London B* 282: 20142953. doi: 10.1098/rspb.2014.2953
- Slatkin M (1991) Inbreeding coefficients and coalescence times. *Genetic Research* 58: 167–175. doi: 10.1017/S0016672300029827
- Shaw KL (2002) Conflict between nuclear and mitochondrial DNA phylogenies of a recent species radiation: what mtDNA reveals and conceals about modes of speciation in Hawaiian crickets. *Proceedings of the National Academy of Sciences* 99: 16122–16127. doi: 10.1073/pnas.242585899
- Swofford DL (2002) PAUP*: Phylogenetic analysis using parsimony (and other methods). Sinauer Associates, Sunderland, MA.
- Tamura K, Stecher G, Peterson D, Filipski A, Kumar S (2013) MEGA6: molecular evolutionary genetics analysis version 6.0. *Molecular Biology and Evolution* 30: 2725–2729. doi: 10.1093/molbev/mst197

- Thomaz D, Guiller A, Clarke B (1996) Extreme divergence of mitochondrial DNA within species of pulmonate land snails. *Proceedings of the Royal Society London B* 263: 363–368. doi: 10.1098/rspb.1996.0056
- Webster M, Sheets HD (2010) A practical introduction to landmark-based geometric morphometrics. *Quantitative Methods in Paleobiology* 16: 163–188. doi: 10.1080/10635-150050207447
- Wiens JJ, Hollingsworth BD (2000) War of the iguanas: Conflicting molecular and morphological phylogenies and long-branch attraction in iguanid lizards. *Systematic Biology* 49: 143–159.
- Wilke T, Davis GM, Qiu DC, Spear RC (2006) Extreme mitochondrial sequence diversity in the intermediate schistosomiasis host *Oncomelania hupensis robertsoni*: Another case of ancestral polymorphism? *Malacologia* 48: 143–157.
- Xia X (2013) DAMBE5: A comprehensive software package for data analysis in molecular biology and evolution. *Molecular Biology and Evolution* 30: 1720–1728. doi: 10.1093/molbev/mst064
- Zelditch ML, Swiderski DL, Sheets HD (2012) *Geometric morphometrics for biologists: a primer*, 2nd edition. Elsevier Academic Press, New York, 488 pp.
- Zielske S, Glaubrecht M, Haase M (2011) Origin and radiation of rissooidean gastropods (Caenogastropoda) in ancient lakes of Sulawesi. *Zoologica Scripta* 40: 221–237. doi: 10.1111/j.1463-6409.2010.00469.x
- Zielske S, Haase M (2014) When snails inform about geology: Pliocene emergence of islands of Vanuatu indicated by a radiation of truncatelloidean freshwater gastropods (Caenogastropoda: Tateidae). *Journal of Zoological Systematics and Evolutionary Research* 52: 217–236. doi: 10.1111/jzs.12053
- Zielske S, Haase M (2014b) New insights into tateid gastropods and their radiation on Fiji based on anatomical and molecular methods (Caenogastropoda: Truncatelloidea). *Zoological Journal of the Linnean Society* 172: 71–102. doi: 10.1111/zoj.12153
- Zielske S, Haase M (2015) Molecular phylogeny and a modified approach of character-based barcoding refining the taxonomy of New Caledonian freshwater gastropods (Caenogastropoda, Truncatelloidea, Tateidae). *Molecular Phylogenetics and Evolution* 89: 171–181. doi: 10.1016/j.ympev.2015.04.020
- Zwickl DJ (2006) Genetic algorithm approaches for the phylogenetic analysis of large biological sequence datasets under the maximum likelihood criterion. PhD Dissertation, University of Texas, Austin.

Taxonomic evaluation of eleven species of *Microcyclops* Claus, 1893 (Copepoda, Cyclopoida) and description of *Microcyclops inarmatus* sp. n. from America

Martha Angélica Gutiérrez-Aguirre¹, Adrián Cervantes-Martínez¹

¹ Universidad de Quintana Roo (UQROO), Unidad Cozumel, Av. Andrés Quintana Roo s/n, 77600, Cozumel, Quintana Roo México

Corresponding author: Martha Angélica Gutiérrez-Aguirre (margutierrez@uqroo.edu.mx)

Academic editor: D. Defaye | Received 10 December 2015 | Accepted 2 June 2016 | Published 6 July 2016

<http://zoobank.org/E0086EEB-7B77-4F71-B6BE-E8637207AF21>

Citation: Gutiérrez-Aguirre MA, Cervantes-Martínez A (2016) Taxonomic evaluation of eleven species of *Microcyclops* Claus, 1893 (Copepoda, Cyclopoida) and description of *Microcyclops inarmatus* sp. n. from America. ZooKeys 603: 33–69. doi: 10.3897/zookeys.603.7480

Abstract

Description and meristic analysis of eleven species of *Microcyclops* recorded in America were performed based on the examination of type specimens and fresh material. Microscopic analysis of oral appendages, such as the shape and armature of the distal coxal endite of the maxilla, the ornamentation on the caudal surface of the antenna, and the intercoxal sclerites and armament of the inner basis of all swimming appendages, were characteristics that allowed the differentiation between species. Among these species, our study confirmed the synonymy of *M. diversus* Kiefer, 1935 with *M. ceibaensis* (Marsh, 1919). The results of our observations showed that *M. alius* (Kiefer, 1935) is a junior synonym of *M. dubitabilis* Kiefer, 1934; the latter being confirmed as a valid species. Also, it is proposed that the records of *M. rubellus* (Lilljeborg, 1901) and *M. varicans* (Sars, 1863) in America should be revised as there are serious doubts about their distribution in America. The analysis suggested that *M. anceps pauxensis* Herbst, 1962 is distinct from *M. anceps* var. *minor* Dussart, 1984 and that both are likely different from *M. anceps anceps* (Richard, 1897). Finally a full morphological description of adult females of *Microcyclops inarmatus* sp. n. is presented.

Keywords

Diversity, Mexico, morphology, species richness

Introduction

In America, 16 species and subspecies of *Microcyclops* Claus, 1893 have been described and recorded: *M. alius* (Kiefer, 1935), *M. anceps anceps* (Richard, 1897), *M. anceps pauxensis* Herbst, 1962, *M. anceps* var. *minor* Dussart, 1984, *M. ceibaensis* (Marsh, 1919), *M. dubitabilis* Kiefer, 1934, *M. echinatus* Fiers, Ghenne & Suárez-Morales, 2000, *M. elongatus* (Lowndes, 1934), *M. finitimus* Dussart, 1984, *M. furcatus* (Daday, 1905), *M. mediasetosus* Dussart & Frutos, 1985, *M. medius* Dussart & Frutos, 1985, *M. pumilis* Pennak & Ward, 1985, *M. rubellus* (Lilljeborg, 1901), *M. diversus* Kiefer, 1935, and *M. varicans* (Sars, 1863).

In her publication of an identification key for South American cyclopoids, Reid (1985) proposed that *Microcyclops diversus* is a probable synonym of *M. ceibaensis* (in 1986, this opinion was based on similarities in the fourth leg observed by the same author) and that *M. anceps* var. *minor* is a synonym of *M. anceps pauxensis*. Rocha (1998) proposed a set of morphological features that would be useful for distinguishing five species previously recorded in Brazil and suggested that *M. alius* is a possible synonym of *M. dubitabilis*. However, Reid (1990) had previously suggested that *M. dubitabilis* is a possible synonym of *M. varicans*.

Therefore, some questions on the taxonomic status of some species of *Microcyclops* in America remain unresolved. These taxonomic problems may be related to the lack of thorough and rigorous species descriptions. Rocha (1998), Mirabdullayev (1998, 2007), and Mirabdullayev and Urazova (2006) have documented morphological features that are useful for differentiating some species of the genus. For instance, they proposed the following morphological features as diagnostic: ornamentation of dorsal margins of prosomites, presence or absence of pores on second endopodite of first leg, ornamentation of the inner margin of basipodite of first leg, ornamentation of caudal ramus and caudal setae, relative lengths of caudal setae, proportions of second endopodite of fourth leg, and general ornamentation of fourth leg.

In Mexico, some species with uncertain taxonomic status have been recorded, including *M. ceibaensis*, *M. anceps*, and *M. dubitabilis* (Elías-Gutiérrez et al. 2008). In this paper, we propose a set of morphological features that are useful for distinguishing between these species, which have been documented by biological inventories of the country. These features include the mouth appendages, the ornamentation of intercoxal sclerites, and the inner margin of the basis of the first to fourth swimming legs.

Methods

The morphological analysis was performed following current standards for the taxonomic study of cyclopoid copepods (see Williamson and Reid 2001).

Material examined. The evaluation included analyses of holotypes, paratypes, and museum specimens deposited in different collections: the Collection of Zooplankton of ECOSUR at Chetumal (**ECO-CH-Z**), the collection of Copepoda of

the Muséum National d'Histoire Naturelle, Paris (**MNHN**), the Staatliches Museum für Naturkunde, Karlsruhe (**SMNK**) and the National Museum of Natural History, Smithsonian Institution, Washington, DC (**USNM**) (Table 2, as Suppl. material 1).

Terminology used for the armament of each appendage(s) follows Huys and Boxshall (1991):

A1	Antennule
A2	Antenna
BspA2	Antennal basipodite
Bsp	Basipodite
Enp1-Enp_n	First to "n" endopodal segment
Exp1-Exp_n	First to "n" exopodal segment
P1, P2, P3, P4	First, second, third, and fourth swimming legs
P5	Free segment of fifth leg

Lateral, outermost terminal, outer median terminal, inner median terminal, innermost terminal, and dorsal caudal setae are coded as setae II, III, IV, V, VI, and VII, respectively.

The morphology of several species was examined using light microscopy: A1, A2, the mouthparts, the entire structure of all of the swimming legs, and other taxonomically relevant structures, such as the frontal or caudal ornamentation of BspA2, the ornamentation of the distal coxal endite of the maxilla, and the ornamentation of maxillular palp, were illustrated with the aid of a camera lucida.

Sources for the morphological data were the types, paratypes, and other museum specimens (Table 2, as Suppl. material 1), and original descriptions of eleven named species and two named subspecies recorded in America. Detailed descriptions based on the microscopic and morphometric analyses of the adult females of each species are presented.

Results

Descriptive section

Below those morphological structures which are shared by all the species examined herein are described.

Antennule 11- or 12-segmented (Fig. 1). In the basic 12-segmented structure (Fig. 1A), each segment was armed with setae (s), spines (sp) or aesthetascs (ae) in the following order: (1) 8s; (2) 4s; (3) 2s; (4) 6s; (5) 3s; (6) 1s + 1sp; (7) 2s; (8) 3s; (9) 2s + 1ae; (10) 2s; (11) 2s + 1 ae; (12) 7s + 1 ae. In the case of the 11-segmented antennule the third and fourth segments are entirely or partially fused (Fig. 1B); then, the third segment bears 8s.

Antenna with coxa (without seta), Bsp (with 2 medial setae + one lateral seta representing Exp), and 3-segmented Enp (Fig. 3B). Labrum with strong teeth on distal

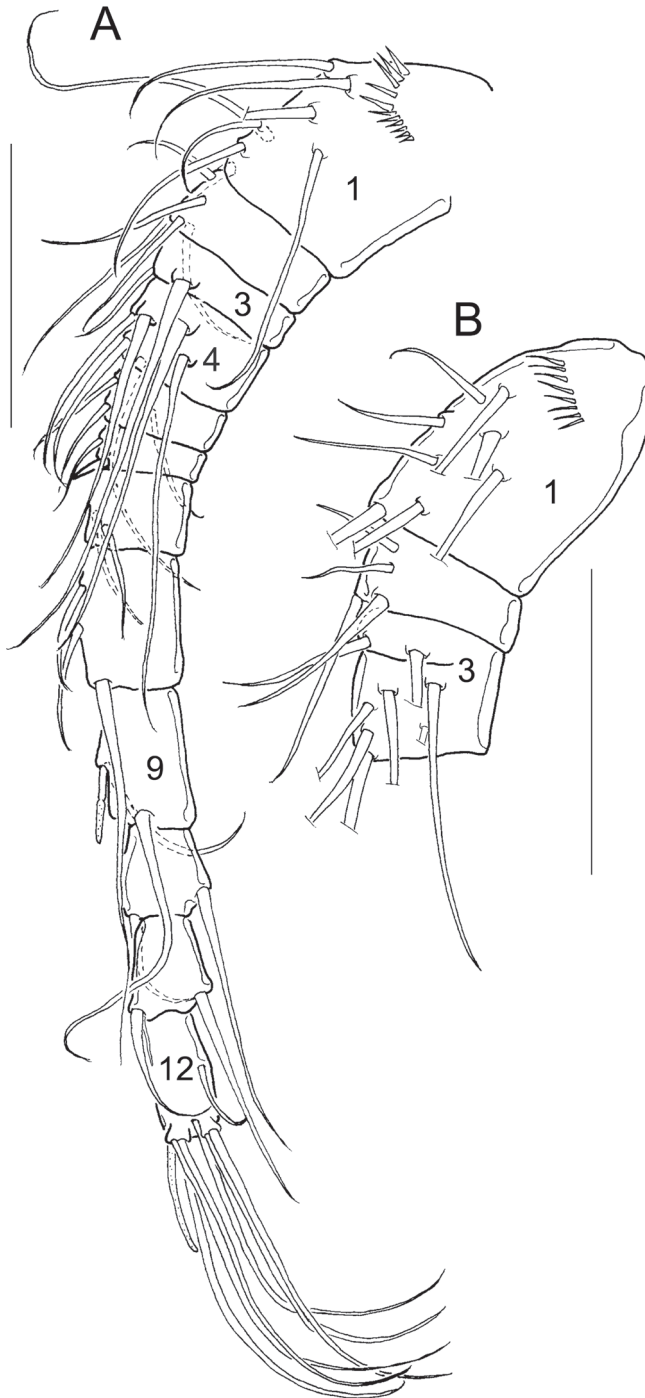


Figure 1. Morphology of antennules. **A** Antennule with 12 segments (*Microcyclops ceibaensis* from km 51-2) **B** Morphological variation in antennules with 11 segments (*M. dubitabilis* from km 51-2). Scale bars: 50 μ m.

Table 1. Setation formula of the swimming legs in the *Microcyclops* species here examined (spine in Roman numerals, seta in Arabic numerals).

	Coxa	Basis	Exp	Enp
P1	0-1	1-I, or 1-0	I-1; III-5	0-1; 1-I-4
P2	0-1	1-0	I-1; IV-5	0-1; 1-I-5
P3	0-1	1-0	I-1; IV-5	0-1; 1-I-5
P4	0-1	1-0	I-0; III-5	0-1; 1-II-3

rim and strong, distal hairs overhanging distal rim (Fig. 6D). Mandible with toothed gnathobase; the innermost teeth bi-toothed. Innermost margin of mandibular gnathobase with one spinulose seta, palp with two long and one short seta. No spinules next to mandibular palp (Fig. 6E).

Praecoxal arthrite and palp of maxillule naked; praecoxal arthrite with 3 chitinized distal claws, and one spinulose seta on caudal side. Inner margin with one biserially plumose seta plus six naked setae (Fig. 6F). Maxilla with praecoxa and coxa partially fused, praecoxal endite with two setae, coxa naked with proximal endite bearing one seta (Fig. 6L) and distal endite with two armed long setae (Fig. 6M). Claw-like basal endite armed, and Enp one- or two-segmented.

Maxilliped with syncoxa bearing 2 or 3 spiniform setae, Bsp with two setae; and Enp two-segmented, first segment with 1 seta, second segment with 3 setae (Fig. 6N).

Armature formula of P1–P4 as in Table 1, endopods and exopods two-segmented in all swimming legs. Urosome five-segmented, fifth pediger bearing one free segment with one apical seta (fifth leg), and one lateral seta inserted on pediger (Fig. 8C). Detailed description of the species is provided in the next section. The material examined for each species is provided in Table 2, as Suppl. material 1.

Order: Cyclopoida Burmeister, 1835

Family: Cyclopidae Rafinesque, 1815

Subfamily Cyclopinae Rafinesque, 1815

Genus *Microcyclops* Claus, 1893

***Microcyclops inarmatus* sp. n.**

<http://zoobank.org/687BDBC3-853D-437E-9310-4146F210094A>

Figures 2–5

Microcyclops varicans Reid, 1992; Trans. Am. Microsc. Soc. 111(3), p: 249–250, figs 8d, 9c.

Holotype. One adult female dissected on two slides: A1, A2 (slide 1, ECOCH-Z-09337); mandible, maxillule, maxilla, maxilliped, P1–P4, and urosome (slide 2, ECOCH-Z-09337). Collected 13.I.1998.

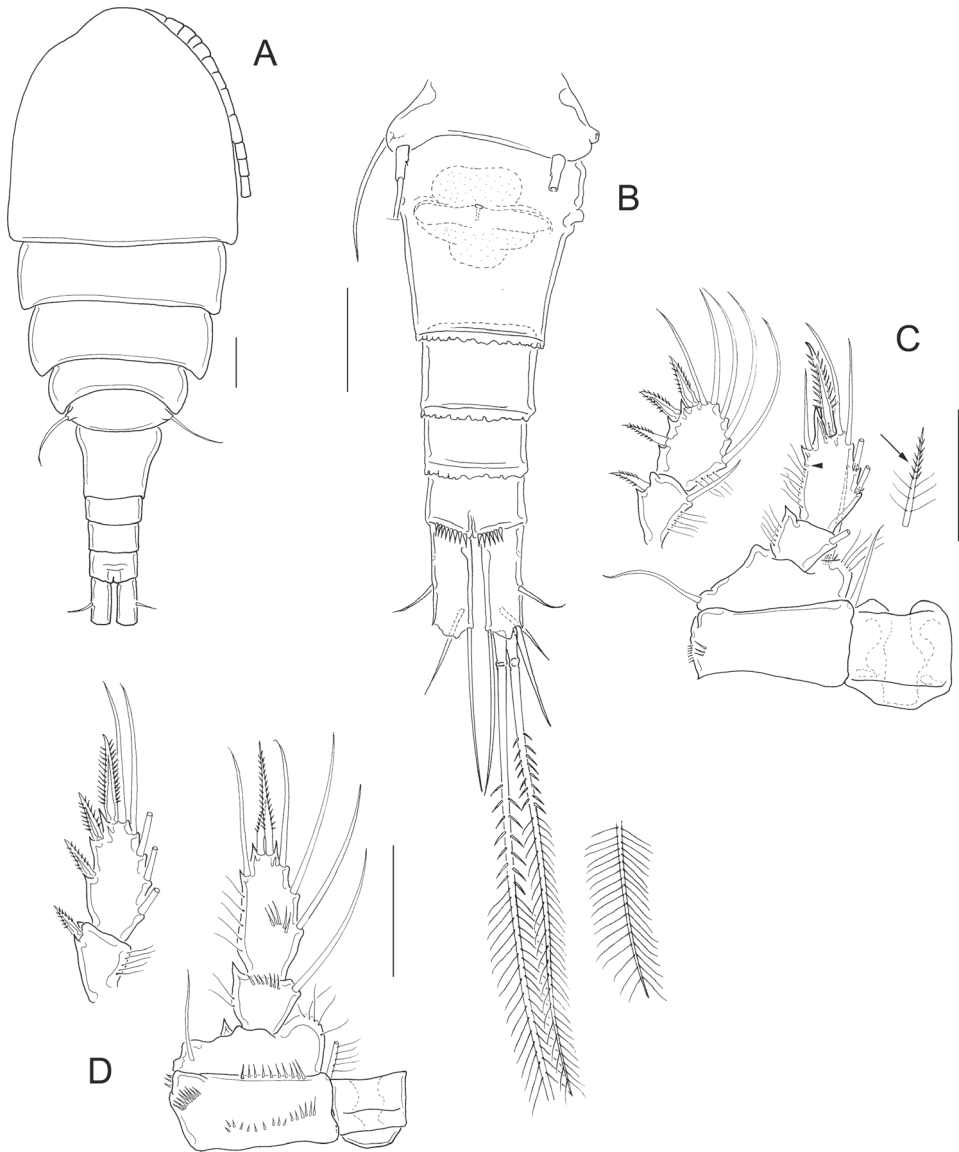


Figure 2. *Microcyclops inarmatus* sp. n. Adult female, holotype (except **A**). **A** Habitus of one paratype specimen (ECOCH-Z-09338) **B** Urosome ventral, note that the last fraction of the inner median terminal caudal seta is separated (ECOCH-Z-09337) **C** P1, caudal (ECOCH-Z-09337) **D** P4, caudal (ECOCH-Z-09337). Scale bars: 50 μ m.

Paratypes. 10 adult females preserved in 90% ethanol with a drop of glycerine. ECOCH-Z-09338. Collected 13.I.1998.

Type locality. A pond in km 51 lado 1, Villahermosa-Frontera highway 18°23'16"N; 92°47'00"W.

Etymology. the name of the species means un-armed in Latin; it refers to the absence of ornamentation on the intercoxal sclerites, the lack of spinules at base of caudal furcal setae, the reduced number of setae on second antennal endopod, and the reduced ornamentation on antennal basis.

Additional material. One adult female collected 1.02.1935 from Laguna Rincon, Haiti (slide SMNK-2391; labelled as *Microcyclops dubitabilis* with A1, maxilla, P1-P4). One adult female collected from Laguna Rincon, Haiti (slide SMNK-2392; labelled as *M. dubitabilis* with urosome).

One adult female collected 05.1986 from Shark river slough, Everglades National Park, Florida, USA (slide 2 of 7, USNM-251321; labelled as *M. varicans* with A1, A2, P1-P4, and urosome).

Diagnosis. Adult female: Dorsal margin of prosomal somites smooth; body length 565 to 615 μm in paratypes. Antennule 12-segmented, not reaching the distal margin of the first prosomal segment (Fig. 2A). Fifth pediger nude; cylindrical free segment of P5 more than 3 times as long as wide, with tiny inner spine; genital double somite expanded proximally. Anal somite with strong spines on ventral distal margin; length to width ratio of caudal ramus less than 3; no spinules at base of lateral and outermost terminal caudal setae (Fig. 2B). Outer median terminal and inner median terminal caudal setae with heteronomous setulation (Fig. 2B). Endopodites and exopodites of P1-P4 bisegmented with setation formula as in Table 1, inner basis of P1 with long spine (long arrow in Fig. 2C), Enp2P1 with one pore on lateral margin (short arrow in Fig. 2C). Intercoxal sclerites of P1-P4 unarmed, long setules on inner margin of basipodites of P1-P4, medial spine of Enp2P4 almost as long as the segment and twice the length of the lateral spine (Fig. 2D).

Adult male: unknown.

Description of female. *Antennule* 12-segmented; antenna with 3-segmented Enp armed with 1, 6, and 7 setae respectively (Fig. 3A, B –position of missing setae in specimens is arrowed). Antennal basis with one group of spinules on the basal-outer margin in caudal view (Fig. 3A, B); frontal surface of the antennal basis with two rows of tiny spinules (Fig. 3C). Nine teeth on mandibular gnathobase (Fig. 3D). Maxillule (Fig. 3E) with unarmed palp; apical region of maxillular palp with two armed setae plus one smooth seta, three setae (one armed) on lateral lobe, proximal seta smooth (Fig. 3F). Distal coxal endite of the maxilla with two long setae: the proximal seta with two tiny spines at its base and bifurcated, distal seta with one row of tiny spines along one margin (Fig. 3G, H). Basipodite with one claw-like projection bearing 5-7 strong spines on the concave margin and one long, armed seta on its base; two-segmented Enp bearing 2 and 3 setae respectively (Fig. 3G). Because of the condition of the microscope slide preparatum we could not verify one basal seta on maxillar Enp1 (arrowed in Fig. 3H). Maxilliped with syncoxa (3 setae), basis (2 setae), and two-segmented Enp bearing 1 and 3 setae. Basis of maxilliped with a row of spinules on frontal and caudal surfaces (Fig. 3I).

Basipodites of P1-P3 with long hair-like setules on the inner margins; one row of tiny spinules along the lateral margins of coxa; intercoxal sclerites naked (Fig. 4A-D).

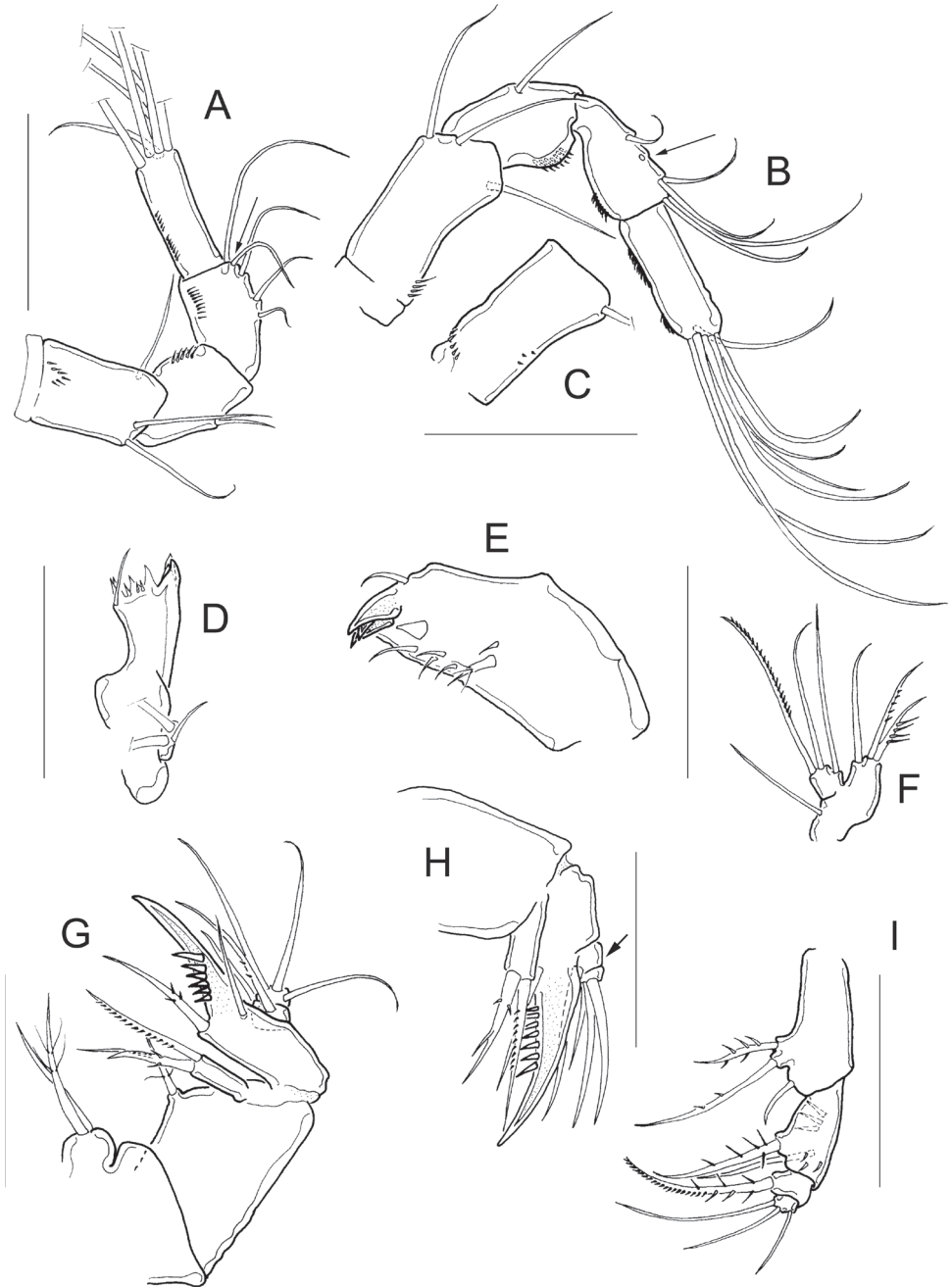


Figure 3. *Microcyclops inarmatus* sp. n. Adult female. **A** Antenna, caudal (USNM-251321), note that the position of missing seta is arrowed **B** Antenna, caudal (ECOCH-Z-09337), note that the position of missing seta is arrowed **C** Antennal basipodite, frontal (ECOCH-Z-09337) **D** Mandible (ECOCH-Z-09337) **E** Maxillule (ECOCH-Z-09337) **F** Maxillular palp (ECOCH-Z-09337) **G** Maxilla (ECOCH-Z-09337) **H** Maxilla (SMNK-2391) **I** Maxilliped (ECOCH-Z-09337). Scale bars: 50 μ m.

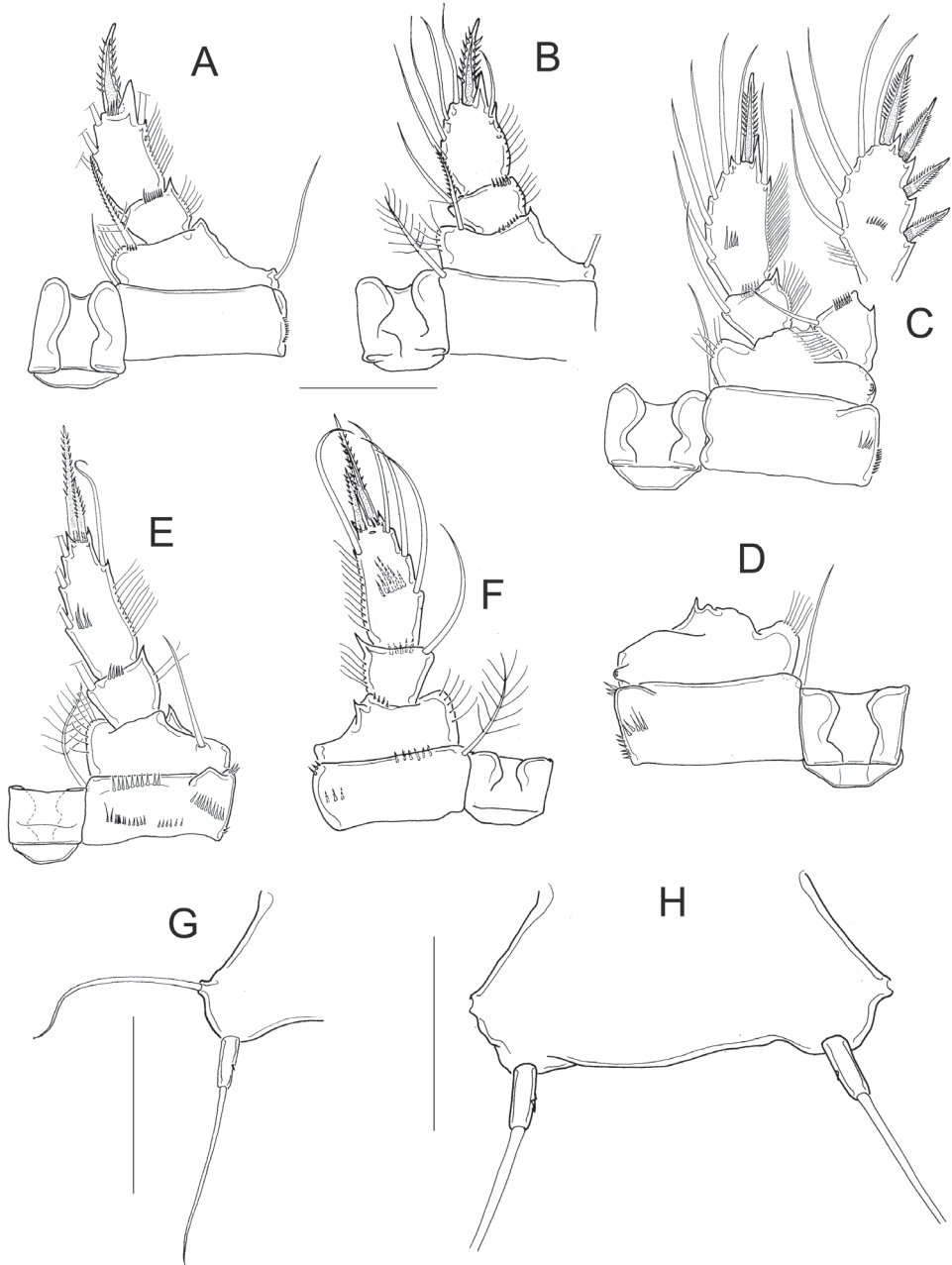


Figure 4. *Microcyclops inarmatus* sp. n. Adult female. **A** P1, frontal (USNM-251321) **B** P1, frontal (SMNK-2391) **C** P2, caudal (ECOCH-Z-09337) **D** P3 coxa, basis, and sclerite, caudal (ECOCH-Z-09337) **E** P4, caudal, Exp unfigured (USNM-251321) **F** P4, frontal, Exp unfigured (SMNK-2391) **G** Fifth pediger and P5 (USNM-251321) **H** Fifth pediger and P5 (SMNK-2392). Scale bars: 50 μ m.

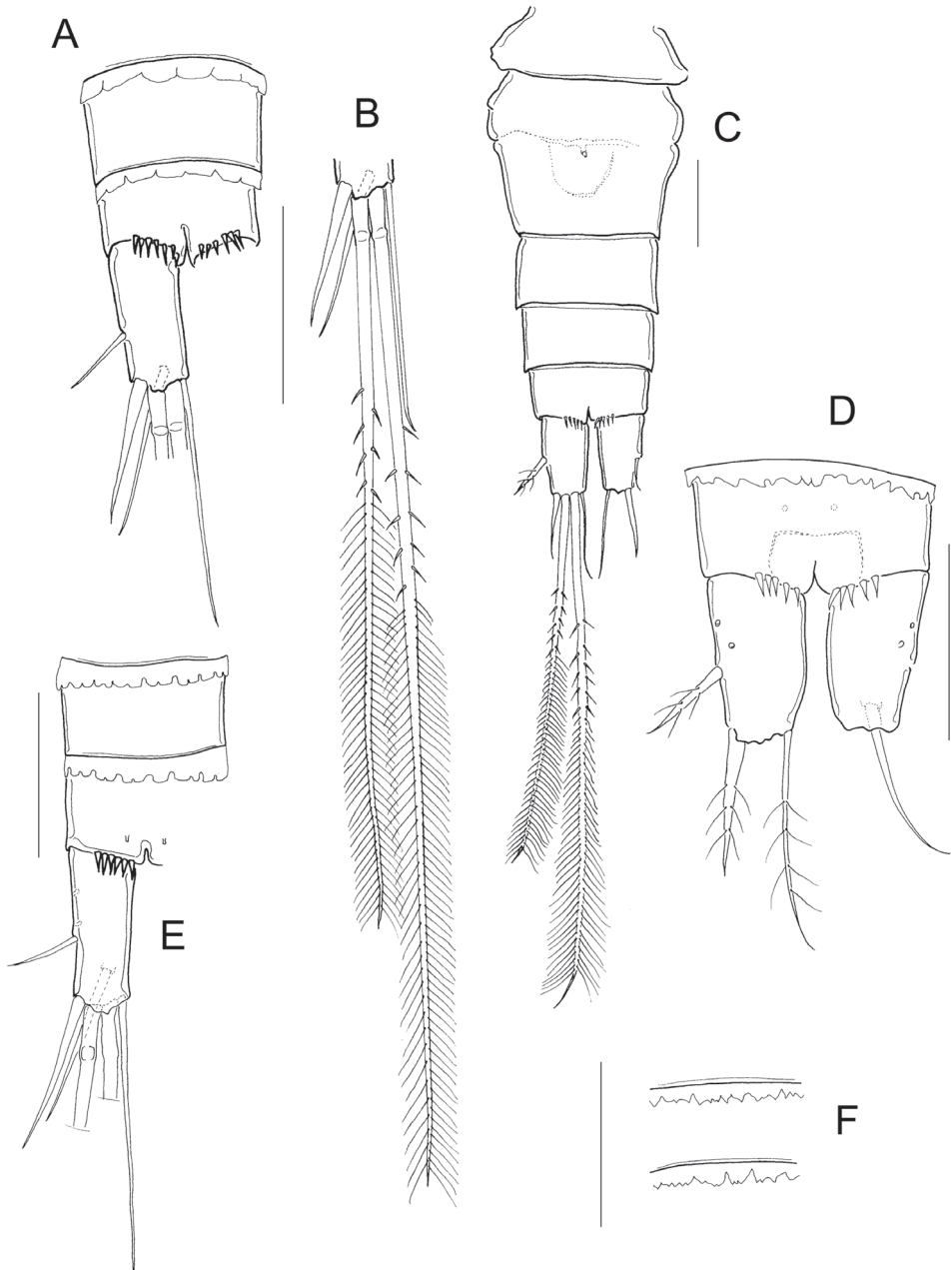


Figure 5. *Microcyclops inarmatus* sp. n. Adult female. **A** Anal somite and caudal rami, ventral (USNM-251321) **B** Terminal caudal setae (USNM-251321) **C** Urosome, ventral (SMNK-2392) **D** Anal somite and caudal rami, ventral (SMNK-2392) **E** Anal somite and caudal rami (ECOCH-Z-0679) **F** Hyaline fringes of urosome (Pajonal). Scale bars: 50 μ m.

Basis of P1 with one long spine on inner margin; spine reaching distal middle of Enp2P1 and armed with heteronomous setulation: hair-like setules on its base, tiny spinules distally (Figs 2C; 4A, B). One pore on the lateral margin of Enp2P1 (Fig. 4A, B). Basipodite of P4 with long hair-like setules on inner margin; P4 intercoxal sclerite quadrangular (Figs 2D; 4E, F), Enp2P4 2.14 ± 0.2 times as long as wide; and medial spine 1.97 ± 0.25 as long as lateral spine and 0.91 ± 0.04 as long as the segment (Figs 2D; 4E, F).

Fifth pediger nude; P5 with one cylindrical free segment, 3.23 ± 0.4 times as long as wide, bearing one tiny medial spinule. Free segment 0.27 ± 0.01 times as long as distal seta (Figs 2B; 4G, H). Hyaline fringes of urosomites serrated (Fig. 2B), petaloid or rounded (Fig. 5 A, C–F). Length to width ratio of caudal ramus 2.54 ± 0.44 , inner margin naked; no spinules at base of lateral caudal (II) and outermost terminal caudal setae (III) (Fig. 2B). Only 5–8 strong spinules present ventrally on the distal margin of anal somite, no spinules dorsally (Fig. 5 A, C–E). Lateral caudal seta (II) inserted at $58.6 \pm 3.9\%$ of caudal ramus.

Dorsal caudal seta (VII) 0.9 ± 0.1 times as long as caudal ramus, and innermost terminal caudal seta (VI) 1.4 ± 0.04 times as long as caudal rami (Fig. 2B). Relative lengths of terminal caudal seta from outermost caudal seta to innermost caudal seta is 1.0 : 4.9 : 7.3 : 1.6 (Figs 2B; 5B, C). Outer median terminal caudal seta (IV) and inner median terminal caudal seta (V) with heteronomous setulation: proximally with spinule-like setules and distally with long and fine setules (Figs 2B; 5B, C).

Microcyclops dubitabilis Kiefer, 1934

Figures 6–8

Description of female. *Antennule* 11, or 12-segmented (intra- and interpopulation variation); 3-segmented endopod of antenna bearing 1, 9, and 7 setae, respectively (Fig. 6A, B). Antennal basis with three long rows of spinules on caudal surface (Fig. 6B): two basal rows, and one median row; frontal surface of antennal basis with two rows of tiny spinules (Fig. 6C). Labrum with 6–7 teeth between two curved lateral teeth, and 3–4 strong spinules on each round projections of the plate (Fig. 6D). Eight teeth on mandibular gnathobase (Fig. 6E). *Maxillule* as in Fig. 6F, maxillular palp with one armed seta plus two smooth setae apically, three smooth setae on lateral lobe, and one proximal nude seta (Fig. 6G, H). Maxilla with armed setae on distal coxal endite: proximal seta with one long spine-like setule at its base and bifurcated apically, distal seta with one row of tiny spines along inner margin (Fig. 6I–K, M). *Basipodite* with claw-like projection bearing 6–8 thin spinules on concave margin and one long seta on its base; this seta armed with two rows of spinules (long spinules on inner margin, and short spinules on outer margin) (Fig. 6I–L). Maxilla with two-segmented Enp bearing 2 and 3 setae respectively (Fig. 6I–L). Maxilliped with syncoxa (3 setae), basis (2 setae), and two-segmented Enp bearing 1 and 3 setae, respectively. Basis of the maxilliped nude, two spinules present on frontal surface of Enp1 (Fig. 6N).

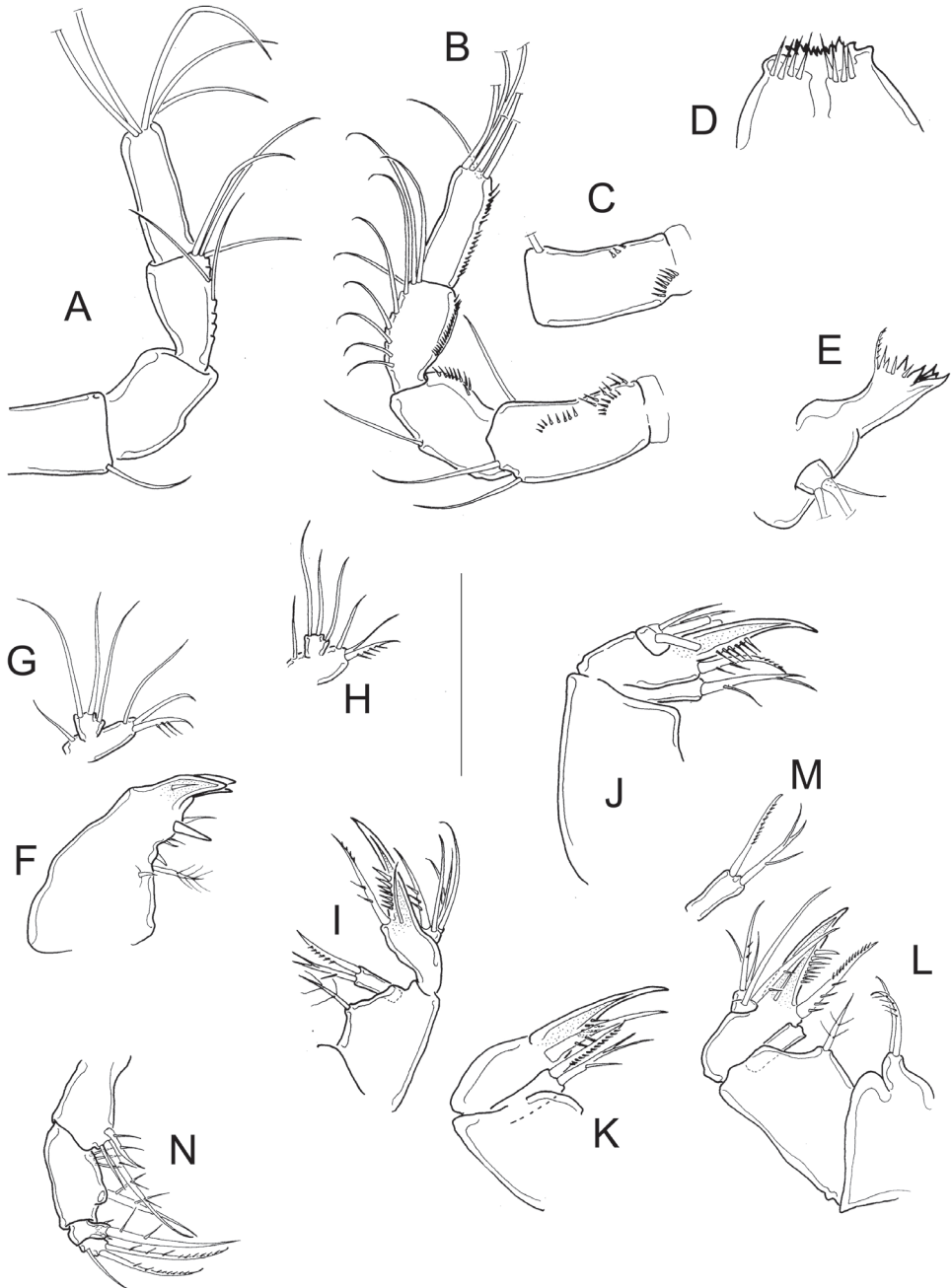


Figure 6. *Microcyclops dubitabilis* Kiefer, 1934. Adult female. **A** Antenna, frontal (SMNK-2204) **B** Antenna, caudal (km 51-1) **C** Antennal basipodite, frontal (km 51-1) **D** Labrum (km 51-1) **E** Mandible (km 51-1) **F** Maxillule (km 51-1) **G** Maxillular palp (km 51-1) **H** Maxillular palp (USNM-251322) **I** Maxilla (USNM-251322) **J** Maxilla (SMNK-2081) **K** Maxilla (SMNK-2204) **L** Maxilla (km 51-1) **M** Distal coxal endite **N** Maxilliped (km 51-1). Scale bar: 50 μ m.

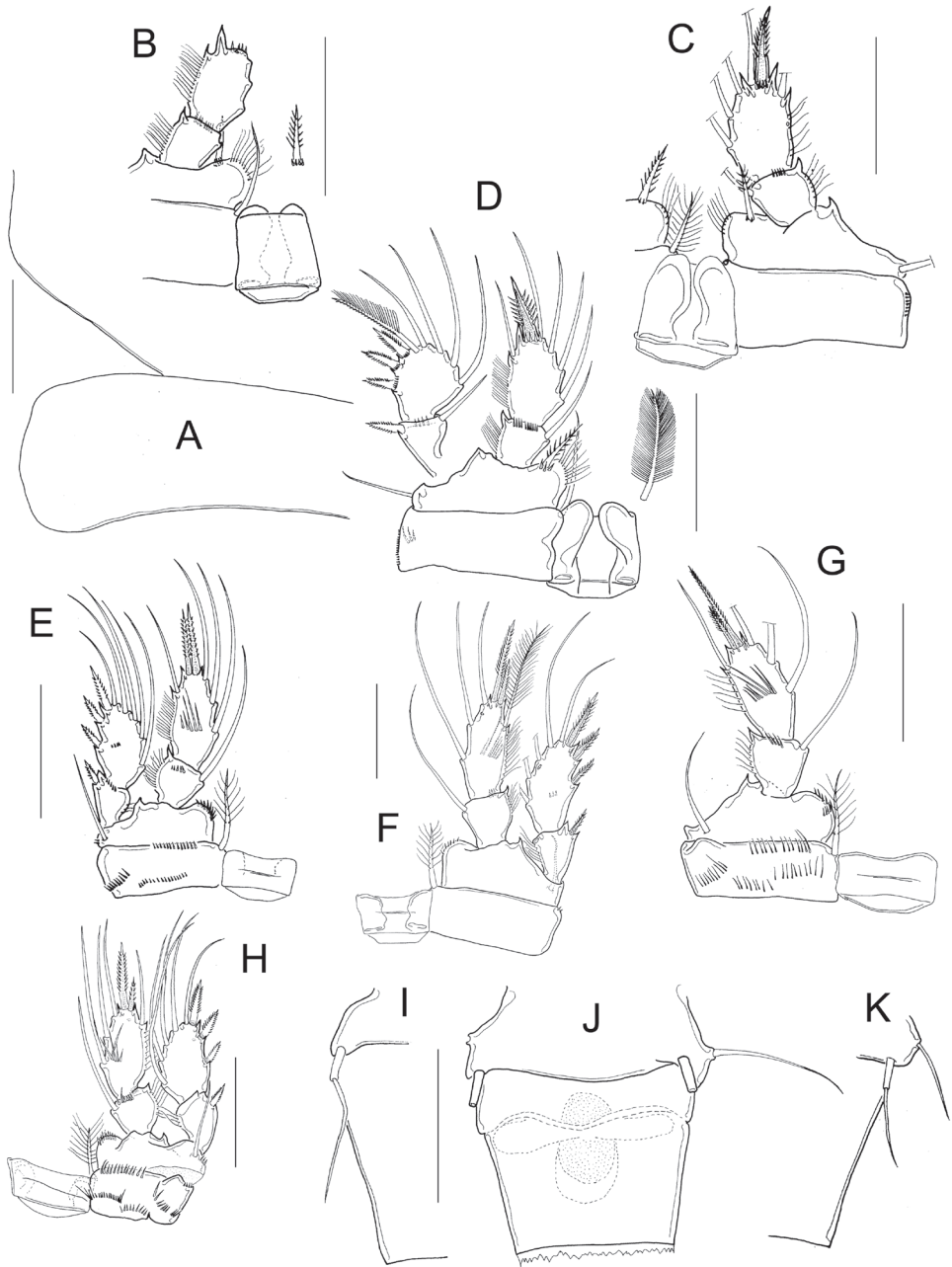


Figure 7. *Microcyclops dubitabilis* Kiefer, 1934. Adult female. **A** First and second prosomal somite, dorsal (SMNK-2189) **B** P1, caudal (USNM-251322) **C** P1, frontal (SMNK-2081) **D** P1, frontal (km 51-1) **E** P4, caudal (USNM-251322) **F** P4, frontal (SMNK-2189) **G** P4, caudal (MNHN-Cp6764) **H** P4, caudal (km 51-1) **I** Fifth pediger, P5, genital double somite, ventral (USNM-251322) **J** Fifth pediger, P5, genital double somite, ventral (MNHN-Cp5398) **K** Fifth pediger, P5, genital double somite, ventral (SMNK-2204). Scale bars: 50 μ m.

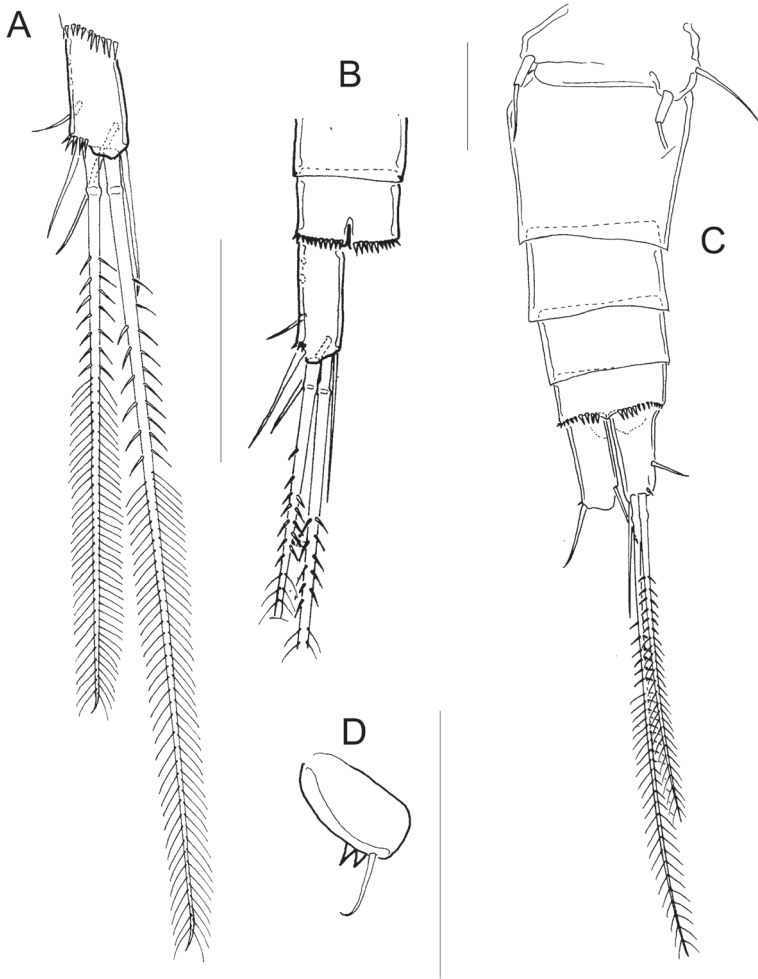


Figure 8. *Microcyclops dubitabilis* Kiefer, 1934. Adult female. **A** Caudal rami, ventral (USNM-251322) **B** Anal somite and caudal rami, ventral (SMNK-2204) **C** Urosome, ventral (SMNK-2081) **D** P6 (km 51-1). Scale bars: 50 μ m.

Dorsal margin of *proosomal somites* smooth (Fig. 7A). Basis of P1 medially hairy. One short spine present on inner margin, spine biserially armed with spinule-like setules (homonomous ornamentation) and reaching slightly beyond distal margin of the Enp1P1. Intercoxal sclerite of P1 naked (Fig. 7B–D). Pore on lateral margin of Enp2P1 sometimes present (interpopulation variation). Inner margin of basis of P2 and P3 hairy, and intercoxal sclerites of these swimming legs naked (unfigured). Inner margin of P4 basis with short hairs; intercoxal sclerite naked, rectangular (Fig. 7E–H), Enp2P4 1.9 ± 0.1 times as long as wide; medial spine 1.8 ± 0.3 times as long as lateral spine, and 0.8 ± 0.1 times as long as segment. Apical spines of Enp2P4 are subequal only in female USNM-251322 (Fig. 7E).

Fifth pediger nude; P5 free segment cylindrical, 3.6 ± 0.8 times as long as wide, without inner spine. Free segment 0.4 ± 0.1 times the length of the distal seta (Figs 7I–K; 8C). Length to width ratio of caudal ramus 2.4 ± 0.2 , inner margin naked. With or without spines at base of seta II (intrapopulation variation), spinules always present at base of setae III. Distal margin of anal somite bearing spinules: medial spinules are longer than lateral ones on ventral surface; spinule row can extend laterally or dorsally (Fig. 8 A–C). Seta II inserted at $71 \pm 5.7\%$ of caudal ramus.

Seta VII 1.02 ± 0.3 times as long as caudal ramus, and seta VI 1.4 ± 0.2 times longer than caudal ramus. Relative lengths of terminal caudal seta from outermost caudal seta to innermost caudal seta are 1.0 : 4.9 : 7.1 : 1.6 (Fig. 8A, C). Seta IV and seta V with heteronomous setulation: proximally with spine-like setules and distally with long and fine setules (Fig. 8A–C). Sixth leg with two medial spines and one lateral seta (Fig. 8D).

Microcyclops ceibaensis (Marsh, 1919)

Figures 9–11

Description of female. *Antennule* 12-segmented (Fig. 9A). Antenna with 3-segmented endopod with 1, 9, and 7 setae, respectively (Fig. 9F). Frontal surface of antennal basis with one basal row of spinules arranged in arc next to medial (inner) margin, and one median row of spinules next to lateral (outer) margin. (Fig. 9D, E). Caudal surface of antennal basis with two basal rows of spinules arranged in arc, plus two rows of long spinules on outer margin (Fig. 9F). Labrum with 7 marginal teeth between two lateral curved teeth, and two rows of long spinules (6) overhanging distal margin (Fig. 9B, C). Gnathobase of the mandible with eight teeth (Fig. 9G). Maxillular palp with three apical setae, three setae on lateral lobe, and one proximal seta. The proximal seta armed on both margins, one seta on lateral lobe and one apical seta with setules (Fig. 9H). Distal coxal endite of the maxilla with two long setae: the proximal seta with two long basal spinules and bifurcated apically, distal seta smooth (Fig. 9I). Basipodite with one claw-like projection bearing thin spinules on concave margin, and one long smooth seta on its base. One-segmented Enp bearing 5 setae (Fig. 9I). Maxilliped with syncoxa (2 setae), basis (2 setae), and two-segmented Enp bearing 1 and 3 setae, respectively. Ornamentation of setae on syncoxa and Enp1 variable (intrapopulation variation, arrowed in Fig. 9J). Syncoxa and basis of maxilliped with a row of spinules on caudal surface next to lateral margin (Fig. 9J).

Dorsal margin of *proosomal somites* slightly serrated (Fig. 10A). Basis of P1–P3 with pilose inner margin. Intercoxal sclerites of P1–P3 with one row of short spinules (Fig. 10B–G), in some populations the sclerite of P3 with two rows of spinules (Fig. 10H). Enp2P1 with two pores on lateral margin (Fig. 10C). Because of the condition of the specimen in slide USNM-222299, it was not possible to verify the presence of spinules on the sclerite as well as the pores on the second endopodal segment of P1 (Fig. 10B).

P1 basis with long medial spine reaching distal third of Enp2P1. Spine ornamented with long setules near base and with short spinule-like setules more distally (Fig.

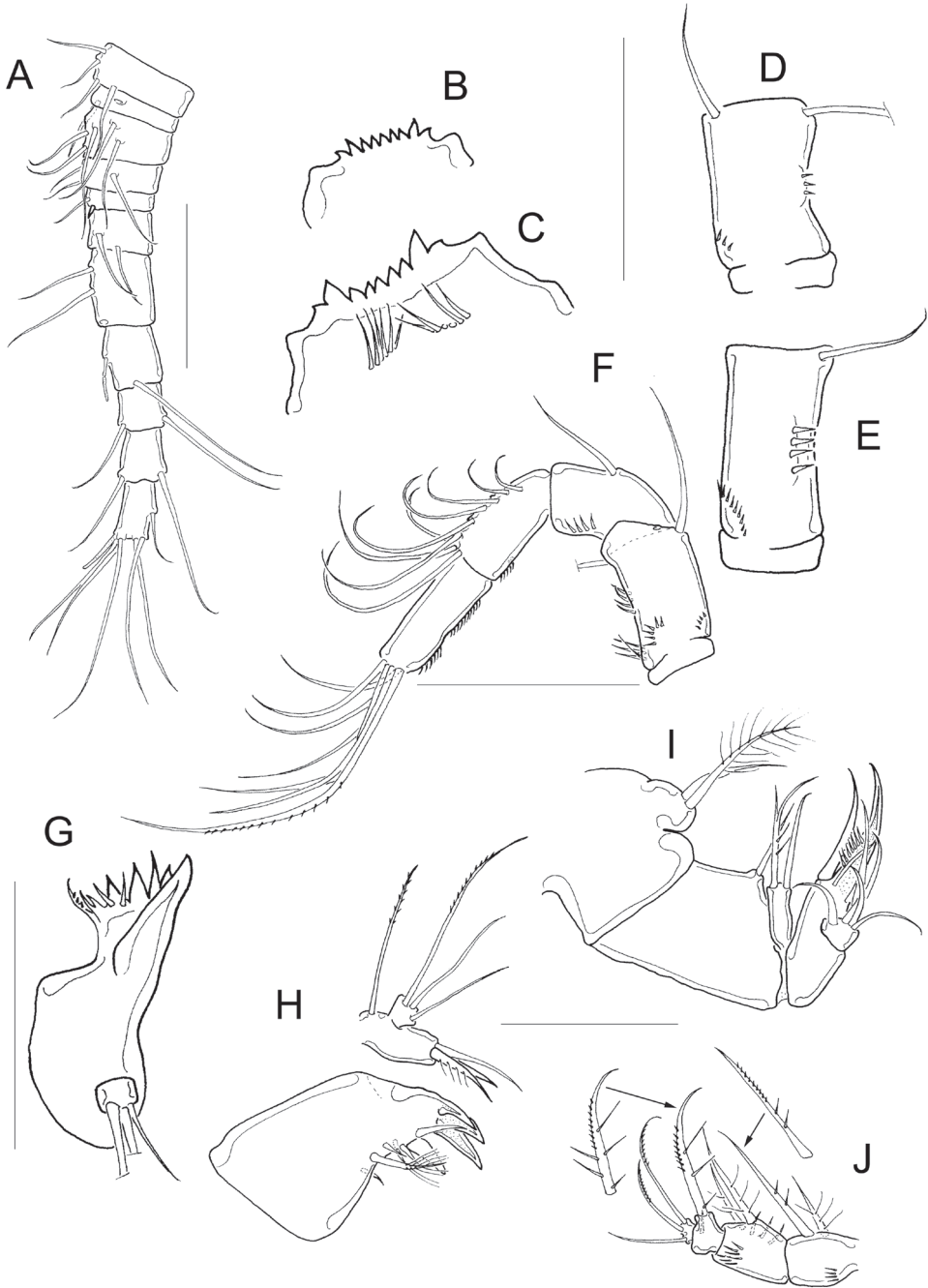


Figure 9. *Microcyclops ceibaensis* (Marsh, 1919). Adult female. **A** Antennule, segments 2-12 (USNM-222299) **B** Labrum (USNM-222299) **C** Labrum (km 51-2) **D** Antennal basipodite, frontal (USNM-222299) **E** Antennal basipodite frontal (km 154) **F** Antenna, caudal (km 154) **G** Mandible (km 51-1) **H** Maxillule (km 154) **I** Maxilla (km 51-2) **J** Maxilliped (km 154). Scale bars: 50 μ m.

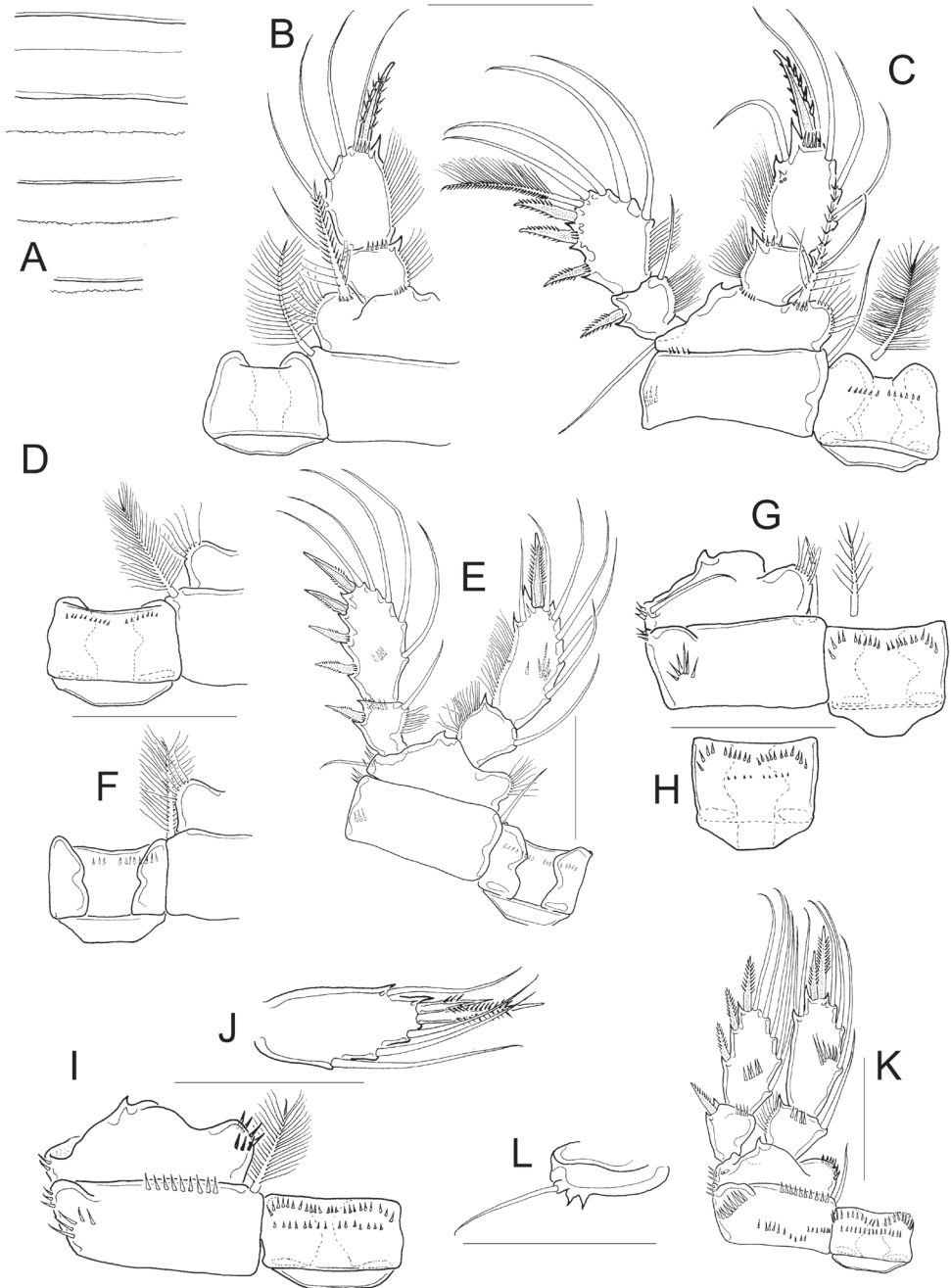


Figure 10. *Microcyclops ceibaensis* (Marsh, 1919). Adult female. **A** Prosomal fringes, dorsal **B** P1, frontal (USNM-222299) **C** P1, caudal (km 51-2) **D** P2 intercoxal sclerite, inner coxa and basis, caudal (USNM-222299) **E** P2, frontal (km 51-2) **F** P3 sclerite, inner coxa and basis, frontal (USNM-222298) **G** P3 intercoxal sclerite, coxa and basis, caudal (km 51-1) **H** P3 intercoxal sclerite, caudal (km 51-2) **I** P4 intercoxal sclerite, coxa and basis, caudal (USNM-222299) **J** Enp3P4 (USNM-222299) **K** P4, caudal (km 51-2) **L** P6. Scale bars: 50 μ m.

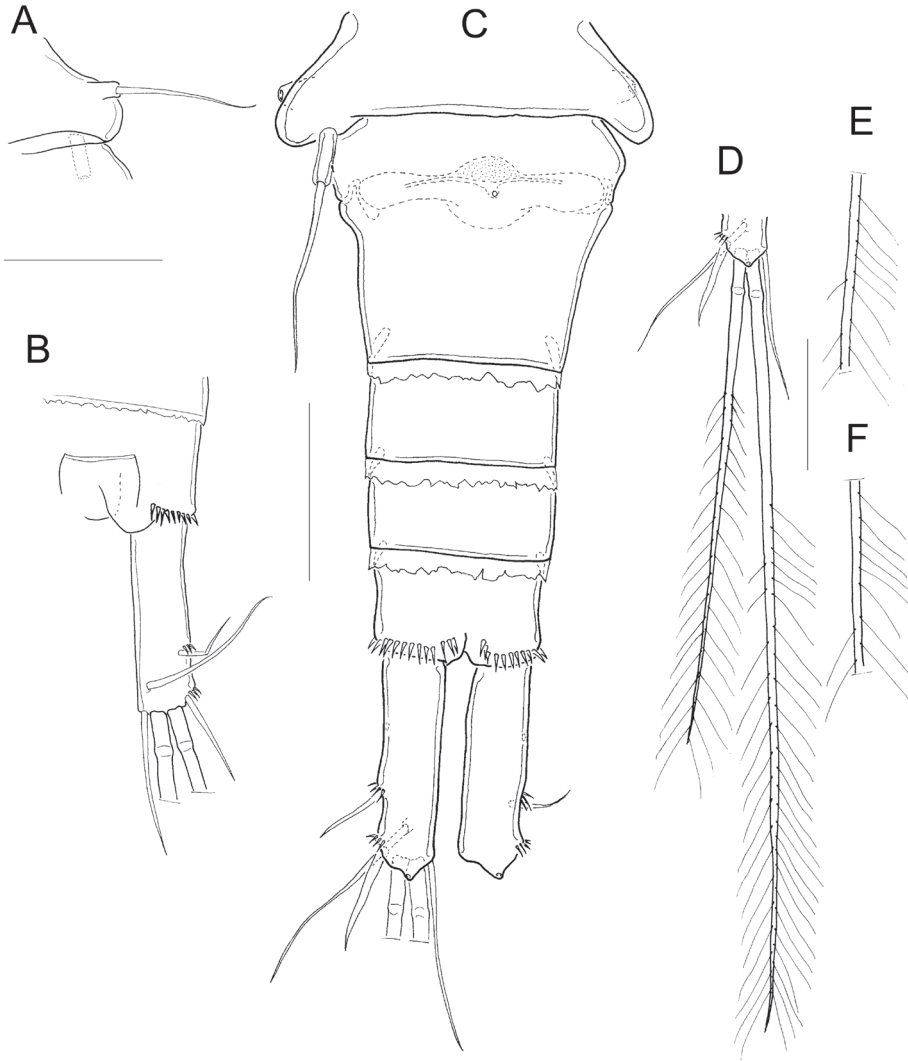


Figure 11. *Microcyclops ceibaensis* (Marsh, 1919). Adult female. **A** Fifth pediger, dorsal (USNM-222299) **B** Anal somite and caudal rami, dorsal (USNM-222299) **C** Urosome, ventral (km 51-1) **D** Caudal ramus and caudal setae, ventral (km 51-1) **E** Detail of inner median caudal seta (km 154) **F** Detail of inner median caudal seta (km 51-1). Scale bars: 50 μ m.

10B, C). Inner margin of P4 basis with strong spinules. Intercoxal sclerite rectangular, and ornamented with two rows of spinules (Fig. 10I, K). $\text{Enp}2\text{P}4$ 2.2 ± 0.1 times as long as wide; medial spine 1.5 ± 0.1 times as long as the lateral spine, and 0.6 ± 0.06 times as long as segment (Fig. 10J, K). Sixth leg with one long seta plus two short spines (Fig. 10L).

Fifth pediger nude (Fig. 11A). Urosomal somites with serrated hyaline fringes (Fig. 11B, C). Fifth leg with one cylindrical free segment 3.8 ± 1.4 times as long as wide;

tiny spinule present on inner margin. P5 free segment 0.3 ± 0.1 times the length of the distal seta (Fig. 11C). Distal margin of anal somite with a continuous row of strong spinules on ventral and dorsal surfaces (Fig. 11B, C). Caudal ramus 3.6 ± 0.4 times longer than wide, inner margin naked. Spinules present at base of caudal setae II and III; seta II inserted at $69 \pm 3.2\%$ of the caudal ramus (Fig. 11C).

Seta VII 0.7 ± 0.1 times as long as caudal ramus, *seta VI* 0.8 ± 0.1 times as long as caudal ramus. Relative lengths of terminal caudal seta from outermost caudal seta to innermost caudal seta: 1.0 : 5.7 : 9.5 : 1.8 (Fig. 11C, D). *Seta IV* and *seta V* with homonomous setulation, with long and fine setules at whole length (Fig. 11D); inner median terminal caudal seta (*V*) with interrupted row of setules along the proximal, lateral margin (Fig. 11E, F).

***Microcyclops echinatus* Fiers, Ghenne & Suárez-Morales, 2000**

Figures 12, 13

Description of female. This description is a complement to the original description of Fiers et al. (2000). Frontal surface of antennal basis with one basal, inner row of spinules arranged in an arc, and one longitudinal row of spinules near lateral margin (Fig. 12A). Antenna with three-segmented endopod bearing 1, 9, and 7 setae, respectively (Fig. 12B). Caudal surface of antennal basis with two rows of long spinules next to exopodal seta, one group of long spinules at basal position, one basal row on inner margin and another basal row on outer margin (Fig. 12B). Nine teeth on the distal margin of the labrum (Fig. 12C). Eight teeth present on gnathobase of mandible (Fig. 12D). Maxillular palp with three apical setae (one of these setae armed with long setules); lateral lobe with three setae, the longer seta armed; proximal seta nude (Fig. 12E). Maxillar basipodite with one claw-like projection bearing thin spines on concave margin and one long seta with one (Fig. 12F) or four tiny spinules (Fiers et al. 2000); maxilla with two-segmented Enp bearing 2 and 3 setae on first and second endopodal segments, respectively (Fig. 12F). Maxilliped with syncoxa (3 setae), basis (2 setae), and two-segmented Enp bearing 1 and 3 setae. Syncoxa and basis of maxilliped with rows of spinules on caudal surface (Fig. 12G).

Two pores on lateral margin of second endopodal segment of P1, very long spinules present at insertion of apical spine of Enp2P1. Long medial spine of P1 basis with heteronomous setulation (Fig. 13A). Inner margin of P1–P3 basis with long hair-like setae (Fig. 13A, B), inner margin of P4 basis with one row of tiny spinules and one row of long setules (Fig. 13C). Intercoxal sclerites of all swimming legs ornamented on caudal surface: P1 with one row of spinules and P2 to P4 with two rows of spinules (Fig. 13A–C). Enp2P4 2.5 ± 0.1 times as long as wide; medial spine is 2.0 ± 0.1 times as long as lateral spine, and 0.8 ± 0.1 times as long as the segment.

Fifth pediger with rows of spinules on ventro-lateral surfaces. Fifth leg with tiny spinule on inner margin (Fig. 13D); cylindrical free segment 3.7 ± 0.1 times longer than wide and 0.45 ± 0.01 times as long as distal seta of P5. Caudal ramus 5.9 ± 0.4

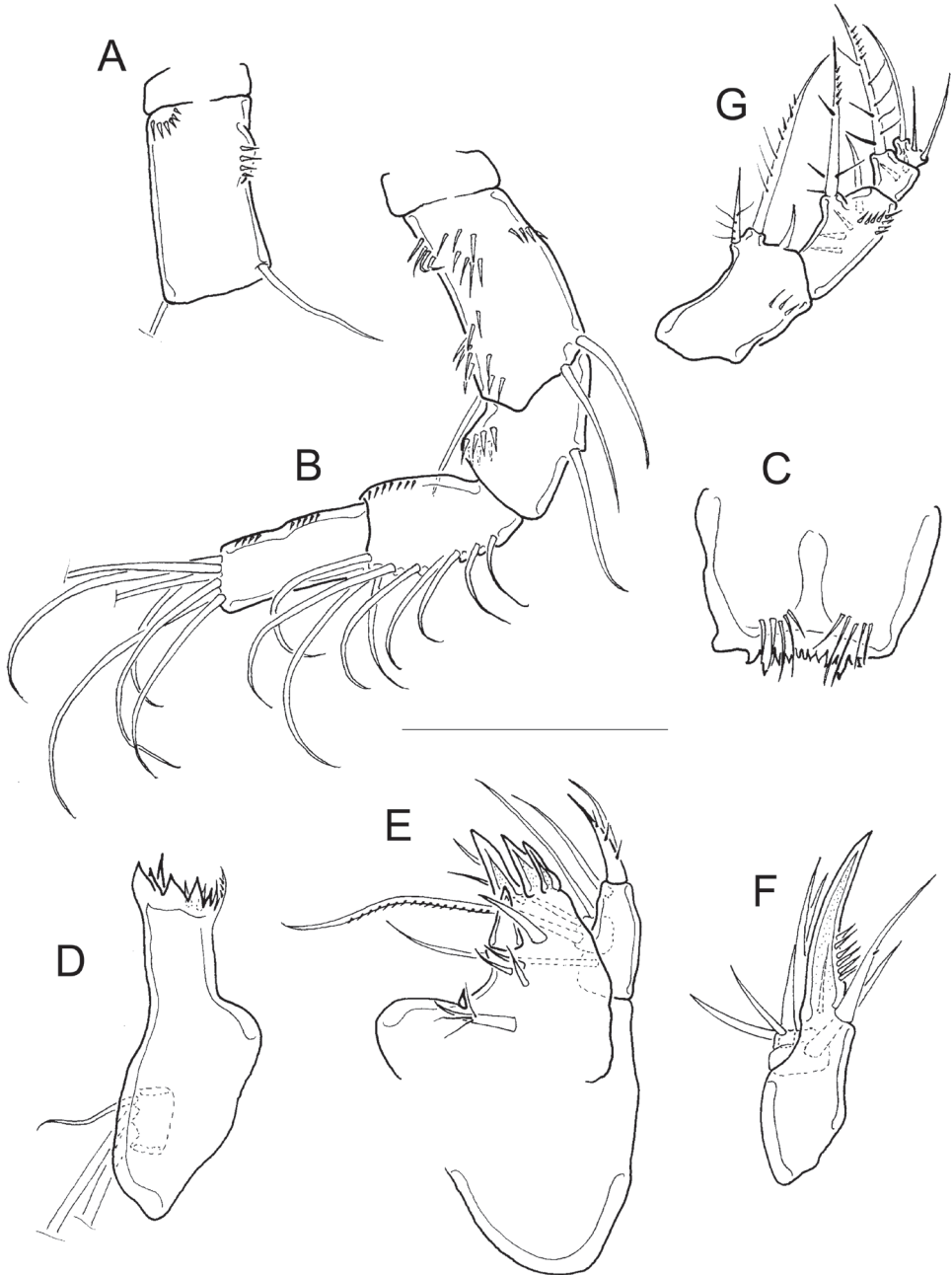


Figure 12. *Microcyclops echinatus* (Fiers et al., 2000). Adult female (km 51-2). **A** Antennal basipodite, frontal **B** Antenna, caudal **C** Labrum **D** Mandible **E** Maxillule **F** Maxilla **G** Maxilliped. Scale bar 50 μ m.

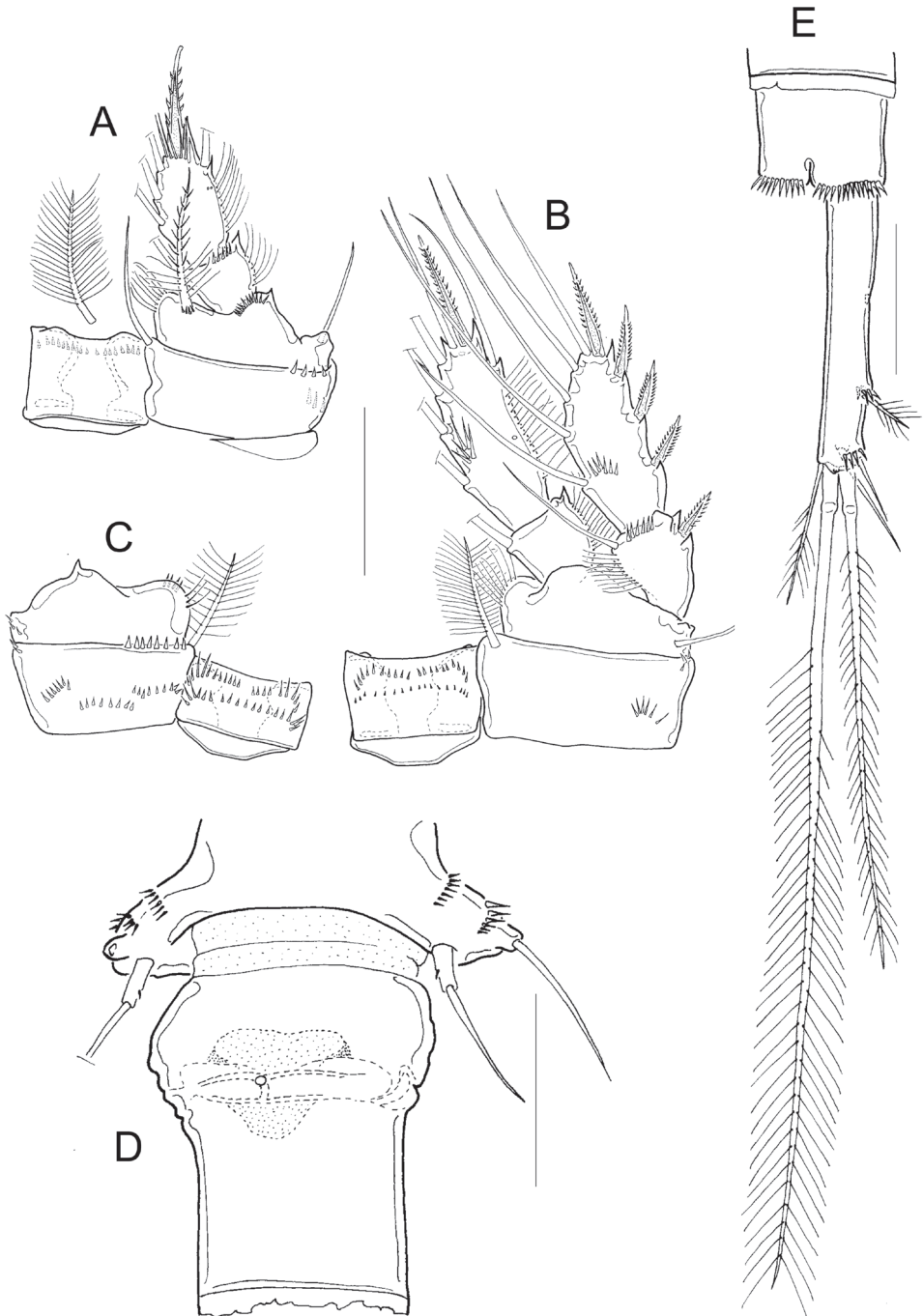


Figure 13. *Microcyclops echinatus* (Fiers et al., 2000). Adult female (Guanal). **A** P1, frontal **B** P3, caudal **C** P4 coxa, basis, sclerite, caudal **D** Fifth pediger, P5 and genital double-somite, ventral **E** Anal somite, caudal rami, and caudal setae, ventral. Scale bars: 50 μ m.

times longer than wide. Seta VII 0.5 ± 0.1 times as long as caudal ramus, seta VI 0.5 ± 0.05 times as long as caudal ramus. Relative lengths of terminal caudal seta from outermost to innermost caudal seta, 1.0 : 6.5 : 10.4 : 2.0. Seta IV and seta V with homonomous setulation, bearing long and fine setules (Fig. 13E).

***Microcyclops finitimus* Dussart, 1984**

Figure 14

Description of female. The following description is complementary to the original description of Dussart (1984). Antennule 12-segmented. Dorsal margin of prosomal somites 1 to 3 smooth (unfigured); hyaline fringe of fifth pediger serrated dorsally (Fig. 14A). Intercoxal sclerite of P1 smooth, inner margin of P1 basis with long hair-like setules, without spine on inner margin (Fig. 14B). Enp2P1 with one pore on lateral margin. Row of long spinules present at base of apical spine and lateral seta of Enp2P1 (Fig. 14C). Inner margin of P4 basis with long setules, intercoxal sclerite quadrangular, with one row of long spinules on caudal surface (Fig. 14D). Enp2P4 2.2 times as long as wide; medial spine 1.4 times as long as lateral spine, and 0.8 times as long as segment.

Anal somite with continuous row of spinules along distal margin (ventrally and dorsally), but on ventral surface medial spinules are longer and stronger than lateral spinules (Fig. 14E). No spinules at base of caudal seta II, but spinules present at base of caudal seta III; length to width ratio of caudal ramus 2.7. Relative lengths of terminal caudal setae from outermost to innermost seta, 1.0 : 6.1 : 8.9 : 2.1. Caudal setae IV, and V with homonomous setulation, bearing long and fine setules (Fig. 14E). Dorsal caudal seta (VII) 0.7 times as long as caudal rami, and innermost caudal seta (VI) 1.2 times longer than caudal rami. Lateral caudal seta (II) inserted at 75.5% of caudal ramus length.

***Microcyclops anceps anceps* (Richard, 1897)**

Figures 15–17

Description of female. Dorsal posterior margin of second prosomal somite with crenulated hyaline fringe (Fig. 15A, B), posterior margin of fourth prosomal somite wrinkled (Fig. 15B). Caudal surface of antennal basis with three oblique rows of tiny spinules near inner margin and two basal (proximal) rows of long spinules near outer margin (Fig. 15C, D, F). Antenna with three-segmented endopod bearing 1, 9, and 7 setae, respectively. Frontal surface of antennal basis with three rows of spinules: one proximal oblique, one near lateral (outer) margin in middle of segment, and one next to exopod seta (Fig. 15E). Mandible with nine teeth on gnathobase (Fig. 15G). Maxillular palp with two armed and one naked setae apically; one armed seta plus two nude setae on lateral lobe, proximal seta with tiny spinules (Fig. 15H). Distal coxal endite of maxilla with two long setae: proximal seta with two long, basal setules and bifurcated

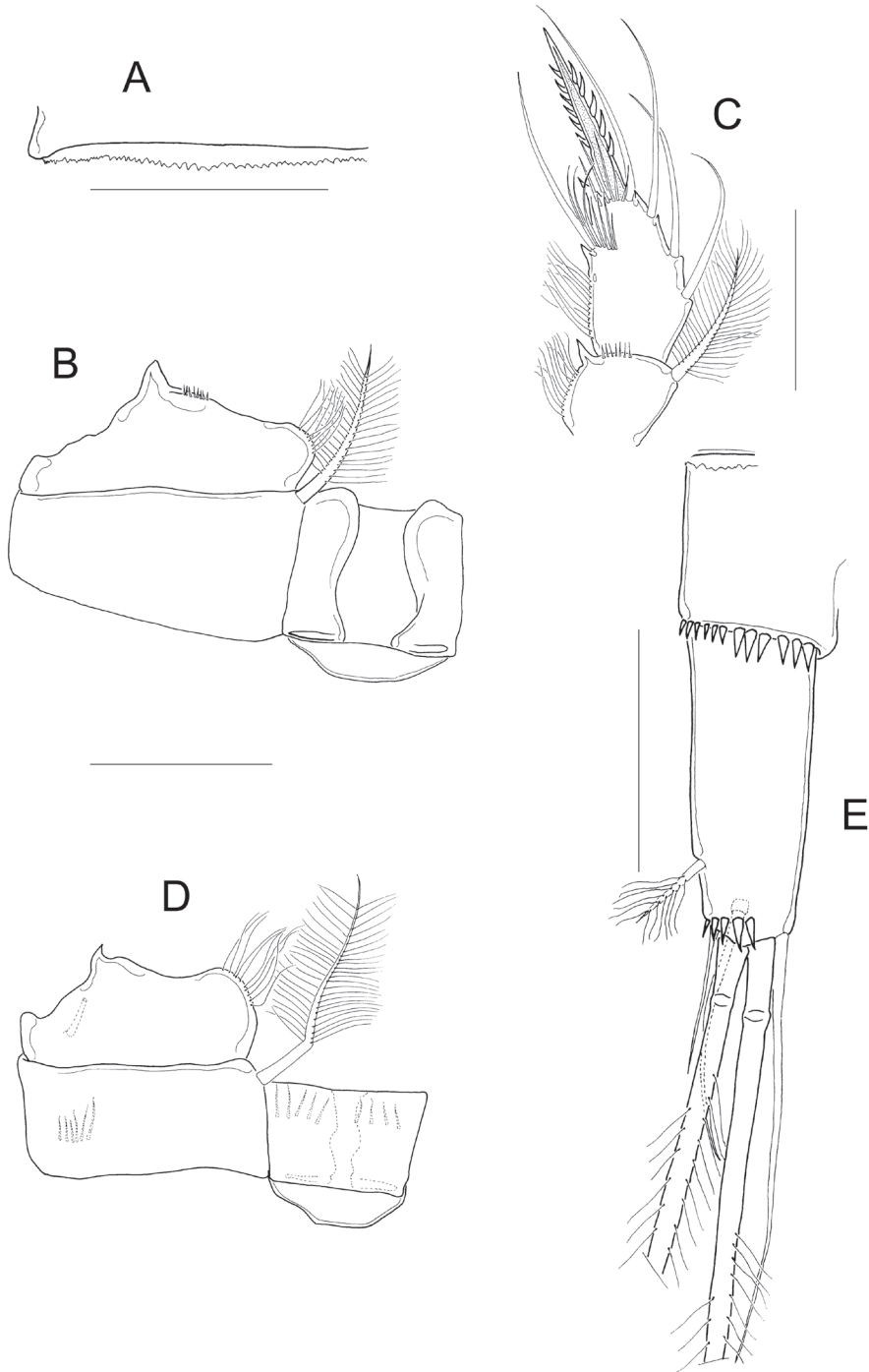


Figure 14. *Microcyclops finitimus* Dussart, 1984. Adult female (MNHN-Cp7294). **A** Fifth pediger and hyaline fringe, dorsal **B** P1, coxa, basis and sclerite, frontal **C** P1, Enp, frontal **D** P4, coxa, basis and intercoxal sclerite, frontal **E** Anal somite, caudal rami, and caudal setae, ventral. Scale bars: 50 μ m.

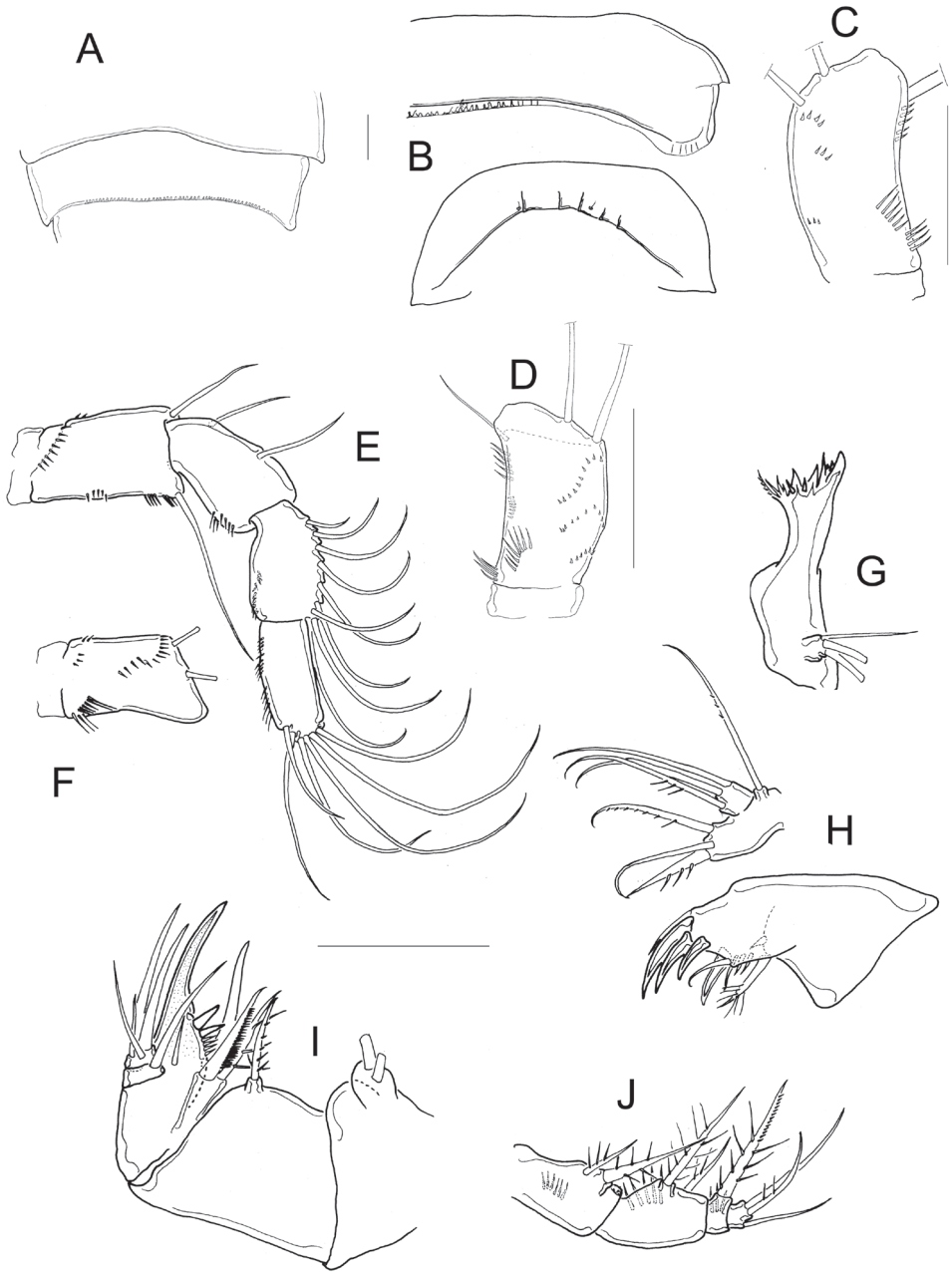


Figure 15. *Microcyclops anceps anceps* (Richard, 1897). Adult female. **A** Second prosomal somite, dorsal (SMNK-2832) **B** Second and fourth prosomal somites, dorsal (Matillas) **C** Antennal basipodite, caudal (MNHN-Cp6876) **D** Antennal basipodite, caudal (MNHN-Cp7296) **E** Antenna, frontal (Matillas) **F** Antennal basipodite, caudal (Matillas) **G** Mandible (Matillas) **H** Maxillule (Matillas) **I** Maxilla (Matillas) **J** Maxilliped (Matillas). Scale bars: 50 μ m.

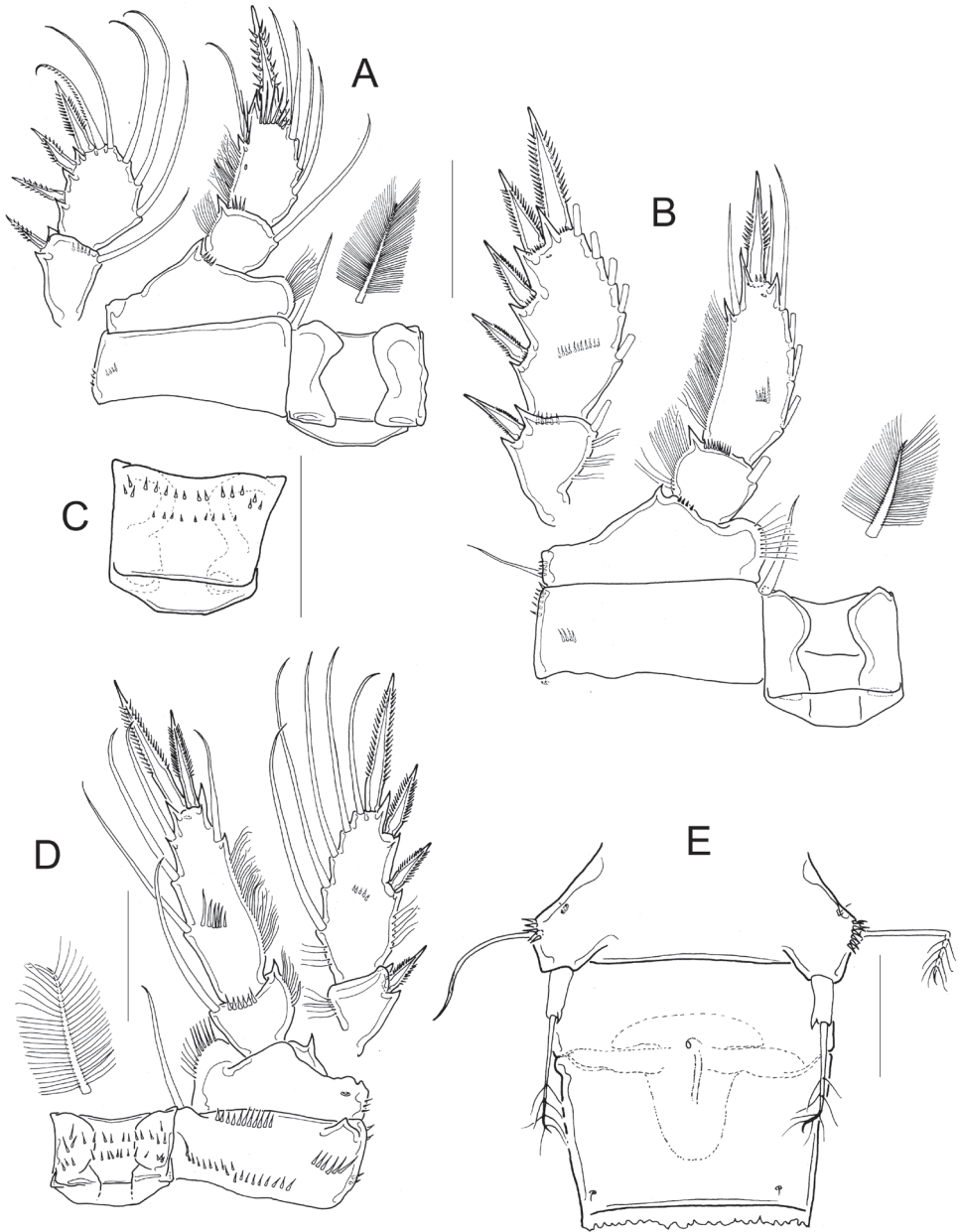


Figure 16. *Microcyclops anceps anceps* (Richard, 1897). Adult female. **A** P1, frontal (Pajonal) **B** P2, frontal (Pajonal) **C** P3 intercoxal sclerite, caudal (Pajonal) **D** P4, caudal (Pajonal) **E** Fifth pediger, genital double-somite (Matillas). Scale bars: 50 μm .

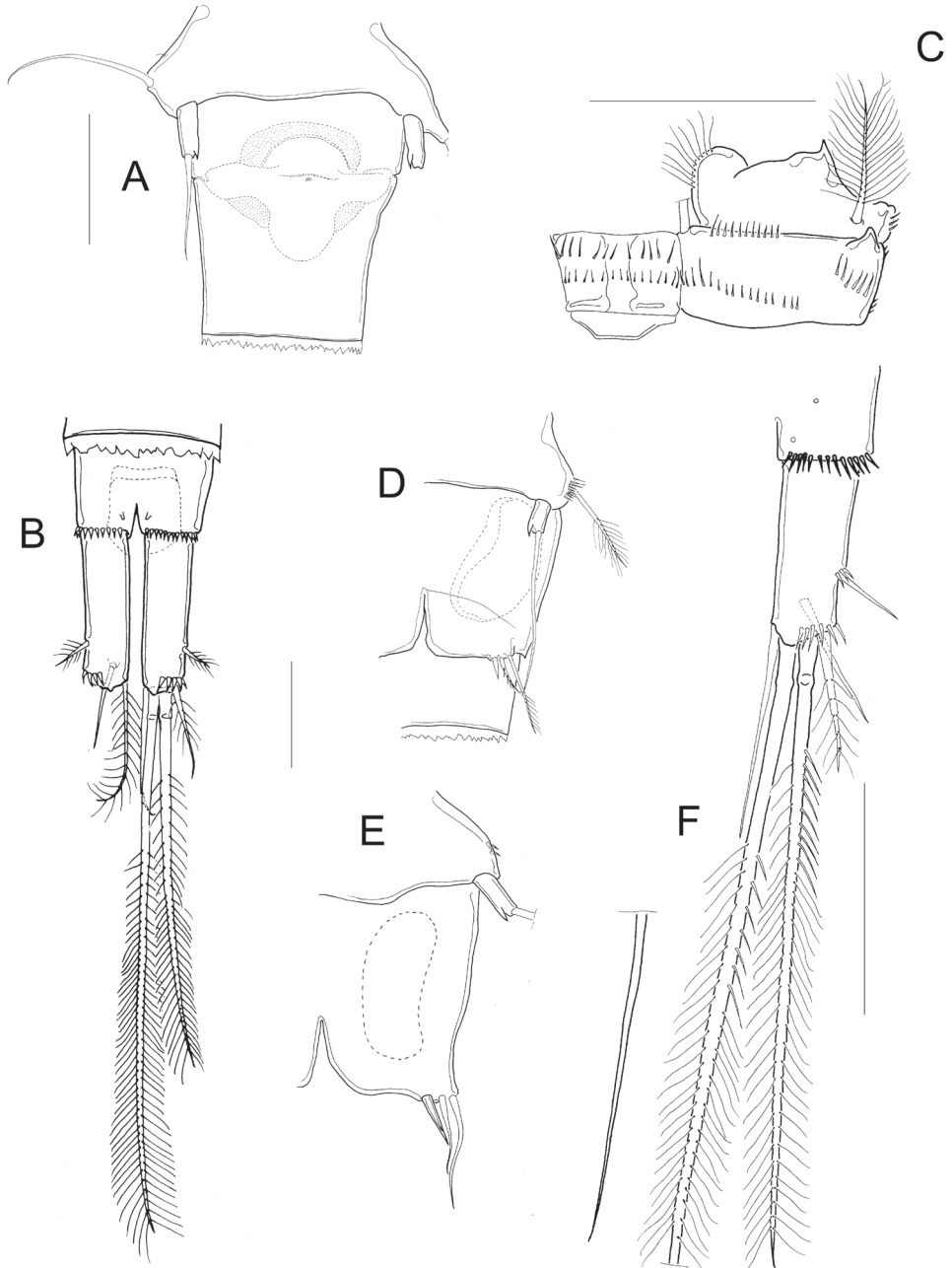


Figure 17. *Microcyclops anceps anceps* (Richard, 1897). Adult female. **A** Fifth pediger, genital double-somite (SMNK-2833) **B** Anal somite, caudal rami and caudal setae (Matillas), ventral. *Microcyclops anceps anceps*. Adult male. **C** P4 coxa, basis, and intercoxal sclerite, caudal (MNHN-Cp6877) **D** Fifth pediger and genital somite (MNHN-Cp6877) **E** Fifth pediger and genital somite (MNHN-Cp7295) **F** Anal somite, caudal rami and caudal setae (MNHN-Cp6876). Scale bars: 50 µm.

apically; distal seta armed with a continuous row of tiny spinules along one (inner) margin (Fig. 15I). Basipodite with claw-like projection bearing two stout teeth followed by a row of tiny spinules, and one long smooth seta on its base; two-segmented Enp bearing 2 and 3 setae, respectively (Fig. 15I). Maxilliped with a row of spinules in syncoxa, Bsp, and Enp1, on frontal view (Fig. 15J).

Inner margin of *basipodite* with long and fine hairs in P1–P3 (Fig. 16A, B). One pore present on lateral margin of Enp2P1. Spine absent on inner margin of BspP1 (Fig. 16A). Inner margin of BspP4 with long. Inner margin of BspP4 with long spinules (Fig. 16D). Intercoxal sclerites naked in P1 and P2 (Fig. 16A, B). Usually one distal row or sometimes two rows of spinules present on intercoxal sclerite of P3 (Fig. 16C). P4 sclerite with two rows of spinules (Fig. 16D): spinules in distal row larger and stronger than those in proximal row (Fig. 16D). Medial apical spine of Enp2P4 1.3 ± 0.1 times as long as lateral apical spine, and 0.7 ± 0.03 times as long as segment; length to width ratio of segment 2.5 ± 0.1 .

Strong spinules present (Figs 16E, 17D) or absent (Fig. 17A) on *fifth pediger* near base of lateral seta of P5. This character shows both inter- and intrapopulation variation; in one population, the females do not have spinules next to lateral seta (MNHN-Cp7296, unfigured here), while the males of the same population do (Fig. 17E).

Free segment of *fifth leg* 2.5 ± 0.2 times longer than wide, with relatively large spinule in distal position (Figs 16E, 17A); free segment 0.4 ± 0.08 times as long as apical seta. Distal margin of anal somite with continuous row of strong spinules on ventral and dorsal surfaces (Figs 17B, F). Caudal ramus 3.7 ± 0.3 times longer than wide, inner margin naked. Spinules present at base of caudal seta III. Caudal seta II inserted at $71.1 \pm 1.15\%$ of caudal ramus length (Fig. 17B).

Seta VII and VI 0.5 ± 0.1 and 0.8 ± 0.1 times as long as caudal ramus, respectively. Relative lengths of terminal caudal seta from outermost to innermost, 1.0 : 4.9 : 7.1 : 1.3 (Fig. 17B). Caudal setae IV and V with homonomous setulation, with hair-like setules only (Fig. 17B).

Discussion

Microcyclops anceps anceps showed the least variation in the qualitative and morphometric characters even though specimens were examined from a wide latitudinal range (Venezuela, Mexico, Guyana, Brazil, Guatemala, and Uruguay).

Microcyclops echinatus (from southeastern Mexico) and *M. ceibaensis* (from Honduras and southeastern Mexico) appeared morphologically similar. Similarities between these species are in: the length and width ratio of Enp2P4; the P4 sclerite with two rows of spines; the length ratio of the terminal caudal setae III and IV; the presence of spines at the insertion of setae II, and III; and the heteronomous ornamentation of the spine on the inner margin of Bsp P1. But the features that separate the specimens of these species were the insertion of the caudal seta II (69.5% in *M. ceibaensis* vs. 73.2% in *M. echinatus*); the length and width ratio of the caudal ramus is 3.6 in *M. ceibaensis*

while 5.9 in *M. echinatus*; the presence of spines on the fifth pediger in *M. echinatus* vs. absence of these spines in *M. ceibaensis*; and the ornamentation of the inner basis of P4 with spine-like setae in *M. ceibaensis* vs. short setae plus hair-like setae in *M. echinatus*.

In 1935, Kiefer described two new species *Cyclops (Microcyclops) diversus* and *Cyclops (Microcyclops) alius* from Uruguay. The microscopic observations performed here, support the opinion of Reid (1986) on the synonymy of *M. ceibaensis* and *M. diversus*. The specimens labelled as *M. diversus* sp. n. share all the morphometric features of the type series of *M. ceibaensis*. Additionally, the structure of P1, P3, P4, and P5; the armament of the caudal surface of the antenna, the number of setae on each endopodal segment of the antenna, and the entire morphology of the urosome, and the caudal ramus in *M. diversus* are indistinguishable from the states found in *M. ceibaensis*.

The type specimens labelled as *M. dubitabilis* (from Trou Caiman, Haiti) and *Microcyclops alius* (from Barra Sta. Luzia, Uruguay) were morphologically similar to: 1) specimens identified as *M. rubellus* [including the specimen analysed by Reid (1992)], 2) some specimens from Southeastern Mexico, 3) *M. alius* from Brazil described by Rocha (1998), and 4) another specimen labelled as *M. dubitabilis* from Guadeloupe. The micro-structural analysis showed that the following features are common in all of the above mentioned specimens: the number of setae on the endopodal segments of the antenna and the number of rows of spines on the caudal surface of antennal basis; the ornamentation of the setae of the maxillular palp; the shape of the maxilla, and in particular, the structure of the distal coxal endite, the basipodite, and the seta on the claw-like projection; the shape and length of the spine on the inner margin of P1 basis; the shape and ornamentation of the intercoxal sclerites and the inner basis of P1, and P4; the meristic characters of P4, all traits of the caudal rami setae; the structure of P5, the anal somite, and the caudal rami. Therefore, *M. alius* is considered here as a junior synonym of *M. dubitabilis*, as it was suggested by Rocha (1998). Also, several specimens recorded under the name *M. rubellus* in the Americas likely refer to *M. dubitabilis*.

Microcyclops dubitabilis clearly differs from *M. varicans* s. str. at least in the next features: the spines at the insertion of caudal seta III are present in *M. dubitabilis*, but absent in *M. varicans*; caudal ramus is 3.5–4 times as long as wide in *M. varicans* and shorter in *M. dubitabilis*. Medial spine of Enp2P4 is around 0.8 times as long as the segment in *M. dubitabilis*, whereas that in *M. varicans* is shorter (around 0.5); and the seta inserted at base of claw-like projection in the maxilla is armed only with strong teeth at its base in *M. varicans*, but this armament is more complex in *M. dubitabilis*. Therefore *M. dubitabilis* is not a synonym of *M. varicans*.

Microcyclops rubellus and *M. varicans* have been recorded in several regions of the world and were thought to be likely cosmopolitan (Reid 1992) and highly variable in morphology. This is especially the case for *M. varicans* (Franke 1989, Alekseev 2002). The type material of *M. rubellus* and *M. varicans* is probably lost and both species were originally described from North Europe (Sars 1863, Lilljeborg 1901). Our review of the descriptions and drawings of *M. rubellus* from some European localities however revealed differences between the European and American specimens here examined

in the medial surface ornamentation of the basis of the fourth swimming leg, in the length proportion of the medial apical spine and the Enp2P4, and the ornamentation of the distal margin of the anal somite (see Einsle 1993). Hence, *M. rubellus* s. str. probably is not distributed in America.

Remarks about the new species

The specimens from southeastern Mexico assigned to the new species *M. inarmatus* were morphologically similar to that from Laguna Rincon, Haiti identified as *M. dubitabilis* (SMNK-2391, 2392) and to the specimen examined by Reid (1992) and classified as *M. varicans*. The shared morphology of the antenna, maxilla, P1 to P5, and urosome is obvious in all of these specimens (figured and described in the descriptive section before).

Microcyclops inarmatus sp. n. can be distinguished from *M. varicans* by the following characters (see also Rylov 1948, Einsle 1993): *M. varicans* has a more elongated caudal rami (3.5-4 times as long as wide), the basipodite of P4 bears short spinules on inner margin, there are more setae on the second endopodite of A2, on the distal margin of anal somite the spinules are present ventral, lateral and dorsally; and the medial spine of the second endopod of fourth leg has around the half length of the segment. All these features clearly differ to *M. inarmatus* sp. n.

The analysis that included specimens from a wide latitudinal range showed a highly conserved morphology primarily in the inner region of each swimming leg and oral appendages. Thus, we may speculate that some reports of *M. varicans* and *M. rubellus* recorded in the Americas are in fact *M. inarmatus* sp. n. and *M. dubitabilis*, respectively.

Microcyclops inarmatus sp. n. has some similarities also to *M. dubitabilis*, but the following features differentiate these two species: setal formula of the antennal endopod (1, 9, 7 in *M. dubitabilis* vs. 1, 6, 7 in *inarmatus*); the ornamentation on the caudal surface of the antennal basis is less complex in *M. inarmatus* than in *M. dubitabilis*; setae on maxillular palp are more armed in *M. inarmatus* than in *M. dubitabilis*; and the basal seta inserted at base of claw-like projection in the maxilla is more simple in *M. inarmatus*, whereas *M. dubitabilis* has two opposite rows of different spines.

The inner margin of the basis of the first swimming leg has a long spine with heteronomous ornamentation in *M. inarmatus*, in comparison to the short, homonomously setulated spine on this site in *M. dubitabilis*. In addition, the inner margin of the basis of the fourth swimming leg bears long hair-like setae and the fourth sclerite is almost as long as wide in *M. inarmatus*, whereas in *M. dubitabilis*, this inner margin bears short setae and the fourth sclerite is wider than long. The free segment of the fifth leg has a tiny spine on the medial margin in *M. inarmatus* (not described in Reid (1992), but clearly observed in the slide USNM-251321), and this spine is absent in *M. dubitabilis*. Finally, the lateral caudal seta is located near the middle of the caudal ramus in *M. inarmatus*, whereas in *M. dubitabilis*, this seta is located in the distal third. In all of the material analysed, no spines were observed at insertion of outermost terminal

caudal seta in *M. inarmatus*, whereas in *M. dubitabilis*, these spines were observed in every specimen.

Other species of *Microcyclops* which has 12-segmented antenna, caudal rami with innermost terminal caudal setae longer than outermost terminal caudal setae, spines present only ventrally on the distal margin of the anal somite, caudal rami short (no more than 3 times as long as wide), one spine on inner basis of P1, and the intercoxal sclerite of P4 quadrangular and naked, are *M. davidi* (Chappuis, 1922) and *M. richardi* (Lindberg, 1942). *Microcyclops inarmatus* sp. n. differs from these species in the surface ornamentation of P4 basipodite: long hair-like setules vs. short spine-like setules in *M. davidi* (*sensu* Mirabdullayev et al. 2002) and *M. richardi* (see Lindberg 1942). The genital double-somite in *M. inarmatus* is short around 0.8 times as long as wide – similar in *M. davidi* –, but it is elongated in *M. richardi*, around 1.4 times longer than wide; and the second endopodite of A2 bears 9 setae in *M. davidi*, but only 6 setae in *M. inarmatus*.

Additionally, in *M. richardi* the free segment of P5 has no spine on medial margin, and the medial spine of Enp2P4 is short (0.6 times the length of the segment) in comparison with the new species. Finally, the seta on the base of the claw-like projection of the maxillar basipodite, is armed with tiny spinules in *M. inarmatus*, whereas in *M. davidi* it bears strong teeth on its base.

Remarks on *M. anceps pauxensis* Herbst, 1962 and *M. anceps* var. *minor* Dussart, 1984

Microcyclops anceps pauxensis and *M. anceps* var. *minor*, described from the Amazonian region and Venezuela respectively, are similar in the number of segments of A1 (12-segmented); the length ratio of Enp2P4 (2.35 vs. 2.46); the intercoxal sclerite of P4 with two rows of spines; the length ratio of the lateral and medial apical spines of Enp2P4 (0.64 vs. 0.51); the length ratio of the medial apical spine of En2P4 and the segment (0.7 in both species), the insertion of the caudal seta II (lateral) is at 68% of the caudal rami length in *M. a. pauxensis*, and 70% in *M. a. minor*, and the continuous row of spines along the ventral and dorsal margins of the anal somite.

However, according to Herbst (1962) and Dussart (1984), the inner basis of P1 is naked in *M. a. pauxensis*, and hairy in *M. a. minor*; the inner basis of P4 bears small setules in *M. a. pauxensis* but this is naked in *M. a. minor*. The ratio between the lengths of the caudal setae VI and III is lower in *M. a. pauxensis* than in *M. a. minor* (1.81 vs. 2.52); the ratio between the lengths of caudal seta VI and caudal rami is higher in *M. a. pauxensis* (1.44) than in *M. a. minor* (1.07); the length ratio between the free segment of P5 and distal seta of P5 is 0.18 in *M. a. pauxensis*, and 0.34 in *M. a. minor*. Other differences between both species were observed in the length ratio between the dorsal caudal seta and caudal ramus (1.5 in *M. a. pauxensis* vs. 0.57 in *M. a. minor*), and the spines on the base of the outer caudal seta (spinules present in

M. a. pauxensis vs. absent in *M. a. minor*). All of these differences suggest that *M. a. minor* is distinct from *M. a. pauxensis*.

Therefore, these taxa may constitute different species. The evaluation of mouthparts and the ornamentation of the inner region of each swimming leg in the type material may facilitate species delimitation. Unfortunately, the type material of both “subspecies” was not available to us.

Conservative characters among species

Based upon morphological and morphometric features, eleven species and two subspecies of *Microcyclops* recorded in America were recognized. The following set of characters distinguishes between species: the ornamentation of the caudal surface of the antennal basis; the ornamentation of the setae of the maxillular palp; the shape and armature of the distal coxal endite of maxilla; and the basal seta in front of the claw-like projection of the maxillar basis. Previously, similar structures have been useful for differentiating other Cyclopinae species, such as *Mesocyclops* (Van de Velde 1984a, 1984b, Hołyńska 2000).

Among the specimens examined, the organization of the spine pattern on the antennal basipodite is similar to that proposed by Van de Velde (1984b) for *Mesocyclops* which is more complex on the caudal side than on the frontal side. Additionally, the caudal surface ornamentation of the antennal basis in *Microcyclops* here examined is similar to that in most New World *Mesocyclops*: the simple ornamentation pattern found in Neotropical *Mesocyclops* was considered by Hołyńska (2000) and Wyngaard et al. (2010) as an ancestral state. The pattern observed in *Microcyclops* is much less complex in comparison to those reported for some eucyclopinae species from the genus *Macrocyclops* (Karanovic and Krajicek 2012), *Paracyclops* (Karaytug 1999) and *Eucyclops* (Alekseev et al. 2006, Mercado-Salas et al. 2015).

The micro-structures of the swimming legs as diagnostic characters have been explored in *Mesocyclops*. In *Mesocyclops*, the coxal and basis armament of the first and fourth trunk limbs are important (Van de Velde 1984a, 1984b). In *Eucyclops*, the coxal seta of P4 or the intercoxal sclerites of all trunk limbs are informative (Alekseev et al. 2006). Our results show that features such as the medial surface ornamentation of basis of all four legs, the shape and ornamentation of the sclerites of P1 to P4, the presence/absence or length and armature of the spine on the inner basis of P1, and the shape or armature of the free segment of P5 were useful for differentiating between species.

Important diagnostic morphometric features for *Microcyclops* were the relative position of the lateral seta on the caudal ramus; the relative length of the outermost terminal caudal seta (III) and the outer median terminal caudal seta (IV); the relative length of caudal seta III and the inner median terminal caudal seta (V); and the length: width ratio of caudal ramus. Traditionally, the length ratio of the second endopod and its apical spines of the fourth trunk limb have been used as features to separate species of

Microcyclops; however, as in another genus such as *Eucyclops* or *Mesocyclops*, the surface micro-structures together with the integumental armature and the meristic characters of the caudal rami are more informative.

This study is the first attempt to clarify the taxonomy of the species of *Microcyclops* recorded in America using detailed morphological analysis.

Conclusion

The microscopic analysis of oral and thoracic appendages facilitated better delineation of *Microcyclops* species recorded in America. The characters that better distinguish between species are the ornamentation of antennal basipodite, the armature of the coxal endite and basipodite of the maxilla, the surface ornamentation of the inner basis of P1, the structure of intercoxal sclerites of the trunk limbs, the length: width ratio of caudal ramus, the length proportion of the caudal setae, and the relative position of the lateral seta on the caudal ramus.

The analysis performed here show that *M. alius* is a junior synonym of *M. dubitabilis*, and support the opinion about the synonymy of *M. ceibaensis* and *M. diversus*.

Microcyclops inarmatus sp. n. can be distinguished from other known species of the genus by the unique combination of several characters such as: morphometric characters of the second endopodite of fourth trunk limb and caudal ramus, presence of 6 setae on the second endopodal segment of antenna, antennal basipodite with just one group of spinules on caudal surface, lack of ornaments on the intercoxal sclerites of all swimming appendages, absence of spinules at base of lateral caudal and outermost terminal caudal setae, and basipodites of first to fourth swimming legs with long hair-like setules on inner margin.

Key to the American species of *Microcyclops* (females)

The key is mainly based on the analysis performed in the descriptive section of this manuscript. Original descriptions were consulted in those species in which no microscopic observations could be made [*Microcyclops anceps pauxensis* (Herbst 1962); *M. anceps* var. *minor* (Dussart 1984); *M. mediasetosus* (Dussart and Frutos 1985); *M. pumilis* (Pennak and Ward 1985); and *M. medius* (Dussart and Frutos 1986)].

- | | | |
|---|---------------------------------------------------------------------------------------------------------------------------------------------------------|----------------------------|
| 1 | Cylindrical free segment of P5 smooth, without inner spine (Fig. 7I–K) | 2 |
| — | Cylindrical free segment of P5 with inner spine (Figs 4G, H; 16E)..... | 5 |
| 2 | Base of the outermost caudal seta (III) with a row of spines (Fig. 8A–C) | 3 |
| — | Base of the outermost caudal seta (III) without a row of spines..... | 4 |
| 3 | Length (L): width (W) ratio of caudal ramus is 4.35; lateral caudal seta inserted at 69% of the total caudal ramus length; inner basis of P4 naked..... | |
| | | <i>Microcyclops medius</i> |

- L: W ratio of caudal ramus is 2.48 ± 0.2 ; lateral caudal seta inserted at 71 ± 5.7 % of the total caudal ramus length (Fig. 8A–C); inner basis of P4 with short hair-like setae (Fig. 7E–H).....*M. dubitabilis*
- 4 L: W ratio of caudal ramus is 5 ± 1 ; lateral caudal seta inserted at 80 % of the total caudal ramus length..... *M. furcatus*
- L: W ratio of caudal ramus is 2.3 ± 0.6 ; lateral caudal seta inserted at 55 % of the total caudal ramus length..... *M. pumilis*
- 5 Inner spine of the cylindrical free segment of P5 tiny, articulated, inserted medially, and does not reach the distal margin of the segment (Figs 4H, 11C, 13D)..... **6**
- Inner spine of the cylindrical free segment of P5 strong, unarticulated; inserted terminally, projected beyond the distal margin of the segment (Figs 16E, 17A)..... **11**
- 6 Length ratio of the innermost (VI): outermost (III) caudal setae is 3.0; L: W ratio of caudal ramus is 2.3; lateral caudal seta inserted at 57 % of the total caudal ramus length.....*M. mediasetosus*
- Length ratio of the innermost (VI): outermost (III) caudal setae is 1.6 to 2.0; L: W ratio of caudal ramus is 2.7 to 6.0; lateral caudal seta inserted at 60 to 75 % of the total caudal ramus length.....7
- 7 Inner basis of P1 with hair-like setae, medial spine absent (Fig. 14B); inner basis of P4 hairy (Fig. 14D); intercoxal sclerite of P1 nude; intercoxal sclerite of P4 armed.....*M. finitimus*
- P1 basis with medial spine (Figs 4A, B; 10B, C; 13A); inner basis of P4 hairy (Fig. 4F), or with strong spine-like setae (Figs 10I, K), or with a combination of both (Fig. 13C); intercoxal sclerite of P1 nude (Fig. 4A, B) or armed (Fig. 13A); intercoxal sclerite of P4 nude (Fig. 2D) or armed (Fig. 10K) **8**
- 8 Inner basis of P1 naked, medial spine reaching the proximal half of Enp2P1 and with homonomous ornamentation; L: W ratio of caudal ramus is 5 to 6, with a row of spines at the base of the lateral caudal seta (II) that extends dorsally; and no spines at the base of the outermost caudal seta (III).....
..... *M. elongatus*
- Inner basis of P1 hairy, medial spine reaching the distal half of Enp2P1 and with heteronomous ornamentation (Figs 2C; 4A, B; 13A); L: W ratio of caudal ramus is 2.5 to 6, with or without spines at the base of both the lateral (II) and the outermost caudal seta (III) **9**
- 9 Anal somite with a row of spines on ventral margin; no spines at the bases of the caudal setae II and III (Figs 5A, C–E); intercoxal sclerites of P1 to P4 unarmed (Fig. 4A–D); basipodite of P4 with long hair-like setae on inner margin (Fig. 2D); one group of spines on caudal view of antennal basis (Fig. 3B); L: W ratio of caudal ramus 2.5 ± 0.4*M. inarmatus* sp. n.
- Anal somite with a row of spines along both ventral and dorsal margins; with spines at the bases of the caudal setae II and III (Fig. 11C); intercoxal sclerites of P1 to P4 armed (Fig. 10C–H, K); basipodite of P4 with strong spine-like

- setae (Figs 10I, K), or with a combination of hair-like setae and spinules (Fig. 13C); more than one group of spines on caudal view of antennal basis (Figs 9F; 12B); L: W ratio of caudal ramus between 3.2 to 6.3..... **10**
- 10 Fifth pediger with spines on ventral and lateral surfaces (Fig. 13D); caudal ramus is 5.9 ± 0.4 times longer than wide (Fig. 13E); inner basis of P4 with heteronomous ornamentation: short spine-like plus long hair-like setae (Fig. 13C); caudal surface of antennal basis with two rows of long spines next to exopodal seta (Fig. 12B) ***M. echinatus***
- Fifth pediger nude ventrally and laterally; caudal ramus is 3.6 ± 0.4 times longer than wide (Fig. 11C); inner basis of P4 with homonomous ornamentation: strong spine-like setae (Figs 10I, K); caudal surface of antennal basis without spines next to exopodal seta (Fig. 9F) ***M. ceibaensis***
- 11 No spines on the base of the caudal setae II and III; inner basis of P4 naked, unarmed ***M. anceps var. minor***
- Spines on the base of caudal seta III, no spines on the base of the caudal seta II (Fig. 17B); inner basis of P4 ornamented (Fig. 16D) **12**
- 12 W ratio of caudal ramus is 3.7 ± 0.3 (Fig. 17B); inner basis of P1 hairy (Fig. 16A); inner basis of P4 with long spine-like setae (Fig. 16D) ***M. anceps anceps***
- L: W ratio of caudal ramus is 2.4; inner basis of P1 naked; inner basis of P4 with short hair-like setae ***M. anceps pauxensis***

Acknowledgements

Danielle Defaye and Paula Rodríguez Moreno-Martin Lefèvre, Muséum National d'Histoire Naturelle, Paris; Hubert Höfer and Hans Walter Mittmann, Staatliches Museum für Naturkunde, Karlsruhe; Chad Walter, Smithsonian Institution National Museum of Natural History, kindly allowed us to review MNHN, SMNK, and NMNH specimens, respectively. The authors received grants from the National Council of Science and Technology (CONACYT) through the Mexican Barcode of Life (MEXBOL). We are grateful to Danielle Defaye, Maria Hołyńska, and Iskandar M. Mirabdullayev who made valuable comments and suggestions to improve the manuscript. We are grateful with the academic edition of two native English-spoken reviewers.

References

- Alekseev VR (2002) Copepoda. In: Fernando CH (Ed.) A Guide to Tropical Freshwater Zooplankton. Backhuys Publishers, Leiden, 123–187.
- Alekseev V, Dumont HJ, Pensaert J, Baribwegure D, Vanfleteren JR (2006) A redescription of *Eucyclops serrulatus* (Fischer, 1851) (Crustacea: Copepoda: Cyclopoida) and some related taxa, with a phylogeny of the *E. serrulatus*-group. Zoologica Scripta 35(2): 123–147. doi: 10.1111/j.1463-6409.2006.00223.x

- Dussart BH (1984) Some Crustacea Copepoda from Venezuela. *Hydrobiologia* 113(1): 25–67. doi: 10.1007/BF00026592
- Dussart BH, Frutos S-M (1985) Sur quelques Copépodes d'Argentine. *Revue d'hydrobiologie Tropicale* 18(4): 305–314.
- Dussart BH, Frutos S-M (1986) Sur quelques Copépodes d'Argentine. 2. Copépodes du Paraná Medio. *Revue d'hydrobiologie Tropicale* 19(3-4): 241–262.
- Einsle U (1993) Crustacea: Copepoda: Calanoida und Cyclopoida. Süßwasserfauna von Mitteleuropa: 8/4-1. Gustav Fischer Verlag, Stuttgart, 209 pp.
- Elías-Gutiérrez M, Suárez-Morales E, Gutiérrez-Aguirre MA, Silva-Briano M, Granados-Ramírez JG, Garfías-Espejo T (2008) Cladocera y Copepoda de las aguas continentales de México, guía ilustrada. Universidad Nacional Autónoma de México FES Iztacala, Comisión Nacional para el Conocimiento y Uso de la Biodiversidad, El Colegio de la Frontera Sur, Consejo Nacional de Ciencia y Tecnología, Secretaría de Medio Ambiente y Recursos Naturales, México, 322 pp.
- Fiers F, Ghenne V, Suárez-Morales E (2000) New species of Continental cyclopoid copepods (Crustacea, Cyclopoida) from the Yucatán Peninsula, Mexico. *Studies on Neotropical Fauna & Environment* 35(3): 209–251. doi: 10.1076/snfe.35.3.209.8862
- Franke U (1989) Katalog zur Sammlung limnischer Copepoden von Prof. Dr. Friedrich Kiefer. *Carolina. Staatliches Museum für Naturkunde, Karlsruhe*, 433 pp.
- Herbst HV (1962) Crustacea aus dem Amazonasgebiet, gesammelt von professor Dr. H Sioli und Dr. R Braun. 1. Litorale und substratgebundene Cyclopoida Gnathostoma (Copepoda). *Crustaceana* 3(4): 259–278. doi: 10.1163/156854062X00508
- Hołyńska M (2000) Revision of the Australasian species of the genus *Mesocyclops* Sars, 1914 (Copepoda: Cyclopidae). *Annales Zoologici* 50(3): 363–447.
- Huys R, Boxshall GA (1991) Copepod Evolution. The Ray Society, London, 468 pp.
- Karanovic T, Krajcicek M (2012) When anthropogenic translocation meets cryptic speciation globalized bouillon originates; molecular variability of the cosmopolitan freshwater cyclopoid *Macrocyclus albidus* (Crustacea: Copepoda). *Annales de Limnologie-International Journal of Limnology* 48(1): 63–80. doi: 10.1051/limn/2011061
- Karayutug S (1999) Genera *Paracyclops*, *Ochridacyclops* and Key to the Eucyclopinæ. Guides to the Identification of the Macroinvertebrates of the Continental Waters of the World, Vol. 14. Backhuys Publishers, Leiden, 217 pp.
- Kiefer F (1935) Neue Süßwassercyclopiden (Crustacea Copepoda) aus Uruguay. *Zoologischer Anzeiger* 109(7/8): 181–188.
- Lilljeborg W (1901) Synopsis specierum huc usque in Suecia observatarum generis *Cyclopis*, sive Bidrag till en Öfversigt af de inom Sverige iakttagna arterna af släktet *Cyclops*. K. Svenska Vetensakad. Forhhandling., Stockholm 35(4): 1–118.
- Lindberg K (1942) Cyclopoïdes nouveaux du continent Indo-Iranien. III-IV. *Records of the Indian Museum Calcutta* 44(1): 15–27.
- Mercado-Salas NF, Suárez-Morales E, Silva-Briano M (2015) Taxonomic revision of the Mexican *Eucyclops* (Copepoda: Cyclopoida) with comments on the biogeography of the genus. *Journal of Natural History* 2015: 1–123. doi: 10.1080/00222933.2015.1061715

- Mirabdullayev IM (1998) Redescription of *Microcyclops rechteyae* Lindberg, 1960 (Crustacea, Copepoda). *Hydrobiologia* 362(1–3): 219–223. doi: 10.1023/A:1003178400061
- Mirabdullayev IM (2007) Redescription of *Microcyclops cunningtoni* (GO Sars, 1909) (Copepoda, Cyclopoida). *Munis Entomology and Zoology* 2(1): 79–85.
- Mirabdullayev IM, Urazova RS (2006) Redescription of the female and first description of the male of *Microcyclops karvei* (Kiefer & Moorthy, 1935) (Copepoda, Cyclopoida). *Zoology in the Middle East* 38(1): 57–62. doi: 10.1080/09397140.2006.10638165
- Mirabdullayev IM, Van Damme K, Dumont H (2002) Freshwater cyclopoids (Crustacea: Copepoda) from the Socotra Archipelago, Yemen, with description of a new species of *Bryocyclops*. *Fauna of Arabia* 19: 261–271.
- Pennak RW, Ward JV (1985) New cyclopoid copepods from interstitial habitats of a Colorado Mountain stream. *Transactions of the American Microscopical Society* 104(3): 216–222. doi: 10.2307/3226433
- Reid JW (1985) Chave de Identificação e lista de referências bibliográficas para as espécies continentais Sulamericanas de vida livre da Ordem Cyclopoida (Crustacea, Copepoda). *Bolm. Instituto de Biociências, Universidade de São Paulo* 9: 17–143.
- Reid JW (1986) A redescription of *Microcyclops ceibaensis* (Marsh, 1919) (Copepoda: Cyclopoida) from Marsh's specimens in the National Museum of Natural History. *Proceedings of the Biological Society of Washington* 99(1): 71–78.
- Reid JW (1990) Continental and coastal free-living Copepoda (Crustacea) of Mexico, Central America and the Caribbean region. In: Navarro D, Robinson JG (Eds) *Centro de Investigaciones de Quintana Roo, Program of Studies in Tropical Conservation*. University of Florida, Chetumal, Quintana Roo, México, 175–213.
- Reid JW (1992) Copepoda (Crustacea) from fresh waters of the Florida Everglades, U.S.A. with a description of *Eucyclops conrowae* n. sp. *Transactions of the American Microscopical Society* 111(3): 229–254. doi: 10.2307/3226612
- Rocha CEF, Da (1998) New morphological characters useful for the taxonomy of the genus *Microcyclops* (Copepoda, Cyclopoida). *Journal of Marine Systems* 15(1–4): 425–431. doi: 10.1016/S0924-7963(97)00091-2
- Rylov VM (1948) *Fauna of U.S.S.R. Crustacea. Freshwater Cyclopoida*. Translated from Russian, 3(3). Zoological Institute of the Academy of Sciences of the U.S.S.R., Leningrad, 314 pp.
- Sars GO (1863) Oversigt af de indenlandske Ferskvands copepoder. *Forh Vidensk Selsk Christiana* 29: 212–262.
- Van de Velde I (1984a) Introduction of new characters in *Mesocyclops* with African species as example. *Crustaceana Supplement* 2: 404–419.
- Van de Velde I (1984b) Revision of the African species of the genus *Mesocyclops* Sars, 1914 (Copepoda: Cyclopidae). *Hydrobiologia* 109(1): 3–66. doi: 10.1007/BF00006297
- Williamson CE, Reid JW (2001) Copepod. In: Thorp JH, Covich AP (Eds) *Ecology and Classification of North American Freshwater Invertebrates*. Academic Press, San Diego California, 915–954. doi: 10.1016/B978-012690647-9/50023-5
- Wyngaard GA, Hołyńska M, Schulte JA II (2010) Phylogeny of the freshwater copepod *Mesocyclops* (Crustacea: Cyclopidae) based on combined molecular and morphological data, with notes on biogeography. *Molecular Phylogenetics and Evolution* 55(3): 753–764. doi: 10.1016/j.ympev.2010.02.029

Supplementary material I

Table 2

Authors: Martha Angélica Gutiérrez-Aguirre, Adrián Cervantes-Martínez

Data type: RTF file

Explanation note: Biological material examined.

Copyright notice: This dataset is made available under the Open Database License (<http://opendatacommons.org/licenses/odbl/1.0/>). The Open Database License (ODbL) is a license agreement intended to allow users to freely share, modify, and use this Dataset while maintaining this same freedom for others, provided that the original source and author(s) are credited.

Two new species of *Pachylaelaps* Berlese, 1888 from the Iberian Peninsula, with a key to European species (Acari, Gamasida, Pachylaelapidae)

Peter Mašán¹, Hasan Hüseyin Özbek², Peter Fenda³

1 Institute of Zoology, Slovak Academy of Sciences, Dúbravská cesta 9, 845-06 Bratislava, Slovakia **2** Faculty of Science and Arts, Erzincan University, 24030 Erzincan, Turkey **3** Department of Zoology, Faculty of Natural Sciences, Comenius University, Ilkovičova 6, 842-15 Bratislava, Slovakia

Corresponding author: Peter Mašán (peter.masan@savba.sk, uzaepema@savba.sk)

Academic editor: F. Faraji | Received 28 April 2016 | Accepted 15 June 2016 | Published 6 July 2016

<http://zoobank.org/86AB7257-735E-499C-B64A-3C87D4D62390>

Citation: Mašán P, Özbek HH, Fenda P (2016) Two new species of *Pachylaelaps* Berlese, 1888 from the Iberian Peninsula, with a key to European species (Acari, Gamasida, Pachylaelapidae). ZooKeys 603: 71–95. doi: 10.3897/zookeys.603.9038

Abstract

Pachylaelaps (Pachylaelaps) pyrenaicus sp. n. and *Pachylaelaps (Longipachylaelaps) brevipilis* sp. n. (Acari, Pachylaelapidae) are described and illustrated based on specimens from litter and soil detritus of forest habitats in Spain (Pyrenees Mts) and Portugal (Serra da Labruja Mts), respectively. An identification key to European species of the genus *Pachylaelaps* Berlese, 1888 is provided.

Keywords

Description, Europe, identification key, Mesostigmata, morphology, soil mites, systematics

Introduction

Pachylaelapid mites (Acari, Mesostigmata, Gamasida, Eviphidoidea) represent a cosmopolitan group of free-living mites with extraordinarily wide ecological and behavioural diversity (including more than 230 known species and 16 genera worldwide). They constitute an important component of the fauna in all soil microhabitats of the

temperate zone of the northern hemisphere. They colonise various soil substrates, especially leaf litter and decomposing organic detritus (Mašán and Halliday 2014).

The genus *Pachylaelaps* Berlese, 1888 belongs to the largest pachylaelapid genera and currently includes 56 valid species. Its continental diversity, based on the original type specimens and excluding those which have been incorrectly classified in the genus at some time, covers Europe (38 spp.), Asia (13 spp.), Africa (3 spp.), South America (1 sp.) and Australia (1 sp.) (Mašán and Halliday 2014, Özbek 2015). The genus was erected by Berlese (1888), placed in the Gamasidae by Berlese (1892) and *Gamasus pectinifer* G. & R. Canestrini, 1881 is generally accepted as its type species by subsequent designation by Berlese (1904) (see discussion of the type species by Mašán and Halliday (2014)). Later, a more comprehensive generic description was provided by Berlese (1904), Evans and Hyatt (1956), Costa (1971), and Koroleva (1977a) who classified the genus in the family Pachylaelapidae. Mašán (2007) clarified the concept of the genus *Pachylaelaps* by removing some species that obviously belong in other genera (e.g. *Onchodellus* Berlese, 1904 and *Pachydellus* Mašán, 2007), and described the new subgenus *Longipachylaelaps*.

When compared with other taxa of edaphic mesostigmatic mites, *Pachylaelaps* are relatively little-known in Europe. The almost identical appearance of individual species, which causes difficulties in species identification, may also explain the small number of papers exclusively devoted to the European species of the genus *Pachylaelaps* (Evans and Hyatt 1956, Hirschmann and Krauss 1965, Koroleva 1977b, 1978, Moraza and Peña 2005). The most recent review and general summary of *Pachylaelaps* species was by Mašán and Halliday (2014), with a checklist of world species.

The main aim of this paper is to describe two new soil-inhabiting species of the little known genus *Pachylaelaps*, compare them with other morphologically similar congeneric species, and provide an updated identification key to the European species of this genus.

Materials and methods

Collected mites were extracted from the litter and soil detritus by means of a modified Berlese-Tullgren funnel equipped with a 40 Watt bulb, and preserved in ethyl alcohol. Before identification, the mites were mounted onto permanent microscope slides, using Swan's chloral hydrate mounting medium. Illustrations were made by H. H. Özbek using a normal optical microscope equipped with a drawing tube. A Leica DM 1000 light microscope equipped with a stage-calibrated ocular micrometer and a Leica EC3 digital camera was used by P. Mašán to obtain measurements and photos. Measurements were made from slide-mounted specimens. Some multiple images were combined using the CombineZP software program (Hadley 2010). Lengths of shields and legs were measured along their midlines, and widths at their widest point (if not otherwise specified in the description). Dorsal setae were measured from the bases of their insertions to their tips. Measurements are mostly presented as ranges (minimum

to maximum). The terminology of dorsal and ventral chaetotaxy follows Lindquist and Evans (1965). The notation for the pore-like structures of the idiosoma is that of Johnston and Moraza (1991).

Systematics

Genus *Pachylaelaps* Berlese

Pachylaelaps Berlese, 1888: 196. Type species *Gamasus pectinifer* G. Canestrini, 1881, by subsequent designation (Berlese 1904).

Diagnosis. *Pachylaelaps* can be reliably diagnosed by the following combination of characters: (1) dorsal shield oblong, suboval, and bearing 30 pairs of mostly subequal setae; (2) dorsocentral setae J2 in normal posterolateral position to setae J1; (3) sternal and genitoventral shield with four and two pairs of setae, respectively; (4) female tarsus II with two spur-like distal setae, pl1 and pl2; (5) sperm induction system of female associated with coxae IV; (6) tibial projections on male palp developed (except for species of *Pachylaelaps pectinifer* group); (7) genu I with 13 setae.

Taxonomic notes. Mašán (2007) divided the genus into two subgenera, *Pachylaelaps* s. str. and *Longipachylaelaps* Mašán, 2007. That taxonomic concept is used also in this paper. The subgenus *Longipachylaelaps* is reliably distinguished from the subgenus *Pachylaelaps* s. str. mainly by the presence of normal needle-like dorsal setae J5, and only one pair of slit-like poroid structures (gdS4) placed on the posterolateral margin of the dorsal shield. In the subgenus *Pachylaelaps* s. str., setae J5 are vestigial, and the posterolateral dorsal shield margin bears two pairs of slit-like poroids, gdZ1 and gdS4.

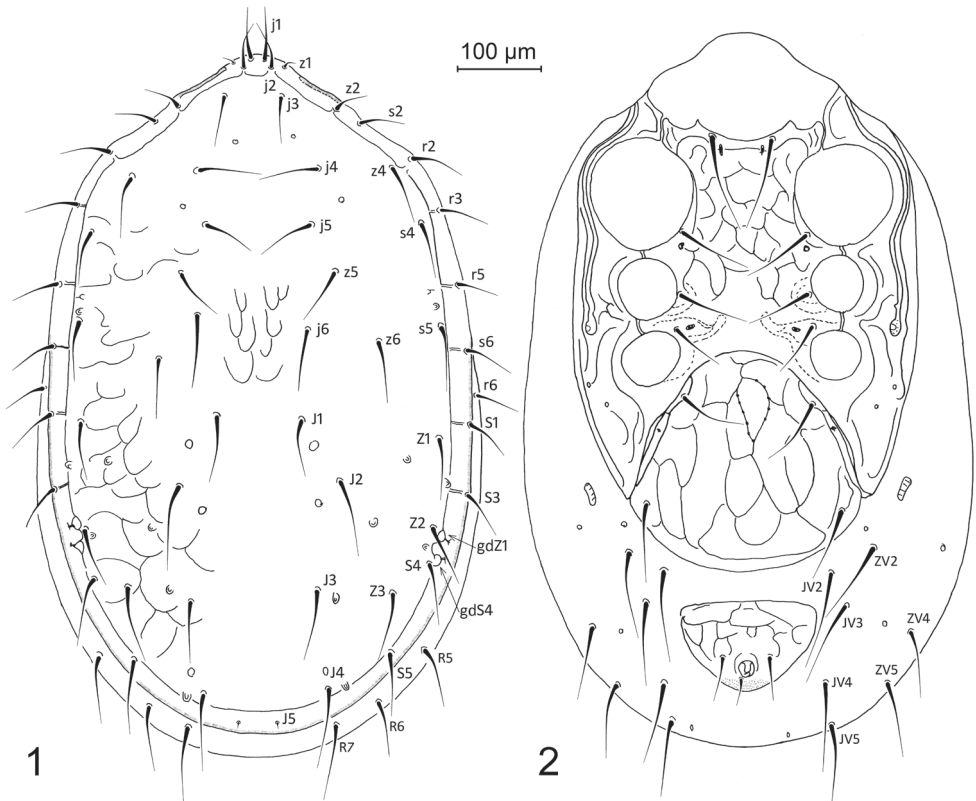
Pachylaelaps (Pachylaelaps) pyrenaicus sp. n.

<http://zoobank.org/4E352060-75DC-4D92-A1FE-8BCDC82CD6B7>

Figures 1–19

Specimens examined. Holotype female: North Spain, Central Pyrenees Mts., Cinca Valley, Bielsa Cadaster, Salinas Village (near-by San Marcial Settlement), pine forest (*Pinus* spp.) with admixed beech (*Fagus sylvatica*), soil detritus with deep layer of raw humus between rock boulders, altitude 1050 m, 42°35'52,2"N, 00°14'20,0"E, 16 June 2007, coll. P. Fendá. Paratypes: four females and one male, with the same data as the holotype. The holotype and four paratypes are deposited at the Institute of Zoology, Slovak Academy of Sciences, Bratislava; one female paratype is deposited at the Acarology Laboratory of Erzincan University, Turkey.

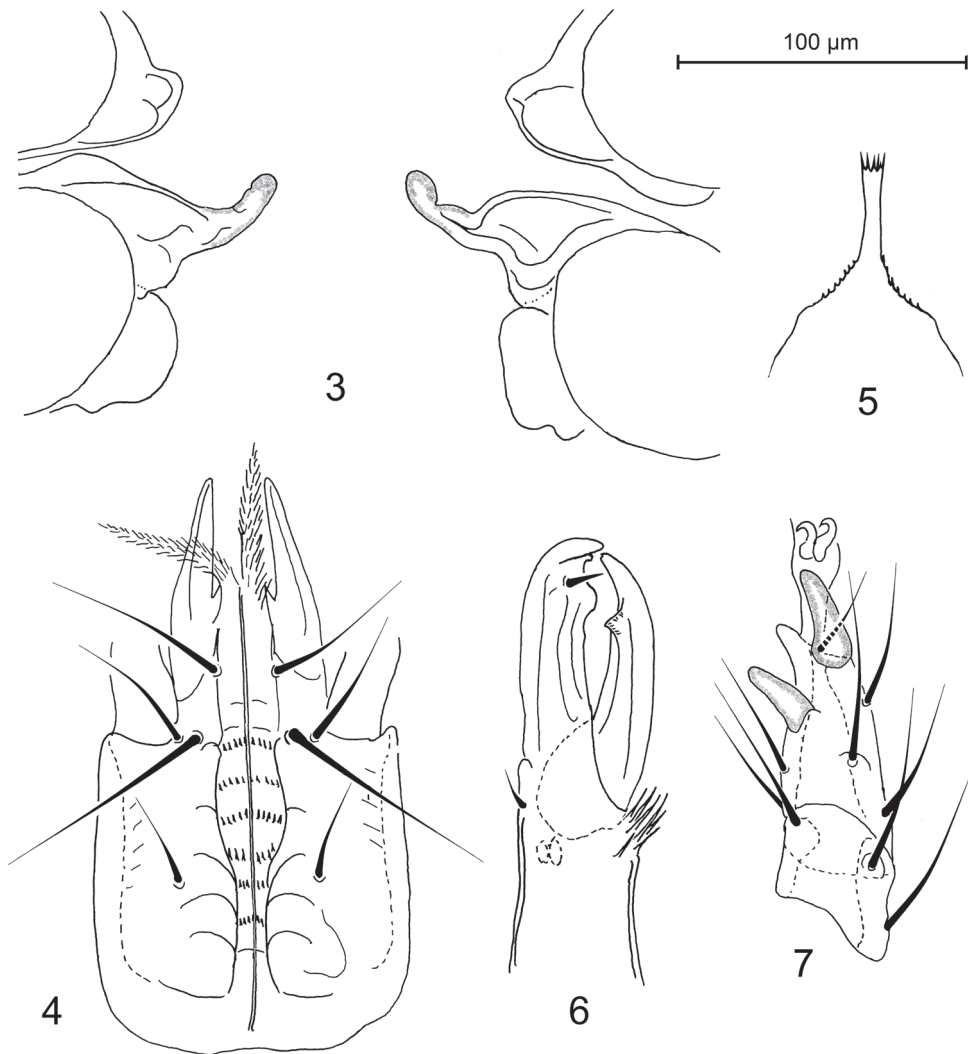
Diagnosis. Slit-like glandular poroids gdZ1 and gdS4 with conspicuously adjacent position. Soft integument with decreased number of 11 pairs of setae in female and eight setal pairs in male. Prestigmatic section of peritreme long, with anterior tip



Figures 1–2. *Pachylaelaps (Pachylaelaps) pyrenaicus*, female, with setal notation of some idiosomal setae and glandular poroids. **1** Dorsal idiosoma **2** Ventral idiosoma.

reaching dorsal surface close to setae z1. Dorsal setae long (the longest setae more than 100 µm in length), and seta j5 with tip reaching base of following seta z5. Cheliceral digits unidentate. Male palptibia with two well developed petal-like projections. In female, ventrodistal femur with small spine-like process associated with a seta. Terminal part of male tarsus II with only one spur-like distal seta (pl1). Sperm induction system with tubular components: tubes irregularly formed, folded, curved or with small bumps on distal sections, progressively widened basally; basal part widely abutting to anterior margin of coxa IV.

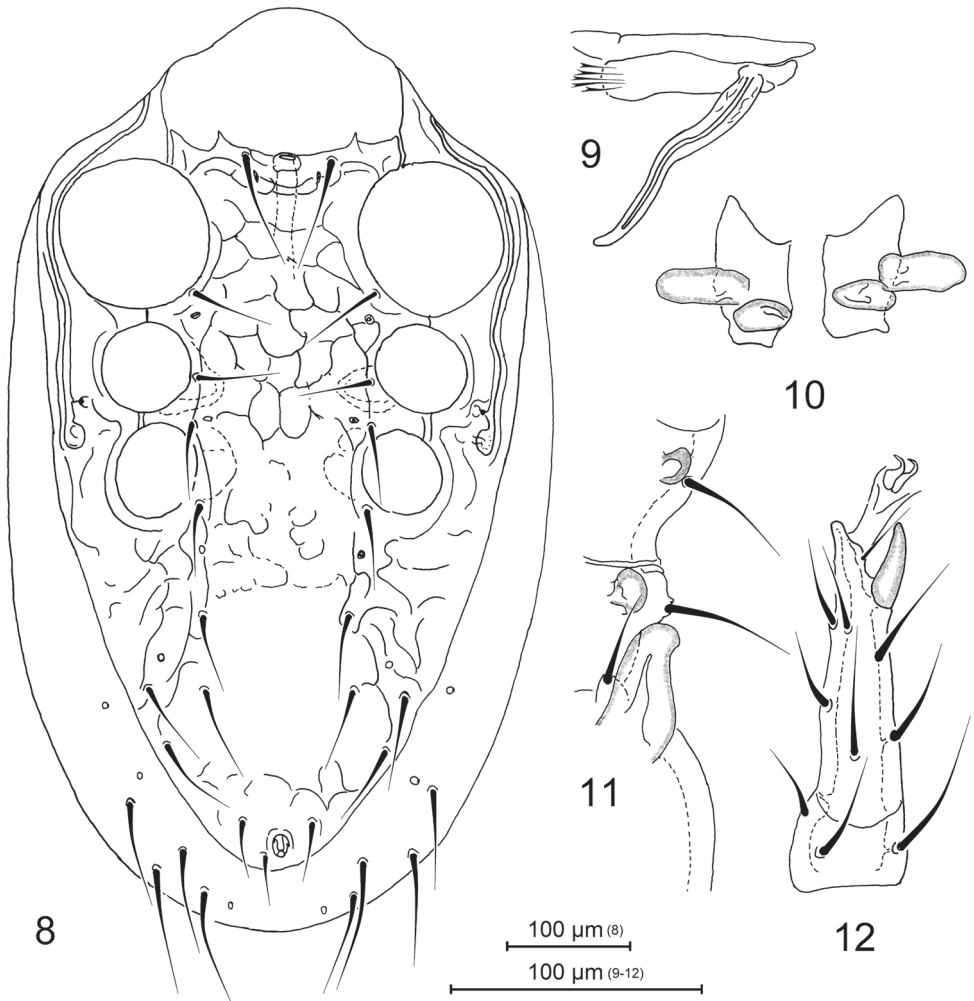
Description. *FEMALE. Dorsal idiosoma* (Figure 1). Dorsal shield 870–915 µm long and 560–610 µm wide, suboval (length/width 1.48–1.63), weakly and unevenly reticulated on surface, and bearing 30 pairs of smooth and needle-shaped dorsal setae. Setae z1 conspicuously shortened, setae J5 strongly reduced in length, vestigial microsetae; other setae relatively longer, subequal and uniform. Length and spacing of some selected dorsal shield setae as follows: j1 53–67 µm, j5 73–83 µm, j5–j5 128–144 µm, j5–z5 72–81 µm, J1–J2 87–111 µm, J2 97–109 µm, J2–J2 216–242 µm, J2–J3 142–172 µm, J3 102–110 µm, J3–J4 118–151 µm, and J4 100–105 µm. Dorsolateral



Figures 3–7. *Pachylaelaps* (*Pachylaelaps*) *pyrenaicus*, female. **3** Sperm induction structures **4** Ventral gnathosoma **5** Epistome **6** Chelicera, lateral view **7** Tarsus II, lateral view.

soft integument with four pairs of marginal setae (r6, R5–R7). Posterolateral poroid structures gdZ1 and gdS4 slit-like, markedly adjacent each other, and placed close to setae Z2 or rarely between setae Z2 and S4.

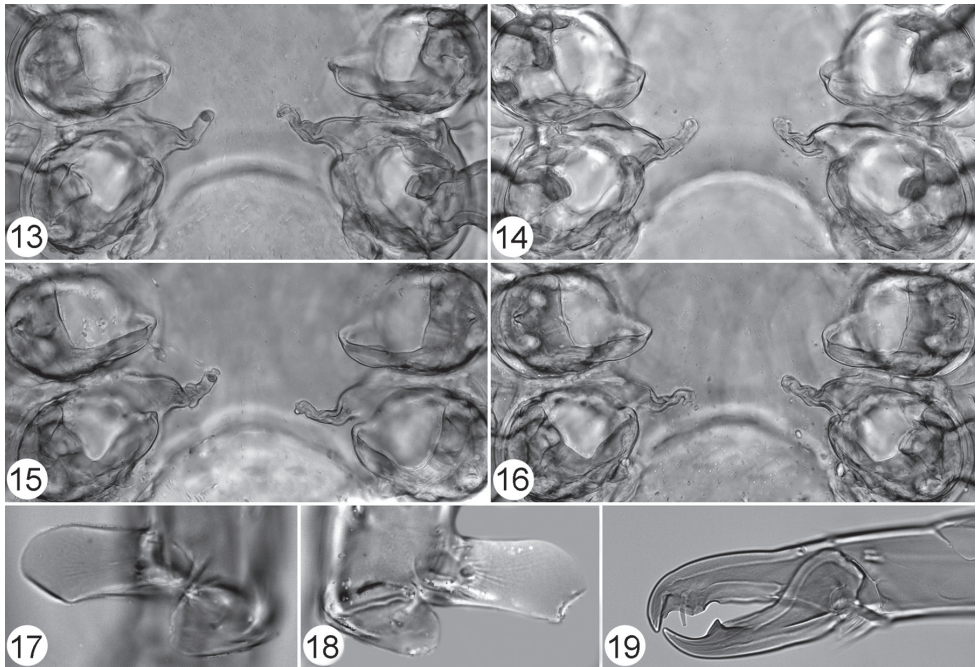
Ventral idiosoma (Figure 2). Sternal shield 272–280 µm long, proportionally 0.82–0.94 shorter than genitiventral shield, with concave anterior margin and two small projections close to bases of sternal setae st1. Genitiventral shield slightly shorter than wide or subequal in length and width (length 295–335 µm, width 308–337 µm, length/width 0.94–0.99). Anal shield subtriangular, 114–137 µm long and 170–199 µm wide (length/width 0.62–0.73); anus with circum-anal setae situated close to pos-



Figures 8–12. *Pachylaelaps (Pachylaelaps) pyrenaicus*, male. **8** Ventral idiosoma **9** Chelicera, ventrolateral view **10** Palptibial projections **11** Projections on medial segments of leg II, ventral view **12** Tarsus II, lateral view.

terior margin of shield. Peritremes well developed, relatively long, with anterior tip reaching dorsal surface close to setae z1. Peritrematal shields with weak longitudinal sculptural lines, other ventral shields distinctly and evenly reticulated on surface. Metapodal platelets minuscule, free and well separate from peritrematal shields. Ventral soft integument with seven pairs of ventral setae (JV2–JV5, ZV2, ZV4, ZV5). Ventral setae similar to those on dorsal idiosoma.

Sperm induction structures (Figures 3, 13–16). Tubes of sperm induction system relatively well developed, well sclerotized, broadened basally, and narrowed distally; worm-like distal section irregularly formed, folded, curved or with small bumps; basal section widely abutting to anterior margin of coxa IV.



Figures 13–19. *Pachylaelaps (Pachylaelaps) pyrenaicus*. **13–16** Sperm induction structures, female, variant forms **17–18** Palptibial projections, male, variant forms **19** Chelicera, female, lateral view. Not scaled.

Gnathosomal structures (Figures 4–6, 19). Corniculi elongated and horn-like; laciniae densely pilose, slightly longer than corniculi; deutosternum slightly widened medially, with six rows of denticles; subcapitular setae smooth and needle-shaped (Figure 4). Epistome with wide subtriangular base, elongate and narrow central neck and thin apical part crenelated on anterior margin; lateral margins of basal part with delicate denticulation; apical section not expanded or only very slightly expanded anteriorly, terminally truncate and with a row of four to seven prongs (Figure 5). Cheliceral digits relatively elongate and slender (Figures 6, 19), 100–110 μm long; fixed digit of chelicera with terminal hook, small and obtuse subapical denticle, and one larger and flattened distal tooth associated with pilus dentilis; movable digit armed with relatively thin terminal hook and one subdistal tooth.

Legs. Leg setation normal for genus (Mašán 2007). Femur II with a small spine-like process on ventral distal surface, process associated with a seta. Tarsus II with two spur-like distal setae pl1 and pl2 (Figure 7).

MALE. Idiosoma (Figure 8). Dorsal shield 810 μm long and 492 μm wide, suboval (length/width 1.65). Sternal, genitiventral, peritrematal, metapodal, and anal plates are fused together to form an entire holovenral shield bearing nine pairs of setae (excluding three circum-anal setae); the shield irregularly reticulate on surface. Dorsolateral and ventral soft integument with eight pairs of setae (see diagnosis). Dorsal and ventral chaetotaxy and other characters as in female.

Gnathosomal structures (Figures 9, 10, 17, 18). Cheliceral spermatodactyl elongated, ensiform, 162 μm long (about 1.5 times as long as movable digit of chelicera), slightly widened in basal section, progressively tapering toward tip and slightly undulate medially; sperm ductus well defined (Figure 9). Palptibiae normal, not thickened (when compared with other palp segments), each bearing a pair of well-developed petal-like projections on proximal ventral surface (see Figures 17 and 18); outer petal markedly larger than inner one, and longer than cross-sectional radius of palptibia.

Legs. Medial segments of legs II spurred on their distal ventral surface: femur with one robust spur, genu and tibia each with a small knob-like spur, as in Figure 11. Femoral spur broadened basally, produced into obtuse and rounded apex; associated axillar seta pv1 inserted in a small tubercle (Figure 11). Terminal part of tarsus II with only one spur-like distal seta pl1; seta pl2 needle-shaped (Figure 12).

Etymology. The epithet of this species is derived from the Latin name “*Pyrenaei Montes*” and alludes to the type locality situated in the Pyrenees Mountains.

Taxonomic notes. The new species may be distinguished from all other congeners especially by the following combination of characters: (1) in female, tubiform spermathecal structures irregular, with worm-like distal sections having some bends, folds and small bumps, and expanded base widely abutting the anterior margin of coxa IV; (2) female chelicera with flat to truncate subdistal tooth on fixed digit; (3) epistome with narrow central projection bearing a row of four to six denticles; (4) male palptibia with two well developed petal-like projections; (5) terminal part of male tarsus II with only one spur-like distal seta, pl1 (6) cheliceral spermatodactyl simple, ensiform, slightly undulate medially, without irregular convexities or projections on its margin.

Mašán (2007) divided the European members of the subgenus *Pachylaelaps* into five clusters of species: (1) the *bellicosus* group (*P. bellicosus* and *P. multidentatus*), with separate position of slit-like poroid structures gdZ1 and gdS4 on dorsal shield, multi-dentate cheliceral digits, spermathecal tubiform structures simple, transparent (weakly sclerotized) and relatively longer, and males apparently absent; (2) the *denticulatus* group (*P. denticulatus* only), possessing separate position of slit-like poroid structures gdZ1 and gdS4, three projections on male palptibia, one spur-like distal seta on tarsus II in male, and bidentate cheliceral digits; (3) the *ensifer* group (*P. armimagnus*, *P. carpathimagnus*, *P. ensifer*, *P. troglophilus* and *P. sacculimagnus*), characterized by the adjacent position of slit-like poroid structures gdZ1 and gdS4, robust size of idiosoma, spermathecal tubiform structures (if detectable) elongated and weakly sclerotized, and presence of 2–4 palptibial projections in male and two spur-like distal setae on tarsus II in both adults; (4) the *imitans* group (*P. imitans*, *P. insularis*, *P. resinae* and *P. terreus*), with adjacent slit-like poroid structures gdZ1 and gdS4 having their openings in a common infundibulum, spermathecal tubiform structures short, conical to cylindrical and strongly sclerotized, two palptibial projections in male, and small lobe-like convexity on ventral margin of cheliceral spermatodactyl; (5) the *pectinifer* group (*P. littoralis* and *P. pectinifer*), characterized by the adjacent position of slit-like poroid structures gdZ1 and gdS4, Y-shaped spermathecal tubiform structures, absence of palptibial projections in male, and presence of two spur-like distal setae on tarsus II in both adults.

In this classification scheme, *Pachylaelaps* (*Pachylaelaps*) *pyrenaicus* should be considered as a species with a separate position among the all above mentioned species groups because it possesses a unique combination of main diagnostic characters. Some morphological characters of *P. (P.) pyrenaicus* are not consistent with those found typically in the individual species groups. The adjacent position of slit-like poroid structures gdZ1 and gdS4 on dorsal shield and unidentate cheliceral digits in the new species are in contradiction with the definition of the *bellicosus* and *denticulatus* groups. The male palptibia has two petal-like projections in *P. (P.) pyrenaicus*, where the *pectinifer* group species does not have these structures developed. In the robust species of the *ensifer* group, tarsus II has two spur-like distal setae in adults, but this character is found in the smaller new species only in females. In addition, in *P. (P.) pyrenaicus*, the tubular structures of sperm induction system have a distinctive form which is not known in the other species of the genus, but is especially different from the members of the *imitans* group that are characterized by short, conical to cylindrical, and strongly sclerotized spermathecal tubes.

***Pachylaelaps* (*Longipachylaelaps*) *brevipilis* sp. n.**

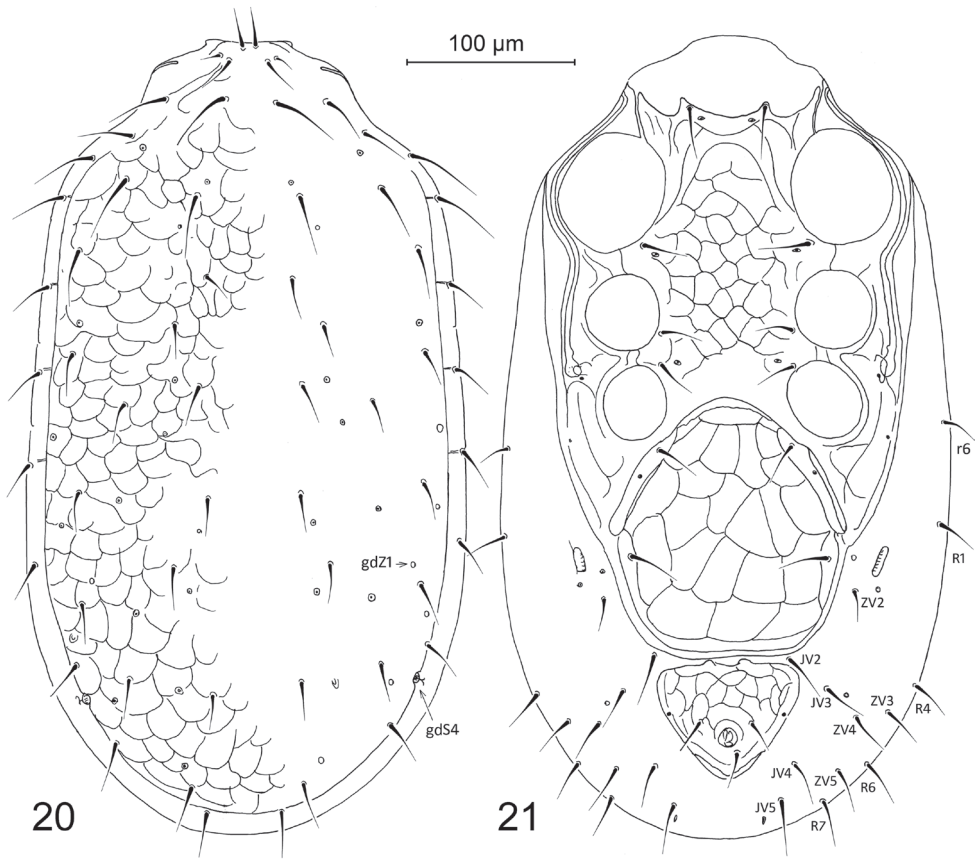
<http://zoobank.org/89C70A15-424B-4D59-9D17-E4642314663B>

Figures 20–42

Specimens examined. Holotype female: North Portugal, Serra da Labruja Mts., San Bento da Porta Aberta Village, Viana do Castelo Cadaster, non-native eucalyptus forest (*Eucalyptus globulus*), humid leaf litter and soil detritus, altitude 260 m, 41°56'02,3"N, 08°37'49,9"W, 10 May 2008, coll. P. Fenda. Paratypes: 45 females and 14 males, with the same data as in holotype. The holotype and paratypes are deposited at the Institute of Zoology, Slovak Academy of Sciences, Bratislava; six paratypes (three females and three males) are deposited at the Acarology Laboratory of Erzincan University, Turkey.

Diagnosis. Soft integument with decreased number of 13 pairs of setae in female and ten setal pairs in male. Dorsal setae J5 well developed, slightly longer than setae J4. Prestigmatic section of peritreme long, with anterior tip reaching dorsal surface close to setae z1. Dorsal setae relatively short (longest setae not exceeding 35 µm in length), with their tips not reaching bases of following setae. Cheliceral digits unidentate; pilus dentilis conspicuously enlarged (in female) or vestigial (in male). Male palptibia with two petal-like projections, shorter than cross-sectional radius of palptibia. Terminal part of male tarsus II with only one spur-like distal seta (pl1). Sperm induction system with tubular components: tubes relatively shorter, with club-shaped apical section, straight or variously curved; basal part not markedly expanded, thin, associated with inner middle surface of coxa IV.

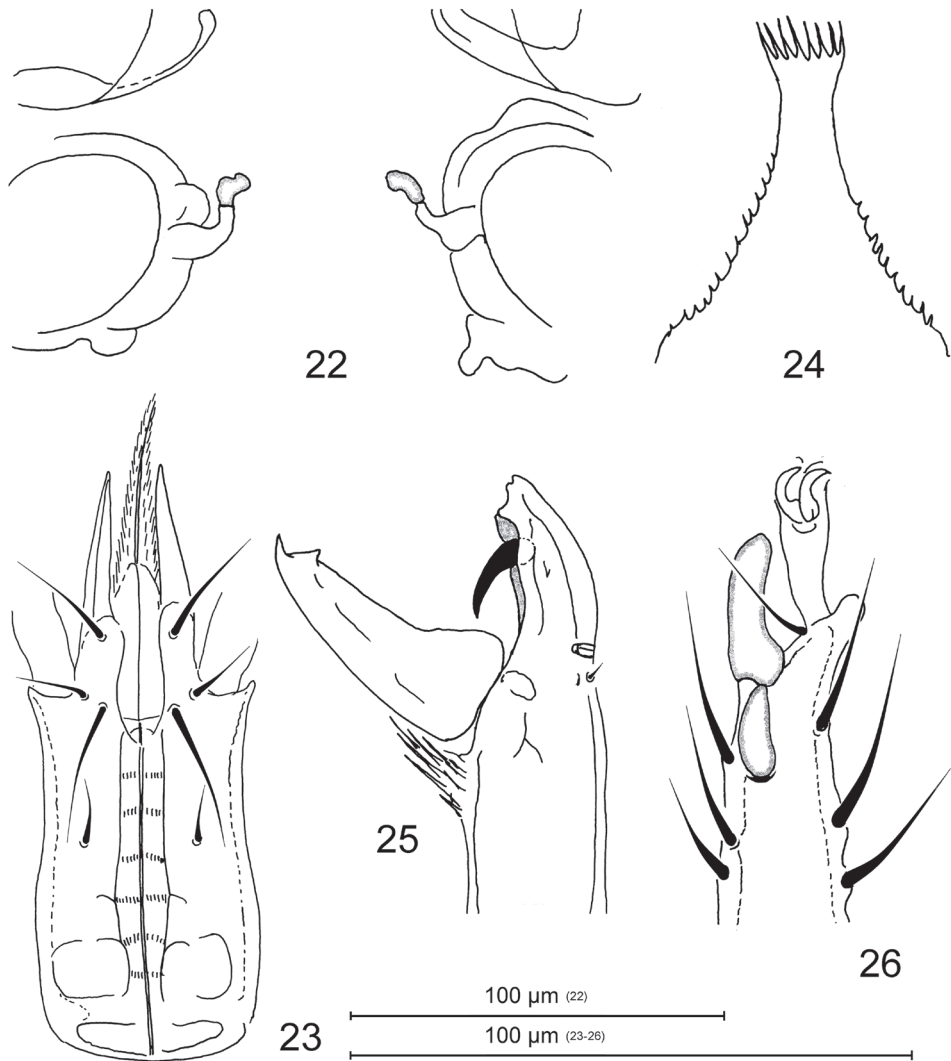
Description. *FEMALE.* Dorsal idiosoma (Figure 20). Dorsal shield 510–565 µm long and 285–315 µm wide, elongated and suboval (length/width 1.75–1.95), delicately and evenly reticulated on surface, and bearing 30 pairs of dorsal setae. Dorsal setae uniform, smooth and needle-shaped, subequal in length, relatively short, and mostly



Figures 20–21. *Pachylaelps (Longipachylaelps) brevipilis*, female, with setal notation of some ventral setae and glandular poroids. **20** Dorsal idiosoma **21** Ventral idiosoma.

with tips not reaching bases of following setae; setae z1 shortest and setae j3, j4, z4, r2, and r3 longest (46–51 µm). Length and spacing of some selected dorsal shield setae as follows: j1 24–29 µm, j5 22–26 µm, j5–j5 53–64 µm, j5–z5 31–41 µm, J1 25–29 µm, J1–J2 44–54 µm, J2 26–31 µm, J2–J2 98–114 µm, J2–J3 88–97 µm, J3 24–30 µm, J3–J4 63–85 µm, J4 22–30 µm, and J5 24–31 µm; setae J4/J5 0.87–0.96. Dorsolateral soft integument with five pairs of marginal setae (r6, R1, R4, R6, R7). One pair of posterolateral poroid structures (gdS4) slit-like, placed between setae S4 and S5.

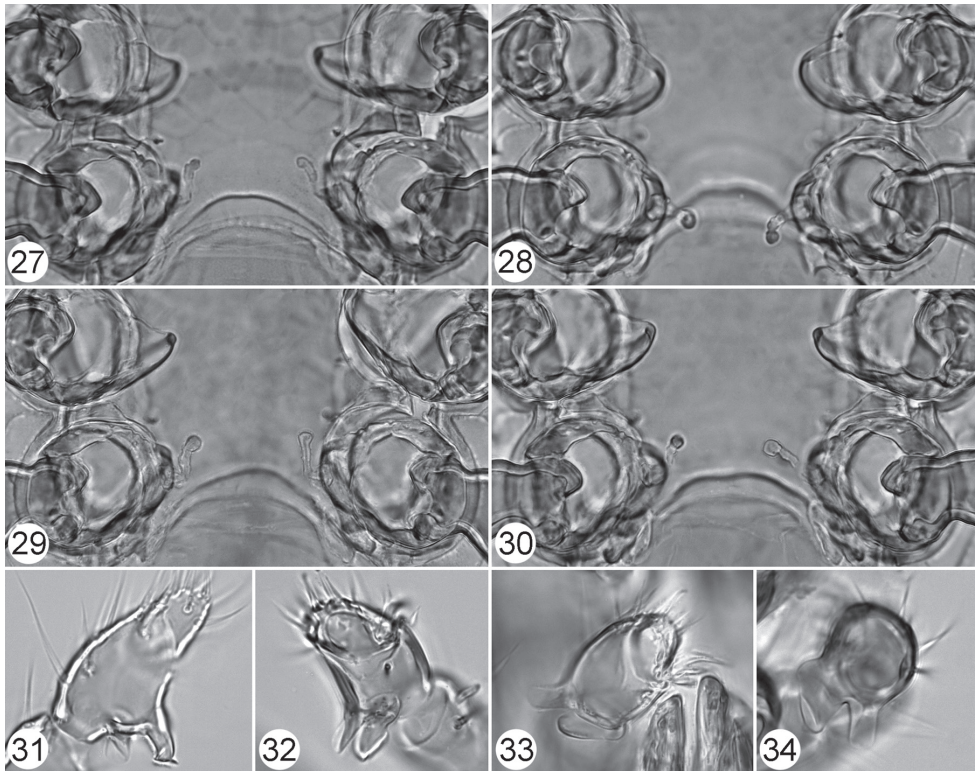
Ventral idiosoma (Figure 21). Sternal shield 190–205 µm long, usually longer than genitiventral shield (length of sternal shield/length of genitiventral shield 0.98–1.12), with concave anterior margin and two small corners close to bases of sternal setae st1. Genitiventral shield slightly longer than wide (length 175–202 µm, width 155–185 µm, length/width 1.05–1.17). Anal shield subtriangular, 70–85 µm long and 95–115 µm wide (length/width 0.65–0.80); anus with circum-anal setae situated close to posterior margin of shield. Peritremes well developed, with anterior tip reaching dorsal surface between setae z1 and z2. Peritrematal shields with weak longitudinal sculp-



Figures 22–26. *Pachylaelaps* (*Longipachylaelaps*) *brevipilis*, female. **22** Sperm induction structures **23** Ventral gnathosoma **24** Epistome **25** Chelicera, lateral view **26** Tarsus II, posterolateral view.

tural lines, other ventral shields distinctly and evenly reticulated on surface. Metapodal platelets minuscule, free on soft integument, and situated at level of setae JV1. Ventral soft integument with eight pairs of ventral setae (JV2–JV5, ZV2–ZV5). Ventral setae similar to those on dorsal idiosoma.

Sperm induction structures (Figures 22, 27–30). Tubes of sperm induction system weakly developed (with well-separated tips), weakly sclerotized in narrow basal and medial part, broadened apically, and club-shaped; basalmost section connected to inner margin of coxa IV; in newly moulted specimens, bulbiform apex of tubes more or less reduced, and almost hyaline (unsclerotised).

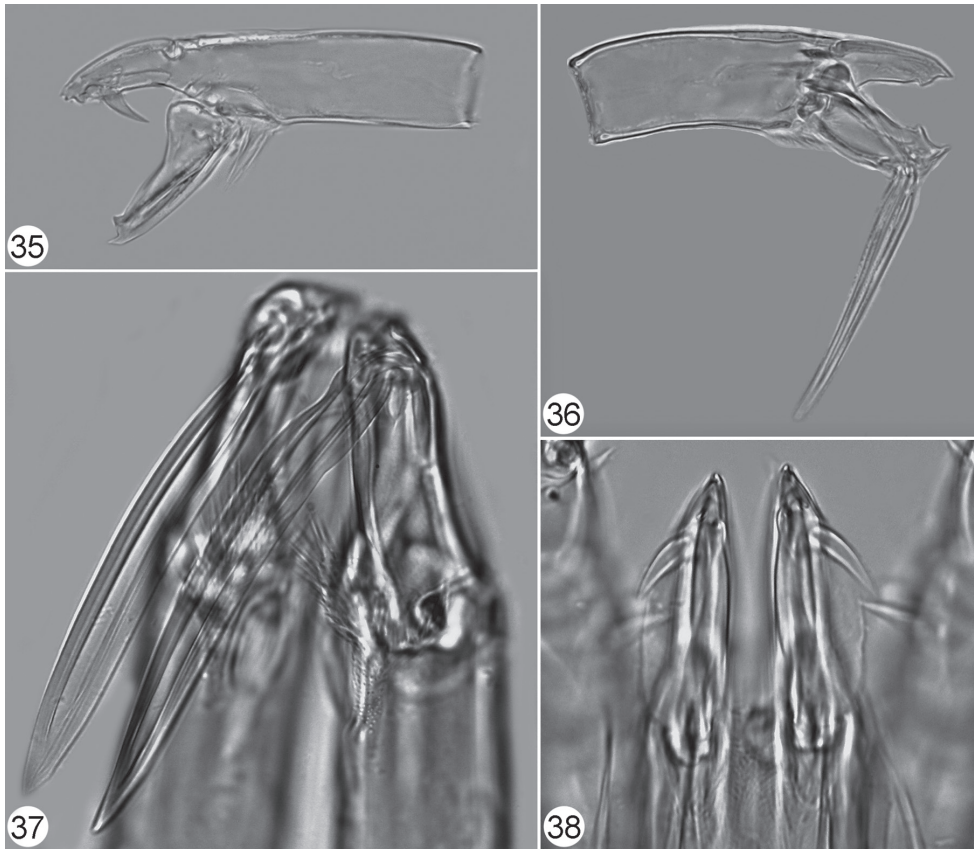


Figures 27–34. *Pachylaelaps (Longipachylaelaps) brevipilis*. **27–30** Sperm induction structures, female, variant forms **31–34** Palptibial projections, male, variant views. Not to scale.

Gnathosomal structures (Figures 23–25, 35, 38). Corniculi elongated and horn-like; laciniae densely pilose, longer than corniculi; deutosternum with six rows of denticles; subcapitular setae smooth and needle-shaped (Figure 23). Epistome with subtriangular and regularly narrowed base, wider central neck and widened apical part densely crenelated on truncate anterior margin; basal part serrate on lateral margins (Figure 24). Fixed digit of chelicera shortened, seemingly truncate; with indistinctive terminal hook reduced to two small denticles, one subdistal tooth, and very robust (hypertrophied) pilus dentilis directed backward (Figures 25, 35, 38). Movable digit of chelicera longer than fixed digit, with a hook and one subapical tooth (Figure 35).

Legs. Leg setation normal for genus (Mašán, 2007). Tarsus II with two spur-like distal setae, pl1 and pl2 (Figure 26).

MALE. Idiosoma (Figure 39). Dorsal shield 470–510 μm long and 250–285 μm wide, elongated and suboval (length/width 1.78–1.88). Sternal, genitiventral, peritrematal, metapodal, and anal plates fused together to form an entire holovenral shield bearing nine pairs of setae (not including three circum-anal setae); shield evenly reticulate on surface. Dorsolateral and ventral soft integument with ten pairs of setae (see diagnosis). Dorsal and ventral chaetotaxy, and other characters as in female.

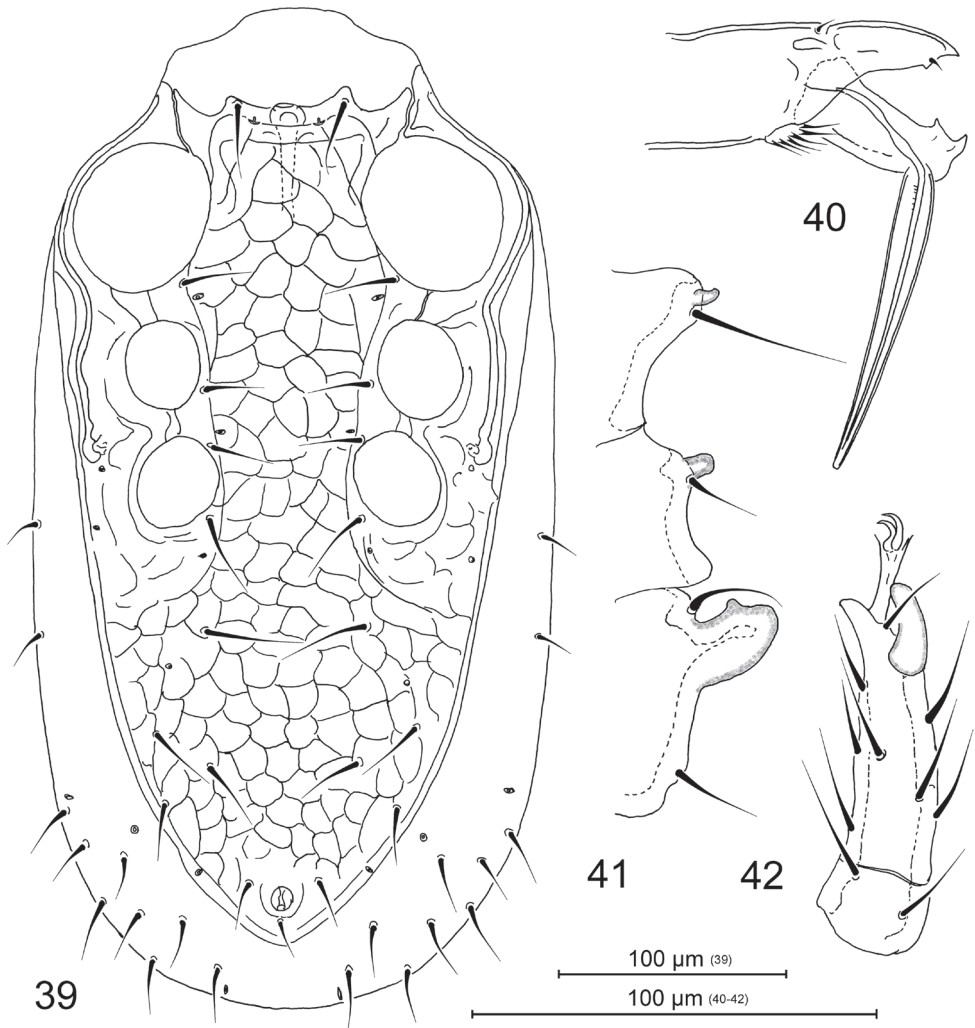


Figures 35–38. *Pachylaelaps* (*Longipachylaelaps*) *brevipilis*. **35** Chelicera, female, lateral view **36** Chelicera, male, lateral view **37** Chelicerae, male, ventrolateral view **38** Chelicerae, female, ventral view. Not to scale.

Gnathosomal structures (Figures 31–34, 36, 37, 40). Palptibiae slightly thickened medially (when compared with other palp segments), each bearing a pair of petal-like projections on proximal ventral surface, as in Figures 31–34; inner petal markedly larger than outer one, but shorter than cross-sectional radius of palptibia. Cheliceral spermatodactyl elongated, ensiform, 75–80 μm long (about 1.7–1.9 times as long as movable digit of chelicera), slightly widened in proximal section and progressively tapering toward the tip; sperm ductus well defined (Figures 36, 37, 40).

Legs. Medial segments of legs II spurred on their distal ventral surface: femur with one robust spur, genu and tibia each with a peg-like spur, as in Figure 41. Femoral spur broadened medially, produced into widely rounded apex, with a small subdistal tubercle (Figure 41). Terminal part of tarsus II with only one spur-like distal seta, p11 (Figure 42).

Etymology. The specific name of the new species is derived from the Latin words “*brevis*” (short) and “*pilum*” (hair), and it alludes to the fact that the species has the shortest idiosomal setae among its congeners.



Figures 39–42. *Pachylaelaps (Longipachylaelaps) brevipilis*, male. **39** Ventral idiosoma **40** Chelicera, lateral view **41** Projections on medial segments of leg II, lateral view **42** Tarsus II, posterolateral view.

Taxonomic notes. The main diagnostic character states for *Pachylaelaps (Longipachylaelaps) brevipilis* are the presence of shorter idiosomal setae (e.g., $j_5 < j_5-z_5$, $J_1 \approx \frac{1}{2} \times J_1-J_2$), the relative length of dorsal setae J4 and J5 (setae J5 negligibly longer than J4, about 1.04–1.14 times as long as J4), the existence of sexual dimorphism in the pilus dentilis (markedly enlarged and spiniform in female, minute and slender in male), the form of the tubular structures of the sperm induction system (tubes shorter, with club-like terminal part), the form and length of the cheliceral spermatodactyl (sword-like, less than twice as long as movable digit), and the length of the dorsal shield (small species, with dorsal shield 470–510 μm long in males, and 510–565 μm long in females).

Table 1. Comparative characteristics of the females of four similar species of the subgenus *Pachylaelaps* (*Longipachylaelaps*).

Character / Species	<i>Pachylaelaps</i> (L.) <i>brevipilis</i> sp. n.	<i>Pachylaelaps</i> (L.) <i>bifurciger</i>	<i>Pachylaelaps</i> (L.) <i>dubius</i>	<i>Pachylaelaps</i> (L.) <i>silviae</i>
Length of dorsal shield	510–565 μ m	910 μ m	unknown	836 μ m
Length of seta J1	J1 \approx $\frac{1}{2}$ J1–J2	J1 \approx $\frac{1}{2}$ x J1–J2	J1 \geq J1–J2	J1 < J1–J2
Length of seta z6	z6 < $\frac{1}{2}$ z6–Z1	z6 \approx $\frac{1}{2}$ x z6–Z1	z6 \leq z6–Z1	z6 > z6–Z1
Length of seta J3	J3 < $\frac{1}{2}$ J3–J4	J3 < $\frac{1}{2}$ J3–J4	J3 \approx J3–J4	J3 < J3–J4
Pilus dentilis	enlarged, spiniform	unknown	enlarged, spiniform	minute, setiform
Genitoventral shield	longer than wide (1.05–1.17)	wider than long (0.87)	longer than wide (1.18)	as long as wide (\approx 1)
Terminal epistome	densely crenelated	bifurcate	unknown	densely crenelated
Spermathecal tubes	club-like distally, shorter (tips distant)	worm-like distally, longer (tips adjacent)	unknown (not detectable ?)	strongly elongated, spirally convoluted

The presence of relatively short dorsal setae (at least in a central row), along with subequal setae J4 and J5, is also the feature of three other *Pachylaelaps* (*Longipachylaelaps*) species, namely *P. (L.) bifurciger*, *P. (L.) dubius* and *P. (L.) silviae*. The new species may be reliably distinguished from the above mentioned congeners by the characters presented in Table 1, and with the help of the identification key provided below.

Key to European species of the genus *Pachylaelaps* (females)

Partial keys to the European species of *Pachylaelaps* may be found in Hirschmann and Krauss (1965), Karg (1971, 1993), Koroleva (1977a), and Mašán (2007). The identification of *Pachylaelaps* species is complicated by the inaccurate and inadequate descriptions of some species. Mašán (2007) and Mašán and Halliday (2014) attempted to clarify the concept of the genus by removing many species that obviously belong in other genera such as *Onchodellus* Berlese, 1904 and *Pachydellus* Mašán, 2007.

Due to vague and inadequate original descriptions, the particular structures of the sperm induction system, palptibial outgrowths and some other important characters remain unknown in a large number of species. Therefore several species are not included in the keys presented in this paper, namely *Pachylaelaps (Pachylaelaps) bicornis* Willmann, 1939 (♀), *Pachylaelaps (Longipachylaelaps) dubius* Hirschmann & Krauss, 1965 (♀), *Pachylaelaps (Pachylaelaps) grandis* Koroleva, 1977 (♀), *Pachylaelaps (Longipachylaelaps) granulifer* Hirschmann & Krauss, 1965 (♀, but ♂ included), *Pachylaelaps (Longipachylaelaps) longisetis* Halbert, 1915 (♂, but ♀ included), *Pachylaelaps (Longipachylaelaps) obirensis* Schmörlzer, 1992 (♀, ♂).

- 1 Dorsal setae J5 developed, needle-like; posterolateral margins of dorsal shield with one pair of slit-like poroid structures, gdS4 (subgenus *Longipachylaelaps* Mašán, 2007).....**2**
- Setae J5 vestigial; posterolateral margins of dorsal shield with two pairs of slit-like poroid structures, gdZ1 and gdS4 (subgenus *Pachylaelaps* s. str.) ..**15**
- 2 Structures of sperm induction system between coxae IV well sclerotized (at least some basal or distal components), usually well discernible and striking in their lines.....**3**
- Structures of sperm induction system weakly sclerotized, hyaline and transparent, scarcely detectable, often poorly developed or fully reduced.....**12**
- 3 Sperm induction system tubular: tubiform structures simple, short or elongated, straight or curved, sometimes variously convoluted, or broadened distally**4**
- Sperm induction system sacculate or otherwise modified: tubiform structures absent and transformed into saccules with short tubiform opening only slightly protuberant above enlarged base, or into specific sickle-shaped structures.....**10**
- 4 Tubiform structures short and straight; movable digit of chelicera with three separate dents: distal hook (often with tiny lateral denticle), and subdistal and medial teeth; length of dorsal shield 750–800 μm
..... ***Pachylaelaps longisetis* Halbert, 1915**
- Tubiform structures longer or otherwise formed; movable digit of chelicera with two separate dents: simple or bifid distal hook (often with tiny lateral denticle), and a subdistal tooth**5**
- 5 Tubiform structures of sperm induction system intermediate in length (with their apices sufficiently separated)**6**
- Tubiform structures long (with distalmost sections adjacent).....**8**
- 6 Dorsal setae short: setae J1 with tips reaching between insertions of setae J1 and J2; setae J4 slightly shorter than setae J5 (J4/J5 0.87–0.96); pilus dentilis conspicuously enlarged, spine-like; smaller species, length of dorsal shield 510–565 μm ***Pachylaelaps brevipilis* sp. n.**
- Dorsal setae long: setae J1 with tips reaching beyond insertions of setae J2; setae J4 at least 1.5 longer than setae J5; pilus dentilis normal, slender; larger species, dorsal shield at least 680 μm in length.....**7**
- 7 Tubiform structures regularly sclerotized; pilus dentilis minute, with upright position; dorsal setae J5 markedly shortened, about 5–6 times shorter than setae J4; genitiventral shield 260–320 μm wide; length of dorsal shield 770–890 μm ***Pachylaelaps sublongisetis* Koroleva, 1977**
- Medial portion of tubiform structures unsclerotized, hyaline; pilus dentilis larger, curved and directed backward; setae J5 less shortened, about 1.5–2.5 times shorter than setae J4; genitiventral shield 188–225 μm wide; length of dorsal shield 680–805 μm***Pachylaelaps longulus* Willmann, 1938**

- 8 Tubiform structures excessively elongated, slightly tapered distally and helically convoluted (with 2–3 bends); length of dorsal shield 836 μm *Pachylaelaps silviae* Moraza & Peña, 2005
- Tubiform structures normal in length, straight or curved, and moderately broadened distally..... 9
- 9 Dorsal setae J5 shortened, about 4–7 times shorter than setae J4; length of dorsal shield 870 μm *Pachylaelaps squamifer* Berlese, 1920
- Setae J5 and J4 subequal in length; length of dorsal shield unknown *Pachylaelaps pulsator* Hirschmann & Krauss, 1965
- 10 Sperm induction system with specific sickle-shaped structures; pilus dentilis relatively robust, spine-like and directed backward; movable cheliceral digit with simple distal hook; genitiventral shield relatively narrower (length/width 1.14–1.27); length of dorsal shield 745–840 μm *Pachylaelaps distinctus* Mašán, 2007
- Sperm induction system sacculate: saccules with short tubiform opening slightly protuberant above enlarged base; pilus dentilis minute, with upright position; movable cheliceral digit with bifid distal hook; genitiventral shield relatively wider (length/width 0.92–1.12) 11
- 11 Sperm ductus inside saccules relatively shorter, straight and directed to anterior margin of coxa IV; base of saccules abutting the coxa IV; dorsal setae J5 30–39 μm long, about 2–3.5 times shorter than setae J4; genitiventral shield relatively narrower (length/width 1.03–1.12); length of dorsal shield 745–885 μm *Pachylaelaps vicarius* Mašán, 2007
- Sperm ductus inside saccules relatively longer, slightly curved and directed between coxae III and IV; base of saccules slightly widened, abutting the coxae III and IV; setae J5 20–25 μm long, about 5–7 times shorter than setae J4; genitiventral shield relatively wider (length/width 0.9–0.95); length of dorsal shield 940–1,050 μm *Pachylaelaps bocharovae* Koroleva, 1978
- 12 Tubiform structures of sperm induction system elongated (with more or less adjacent tips), straight or slightly curved 13
- Tubiform structures shortened (with well separated tips) or not detectable.. 14
- 13 Tubiform structures thin and long, worm-like; margins of genitiventral and anal shield straight and markedly separated; dorsal setae J4 and J5 short and subequal in length; epistome with distal projection narrow and bifurcate apically (often with small denticle between lateral cusps); length of dorsal shield 910 μm *Pachylaelaps bifurciger* Berlese, 1920
- Tubiform structures broadened, with slightly club-like tip; margins of genitiventral and anal shield undulate and closely abutting each other; setae J5 30–33 μm long, about 4–4.5 times shorter than setae J4; distal projection of epistome wide and densely crenelated anteriorly; length of dorsal shield 780–840 μm *Pachylaelaps undulatus* Evans & Hyatt, 1956
- 14 Tubiform structures short, broad, conical and delicately striated transversally; pilus dentilis relatively well developed, directed backward; dorsal setae J5 47–61 μm

- long, about 1.5–2 times shorter than setae J4; length of dorsal shield 685–835 μm ***Pachylaelaps carpathicus* Mašán, 2007**
- Tubiform structures not detectable (only rudimentary and tenuous structures rarely present); pilus dentilis small, with upright position; setae J5 15–25 μm long, about 3.5–6.5 times shorter than setae J4; length of dorsal shield 740–930 μm ***Pachylaelaps perlucidus* Mašán, 2007**
- 15 Two slit-like poroid structures well separated on posterolateral dorsal surface: gdZ1 situated between setae Z1–Z2 (close to Z2) and gdS4 between setae S4–S5 (close to S4) **16**
- Two slit-like poroid structures with more adjacent position on posterolateral dorsal surface: gdZ1 and gdS4 situated between setae Z2 and S4, or close to setae Z2 **18**
- 16 Cheliceral digits bidentate; length of dorsal shield 880 μm ***Pachylaelaps denticulatus* Hirschmann & Krauss, 1965 sensu Koroleva, 1977**
- Cheliceral digits multidentate: movable digit with 7–12 denticles..... **17**
- 17 Lateromarginal and ventral soft integument with 11 pairs of setae; tubiform structures tenuous, worm-like and hyaline (hardly discernible); length of dorsal shield 615–670 μm ... ***Pachylaelaps multidentatus* Evans & Hyatt, 1956**
- Lateromarginal and ventral soft integument with 14 pairs of setae; tubiform structures relatively broad, tapered apically, directed posteromedially, weakly sclerotized but well discernible; length of dorsal shield 650–750 μm ***Pachylaelaps bellicosus* Berlese, 1920**
- 18 Tubiform structures of sperm induction system Y-shaped, with greatly widened bases, straight and tubular distal sections, and subglobular teat-like apices; basal part V-shaped, with well sclerotized sides..... **19**
- Tubiform structures otherwise formed or not detectable..... **20**
- 19 Openings of slit-like poroids gdZ1 and gdS4 closely adjacent; sternal surface with transversal linear pattern; genitiventral shield longer than wide (length/width 1.05–1.2); length of dorsal shield 720–970 μm ***Pachylaelaps littoralis* Halbert, 1915**
- Openings of slit-like poroids gdZ1 and gdS42 relatively separate; sternal region with transversal-longitudinal linear pattern; genitiventral shield usually subequal in length and width (length/width 0.95–1.1); length of dorsal shield 690–860 μm ***Pachylaelaps pectinifer* (G. & R. Canestrini, 1882)**
- 20 Sperm induction system with short, conical to cylindrical, and evenly sclerotized structures **21**
- Sperm induction system not detectable or with normal, elongated and tubiform structures **24**
- 21 Lateromarginal and ventral soft integument with 9–10 pairs of setae; cheliceral digits slim and elongated: subdistal and submedial tooth of movable digit small, subequal in size and with well separated position; length of dorsal shield 680–800 μm ***Pachylaelaps resinae* Karg, 1971**

- Lateromarginal and ventral soft integument with 15–16 pairs of setae; cheliceral digits relatively shorter: movable digit with more adjacent subdistal and submedial tooth, submedial tooth distinctly larger than small subdistal tooth.....**22**
- 22 Smaller species with dorsal shield under 850 μm in length (sternal shield less than 275 μm in length, genitiventral shield less than 305 μm in width); transversal curved sculptural line on sternal surface between setae st2 discontinuous medially; length of dorsal shield 750–800 μm
.....*Pachylaelaps terreus* Mašán, 2007
- Larger species with dorsal shield more than 850 μm in length (sternal shield more than 275 μm in length, genitiventral shield more than 305 μm in width); transversal curved sculptural line on sternal surface continuous**23**
- 23 Sclerotized structures with sperm ductus stout, widened basally and completely abutting inner surface of coxae IV, and relatively short (with well separate apices); length of dorsal shield 880–1,022 μm
.....*Pachylaelaps insularis* Berlese, 1920
- Sclerotized structures with sperm ductus slim, narrow, and relatively long; length of dorsal shield 950–1,140 μm ..*Pachylaelaps imitans* Berlese, 1920
- 24 Smaller species with dorsal shield under 950 μm in length; tubiform structures of sperm induction system evenly sclerotized and relatively shorter (with their apices sufficiently separated); dorsolateral and ventral soft integument with 11 pairs of setae*Pachylaelaps pyrenaicus* sp. n.
- Larger species with dorsal shield between 1,150 and 1,400 μm in length; tubiform structures not detectable (unsclerotized or absent), or unevenly sclerotized and obviously elongate, with adjacent apical or distal sections; apical or distal section of tubes more sclerotized than basal part; dorsolateral and ventral soft integument with at least 13 pairs of setae.....**25**
- 25 Tubiform structures well developed, relatively long**26**
- Tubiform structures not detectable**28**
- 26 Tubiform structures penis-like, straight or slightly curved, directed anteriorly, with slightly broadened base and more sclerotized tip; length of dorsal shield 1,185–1,330 μm*Pachylaelaps armimagnus* Mašán, 2007
- Tubiform structures more elongated, worm-like to saccule-like, well broadened basally, strongly curved and directed posteriorly**27**
- 27 Distal portions of tubiform structures relatively wide, saccule-like, closely adjacent, and uniformly sclerotized; lateromarginal and ventral soft integument with 13–14 pairs of setae; length of dorsal shield 1,320–1,350 μm
.....*Pachylaelaps sacculimagnus* Mašán, 2007
- Distal portions of tubiform structures narrow, worm-like, well distant, and with thickened terminal sclerotization; lateromarginal and ventral soft integument with 15 pairs of setae; length of dorsal shield 1,180–1,310 μm
.....*Pachylaelaps troglophilus* Willmann, 1940

- 28 Lateromarginal and ventral soft integument with increased number of 20–21 pairs of setae; genitiventral shield relatively narrower (length/width 1.08–1.19); length of dorsal shield 1,245–1,300 μm *Pachylaelaps ensifer* Oudemans, 1904
- Lateromarginal and ventral soft integument with 15 pairs of setae; genitiventral shield relatively wider (length/width 0.96–1.05); length of dorsal shield 1,190–1,400 μm*Pachylaelaps carpathimagnus* Mašán, 2007

Key to European species of the genus *Pachylaelaps* (males)

- 1 Dorsal setae J5 well developed, needle-like; posterolateral margins of dorsal shield with one pair of slit-like poroid structures, gdS4 (subgenus *Longipachylaelaps* Mašán, 2007) **2**
- Setae J5 vestigial; posterolateral margins of dorsal shield with two pairs of slit-like poroid structures, gdZ1 and gdS4 (subgenus *Pachylaelaps* s. str.) **18**
- 2 Apex of cheliceral spermatodactyl with special horseshoe-like process; length of dorsal shield 810 μm *Pachylaelaps virago* Berlese, 1920
- Apex of spermatodactyl regularly formed, never with additional process **3**
- 3 Cheliceral spermatodactyl wider, with obvious basal or medial expansion and narrow distal section **4**
- Spermatodactyl narrower, sword-like to stiletto-like, with almost parallel lateral margins in medial section and moderately tapered distal section **7**
- 4 Cheliceral spermatodactyl widened in basal section and relatively longer (spermatodactyl length/movable digit length 2.9–3.3); dorsal setae J5 less than two times longer than setae J4 **5**
- Spermatodactyl widened in medial section and relatively shorter (spermatodactyl length/movable digit length 1.8–2.3); setae J5 at least two times shorter than setae J4..... **6**
- 5 Dorsal setae J5 and J4 subequal in length; length of dorsal shield unknown *Pachylaelaps pulsator* Hirschmann & Krauss, 1965
- Dorsal setae J5 about 1.5 times shorter than setae J4; length of dorsal shield unknown *Pachylaelaps longicrinitus* Hirschmann & Krauss, 1965
- 6 Dorsal setae J5 less shortened, about 2–3.5 times shorter than setae J4; two petal-like palptibial projections basally fused; length of dorsal shield 670–735 μm *Pachylaelaps distinctus* Mašán, 2007
- Setae J5 more shortened, about 4–7 times shorter than setae J4; two petal-like palptibial projections free; length of dorsal shield 750 μm *Pachylaelaps squamifer* Berlese, 1920
- 7 Petal-like palptibial projections smaller, shorter than cross-sectional radius of palptibia **8**
- Petal-like palptibial projections larger, longer than cross-sectional radius of palptibia **11**

- 8 Dorsal setae J4 and J5 subequal or only negligibly differing in length; dorso-central setae shorter: setae J1 with tips reaching between insertions of setae J1 and J2..... **9**
- Dorsal setae J4 at least 1.5 times longer than setae J5; dorsocentral setae longer: setae J1 with tips reaching or overlapping the insertions of setae J2..... **10**
- 9 Cheliceral spermatodactyl laterally flattened, sword-like, shorter (less than two times the movable digit); most dorsal setae short: $z6 < z6-Z1$, $s4 < s4-s5$, $Z2 < Z2-Z3$; length of dorsal shield 470–510 μm
..... *Pachylaelaps brevipilis* sp. n.
- Spermatodactyl tubular, slightly sinuous, spear-shaped, longer (about three times the movable digit); most dorsal setae long: $z6 > z6-Z1$, $s4 > s4-s5$, $Z2 > Z2-Z3$; length (mean) of dorsal shield 836 μm
..... *Pachylaelaps silviae* Moraza & Peña, 2005
- 10 Cheliceral spermatodactyl widest in distal section; length of dorsal shield unknown *Pachylaelaps granulifer* Hirschmann & Krauss, 1965
- Spermatodactyl widest in basal section; length of dorsal shield unknown.....
..... *Pachylaelaps gibbosus* Hirschmann & Krauss, 1965
- 11 Two palptibial projections with parallel contiguous margins and adjacent apices..... **12**
- Two palptibial projections with divergent contiguous margins and apices well separated..... **13**
- 12 Larger palptibial projection with widely rounded anterior margin; dorsal setae J5 38–51 μm long, about 1.5–2.5 times shorter than setae J4 (70–92 μm long); length of dorsal shield 645–735 μm
..... *Pachylaelaps longulus* Willmann, 1938
- Larger palptibial projection regularly tapered and with obtusely pointed apex; setae J5 about 30 μm long, about four times shorter than setae J4 (120–130 μm long); length of dorsal shield 710–780 μm
..... *Pachylaelaps sublongisetis* Koroleva, 1977
- 13 One of the palptibial projections with needle-like process on distal margin... **14**
- Palptibial projections never with needle-like process on distal margin..... **15**
- 14 Distal margin of larger palptibial projection irregular, with two apices: anteriorly directed apex needle-like, laterally situated apex expanded and widely rounded; cheliceral spermatodactyl wider, with small subapical incision; length of dorsal shield 640–715 μm *Pachylaelaps carpathicus* Mašán, 2007
- Distal margin of larger palptibial projection regularly curved, with one needle-like apex directed laterally; spermatodactyl narrower, with regularly tapered apex; length of dorsal shield 870–950 μm
..... *Pachylaelaps bocharovae* Koroleva, 1978
- 15 Cheliceral spermatodactyl relatively longer (spermatodactyl length/movable digit length 1.8–2.4)..... **16**
- Spermatodactyl relatively shorter (spermatodactyl length/movable digit length 1.6–1.8)..... **17**

- 16 Terminal hook of cheliceral fixed digit bifid; cheliceral spermatodactyl relatively shorter (spermatodactyl length/movable digit length 1.8–2); length of dorsal shield 745–900 μm ***Pachylaelaps perlucidus* Mašán, 2007**
- Terminal hook of cheliceral fixed digit simple; spermatodactyl relatively longer (spermatodactyl length/movable digit length 2.2–2.4); length of dorsal shield unknown ***Pachylaelaps conifer* Hirschmann & Krauss, 1965**
- 17 Dorsal setae relatively longer: setae J3 with tips reaching to the bases of setae J5; cheliceral spermatodactyl relatively shorter (spermatodactyl length/movable digit length 1.6); length of dorsal shield unknown.....
- ***Pachylaelaps decipiens* Hirschmann & Krauss, 1965**
- Dorsal setae relatively shorter: setae J3 with tips reaching between the bases of setae J3 and J5; spermatodactyl relatively longer (spermatodactyl length/movable digit length 1.8); length of dorsal shield unknown.....
- ***Pachylaelaps hestulifer* Hirschmann & Krauss, 1965**
- 18 Tarsus II with one spur-like distal seta (pl1) **19**
- Tarsus II with two spur-like distal setae (pl1, pl2)..... **23**
- 19 Palptibial projections wider, each with widely rounded apex; cheliceral spermatodactyl with at least one small lobe-like convexity situated on ventral proximal margin **20**
- Palptibial projections narrower, at least one of them with needle-like apex; cheliceral spermatodactyl with straight margins, without lobe-like convexities on its margins **21**
20. Two slit-like poroid structures on posterolateral dorsal surface well separated: gdZ1 situated between setae Z1–Z2 (close to Z2) and gdS4 between setae S4–S5 (close to S4); length of dorsal shield 760–840 μm ***Pachylaelaps denticulatus* Hirschmann & Krauss, 1965 sensu Koroleva, 1977**
- Two slit-like poroid structures with more adjacent position on posterolateral dorsal surface: gdZ1 and gdS4 situated close to setae Z2.....
- ***Pachylaelaps pyrenaicus* sp. n.**
- 21 Cheliceral spermatodactyl with two small lobe-like convexities situated on dorsal distal margin and ventral proximal margin; length of dorsal shield 740 μm ***Pachylaelaps terreus* Mašán, 2007**
- Spermatodactyl with one small lobe-like convexity situated on ventral proximal margin **22**
- 22 Larger species, dorsal shield more than 750 μm in length; length of dorsal shield 980 μm ***Pachylaelaps imitans* Berlese, 1920**
- Smaller species, dorsal shield less than 750 μm in length; length of dorsal shield 610–665 μm ***Pachylaelaps resinae* Karg, 1971**
- 23 Palptibia smooth, without projections **24**
- Palptibia with projections **25**
- 24 Openings of slit-like poroids gdZ1 and gdS4 closely adjacent; projection on genu II small, subconical, with thin and rounded apex; cheliceral sperma-

- todactyl about 1.5 times longer than movable digit; length of dorsal shield 700–830 μm *Pachylaelaps littoralis* Halbert, 1915
 – Openings of slit-like poroids gdZ1 and gdS42 relatively separate; projection on genu II robust, subcylindrical, with flat to truncate apex; spermatodactyl about two times longer than movable digit; length of dorsal shield 650–770 μm *Pachylaelaps pectinifer* (G. & R. Canestrini, 1882)
 25 Smaller species with dorsal shield less than 1,000 μm in length; palptibia with two projections; cheliceral spermatodactyl relatively shorter (spermatodactyl length/movable digit length about 1.6); length of dorsal shield 825–840 μm ...
 *Pachylaelaps insularis* Berlese, 1920
 – Larger species with dorsal shield more than 1,000 μm in length; palptibia with 2–4 projections; cheliceral spermatodactyl relatively longer (spermatodactyl length/movable digit length more than 2.5)..... 26
 26 Palptibia thickened: palptibial petal-like projections well developed and sclerotized, longer than cross-sectional radius of palptibia; proximal section of cheliceral spermatodactyl relatively wide and with punctate ornamentation on surface 27
 – Palptibia normal: palptibial petal-like projections weakly developed and sclerotized, shorter than cross-sectional radius of palptibia; proximal section of spermatodactyl relatively narrow and without punctation 29
 27 Palptibia with two petal-like projections and a setiform structure, smaller petal-like projection with spinous apex; cheliceral spermatodactyl with small convexity on ventral proximal margin; length of dorsal shield 1,080–1,170 μm *Pachylaelaps troglophilus* Willmann, 1940
 – Palptibia with three petal-like projections (one of them with spinous apex) and a setiform structure; spermatodactyl without small convexity on ventral margin 28
 28 Setiform structure associated with palptibial projections simple, tenuous and tubular; cheliceral spermatodactyl with regularly convergent lateral margins, lanceolate in subdistal part; length of dorsal shield 1,245–1,255 μm
 *Pachylaelaps armimagnus* Mašán, 2007
 – Setiform structure associated with palptibial projections flattened, plank-like, bifurcate apically, with two sharp points; spermatodactyl knife-like, with almost parallel lateral margins, slight subapical narrowing and rostrum-like tip; length of dorsal shield 1,230–1,360 μm
 *Pachylaelaps sacculimagnus* Mašán, 2007
 29 Palptibia with two separate or fused scale-like projections, the projections with rounded or obtusely pointed distal margin; length of dorsal shield 1,235–1,245 μm *Pachylaelaps ensifer* Oudemans, 1904
 – Palptibia with four scale-like projections, the largest lateral projection hook-shaped subapically, sharply pointed; length of dorsal shield 1,170–1,325 μm *Pachylaelaps carpathimagnus* Mašán, 2007

Acknowledgements

This study was supported by the Scientific Grant Agency of the Ministry of Education of Slovak Republic and the Academy of Sciences [VEGA Grant No. 2/0091/14: Arboricolous mites (Acari: Mesostigmata) associated with wood-destroying insects and fungi in Slovakia, with consideration on taxonomy, ecology and chorology of individual species.].

References

- Berlese A (1888) Acari austro-americi quos collegit Aloysius Balzan. Manipulus primus. Species novas circiter quinquaginta complectens. Bolletino della Società Entomologica Italiana 20: 171–222. [Plates 5–13]
- Berlese A (1892) Acari, Myriopoda et Scorpiones hucusque in Italia reperta. Ordo Mesostigmata (Gamasidae). Sumptibus Auctoris, Patavii, 143 pp.
- Berlese A (1904) Illustrazione iconografica degli Acari mirmecofili. Redia 1: 299–474. [Plates VII–XX]
- Costa M (1971) Mites of the genus *Pachylaelaps* Berlese (Acari: Mesostigmata, Pachylaelapidae) from litter in Israel. Israel Journal of Zoology 20: 253–277.
- Evans GO, Hyatt KH (1956) British mites of the genus *Pachylaelaps* Berlese (Gamasina – Pachylaelaptidae). Entomologist's Monthly Magazine 92: 118–129.
- Hadley A (2010) CombineZP. <http://www.hadleyweb.pwp.blueyonder.co.uk/>
- Hirschmann W, Krauss W (1965) Gangsystematik der Parasitiformes. Teil 8. Gamasiden. Bestimmungstabellen von 55 *Pachylaelaps*-Arten. Acarologie, Schriftenreihe für vergleichende Milbenkunde 7: 1–5. [Plates 1–28]
- Johnston DE, Moraza ML (1991) The idiosomal adenotaxy and poroidotaxy of Zerconidae (Mesostigmata: Zerconina). In: Dusbábek F, Bukva V (Eds) Modern Acarology. Academia Press, Prague, Vol. 2, 349–356.
- Karg W (1971) Acari (Acarina), Milben, Unterordnung Anactinochaeta (Parasitiformes). Die freilebenden Gamasina (Gamasides), Raubmilben. Die Tierwelt Deutschlands 59: 1–475.
- Karg W (1993) Acari (Acarina), Milben. Parasitiformes (Anactinochaeta). Cohors Gamasina Leach. Raubmilben. 2. Überarbeitete Auflage. Die Tierwelt Deutschlands 59: 1–523.
- Koroleva EV (1977a) Family Pachylaelaptidae Vitzthum, 1931. In: Ghilyarov MS, Bregetova NG (Eds) Key to the Soil Inhabiting Mites, Mesostigmata. Nauka Press, Leningrad, 411–483. [In Russian]
- Koroleva EV (1977b) Novye vidy kleshchei roda *Pachylaelaps* Berlese, 1888 (Parasitiformes, Pachylaelaptidae). Parazitologicheskyy Sbornik 27: 119–148.
- Koroleva EV (1978) A new species of the genus *Pachylaelaps* (Parasitiformes, Pachylaelaptidae) from North Osetia and cycle of its development. Zoologicheskyy Zhurnal 57: 1430–1434. [In Russian]
- Lindquist EE, Evans GO (1965) Taxonomic concepts in the Ascidae, with a modified setal nomenclature for the idiosoma of the Gamasina (Acarina: Mesostigmata). Memoirs of the Entomological Society of Canada 47: 1–64. doi: 10.4039/entm9747fv

- Mašán P (2007) A Review of the family Pachylaelapidae in Slovakia, with systematics and ecology of European species (Acari: Mesostigmata: Eviphidoidea). NOI Press, Bratislava, 247 pp.
- Mašán P, Halliday B (2014) Review of the mite family Pachylaelapidae (Acari: Mesostigmata). *Zootaxa* 3776: 1–66. doi: 10.11646/zootaxa.3776.1.1
- Moraza ML, Peña MA (2005) The family Pachylaelapidae Vitzthum, 1931 on Tenerife Island (Canary Islands), with description of seven new species of the genus *Pachylaelaps* (Acari, Mesostigmata: Pachylaelapidae). *Acarologia* 45: 103–129.
- Özbek HH (2015) An unusual new species of *Pachylaelaps* (Acari: Pachylaelapidae) from Turkey. *International Journal of Acarology* 41: 67–70. doi: 10.1080/01647954.2014.988645

Fangumellus flavobadius: a new genus and species of plant bug from Laos (Heteroptera, Miridae, Mirinae, Mirini)

Tomohide Yasunaga¹, Minsuk Oh², Seunghwan Lee^{2,3}

1 Research Associate, Division of Invertebrate Zoology, American Museum of Natural History, New York c/o Nimeshi 2-33-2, Nagasaki 852-8061, Japan **2** Biosystematics Laboratory, Research Institute for Agriculture and Life Sciences, Seoul National University, Seoul 151-921, Republic of Korea **3** Department of Agricultural Biotechnology, Seoul National University, Seoul 151-921, Republic of Korea

Corresponding author: *Seunghwan Lee* (seung@snu.ac.kr)

Academic editor: *G. Zhang* | Received 1 May 2016 | Accepted 16 June 2016 | Published 6 July 2016

<http://zoobank.org/DA5D9159-AB1A-4517-B897-4B04C9C02FBC>

Citation: Yasunaga T, Oh M, Lee S (2016) *Fangumellus flavobadius*: a new genus and species of plant bug from Laos (Heteroptera, Miridae, Mirinae, Mirini). ZooKeys 603: 97–103. doi: 10.3897/zookeys.603.9063

Abstract

A new species of the plant bug tribe Mirini representing a new genus, *Fangumellus flavobadius*, is described from Laos. This genus is characterized primarily by the medium-sized, ovoid, tumid body, less shiny, roughened, almost impunctate dorsal surface, short antenna and labium, short pygophore, and atypical shape of parameres and endosoma. The phylogenetic relationship to other known mirine genera is also discussed.

Keywords

Miridae, Mirinae, Mirini, new genus, new species, *Fangumellus flavobadius*, Laos, taxonomy

Introduction

Fauna of the plant bug family Miridae in the Lao People's Democratic Republic is still in great need of investigation. This paper represents a part of recent attempt to document the plant bug fauna of Laos, subsequent to Oh et al. (2015) and Yasunaga and Duwal (2015).

The present work documents an undescribed species of the plant bug family Miridae, which cannot be placed in any known genera. This bug, belonging to the tribe Mirini of the subfamily Mirinae, has several atypical features, in particular the shape of the pygophore and parameres, although its conventional ovoid body form is reminiscent of some taxa of *Lygus*-complex. Among nearly 300 described genera in the Mirini, approximately 40 genera may be assigned to this complex group in Asia (Schwartz and Footitt 1998, Yasunaga et al. 2002). We herein describe a new genus *Fangumellus* to accommodate this peculiar new mirid species, *F. flavobadius*, and discuss its phylogenetic position.

Materials and methods

The holotype is deposited in Biosystematics Laboratory, Research Institute for Agriculture and Life Sciences, Seoul National University, Seoul, Korea (SNUK). Matrix code label is attached to the holotype, which uniquely identifies each specimen and is referred to as ‘unique specimen identifiers’ (USIs). The USI code [AMNH_PBI 0123] comprises a dataset code (AMNH_PBI) and a unique specimen number (0123). These data were digitized on the Arthropod Easy Capture (formerly the Planetary Biodiversity Inventory) database maintained by the American Museum of Natural History, New York, USA (<http://research.amnh.org/pbi/>) and are incorporated with <http://www.discoverlife.org>.

All measurements are in millimeters. Terminology of the male genitalia follows Schwartz and Footitt (1998) and Yasunaga and Schwartz (2007). Further information on known taxa mentioned in the text is available on website (Schuh 2002–2014). Digital images used in this paper were captured using a Diagnostic Instruments Insight Camera 14.2 Color Mosaic, with a SPOT Insight System. The following abbreviations are used for the male genitalia (Fig 2): GP, secondary gonopore; HP, hypophysis; PT, phallosome; SD, seminal duct; SL, sensory lobe; SP, spiculum.

Results

Fangumellus gen. n.

<http://zoobank.org/09B11573-23B5-4AEB-A0D1-6A6B437FCAB7>

Type species. *Fangumellus flavobadius* sp. n.

Diagnosis. Distinguished from other genera in tribe Mirini by the following combination of characters: Medium-sized, ovoid, tumid body; less shining, partly matte, almost impunctate dorsal surface; short antenna and labium; short pygophore; and unique shape of parameres and endosoma (Fig. 2), especially sinuate distal portion of right paramere.

Description. Male: Body medium-sized, ovoid, tumid (Fig. 1A); dorsal surface weakly shining, with uniformly distributed, pale brown, short, reclining setae. **Head:**

Vertical, smooth; eye rather small; vertex weakly carinate basally; frons neither serrate nor sulcate; clypeus weakly swollen (Fig. 1C). **Antenna:** Generally short, not thickened or clavate, lacking noticeable long setae or spines; segment I subequal in length to IV; segment II almost linear, about as thick as I, shorter than basal width of pronotum; segments III and IV filiform. **Labium:** Short, slender, reaching subapical part of mesocoxa (Fig. 1B). **Thorax:** Pronotum shagreened or matte, shallowly and irregularly punctate, with narrow calli, not carinate laterally; collar somewhat arched, about as thick as base of antennal segment II; scutellum weakly shining, rather tumid, shallowly and transversely wrinkled; pleura weakly shagreened or matte; metathoracic scent efferent system as in Fig. 1D. **Hemelytron:** Less shining, weakly shagreened, with uniformly distributed, whitish, silky, reclining setae. **Legs:** Generally short; tibial spines dark, short, sparsely distributed; meta-tarsomere I subequal in length to II; meta-tarsomere III longer than I or II. **Genitalia** (Fig. 2): Pygophore short, with triangular apex (Fig. 2A). Parameres quite atypical in shape, generally slender and elongate (Fig. 2A–D); left paramere with hooked apex of hypophysis and a thumblike, blunt-tipped protuberance on sensory lobe (Fig. 2D); right paramere sigmoid, with somewhat spiral or coiled hypophysis (Fig. 2C). Endosoma as in Fig. 2A–D, with a slender, apically hooked spiculum; secondary gonopore thick-rimmed, without any accompanied sclerite; seminal duct well expanded subapically (Fig. 2H); phallosome slender, with a folded apex (Fig. 2F). **Female:** Unknown.

Etymology. Named after the King ‘Fa Ngum’ who first established a unified kingdom (Lan Xang Kingdom) in Laos in 14th century, combined with Latin diminutive (-ellus); masculine.

Discussion. This new genus is at first sight reminiscent of *Pachylygus* Yasunaga or some taxa of *Lygus* (in broad sense, see Schwartz and Footitt 1998, Yasunaga et al. 2002). However, the less punctate and rather shagreened dorsal surface and atypical shape of the parameres suggest that *Fangumellus* is evidently not closely related to those taxa. It is our opinion that comparison with *Paramiridius* Miyamoto & Yasunaga may merit careful consideration. One of *Paramiridius* species recently described from Laos, *P. laomontanus* Oh, Yasunaga & Lee, has some similarities in general appearance and male genitalia (e.g., ovoid body, impunctate dorsum, short labium, slender and apically hooked left paramere, thick-rimmed secondary gonopore, and apically expanded seminal duct) (Oh et al. 2015). Nonetheless, some of these similarities appear homoplasious or are shared by other mirine taxa. We currently cannot determine any sister taxon closely related to *Fangumellus*; a broader survey including the female genitalic structure is required to demonstrate its closest relative.

We can only suggest herein that the two unique characters exhibited on the parameres are in all likelihood autapomorphies for the new taxon (sigmoid, spiral, elongate hypophysis of right paramere and a thumb-like, subbasal protuberance of left paramere, which are not possessed by any other known mirine genera). In addition, the surface structure of *Fangumellus* (e.g., shagreened, impunctate dorsum with rather stiff vestiture) may be presumed as a derived character.

***Fangumellus flavobadius* sp. n.**

<http://zoobank.org/31A8801B-B1B5-45CA-96BB-3E1C9E1AF025>

Figs 1–2

Type material. Holotype male. LAOS: Xiang Khoang Prov., Kham Dist., Phosabous National Protected Area, Namchack Village, [N19°50'57", E103°47'51", 670m alt.], light trap, 2 May 2015, Oh (Coll. No: 150429-MS-29) (AMNH_PBI 00380463).

Diagnosis. Recognized by the characters mentioned in generic diagnosis and distinctive color pattern. Most similar in general appearance to certain species of *Lygus* Hahn, *Pachylygus* Yasunaga or *Peltdolygus* Poppius (cf. Schwartz and Foottit 1998, Yasunaga et al. 2002); distinguished by somewhat shagreened pronotum without clear punctures, rather flat, not developed scutellum and unique shape of parameres.

Description. Male: Body yellow, partly tinged with olive green (yellow parts assumed to be more or less greenish when alive); dorsal surface weakly shining, rather matte or roughened, with reddish brown pattern on hemelytron (Fig. 1A). **Head:** Pale brown, shining (Fig. 1C); apex of clypeus narrowly rouge (Fig. 1D). **Antenna:** Dark brown; basal quarter of segment II pale reddish brown; basal 1/3 parts of segments II and III creamy yellow. Labium shiny pale brown; apical half of segment IV darkened (Fig. 1B, D). **Thorax:** Pronotum yellowish brown, weakly wrinkled and faintly punctate, with pale olive disk; calli and collar yellowish brown; mesoscutum pale brown; scutellum olive green, shallowly wrinkled; pleura including scent efferent system yellowish brown; propleuron faintly punctate as in disk (Fig. 1D). **Hemelytron:** Pale brown, weakly shining, with two reddish brown, noticeable maculae at base of corium across base of clavus and at posterior half of corium to embolium (Fig. 1A); clavus with an obscure mark at middle and narrowly reddish brown apex; cuneus yellowish brown, with darkened apex; membrane smoky brown, with a yellow spot posterior to apex of cuneus. **Legs:** Coxae and legs yellowish brown (Fig. 1B); each coxa and trochanter slightly tinged with olive; apex of metafemur slightly darkened; apices of all tibia reddish brown; all tarsi pale reddish brown; each tarsomere III dark brown. **Abdomen:** Yellow, widely tinged with green; median parts of abdominal tergites sanguineous. Male genitalia as mentioned in generic description. **Female:** Unknown.

Measurements (in mm). Holotype male: Total body length 5.72; head width including eyes 1.18; head height 0.82; vertex width 0.46; lengths of antennal segments I–IV 0.56, 1.80, 0.73, 0.55; total length of labium 1.56; mesal pronotal length 1.18; basal pronotal width 2.21; maximum width across hemelytron 2.63; lengths of metafemur, tibia and tarsus 1.80, 2.57, 0.62; and lengths of meta-tarsomeres I–III 0.21, 0.22, 0.35.

Etymology. From Latin, flavus (= yellow) combined with badius (= maroon or chestnut brown), referring to the basic color pattern of this new species; an adjective.

Distribution. Laos (Xiang Khoang).

Biology. Unknown; only one male was collected using UV light trap.

Discussion. This new species evidently represents a member of *Lygus* sensu lato. In the key to species of this complex group from Indo-Australian region (Poppius 1914),

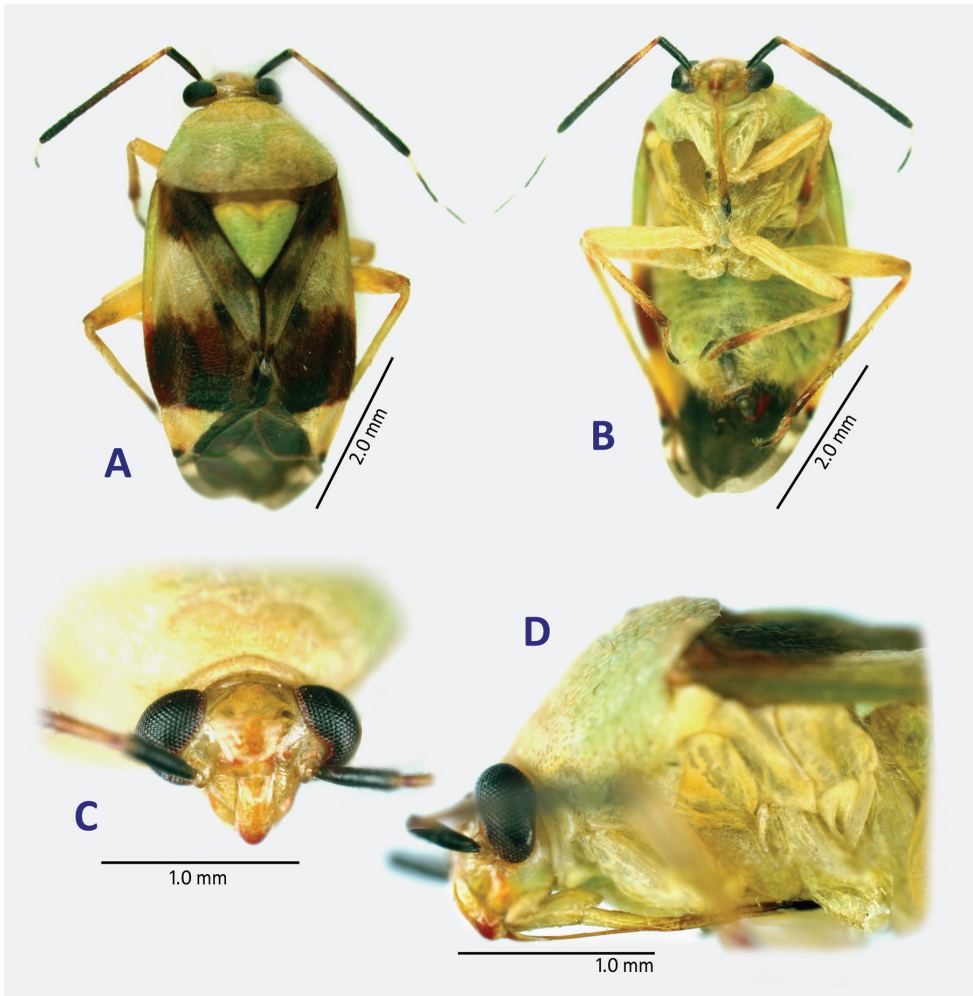


Figure 1. Habitus images of *Fangumellus flavobadius*, holotype male. **A** dorsal view **B** ventral view **C** head in frontal view **D** head and thorax in left lateral view.

Fangumellus flavobadius actually keys out to *Lygus* [s.l.] *dohrni* Poppius, 1914, described from Sumatra, Indonesia. However, this mirid is distinct in having the following characters: Body elongate and large (6.5 mm in total length, 2.5 mm maximum width); apex of clypeus; dark membrane with yellow veins; antennal segment II 2.5 times as long as segment I; scutellum flat; clavus and corium rather strongly punctate than pronotum; and tibiae with brown spines, each of which has a dark, small dot. Judging from the original description by Poppius (1914), his taxon is more probably close to *Castanopsides* Yasunaga-*Mahania* Poppius group (cf. Yasunaga and Duwal 2006). Although several recent works (e.g., Schwartz and Chérot 2005) carefully revised the generic placements for the species assigned to the *Lygus*-complex, dozens of species are still placed in *Lygus* sensu lato, and, needless to say, require further critical revisions.

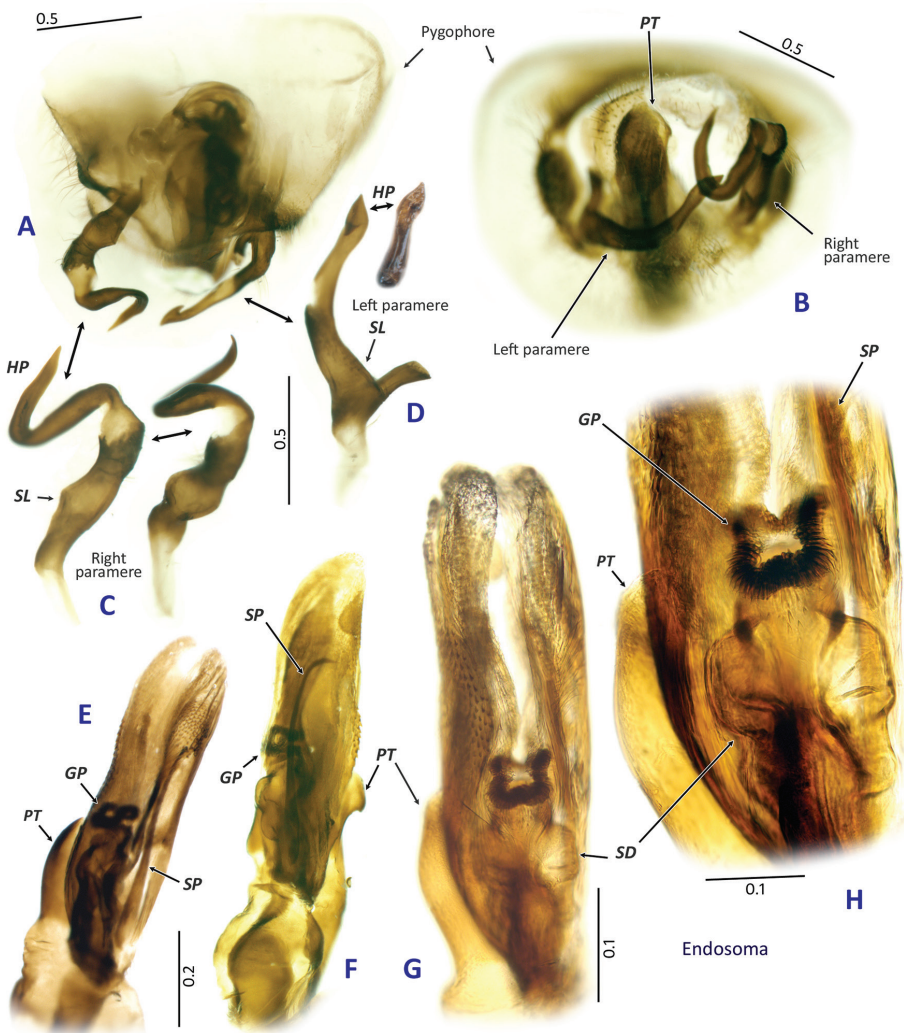


Figure 2. Male genitalia of *Fangumellus flavobadius*. **A** pygophore in ventral view **B** pygophore in caudal view **C** right paramere **D** left paramere **E–H** endosoma. Abbreviations corresponding to those mentioned in materials and methods section.

Acknowledgements

The authors express their gratitude to Dr. Michael D. Schwartz (Agriculture & Agri-Food Canada, Ottawa, Ontario), an anonymous reviewer, and Dr. Guanyang Zhang (subject editor, ZooKeys), for improving the manuscript with valuable comments. This work was supported by a grant from the National Institute of Biological Resources (NIBR), funded by the Ministry of Environment (MOE) of the Republic of Korea (NIBR201504201).

References

- Oh M, Yasunaga T, Lee S (2015) First record of the plant bug genus *Paramiridius* Miyamoto & Yasunaga (Heteroptera, Miridae, Mirinae) from Indochina, with descriptions of two new species from Laos. *ZooKeys* 546: 51–59. doi: 10.3897/zookeys.546.6335
- Poppius B (1914) Zur Kenntnis der Indo-Australischen *Lygus*-Arten. *Annales Historico-Naturales Musei Nationalis Hungarici* 12: 337–398.
- Schuh RT (2002–2014) On-line Systematic Catalog of Plant Bugs (Insecta: Heteroptera: Miridae). Available from: <http://research.amnh.org/pbi/catalog/> [Accessed 1 May 2016]
- Schwartz MD, Chérot F (2005) *Miscellanea Miridologica* (Insecta: Heteroptera). *Zootaxa* 814: 1–24.
- Schwartz MD, Footitt RG (1998) Revision of the Nearctic species of the genus *Lygus* Hahn, with review of the Palearctic species (Heteroptera: Miridae). *Memoirs on Entomology, International* 10: 1–428.
- Schwartz MD, Kerzhner IM (1997) Type specimens and identity of some Chinese species of the “*Lygus* complex” (Heteroptera: Miridae). *Zoosystematica Rossica* 5: 249–256.
- Yasunaga T, Duwal RK (2008) New species of the mirine plant bug genus *Castanopsides* Yasunaga and its assumed sister genus *Mabania* Poppius from Nepal, with a new synonymy of the genus *Liocapsus* Poppius (Heteroptera, Miridae, Mirinae). In: Grozeva S, Simov, N (Eds) *Advances in Heteroptera Research*. Pensoft Publishers, Sofia and Moscow, 403–417.
- Yasunaga T, Duwal RK (2015) Further records and descriptions of the plant bug subfamily Phylinae (Hemiptera: Heteroptera: Miridae) from Thailand. *Zootaxa* 3981(2): 193–219. doi: 10.11646/zootaxa.3981.2.3
- Yasunaga T, Schwartz MD (2007) Revision of the mirine plant bug genus *Philostephanus* Distant and allies (Heteroptera: Miridae: Mirinae: Mirini). *Tijdschrift voor Entomologie* 150: 100–180. doi: 10.1163/22119434-900000216
- Yasunaga T, Schwartz MD, Chérot F (2002) New genera, species, synonymies, and combinations in the “*Lygus* complex” from Japan, with discussion on *Peltidolygus* Poppius and *Warrisia* Carvalho (Heteroptera: Miridae: Mirinae). *American Museum Novitates* 3378: 1–26. doi: 10.1206/0003-0082(2002)378<0001:NGSSAC>2.0.CO;2

Taxonomic revision of the Malagasy *Nesomyrmex madecassus* species-group using a quantitative morphometric approach

Sándor Csősz¹, Brian L. Fisher¹

¹ Entomology, California Academy of Sciences, 55 Music Concourse Drive, San Francisco, CA 94118, U.S.A.

Corresponding author: Sándor Csősz (sandorcsosz2@mail.com)

Academic editor: M. Borowiec | Received 26 February 2016 | Accepted 15 July 2016 | Published 6 July 2016

<http://zoobank.org/D44B76A7-9C02-45D8-B9F4-996BFCB01579>

Citation: Csősz S, Fisher BL (2016) Taxonomic revision of the Malagasy *Nesomyrmex madecassus* species-group using a quantitative morphometric approach. ZooKeys 603: 105–130. doi: 10.3897/zookeys.603.8271

Abstract

Here we reveal the diversity of the next fragment of the Malagasy elements of the ant genus *Nesomyrmex* using a combination of advanced exploratory analyses on quantitative morphological data. The diversity of the *Nesomyrmex madecassus* species-group was assessed via hypothesis-free *nest centroid clustering* combined with *recursive partitioning* to estimate the number of clusters and determine the most probable boundaries between them. This combination of methods provides a highly automated species delineation protocol based on continuous morphometric data, and thereby it obviates the need of subjective interpretation of morphological patterns. Delimitations of clusters recognized by these exploratory analyses were tested via confirmatory Linear Discriminant Analysis (LDA). Our results suggest the existence of four morphologically distinct species, *Nesomyrmex flavus* **sp. n.**, *N. gibber*, *N. madecassus* and *N. nitidus* **sp. n.**; all are described here and an identification key for their worker castes using morphometric data is given. Two members of the newly outlined *madecassus* species-group, *N. flavus* **sp. n.** and *N. nitidus* **sp. n.**, represent true cryptic species. Geographic maps depicting species distributions and elevational information for the sites where populations of particular species were collected are also provided.

Keywords

Madagascar, taxonomy, morphometry, species delimitation, exploratory analyses, gap statistic, biogeography

Introduction

The ant fauna of the Malagasy zoogeographical region, i.e. Madagascar and its surrounding islands (Bolton 1994), has recently been the subject of intensive systematic research (Fisher 2009, Blaimer and Fisher 2013, Yoshimura and Fisher 2012, Hita-Garcia and Fisher 2014). Thanks to these efforts to explore Malagasy biodiversity, our knowledge of the island's myrmecofauna has increased considerably. These latest findings support earlier assumptions about the high species diversity of the region. The goal of the current paper is to contribute to this endeavor and clarify the taxonomy of another segment of the Malagasy *Nesomyrmex* fauna, the *Nesomyrmex madecassus* species-group.

The four species in this group are known to nest in small diameter (pencil size) dead twigs above ground. They can be found foraging on tree trunks and occasionally in the leaf litter at higher elevations. There is also the occasional record of nests in rotten logs at higher elevations. But in general, to collect these species, the best approach is to break open small dead twigs. We know little of their biology but field observations suggest they are generalist scavengers. Morphological diversity is assessed via a taxonomic protocol NC-PART clustering introduced by Csősz and Fisher (2016a, 2016b) based on multivariate analyses of quantitative morphological data. This method incorporates elements of NC-clustering (Seifert et al. 2014) and the partitioning algorithms known as 'part' (Nilsen et al. 2013). Benefits of the combined application of Nest Centroid clustering (NC clustering) and Partitioning Algorithm based on Recursive Thresholding (PART) was described in detail in Csősz and Fisher (2016a, 2016b) and its efficiency in species delimitation has proven in two *Nesomyrmex* species-groups and in a fragment of the Malagasy *Camponotus* fauna (Rakotonirina et al. 2016). The NC clustering searches for discontinuity in morphometric data by sorting all similar cases into clusters in a two-step procedure. This technique has proved efficient at pattern recognition within large and complex datasets, but the number of clusters is still subjectively defined based on the obtained dendrogram. The partitioning method PART allows for estimation on the number of clusters via recursive application of the Gap statistic (Tibshirani et al. 2001) algorithm and automated assignment of each sample in either clusters.

Multivariate evaluation of morphological data has revealed that the *N. madecassus* species-group incorporates four well-outlined clusters in the Malagasy zoogeographical region, all representing species. Two of them, *Nesomyrmex gibber* (Donisthorpe, 1946) and *N. madecassus* (Forel, 1892) are already described taxa, but two new species, *N. flavus* sp. n. and *N. nitidus* sp. n., are being described here based on worker caste. The latter two species represent true cryptic species (Seifert 2009) which can be convincingly separated by using a combination of morphometric data. We provide a combined key that uses a traditional, character-based key, and a separation of the two cryptic taxa, *N. flavus* sp. n. and *N. nitidus* sp. n. is supported by a character combination. Morphological patterns are linked to geographic map elevations of the sites where populations were collected and are also provided as predictor variables.

Material and methods

The group was defined earlier by Csósz and Fisher (2015) as one of the four remarkable lineages occurring in the region, and defined as follows: “Pronotal spines absent. Anterodorsal spines on petiolar node absent. Propodeal spines short, lamelliform to absent. Vertex ground sculpture smooth. Vertex main sculpture not defined. Metanotal depression present. Median clypeal notch present or absent. Median clypeal notch shape/depth 0–15 μm . Antennomere count: 12. Absolute cephalic size (CS): 571 μm [405, 785]. Cephalic length vs. maximum width of head capsule (CL/CWb): 1.231 [1.092, 1.567]. Postocular distance vs. cephalic length (PoOc/CL): 0.479 [0.407, 0.544]. Scape length vs. absolute cephalic size (SL/CS): 0.718 [0.492, 0.831]. Eye length vs. absolute cephalic size (EL/CS): 0.249 [0.1934, 0.279]. Petiole width vs. absolute cephalic size (PEW/CS): 0.217 [0.181, 0.256]. Postpetiole width vs. absolute cephalic size (PPW/CS): 0.331 [0.243, 0.398]. Petiolar node height vs. absolute cephalic size (PEW/CS): 0.122 [0.072, 0.158].

In the present study, 18 continuous morphometric traits were recorded in 231 worker individuals belonging to 172 nest samples collected in the Malagasy region.

The material is deposited in the following institutions, abbreviations after Evenhuis (2013): CASC (California Academy of Sciences, San Francisco, California, U.S.A.), MCZ (Museum of Comparative Zoology, Cambridge, Massachusetts, U.S.A.), MHNG (Muséum d’Histoire Naturelle, Geneva, Switzerland) and Phil S. Ward’s collection (University of California Davis Davis, California, U.S.A.).

All images and specimens used in this study are available online on AntWeb (<http://www.antweb.org>). Images are linked to their specimens via the unique specimen code affixed to each pin (CASENT0101667). Online specimen identifiers follow this format: <http://www.antweb.org/specimen/CASENT0101667>.

Digital color montage images were created using a JVC KY-F75 digital camera and Syncroscopy Auto-Montage software (version 5.0), or a Leica DFC 425 camera in combination with the Leica Application Suite software (version 3.8). Distribution maps were generated in R (R Core Team 2015) via ‘*phylo.to.map*’ function using package *phytools* (Revell 2012).

The measurements were taken with a Leica MZ 12.5 stereomicroscope equipped with an ocular micrometer at a magnification of 100 \times . Measurements and indices are presented as arithmetic means with minimum and maximum values in parentheses. Body size dimensions are expressed in μm . Due to the abundance of worker individuals available relative to queen and male specimens, the present revision is based on worker caste only. Worker-based revision is further facilitated by the fact that the name-bearing type specimens of the vast majority of existing ant taxa belong to the worker caste. All measurements were made by the first author. For the definition of morphometric characters, earlier protocols (Csósz et al. 2015, Csósz and Fisher 2015, 2016a, 2016b) were considered. Explanations and abbreviations for measured characters are as follows:

- CL** Maximum cephalic length in median line. The head must be carefully tilted to the position providing the true maximum. Excavations of hind vertex and/or clypeus reduce CL.
- CW** Maximum width of the head. Includes compound eyes.
- CWb** Maximum width of head capsule without the compound eyes. Measured just posterior of the eyes.
- CS** Absolute cephalic size. The arithmetic mean of CL and CWb.
- EL** Maximum diameter of the compound eye.
- FRS** Frontal carina distance. Distance of the frontal carinae immediately caudal of the posterior intersection points between frontal carinae and the torular lamellae. If these dorsal lamellae do not laterally surpass the frontal carinae, the deepest point of scape corner pits may be taken as the reference line. These pits take up the inner corner of the scape base when the scape is directed caudally and produces a dark triangular shadow in the lateral frontal lobes immediately posterior to the dorsal lamellae of the scape joint capsule.
- ML (Weber length)** Mesosoma length from caudalmost point of propodeal lobe to transition point between anterior pronotal slope and anterior pronotal shield. Preferentially measured in lateral view; if the transition point is not well defined, use dorsal view and take the center of the dark-shaded borderline between pronotal slope and pronotal shield as anterior reference point. In gynes: length from caudalmost point of propodeal lobe to the most distant point of steep anterior pronotal face.
- MW** Mesosoma width. In workers MW is defined as the longest width of the pronotum in dorsal view excluding the pronotal spines.
- MPST** Maximum distance from the center of the propodeal stigma to the anteroventral corner of the ventrolateral margin of the metapleuron.
- NOH** maximum height of the petiolar node. Measured in lateral view from the uppermost point of the petiolar node perpendicular to a reference line extending from the petiolar spiracle to the imaginary midpoint of the transition between dorso-caudal slope and dorsal profile of caudal cylinder of the petiole.
- NOL** Length of the petiolar node. Measured in lateral view from the center of petiolar spiracle to dorso-caudal corner of caudal cylinder. Do not erroneously take as the reference point the dorso-caudal corner of the helcium, which is sometimes visible.
- PEH** maximum petiole height. The chord of the ventral petiolar profile at node level is the reference line perpendicular to the line describing the maximum height of petiole.
- PEL** Diagonal petiolar length in lateral view; measured from anterior corner of subpetiolar process to dorso-caudal corner of caudal cylinder.
- PEW** Maximum width of petiole in dorsal view. Nodal spines are not considered.
- PoOC** Postocular distance. Use a cross-scaled ocular micrometer and adjust the head to the measuring position of CL. Caudal measuring point: median

- occipital margin; frontal measuring point: median head at the level of the posterior eye margin.
- PPH** Maximum height of the postpetiole in lateral view. Measured perpendicularly to a line defined by the linear section of the segment border between dorsal and ventral petiolar sclerite.
- PPL** Postpetiole length. The longest anatomical line that is perpendicular to the posterior margin of the postpetiole and is between the posterior postpetiolar margin and the anterior postpetiolar margin.
- PPW** Postpetiole width. Maximum width of postpetiole in dorsal view.
- SL** Scape length. Maximum straight line scape length excluding the articular condyle.

In verbal descriptions of taxa based on external morphological traits, recent taxonomic papers (Csősz and Fisher 2015, 2016) were considered. Definitions of surface sculpturing are linked to Harris (1979). Body size is given in μm , means of morphometric ratios as well as minimum and maximum values are given in parentheses with up to three digits. Inclinations of pilosity given in degrees. Definitions of species-groups as well as descriptions of species are surveyed in alphabetic order.

Statistical framework—hypothesis formation and testing. The present statistic framework follows the procedure applied in Csősz and Fisher (2016a, 2016b). Advantages and limitations of the present procedure are discussed there.

Generating prior species hypotheses via the combined application of NC clustering and PART. This method searches for discontinuities in continuous morphometric data and sorts all similar cases into the same cluster in a two-step procedure. The first step reduces dimensionality in data with cumulative linear discriminant analysis (LDA) using nest samples (i.e. individuals collected from the same nest are assumed genetically closely related, often sisters) as groups (Seifert et al. 2014). The second step calculates pairwise distances between samples using LD scores as input and the distance matrix is displayed in a dendrogram. The NC-clustering was done via packages *cluster* (Maechler et al. 2014) and *MASS* (Venables and Ripley 2002).

The ideal number of clusters was determined by Partitioning Algorithm based on Recursive Thresholding via the package *clusterGenomics* (Nilsen and Lingjaerde 2013) using the function ‘part’, which also assigns observations (i.e. specimens, or samples) into partitions. The method estimates the number of clusters in a data based on recursive application of the Gap statistic (Tibshirani et al. 2001) and is able to discover both top-level clusters as well as sub-clusters nested within the main clusters. If more than one cluster is returned by the Gap statistic, it is re-optimized on each subset of cases corresponding to a cluster until a stopping threshold is reached or the subset under evaluation has less than $2 \cdot \text{minSize}$ cases (Nilsen et al. 2013). Two clustering methods, “hclust” and “kmeans” are used to determine the optimal number of clusters with 1000 bootstrap iterations. The results of PART are mapped on the dendrogram by colored bars via function ‘mark.dendrogram’ found in (Beleites and Sergio 2015). The script written in R and can be found in Supporting In-

formation. The script is published by Csősz and Fisher (2016a, 2016b) and is freely accessible.

Arriving at final species hypothesis using confirmatory Linear Discriminant Analysis (LDA) and LDA ratio extractor. To provide increased reliability of species delimitation, hypotheses on clusters and classification of cases via exploratory processes were confirmed by LDA Leave-one-out cross-validation (LOOCV). Classification hypotheses were imposed for all samples congruently classified by partitioning methods while wild-card settings (i.e. no prior hypothesis imposed on its classification) were given to samples that were incongruently classified by the two methods or proved to be outliers.

Interpreting discriminant functions as identification tools. In this paper discriminant function analysis is used to determine which variables discriminate between two or more cryptic species. The discriminant functions (D2 and D4) provided in the key and differential diagnoses offer moderately time consuming but accurate opportunities to identify every single individual. The linear equation of the discriminant functions are as follows: $D_m = a_1 * x_1 + a_m * x_m + c$, where c is a constant, a_1 through a_m are the characters in micrometer and x_1 and x_m are coefficients. The equation must be calculated with the trait names (e.g. SL) substituted with the length of the corresponding traits in micrometer (e.g. 625). The dimensionless number (D_m) returned by the equation must fit either of the species' scores showing the identity of that particular individual.

Results

Altogether, four remarkable clusters were recognized by both clustering algorithms “hclust” and ‘kmeans’ using function ‘part’. The pattern returned by these partitioning algorithms can be fitted on the hierarchical structure seen on the dendrogram generated by NC clustering (Fig. 1). The grouping hypotheses generated by the combination of hypothesis-free exploratory analyses was validated by Linear Discriminant Analysis with leave-one-out cross-validation (LOOCV-LDA). The overall classification success is 98% (Table 1), hence the four clusters solution is accepted as the final species hypothesis. The four species described here are as follows in alphabetic order: *N. flavus* sp. n., *Nesomyrmex gibber* (Donisthorpe, 1946), *N. madecassus* (Forel, 1892) and *N. nitidus* sp. n.. Two of the four morphologically diagnosable OTUs, *gibber* and *madecassus*, differ in many qualitative characters (e.g. shape of propodeal spines, petiolar node,

Table 1. Classification matrix obtained by Leave One Out Cross Validation LDA. The last column (percent.correct) shows the classification success in percentage.

	flavus	gibber	madecassus	nitidus	percent.correct
flavus	59	0	2	0	96.7
gibber	0	7	0	0	100
madecassus	2	0	82	0	96.7
nitidus	0	0	0	79	100

Table 2. Mean of morphometric ratios calculated species-wise on individual level. Morphometric traits are divided by absolute cephalic size (CS), \pm SD are provided in the upper row, minimum and maximum values are given in parentheses in the lower row.

	flavus (n = 61)	gibber (n = 7)	madecassus (n = 84)	nitidus (n = 79)
CS	602 \pm 35	724 \pm 33	692 \pm 37	496 \pm 26
	[533, 699]	[655, 752]	[616, 763]	[460, 574]
CL/CW	1.21 \pm 0.04	1.11 \pm 0.02	1.15 \pm 0.02	1.19 \pm 0.03
	[1.15, 1.31]	[1.09, 1.13]	[1.10, 1.20]	[1.12, 1.31]
CL/CWb	1.26 \pm 0.04	1.17 \pm 0.02	1.18 \pm 0.02	1.23 \pm 0.03
	[1.19, 1.36]	[1.14, 1.18]	[1.13, 1.22]	[1.16, 1.35]
PO _o C/CL	0.48 \pm 0.01	0.41 \pm 0.01	0.46 \pm 0.01	0.48 \pm 0.01
	[0.46, 0.50]	[0.39, 0.42]	[0.43, 0.48]	[0.46, 0.50]
FRS/CS	0.30 \pm 0.01	0.33 \pm 0.01	0.31 \pm 0.01	0.31 \pm 0.01
	[0.28, 0.32]	[0.32, 0.34]	[0.29, 0.33]	[0.29, 0.33]
SL/CS	0.80 \pm 0.02	0.80 \pm 0.01	0.78 \pm 0.02	0.74 \pm 0.02
	[0.76, 0.83]	[0.78, 0.82]	[0.72, 0.82]	[0.69, 0.78]
EL/CS	0.25 \pm 0.01	0.25 \pm 0.01	0.26 \pm 0.01	0.26 \pm 0.01
	[0.23, 0.27]	[0.24, 0.26]	[0.24, 0.28]	[0.23, 0.27]
MW/CS	0.60 \pm 0.02	0.64 \pm 0.01	0.62 \pm 0.02	0.60 \pm 0.01
	[0.57, 0.66]	[0.63, 0.65]	[0.56, 0.66]	[0.57, 0.63]
PEW/CS	0.22 \pm 0.01	0.21 \pm 0.01	0.22 \pm 0.01	0.22 \pm 0.01
	[0.21, 0.24]	[0.20, 0.23]	[0.19, 0.24]	[0.19, 0.24]
PPW/CS	0.35 \pm 0.01	0.30 \pm 0.02	0.35 \pm 0.02	0.33 \pm 0.02
	[0.33, 0.40]	[0.27, 0.32]	[0.29, 0.39]	[0.30, 0.36]
ML/CS	1.38 \pm 0.04	1.41 \pm 0.01	1.35 \pm 0.04	1.31 \pm 0.03
	[1.29, 1.50]	[1.39, 1.42]	[1.26, 1.45]	[1.25, 1.41]
PEL/CS	0.53 \pm 0.02	0.50 \pm 0.03	0.50 \pm 0.02	0.51 \pm 0.02
	[0.48, 0.57]	[0.46, 0.53]	[0.44, 0.55]	[0.47, 0.58]
NOL/CS	0.35 \pm 0.02	0.33 \pm 0.01	0.33 \pm 0.02	0.34 \pm 0.02
	[0.30, 0.39]	[0.32, 0.34]	[0.28, 0.38]	[0.31, 0.39]
MPST/CS	0.44 \pm 0.01	0.46 \pm 0.01	0.44 \pm 0.02	0.43 \pm 0.02
	[0.41, 0.47]	[0.45, 0.47]	[0.41, 0.49]	[0.40, 0.48]
PEH/CS	0.28 \pm 0.01	0.29 \pm 0.00	0.28 \pm 0.01	0.27 \pm 0.01
	[0.26, 0.30]	[0.29, 0.30]	[0.25, 0.32]	[0.25, 0.31]
NOH/CS	0.13 \pm 0.01	0.15 \pm 0.01	0.13 \pm 0.01	0.12 \pm 0.01
	[0.11, 0.15]	[0.14, 0.17]	[0.11, 0.16]	[0.10, 0.15]
PPH/CS	0.27 \pm 0.01	0.26 \pm 0.01	0.27 \pm 0.01	0.26 \pm 0.01
	[0.25, 0.30]	[0.24, 0.27]	[0.24, 0.31]	[0.24, 0.28]
PPL/CS	0.30 \pm 0.02	0.26 \pm 0.02	0.27 \pm 0.02	0.27 \pm 0.02
	[0.25, 0.34]	[0.24, 0.29]	[0.23, 0.30]	[0.23, 0.31]

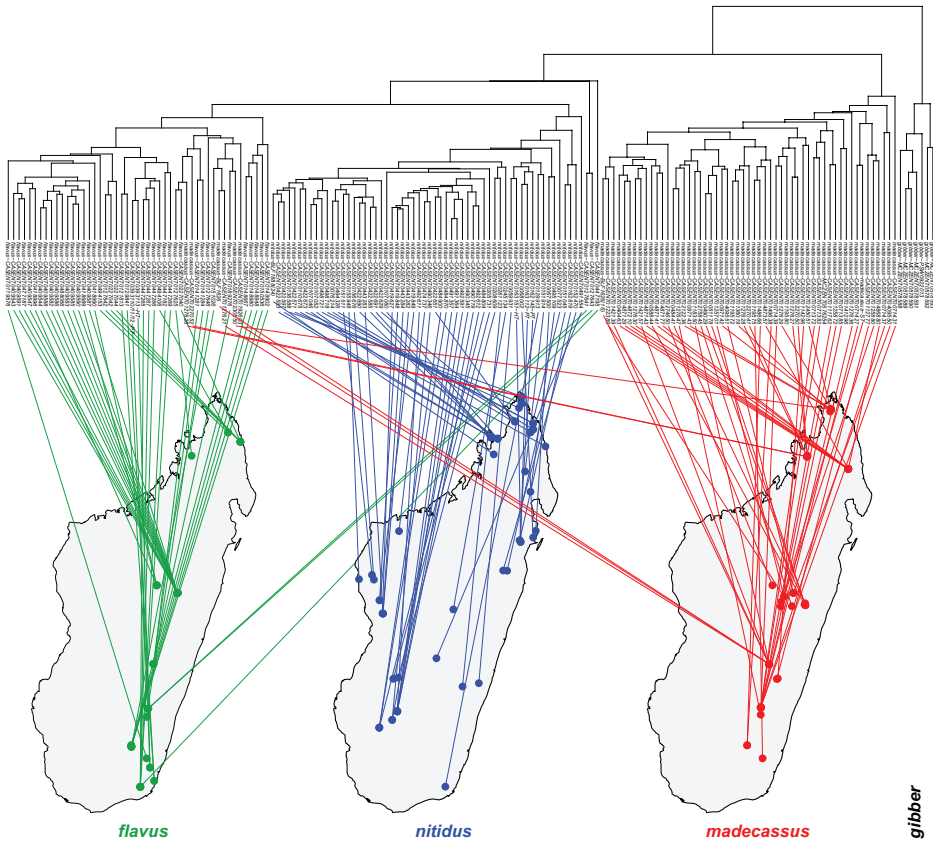


Figure 2. Dendrogram to geographic map. Dendrogram solution is linked on the map of Madagascar. Color codes for species are as follows: *Nesomyrmex flavus* sp. n.: green, *N. gibber*: black, *N. madecassus*: red, *N. nitidus* sp. n.: blue. Samples of *N. gibber* found in Mauritius, East to Madagascar (not shown).

surface sculpturing etc.), but the two others, *flavus* and *nitidus*, represent true cryptic species in the sense of Seifert (2009). Morphometric data for species calculated on individuals are given in Table 2. Three of four species, *N. flavus* sp. n., *N. madecassus* (Forel, 1892) and *N. nitidus* sp. n. occur in Madagascar exhibiting different but overlapping geographic distribution (Fig. 2) and elevational ranges (Fig. 3). *Nesomyrmex gibber* is known to occur only in Mauritius.

Synopsis of Malagasy members of the *Nesomyrmex madecassus* species-group

flavus Csősz & Fisher, sp. n.
gibber (Donisthorpe, 1946)
madecassus (Forel, 1892)
nitidus Csősz & Fisher, sp. n.

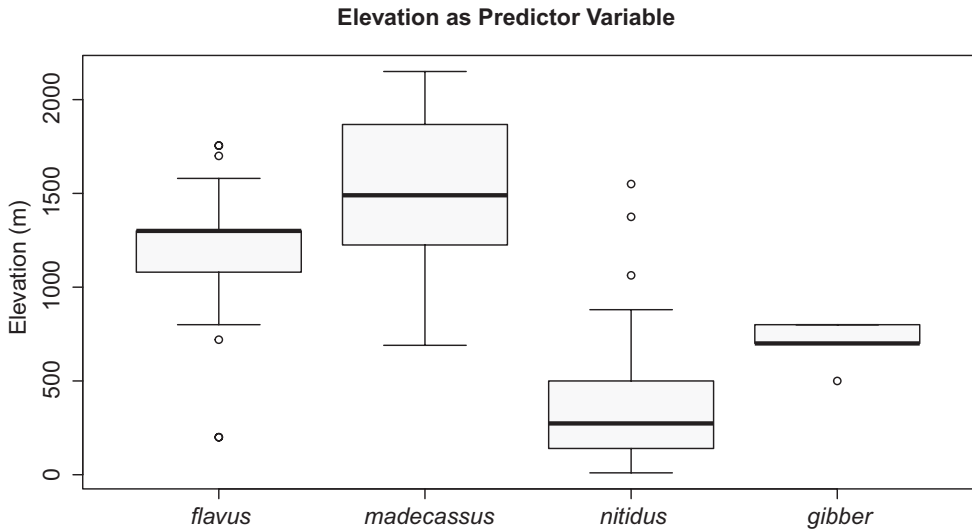


Figure 3. Boxplot for elevational distribution of *Nesomyrmex madecassus* group species. Black line: median, grey box: upper and lower quartiles, whisker: minimum, maximum values, open circles: outliers.

Key to workers of the *Nesomyrmex madecassus* group species

- 1 Mesothoracic hump conspicuous. Mauritius only ***gibber***
- Mesothoracic hump absent. Madagascar **2**
- 2 Dark brown to black ***madecassus*** (dark phenotype)
- Yellow to light brown **3**
- 3 Postocular area (PoOC) longer relative to cephalic width including compound eyes (CW): $CW/PoOC > 1.85$ (min. 1.77, max. 2.07), [5-95% percentiles: min. 1.85, max. 2.01] ***madecassus*** (ocher phenotype)
- Postocular area (PoOC) shorter relative to cephalic width including compound eyes (CW): $CW/PoOC < 1.85$ (min. 1.52, max. 1.89), [5-95% percentiles: min. 1.60, max. 1.84] **4**
- 4 Occur at higher altitudes/elevations: mean = 1190 m, [min. 200, max. 1755 m]. For precise morphological separations a discriminant $D2 (+0.0847*SL -0.0625*MW -15.038)$ function is available. $D2$ scores (n = 61) = +3.09 [+0.98, +5.33] ***flavus***
- Distributed in lower elevations: mean = 383 m, [min. 10, max. 1550 m]. For precise morphological separations a discriminant $D2$ function is available. $D2$ scores (n = 79) = -2.39 [-4.63, +0.19] ***nitidus***

***Nesomyrmex flavus* Csösz & Fisher, sp. n.**

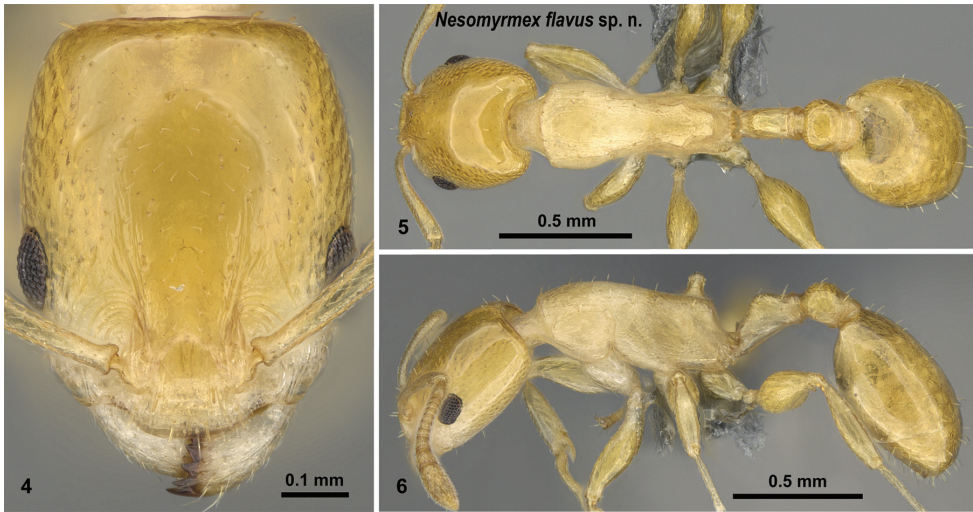
<http://zoobank.org/FD4F716F-93CB-42AB-95F9-26C76A65386B>

Figs 4–6, Table 2

Type material investigated. Holotype: **CASENT0393113**, collection code: BLF36563: MADAGASCAR, Prov. Toliara, Anosy Region, Anosyenne Mts, 31.2 km NW Manantenina, N -24.13894, E 47.06804, alt 1125 m, B.L. Fisher, F.A. Esteves et al., 2_26_2015, (1w, CAS);

Paratypes: Five workers, four gynes and two males with the same label data with the holotype under CASENT codes: **CASENT0393110**, collection code: BLF36563 (1w, 1q, CAS); **CASENT0393111**, collection code: BLF36563 (1w, 1q, CAS); **CASENT0393112**, collection code: BLF36563 (1w, 1q, CAS); **CASENT0393113**, collection code: BLF36563 (1q, CAS); **CASENT0393114**, collection code: BLF36563 (1w, 1m, CAS); **CASENT0393115**, collection code: BLF36563 (1w, 1m, CAS)

Material examined. MADAGASCAR: **CASENT0119576** (collection code: BLF14982, 1w, CAS, CASENT0119576): Prov. Fianarantsoa, Parc National Befotaka-Midongy, Papango 28.5 km S Midongy-Sud, Mount Papango, N -23.84083, E 46.9575, alt 1250 m, B.L. Fisher et al., 11_17_2006; **CASENT0121813** (collection code: BLF15514, 1w, CAS, CASENT0121813): Prov. Toliara, Forêt Ivohibe 55.0 km N Tolagnaro, N -24.569, E 47.204, alt 200 m, B.L. Fisher et al., 12_3_2006; **CASENT0129841** (collection code: BLF15450, 1w, CAS): Prov. Toliara, Forêt Ivohibe 55.0 km N Tolagnaro, N -24.569, E 47.204, alt 200 m, B.L. Fisher et al., 12_2_2006; **CASENT0127625** (collection code: BLF01972, 2w, CAS): Prov. Antsiranana, Prov. Antsiranana R.S. Manongarivo 17.3 km 218° SW Antanambao, N -14.02167, E 48.4183, alt 1580 m, B.L. Fisher, 10_27_1998; **CASENT0127641** (collection code: BLF00748, 1w, CAS): Prov. Fianarantsoa, 43 km S Ambalavao, Rés. Andringitra, N -22.23333, E 47, alt 800 m, B.L. Fisher, 10_6_1993; **CASENT0127642** (collection code: BLF01023, 1w, CAS): Prov. Toamasina, 6.9 km NE Ambanizana, Ambohitsitondroina, N -13.56667, E 50, alt 1080 m, B.L. Fisher, 12_9_1993; **CASENT0127643** (collection code: BLF00740, 1w, CAS): Prov. Fianarantsoa, 45 km S Ambalavao, N -22.21667, E 47.0167, alt 720 m, B.L. Fisher, 10_1_1993; **CASENT0127646** (collection code: BLF01751, 2w, CAS): Prov. Fianarantsoa, R.S. Ivohibe, 6.5 km ESE Ivohibe, N -22.49667, E 46.955, alt 1575 m, B.L. Fisher (Sylvain), 10_24_1997; **CASENT0141281** (collection code: BLF20452, 1w, CAS), **CASENT0141284** (collection code: BLF20457, 2w, CAS): Prov. Fianarantsoa, Parc naturel communautaire, 26.8 km SW Ambositra, N -20.775, E 47.1836, alt 1755 m, B.L. Fisher et al., 5_20_2008; **CASENT0148667** (collection code: BLF21477, 1w, CAS), **CASENT0149902** (collection code: BLF21545, 1w, CAS): Prov. Toliara, Réserve Spéciale Kalambatritra, Betanana, N -23.4144, E 46.459, alt 1360 m, B.L. Fisher et al., 2_8_2009; **CASENT0148948** (collection code: BLF21630, 1w, CAS), **CASENT0148980** (collection code: BLF21600, 1w, CAS), **CASENT0150536** (collection code: BLF21632, 1w, CAS), Prov. Toliara, Réserve Spéciale Kalambatritra, Ampanihy, N -23.4635, E 46.4631, alt 1270 m, B.L. Fisher et al., 2_9_2009;



Figures 4–6. *Nesomyrmex flavus* sp. n. holotype worker (CASENT0393113). Head in full-face view (4), dorsal view of the body (5), lateral view of the body (6).

CASENT0151026 (collection code: BLF21705, 1w, CAS): Prov. Toliara, Réserve Spéciale Kalambatritra, Ampanihy, N -23.463, E 46.4706, alt 1269 m, B.L. Fisher et al., 2_10_2009; **CASENT0189276** (collection code: BLF01626, 3w, CAS, CASENT0189276): Prov. Fianarantsoa, 29 km SSW Ambositra, Ankazomivady, N -20.77667, E 47.165, alt 1700 m, B.L. Fisher, 1_14_1998; **CASENT0227040** (collection code: BLF1972(8), 1w, CAS), **CASENT0227042** (collection code: BLF01014, 1w, CAS), **CASENT0227044** (collection code: BLF01014, 1w, CAS): Prov. Toamasina, 6.9 km NE Ambanizana, Ambohitsitondroina, N -13.56667, E 50, alt 1080 m, B.L. Fisher, 12_9_1993; **CASENT0409543** (collection code: BLF02398, 1w, CAS), **CASENT0409544** (collection code: BLF02398, 1w, CAS), **CASENT0409547** (collection code: BLF02398, 1w, CAS), **CASENT0409582** (collection code: BLF02451, 2w, CAS), **CASENT0409583** (collection code: BLF02421, 2w, CAS), **CASENT0409585** (collection code: BLF02451, 2w, CAS), **CASENT0409586** (collection code: BLF02435, 2w, CAS), **CASENT0409587** (collection code: BLF02435, 1w, CAS), **CASENT0409588** (collection code: BLF02465, 2w, CAS), **CASENT0409590** (collection code: BLF02465, 2w, CAS), **CASENT0409591** (collection code: BLF02447, 1w, CAS): Prov. Antananarivo, 3 km 41° NE Andranomay, 11.5 km 147° SSE Anjozorobe, N -18.47333, E 47.96, alt 1300 m, Fisher, Griswold et al., 12_5_2000; **CASENT0418989** (collection code: BLF03695, 1w, CAS), **CASENT0418990** (collection code: BLF03695, 1w, CAS), **CASENT0418996** (collection code: BLF03695, 2w, CAS): Prov. Antananarivo, Réserve Spéciale d'Ambohitantely, Forêt d'Ambohitantely, 20.9 km 72° NE d'Ankazobe, N -18.22528, E 47.2868, alt 1410 m, Fisher, Griswold et al., 4_17_2001; **CASENT0447182** (collection code: BLF05014, 1w, CAS), **CASENT0447195** (collection code: BLF05014, 1w, CAS), **CASENT0447265** (collection code: BLF05014, 1w, CAS), **CASENT0447266** (col-

lection code: BLF05014, 1w, CAS), **CASENT0447267** (collection code: BLF05014, 1w, CAS), **CASENT0447269** (collection code: BLF05014, 1w, CAS): Prov. Toliara, Parc National d'Andohahela, Col du Sedro, 3.8 km 113° ESE Mahamavo, 37.6 km 341° NNW Tolagnaro, N -24.76389, E 46.7517, alt 900 m, Fisher-Griswold Arthropod Team, 1_21_2002; **CASENT0477187** (collection code: BLF02543, 2w, CAS),; **CASENT0488066** (collection code: BLF02544, 1w, CAS): Prov. Antananarivo, 3 km 41° NE Andranomay, 11.5 km 147° SSE Anjozorobe, N -18.47333, E 47.96, alt 1300 m, Griswold et al., 12_5_2000; **CASENT0494106** (collection code: BLF09806, 1w, CAS),; **CASENT0494153** (collection code: BLF09859, 2w, CAS): Prov. Antsiranana, Forêt de Binara, 9.4 km 235° SW Daraina, N -13.26333, E 49.6, alt 1100 m, B.L. Fisher, 12_5_2003;

Description of workers. Body color: yellow. Body color pattern: Body concolorous. Absolute cephalic size: 602 [533, 699]. Cephalic length vs. Maximum width of head capsule (CL/CWb): 1.26 [1.19, 1.36]. Postocular distance vs. cephalic length (PoOc/CL): 0.48 [0.46, 0.50]. Postocular sides of cranium contour frontal view orientation: converging posteriorly. Postocular sides of cranium contour frontal view shape: convex. Vertex contour line in frontal view shape: straight; slightly concave. Vertex sculpture: main sculpture inconspicuous, ground sculpture smooth. Gena contour line in frontal view shape: convex. Genae contour from anterior view orientation: converging; strongly converging. Gena sculpture: NOT CODED. Concentric carinae laterally surrounding antennal foramen: present. Eye length vs. absolute cephalic size (EL/CS): 0.25 [0.23, 0.27]. Frontal carina distance vs. absolute cephalic size (FRS/CS): 0.30 [0.28, 0.32]. Longitudinal carinae on median region of frons: present. Longitudinal carinae on medial region of frons shape: variable. Smooth median region on frons: present. Antennomere count: 12. Scape length vs. absolute cephalic size (SL/CS): 0.80 [0.76, 0.83]. Median clypeal notch: variable. Ground sculpture of submedian area of clypeus: present. Median carina of clypeus: absent. Lateral carinae of clypeus: present. Metanotal depression: variable. Dorsal region of mesosoma sculpture: fine areolate ground sculpture, superimposed by dispersed rugae. Lateral region of pronotum sculpture: areolate ground sculpture, main sculpture dispersed costate. Mesopleuron sculpture: fine areolate ground sculpture, superimposed by dispersed rugulae. Metapleuron sculpture: fine areolate ground sculpture, superimposed by dispersed rugulae. Petiole width vs. absolute cephalic size (PEW/CS): 0.22 [0.21, 0.24]. Anterior profile of petiolar node contour line in lateral view shape: concave. Dorso-caudal petiolar profile contour line in lateral view shape: convex; strongly convex. Dorsal region of petiole sculpture: ground sculpture smooth, main sculpture absent. Postpetiole width vs. absolute cephalic size (PPW/CS): 0.35 [0.33, 0.40]. Dorsal region of postpetiole sculpture: ground sculpture smooth, main sculpture dispersed rugose; ground sculpture smooth, main sculpture absent.

Diagnosis. Workers of *N. flavus* cannot be confused with *N. gibber* because the conspicuous mesothoracic hump which is a diagnostic character of the latter species is absent in *N. flavus* workers. This species can be easily separated from dark phenotypes of *N. madecassus* by color: the dark madecassus phenotypes are dark brown but the workers of *N. flavus* are light yellow. Morphometric ratio (PoOC/CW) and discri-

minant D4 function helps to separate *N. flavus* from other *madecassus* phenotypes; further details are given in diagnosis under *N. madecassus*.

The workers of this species are the most similar to that of *N. nitidus*. The elevational distribution of the two species may provide hints useful for separation (Fig. 3) but the ranges broadly overlap. These taxa represent true cryptic species which cannot be identified based on qualitative characters (i.e. sculpture, shape or color), and their overlapping range means ratios cannot be used for identification. Therefore, only a discriminant D2 function with a greatly reduced character set ($D2 = +0.0847*SL - 0.0625*MW - 15.038$) yields complete separation (morphometric data are in micrometer):

$$\textit{flavus} \text{ D2 (n = 61) = +3.09 [+0.98, +5.33]}$$

$$\textit{nitidus} \text{ D2 (n = 79) = -2.39 [-4.63, +0.19]}$$

For now, this remains the simplest method available to separate workers of these two taxa, but in the future, when more information about these species has been accumulated, we hope to find a reliable and easy-to-use diagnostic trait.

Biology and distribution. This species is known to occur in Madagascar's rain forests at high altitudes between 200 and 1755 m, mean: 1190 m (Fig. 3). This species is known to forage in low vegetation and nests can often be found in dead twigs. This species has occasionally been collected in leaf litter (leaf mold, rotten wood), or in rotten tree stumps.

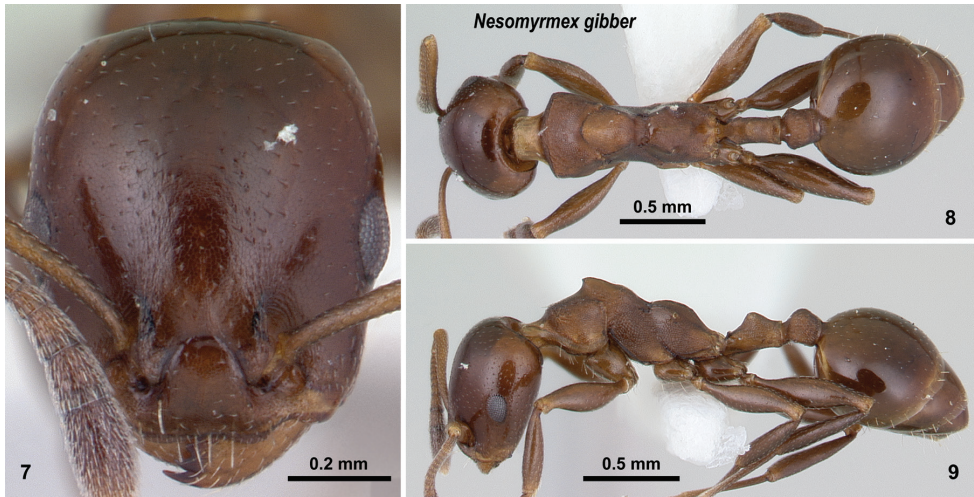
Nesomyrmex gibber (Donisthorpe, 1946)

Figs 7–9, Table 2

Type material investigated. Holotype: “Ireneopone gibber, H. Donisthorpe, 1946 TYPE” Mauritius, Calebasses Mt., 22. X. 1944, No 72 leg. R. Mamet (1w, BMNH, London, U.K., CASENT0102303), [type specimen was morphometrically not investigated, AntWeb images were used for comparison]

Material examined. MAURITIUS: MCZENT0578588 (1w, MCZ), **MCZENT0578589** (1w, MCZ), **MCZENT0578590** (1w, MCZ), **MCZENT0578591** (1w, MCZ), **MCZENT0578592** (1w, MCZ), **MCZENT0578593** (1w, MCZ, CASENT0178539): Le Pouce Mt., N -20.19, E 57.52, alt 700–800 m, W.L. Brown, 1_29_1977; **CASENT0922013**, (collection code: PSW10502, 1w, PSW, CASENT0922013): Basin Blanc, Mauritius, N -20.45, E 57.4667, alt 500 m, P.S. Ward, 5_06_1989.

Description of workers. Body color: brown. Body color pattern: Body concolorous. Absolute cephalic size: 724 [655, 752]. Cephalic length vs. Maximum width of head capsule (CL/CWb): 1.17 [1.14, 1.18]. Postocular distance vs. cephalic length (PoOc/CL): 0.41 [0.39, 0.42]. Postocular sides of cranium contour frontal view orientation: converging posteriorly. Postocular sides of cranium contour frontal view shape: convex. Vertex contour line in frontal view shape: straight; slightly concave. Vertex sculpture:



Figures 7–9. *Nesomyrmex gibber* non-type worker (CASENT0178540). Head in full-face view (7), dorsal view of the body (8), lateral view of the body (9).

main sculpture absent, ground sculpture areolate. Gena contour line in frontal view shape: convex. Genae contour from anterior view orientation: converging; strongly converging. Gena sculpture: ground sculpture areolate, main sculpture absent. Concentric carinae laterally surrounding antennal foramen: absent. Eye length vs. absolute cephalic size (EL/CS): 0.25 [0.24, 0.26]. Frontal carina distance vs. absolute cephalic size (FRS/CS): 0.33 [0.32, 0.34]. Longitudinal carinae on median region of frons: absent. Smooth median region on frons: present. Antennomere count: 12. Scape length vs. absolute cephalic size (SL/CS): 0.80 [0.78, 0.82]. Median clypeal notch: present. Ground sculpture of submedian area of clypeus: present. Median carina of clypeus: absent. Lateral carinae of clypeus: absent. Metanotal depression: present. Dorsal region of mesosoma sculpture: ground sculpture areolate, main sculpture absent. Lateral region of pronotum sculpture: ground sculpture areolate, main sculpture absent. Mesopleuron sculpture: ground sculpture areolate, main sculpture absent. Metapleuron sculpture: ground sculpture areolate, main sculpture absent. Petiole width vs. absolute cephalic size (PEW/CS): 0.21 [0.20, 0.23]. Anterior profile of petiolar node contour line in lateral view shape: concave. Dorso-caudal petiolar profile contour line in lateral view shape: strongly convex. Dorsal region of petiole sculpture: ground sculpture areolate, main sculpture absent. Postpetiole width vs. absolute cephalic size (PPW/CS): 0.30 [0.27, 0.32]. Dorsal region of postpetiole sculpture: ground sculpture areolate, main sculpture absent.

Diagnosis. This species is easily distinguished from all the other taxa treated in this revisionary work by the presence of the conspicuous mesothoracic hump on the mesosoma of workers (Fig. 9).

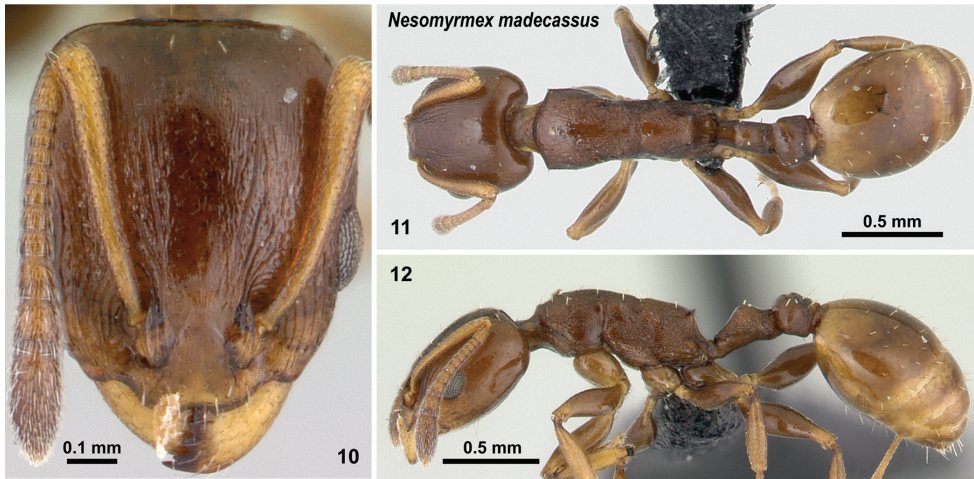
Biology and distribution. Endemic to Mauritius island. Occur in rainforests in higher altitude between 500 and 800 meters, (mean = 714 m). This species can be collected on low vegetation and in dead stems.

***Nesomyrmex madecassus* (Forel, 1892)**

Figs 10–12, Table 2

Type material investigated. Syntype workers: CASENT0101667, (collection code: ANTC3246), CASENT0101687 (collection code: ANTC3247): [MADAGASCAR, Prov.] Antsiranana, Forêt d' Andrangoloaka [Antananarivo, -18.91 N, 47.55 E], Madagascar (Sikora)", (CASENT0101667, CASENT0101687, MHNG);

Material examined. Dark (wild type) phenotype: MADAGASCAR: BLF1626 (collection code: BLF1626, 3w, CAS), **BLF1626(16)** (collection code: BLF1626(16), 2w, CAS): Fianarantsoa, 29 km SSW Ambositra, Ankazomivady, N -20.77667, E 47.165, alt 1700 m, B.L. Fisher, 1_14_1998; **CASENT0040463** (collection code: BLF09324, 1w, CAS): Antsiranana, Parc National de Marojejy, 25.4 km 30° NNE Andapa, 10.9 km 311° NW Manantenina, N -14.445, E 49.735, alt 2000 m, B.L. Fisher, 11_23_2003; **CASENT0048441** (collection code: BLF10513, 2w, CAS): Toamasina, Analamay, N -18.80623, E 48.33707, alt 1068 m, Malagasy ant team, 3_21_2004; **CASENT0049029** (collection code: BLF10704, 2w, CAS): Toamasina, Torotorofotsy, N -18.87082, E 48.34737, alt 1070 m, Malagasy ant team, 3_29_2004; **CASENT0051178** (collection code: BLF10689, 2w, CAS): Toamasina, Torotorofotsy, N -18.87082, E 48.34737, alt 1070 m, Malagasy ant team, 3_28_2004; **CASENT0058844** (collection code: BLF11968, 1w, CAS): Toamasina, Forêt Ambatovy, 14.3 km 57° Moramanga, N -18.85083, E 48.32, alt 1075 m, B.L. Fisher, 4_12_2005; **CASENT0071372** (collection code: BLF13809, 1w, CAS), **CASENT0071382** (collection code: BLF13794, 1w, CAS), **CASENT0071385** (collection code: BLF13811, 1w, CAS), **CASENT0071427** (collection code: BLF13798, 1w, CAS), **CASENT0071431** (collection code: BLF13800, 1w, CAS), **CASENT0071437** (collection code: BLF13785, 1w, CAS), **CASENT0071439** (collection code: BLF13775, 1w, CAS): Fianarantsoa, Parc National d'Andringitra, Plateau d'Andohariana, 39.8 km 204° Ambalavao, N -22.18767, E 46.90083, alt 2150 m, B.L. Fisher et al., 4_16_2006; **CASENT0097142** (collection code: MA-01-01D-01, 1w, CAS), **CASENT0097143** (collection code: MA-01-01D-01, 1w, CAS): Diego-Suarez, Parc National Montagne d'Ambre [Petit Lac road], N -12.52028, E 49.17917, alt 1125 m, Irwin, Schlinger, Harin'H, 1_25_2001; **CASENT0111762** (collection code: MG-29-06, 1w, CAS): Fianarantsoa, Miandritsara Forest, 40Km S of Ambositra, N -20.79267, E 47.17567, alt 822 m, Rin'ha, Mike, 1_5_2005; **CASENT0112777** (collection code: MA-02-09C-60, 1w, CAS): Fianarantsoa, Belle Vue trail, Ranomafana National Park, Fianarantsoa Prov., N -21.2665, E 47.42017, alt 1020 m, R. Harin'Hala, 5_4_2003; **CASENT0114296** (collection code: MA-02-09D-06, 1w, CAS): Fianarantsoa, JIRAMA water works near river, Ranomafana National Park, Fianarantsoa Prov., N -21.2485, E 47.45217, alt 690 m, R. Harin'Hala, 12_6_2001; **CASENT0118350** (collection code: MG-29-04, 1w, CAS): Fianarantsoa, Miandritsara Forest, 40Km S of Ambositra, N -20.79267, E 47.17567, alt 822 m, Rin'ha, Mike, 11_14_2004; **CASENT0122389** (collection code: BLF17425, 1w, CAS), **CASENT0125701** (collection code: BLF17430, 1w, CAS), **CASENT0125880**



Figures 10–12. *Nesomyrmex madecassus* non-type worker (CASENT0487142). Head in full-face view (**10**), dorsal view of the body (**11**), lateral view of the body (**12**).

(collection code: BLF17420, 1w, CAS): Antananarivo, Kaloy, N -18.58998, E 47.65102, alt 1423 m, B.L. Fisher et al., 4_27_2007; **CASENT0125872** (collection code: BLF17314, 1w, CAS): Antananarivo, Ambohimanga, N -18.76125, E 47.56447, alt 1361 m, B.L. Fisher et al., 4_26_2007; **CASENT0127628** (collection code: BLF01989, 1w, CAS): Antsiranana, R.S. Manongarivo, 20.4 km 219° SW Antanambao, N -14.04667, E 48.40167, alt 1860 m, B.L. Fisher, 11_3_1998; **CASENT0127627** (collection code: BLF01972, 3w, CAS): Antsiranana, Prov. Antsiranana R.S. Manongarivo 17.3 km 218° SW Antanambao, N -14.02167, E 48.41833, alt 1580 m, B.L. Fisher, 10_27_1998; **CASENT0127629** (collection code: MA-01-01A-01, 1w, CAS): Diego-Suarez, Parc National Montagne d'Ambre [1st campsite], N -12.51444, E 49.18139, alt 960 m, Irwin, Schlinger, Harin'H, 1_21_2001; **CASENT0127630** (collection code: ANTC8395, 2w, CAS): Antsiranana, RNI Marojejy, 11 km NW Manantenina, N -14.45, E 49.73333, alt 1875 m, E.L. Quinter, 11_13_1996; **CASENT0127636** (collection code: ASS(03)-1, 2w, CAS): Fianarantsoa, Rés. Andringitra, Plateau d'Andohariana, base of Pic d'Ivangomena, N -22.2, E 46.9, alt 2050 m, Goodman leg., 9_3_1995; **CASENT0127647** (collection code: BLF01755, 2w, CAS): Fianarantsoa, 8.0 km NE Ivohibe, N -22.42167, E 46.89833, alt 1200 m, B.L. Fisher (Sylvain), 11_3_1997; **CASENT0136019** (collection code: BLF18083, 1w, CAS): Antsiranana, Parc National Montagne d'Ambre, Lac maudit, N -12.58502, E 49.15147, alt 1250 m, B.L. Fisher et al., 11_13_2007; **CASENT0142139** (collection code: BLF20488, 1w, CAS), **CASENT0142157** (collection code: BLF20480, 1w, CAS): Fianarantsoa, Parc naturel communautaire, 28.5 km SW Ambositra, N -20.78414, E 47.16699, alt 1780 m, B.L. Fisher et al., 5_21_2008; **CASENT0212236** (collection code: BLF26175, 1w, CAS): Antsiranana, Parc National Montagne d'Ambre, N -12.51778, E 49.17957, alt 1000 m, B.L. Fisher et al., 3_6_2011; **CASENT0227041** (collection code: BLF01989, 1w,

CAS, CASENT0227040), **CASENT0227050** (collection code: BLF01989, 1w, CAS), **CASENT0227052** (collection code: BLF01989, 1w, CAS): Antsiranana, R.S. Manongarivo, 20.4 km 219° SW Antanambao, N -14.04667, E 48.40167, alt 1860 m, B.L. Fisher, 11_3_1998; **CASENT0230550** (collection code: BLF26169, 1w, CAS), **CASENT0245051** (collection code: BLF26169, 1w, CAS, CASENT0409551): Antsiranana, Parc National Montagne d'Ambre, N -12.51778, E 49.17957, alt 1000 m, B.L. Fisher et al., 3_6_2011; **CASENT0274650** (collection code: BLF28278, 1w, CAS): Antananarivo, Réserve Speciale d'Ambohitantly, N -18.22444, E 47.2774, alt 1490 m, B.L. Fisher et al., 3_9_2012; **CASENT0275845** (collection code: BLF28339, 1w, CAS): Antananarivo, Mandraka Park, N -18.9019, E 47.90786, alt 1360 m, B.L. Fisher et al., 3_11_2012; **CASENT0409550** (collection code: BLF02398, 1w, CAS), **CASENT0409551** (collection code: BLF02398, 1w, CAS): Antananarivo, 3 km 41° NE Andranomay, 11.5 km 147° SSE Anjozorobe, N -18.47333, E 47.96, alt 1300 m, Fisher, Griswold et al., 12_5_2000; **CASENT0486880** (collection code: BLF09120, 1w, CAS), **CASENT0487129** (collection code: BLF09369, 2w, CAS), **CASENT0487141** (collection code: BLF09412, 2w, CAS), **CASENT0487143** (collection code: BLF09412, 2w, CAS), **CASENT0487177** (collection code: BLF09372, 2w, CAS), **CASENT0487210** (collection code: BLF09416, 2w, CAS), **CASENT0487357** (collection code: BLF09315, 4w, CAS): Antsiranana, Parc National de Marojejy, 25.7 km 32° NNE Andapa, 10.3 km 314° NW Manantenina, N -14.445, E 49.74167, alt 1575 m, B.L. Fisher, 11_22_2003; MCZENT0576254 (1w, MCZ): Antsiranana, 10k NE Antananarivo lac Alarobie, G.D. Alpert, 3_10_1991;

Ocher phenotype: **CASENT0119572** (collection code: BLF15013, 1w, CAS), **CASENT0119575** (collection code: BLF15088, 1w, CAS), **CASENT0119580** (collection code: BLF15089, 1w, CAS): Fianarantsoa, Parc National Befotaka-Midongy, Papango 28.5km S Midongy-Sud, Mount Papango, N -23.84083, E 46.9575, alt 1250 m, B.L. Fisher et al., 11_19_2006; **CASENT0149638** (collection code: BLF21513, 1w, CAS, CASENT0149638): Toliara, Réserve Spéciale Kalambatritra, N -23.4185, E 46.4583, alt 1365 m, B.L. Fisher et al., 2_8_2009; **CASENT0148666** (collection code: BLF21476, 1w, CAS): Toliara, Réserve Spéciale Kalambatritra, Betanana, N -23.4144, E 46.459, alt 1360 m, B.L. Fisher et al., 2_8_2009; **CASENT0192603** (collection code: BLF01626, 1w, CAS): Fianarantsoa, 29 km SSW Ambositra, Ankazomivady, N -20.77667, E 47.165, alt 1700 m, B.L. Fisher, 1_14_1998; **CASENT0141296** (collection code: BLF20465, 1w, CAS): Fianarantsoa, Parc naturel communautaire, 28.5 km SW Ambositra, N -20.78414, E 47.16699, alt 1780 m, B.L. Fisher et al., 5_21_2008; **CASENT0127621** (collection code: BLF01626, 4w, CAS): Fianarantsoa, 29 km SSW Ambositra, Ankazomivady, N -20.77667, E 47.165, alt 1700 m, B.L. Fisher, 1_14_1998; **CASENT0127626** (collection code: BLF01989, 1w, CAS): Antsiranana, R.S. Manongarivo, 20.4 km 219° SW Antanambao, N -14.04667, E 48.40167, alt 1860 m, B.L. Fisher, 11_3_1998;

Description of workers. Body color: brown; black; rarely yellow. Body color pattern: Body concolorous. If yellow, body concolorous, clava, femora and 1st gastral tergite darker. Absolute cephalic size: 692 [616, 763]. Cephalic length vs. Maximum

width of head capsule (CL/CWb): 1.18 [1.13, 1.22]. Postocular distance vs. cephalic length (PoOc/CL): 0.46 [0.43, 0.48]. Postocular sides of cranium contour frontal view orientation: converging posteriorly. Postocular sides of cranium contour frontal view shape: convex. Vertex contour line in frontal view shape: straight; slightly concave. Vertex sculpture: main sculpture inconspicuous, ground sculpture smooth. Gena contour line in frontal view shape: convex. Genae contour from anterior view orientation: converging. Gena sculpture: rugoso-reticulate with feeble areolate ground sculpture. Concentric carinae laterally surrounding antennal foramen: present. Eye length vs. absolute cephalic size (EL/CS): 0.26 [0.24, 0.28]. Frontal carina distance vs. absolute cephalic size (FRS/CS): 0.31 [0.29, 0.33]. Longitudinal carinae on median region of frons: absent. Smooth median region on frons: present. Antennomere count: 12. Scape length vs. absolute cephalic size (SL/CS): 0.78 [0.72, 0.82]. Median clypeal notch: variable. Ground sculpture of submedian area of clypeus: present. Median carina of clypeus: absent. Lateral carinae of clypeus: present. Metanotal depression: variable. Dorsal region of mesosoma sculpture: areolate ground sculpture, superimposed by dispersed rugae. Lateral region of pronotum sculpture: areolate ground sculpture, main sculpture dispersed costate. Mesopleuron sculpture: ground sculpture areolate, main sculpture absent. Metapleuron sculpture: ground sculpture areolate, main sculpture absent. Petiole width vs. absolute cephalic size (PEW/CS): 0.22 [0.19, 0.24]. Anterior profile of petiolar node contour line in lateral view shape: concave. Dorsal-caudal petiolar profile contour line in lateral view shape: convex. Dorsal region of petiole sculpture: ground sculpture areolate, main sculpture absent. Postpetiole width vs. absolute cephalic size (PPW/CS): 0.35 [0.29, 0.39]. Dorsal region of postpetiole sculpture: ground sculpture areolate, main sculpture absent.

Diagnosis. Workers of this species differ from that of *N. gibber* by having no mesothoracic hump, and from *N. flavus* sp. n. and *N. nitidus* sp. n. by its dark brown color versus the light yellow hue of the two latter species.

The dark color in *madecassus* populations is dominant across the entire known distributional area, and comprises ~95% of the examined material. However, a rare, lighter-colored *madecassus* phenotype (ocher phenotype) was also found in a few localities. There is no evidence, other than color, that would support heterospecificity of these two discrete phenotypes of *N. madecassus* workers and no correlation was found between elevational cline and color. Only one mixed sample is known to include both ocher and dark phenotype. Ocher *madecassus* phenotypes are darker than the majority of *N. flavus* and *N. nitidus* workers and also differ from the latter species by having brown femora and a dark patch on the first gastral tergite.

Nesomyrmex madecassus workers (including ocher phenotypes) can be separated from those of *N. flavus* and *N. nitidus* using the ratio of postocular area to cephalic width including compound eyes (PoOC/CW), which yielded only three misclassified cases:

madecassus (n = 84) = 1.92 (1.77, 2.07), [5-95% percentiles: min. 1.85, max. 2.01]

flavus (n = 61) = 1.73 (1.53, 1.89), [5-95% percentiles: min. 1.60, max. 1.84]

nitidus (n = 79) = 1.73 (1.52, 1.85), [5-95% percentiles: min. 1.63, max. 1.83]

A more precise means to separate other *madecassus* phenotype from workers of *N. flavus* and *N. nitidus* may be necessary. In these cases, a discriminant D4 function ($D4 = +0.0511*PoOC -0.0486*CW -0.0702*PEW +0.0435*PEL +8.3829$) provides a moderately time consuming classification tool yielding non-overlapping ranges between *madecassus* workers and that of *flavus* and *nitidus* (morphometric data are given in micrometers):

madecassus D4 (n = 84) = -1.70 [-4.61, 0.26]

flavus D4 (n = 61) = +2.39 [0.42, 5.02]

nitidus D4 (n = 79) = +3.18 [0.51, 5.98]

Biology and distribution. This species is known to occur in Madagascar's rain forests at very high altitudes between 690 and 2150 m, mean: 1538 m (Fig. 3). This species is known to forage in low vegetation, nests can often be found in dead twigs, or rarely in leaf litter (leaf mold, rotten wood), or in rotten tree stumps.

***Nesomyrmex nitidus* Csősz & Fisher, sp. n.**

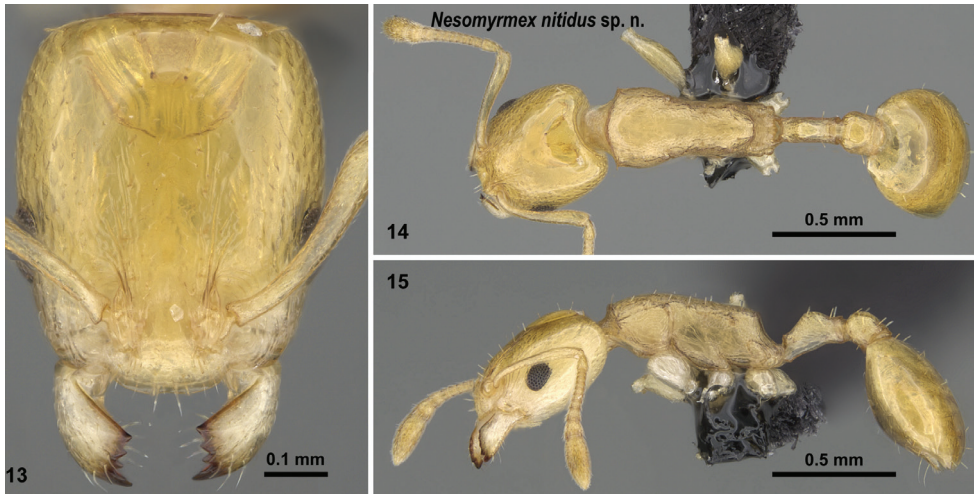
<http://zoobank.org/F0E325CD-99C1-4CB0-817D-4D7EC060AD8F>

Figs 13–15, Table 2

Type material investigated. Holotype: CASENT0163151, collection code: BLF24792: MADAGASCAR, Prov. Toamasina, Réserve Spéciale Ambatovaky, Sandrangato river, N -16.81753, E 49.29498, alt 360 m, B.L. Fisher et al. 2_25_2010, (1w, CAS);

Paratypes: two workers and one gyne from the same locality under CASENT codes: **CASENT0163112**, collection code: BLF24794: MADAGASCAR, Prov. Toamasina, Réserve Spéciale Ambatovaky, Sandrangato river, N -16.81753, E 49.29498, alt 360 m, B.L. Fisher et al. 2_25_2010, (1w, CAS); **CASENT0162145**, collection code: BLF24570: MADAGASCAR, Prov. Toamasina, Réserve Spéciale Ambatovaky, Sandrangato river, N -16.7633, E 49.26692, alt 520 m, B.L. Fisher et al. 2_26_2010, (1w, CAS); **CASENT0161445**, collection code: BLF25001: MADAGASCAR, Prov. Toamasina, Réserve Spéciale Ambatovaky, Sandrangato river, N -16.81209, E 49.29216, alt 460 m, B.L. Fisher et al. 2_22_2010, (1q, CAS);

Material examined. MADAGASCAR: BLF1888(24) (collection code: BLF01888, 1w, CAS): Prov. Antsiranana, R.S. Manongarivo, 12.8 km 228° SW Antanambao, N -13.97667, E 48.42333, alt 780 m, B.L. Fisher, 10_12_1998; **CASENT0059931** (collection code: BLF12392, 1w, CAS): Prov. Fianarantsoa, 7.6 km 122° Kianjavato, Forêt Classée Vatovavy, N -21.4, E 47.94, alt 175 m, B.L. Fisher et al., 6_6_2005; **CASENT0067500** (collection code: BLF12687, 1w, CAS): Prov. Toamasina, Parc National Mananara-Nord, 7.1 km 261° Antanambe, N -16.455, E 49.7875, alt 225 m, B.L. Fisher et al., 11_16_2005; **CASENT0068002** (collection code: BLF12780, 2w, CAS): Prov. Toamasina, Res. Ambodiriana, 4.8 km 306° Manompana, along Manom-



Figures 13–15. *Nesomyrmex nitidus* sp. n. holotype worker (CASENT0163151). Head in full-face view (13), dorsal view of the body (14), lateral view of the body (15).

pana river, N -16.67233, E 49.70117, alt 125 m, B.L.Fisher et al., 11_18_2005; **CASENT0076214** (collection code: BLF09620, 1w, CAS): Prov. Antsiranana, Forêt de Binara, 7.5 km 230° SW Daraina, N -13.255, E 49.61667, alt 375 m, B.L. Fisher, 12_2_2003; **CASENT0077523** (collection code: BLF09713, 1w, CAS): Prov. Antsiranana, Forêt de Binara, 9.1km 233° SW Daraina, N -13.26333, E 49.60333, alt 650-800 m, B.L. Fisher, 12_4_2003; **CASENT0107046** (collection code: BLF11562, 1w, CAS), **CASENT0107052** (collection code: BLF11562, 1w, CAS): Prov. Antsiranana, Forêt Ambato, 26.6 km 33° Ambanja, N -13.4645, E 48.55167, alt 150 m, B.L. Fisher, 12_9_2004; **CASENT0107060** (collection code: BLF11610, 1w, CAS): Prov. Antsiranana, Forêt Ambato, 26.6 km 33° Ambanja, N -13.4645, E 48.55167, alt 150 m, B.L. Fisher, 12_10_2004; **CASENT0110675** (collection code: BLF11220, 1w, CAS): Prov. Antsiranana, Ambondrobe, 41.1km 175° Vohemar, N -13.71533, E 50.10167, alt 10 m, B.L. Fisher, 11_30_2004; **CASENT0129913** (collection code: BLF15100, 1w, CAS): Prov. Toliara, Parc National Andohahela, Col de Tanatana, 33.3km NW Tolagnaro, N -24.7585, E 46.85367, alt 275 m, B.L. Fisher et al., 11_22_2006; **CASENT0136588** (collection code: BLF18628, 1w, CAS): Prov. Antsiranana, Forêt d'Ampombofofo, N -12.09949, E 49.33874, alt 25 m, B.L. Fisher et al., 11_21_2007; **CASENT0151045** (collection code: BLF22399, 1w, CAS): Prov. Toamasina, Parc National de Zahamena, Sahavorondrano River, N -17.75257, E 48.85725, alt 765 m, B.L. Fisher et al., 2_23_2009; **CASENT0151511** (collection code: BLF23080, 1w, CAS): Prov. Mahajanga, Réserve forestière Beanka, 50.2 km E Maintirano, N -17.88756, E 44.47265, alt 153 m, B.L.Fisher et al., 10_31_2009; **CASENT0151914** (collection code: BLF22603, 1w, CAS, CASENT0151914): Prov. Antsiranana, Betaolana Forest, along Bekona River, N -14.52996, E 49.44039, alt 880 m, B.L. Fisher et al., 3_5_2009; **CASENT0152470** (collection code: BLF22141, 1w, CAS, CASENT0152470): Prov.

Toamasina, Parc National de Zahamena, Tetezambatana forest, near junction of Nosivola and Manakambahiny Rivers, N -17.74298, E 48.72936, alt 860 m, B.L. Fisher et al., 2_19_2009; **CASENT0155948** (collection code: BLF22797, 1w, CAS): Prov. Mahajanga, Réserve forestière Beanka, 50.2 km E Maintirano, N -18.02649, E 44.05051, alt 250 m, B.L. Fisher et al., 10_19_2009; **CASENT0156676** (collection code: BLF22969, 1w, CAS): Prov. Mahajanga, Réserve forestière Beanka, 53.6 km E Maintirano, N -18.04014, E 44.53394, alt 272 m, B.L. Fisher et al., 10_25_2009; **CASENT0162145** (collection code: BLF24570, 2w, CAS): Prov. Toamasina, Réserve Spéciale Ambatovaky, Sandrangato river, N -16.7633, E 49.26692, alt 520 m, B.L. Fisher et al., 2_22_2010; **CASENT0162819** (collection code: BLF24484, 1w, CAS): Prov. Toamasina, Réserve Spéciale Ambatovaky, Sandrangato river, N -16.76912, E 49.26704, alt 475 m, B.L. Fisher et al., 2_21_2010; **CASENT0163112** (collection code: BLF24794, 1w, CAS), **CASENT0163151** (collection code: BLF24792, 1w, CAS): Prov. Toamasina, Réserve Spéciale Ambatovaky, Sandrangato river, N -16.81753, E 49.29498, alt 360 m, B.L. Fisher et al., 2_25_2010; **CASENT0205731** (collection code: BLF25790, 1w, CAS): Prov. Toliara, Makay Mts., N -21.25864, E 45.16412, alt 500 m, B.L. Fisher et al., 12_8_2010; **CASENT0208609** (collection code: BLF25261, 1w, CAS): Prov. Toliara, Makay Mts., N -21.21985, E 45.32396, alt 500 m, B.L. Fisher et al., 11_25_2010; **CASENT0245134** (collection code: BLF26356, 1w, CAS): Prov. Antananarivo, Ankalalahana, N -19.00659, E 47.1122, alt 1375 m, B.L. Fisher et al., 3_29_2011; **CASENT0261123** (collection code: BLF27634, 2w, CAS): Prov. Fianarantsoa, Andrambovato along river Tatamaly, N -21.51082, E 47.40992, alt 1063 m, B.L. Fisher et al., 10_24_2011; **CASENT0419627** (collection code: BLF04344, 1w, CAS): Prov. Mahajanga, Parc National Tsingy de Bemaraha, 2.5 km 62° ENE Bekopaka, Ankidrodroa River, N -19.13222, E 44.81467, alt 100 m, Fisher-Griswold Arthropod Team, 11_11_2001; **CASENT0419848** (collection code: BLF04434, 1w, CAS), **CASENT0419849** (collection code: BLF04434, 1w, CAS): Prov. Mahajanga, Parc National Tsingy de Bemaraha, 10.6 km ESE 123° Antsalova, N -18.70944, E 44.71817, alt 150 m, Fisher-Griswold Arthropod Team, 11_16_2001; **CASENT0422571** (collection code: BLF03132, 1w, CAS): Prov. Antsiranana, Montagne des Français, 7.2 km 142° SE Antsiranana (=Diego Suarez), N -12.32278, E 49.33817, alt 180 m, Fisher, Griswold et al., 2_22_2001; **CASENT0422585** (collection code: BLF03426, 1w, CAS), **CASENT0422593** (collection code: BLF03426, 1w, CAS), **CASENT0422597** (collection code: BLF03426, 2w, CAS): Prov. Antsiranana, Nosy Be, Réserve Naturelle Intégrale de Lokobe, 6.3 km 112° ESE Hellville, N -13.41933, E 48.33117, alt 30 m, Fisher, Griswold et al., 3_19_2001; **CASENT0422629** (collection code: BLF02859, 2w, CAS), **CASENT0422651** (collection code: BLF02859, 1w, CAS): Prov. Antsiranana, Réserve Spéciale de l'Ankarana, 22.9 km 224° SW Anivorano Nord, N -12.90889, E 49.10983, alt 80 m, Fisher, Griswold et al., 2_10_2001; **CASENT0422673** (collection code: BLF02660, 1w, CAS): Prov. Antsiranana, Réserve Spéciale d'Ambre, 3.5 km 235° SW Sakaramy, N -12.46889, E 49.24217, alt 325 m, Fisher, Griswold et al., 1_26_2001; **CASENT0422690** (collection code: BLF03426, 1w, CAS), **CASENT0422691** (collection code: BLF03426, 2w, CAS):

Prov. Antsiranana, Nosy Be, Réserve Naturelle Intégrale de Lokobe, 6.3 km 112° ESE Hellville, N -13.41933, E 48.33117, alt 30 m, Fisher, Griswold et al., 3_19_2001; **CASENT0443282** (collection code: BLF04234, 2w, CAS), **CASENT0443283** (collection code: BLF04234, 2w, CAS), **CASENT0443284** (collection code: BLF04234, 2w, CAS): Prov. Mahajanga, Parc National Tsingy de Bemaraha, 3.4 km 93° E Bekopaka, Tombeau Vazimba, N -19.14194, E 44.828, alt 50 m, Fisher-Griswold Arthropod Team, 11_6_2001; **CASENT0474737** (collection code: BLF06448, 1w, CAS): Prov. Mahajanga, Parc National de Namoroka, 9.8 km 300° WNW Vilanandro, N -16.46667, E 45.35, alt 140 m, Fisher, Griswold et al., 11_4_2002; **CASENT0484804** (collection code: BLF07511, 2w, CAS), **CASENT0484870** (collection code: BLF07511, 2w, CAS), **CASENT0484900** (collection code: BLF07511, 1w, CAS): Prov. Toliara, Parc National de Zombitse, 19.8 km 84° E Sakaraha, N -22.84333, E 44.71, alt 770 m, Fisher, Griswold et al., 2_5_2003; **CASENT0490345** (collection code: BLF07384, 1w, CAS), **CASENT0490346** (collection code: BLF07384, 2w, CAS): Prov. Fianarantsoa, Forêt d'Analalava, 29.6 km 280° W Ranohira, N -22.59167, E 45.12833, alt 700 m, Fisher, Griswold et al., 2_1_2003; **CASENT0490719** (collection code: BLF07703, 2w, CAS), **CASENT0491357** (collection code: BLF07762, 2w, CAS), **CASENT0491554** (collection code: BLF07293, 1w, CAS): Prov. Fianarantsoa, Forêt d'Atsirakambiaty, 7.6 km 285° WNW Itremo, N -20.59333, E 46.56333, alt 1550 m, Fisher, Griswold et al., 1_22_2003; **CASENT0491364** (collection code: BLF07761, 2w, CAS), **CASENT0492591** (collection code: BLF07652, 2w, CAS), **CASENT0492611** (collection code: BLF07652, 2w, CAS), **CASENT0492612** (collection code: BLF07652, 2w, CAS): Prov. Fianarantsoa, Parc National d'Isalo, Sahanafa River, 29.2 km 351° N Ranohira, N -22.31333, E 45.29167, alt 500 m, Fisher, Griswold et al., 2_10_2003; **CASENT0494326** (collection code: BLF09951, 1w, CAS): Prov. Antsiranana, Forêt de Bekaraoka, 6.8 km 60° ENE Daraina, N -13.16667, E 49.71, alt 150 m, B.L. Fisher, 12_8_2003; **CASENT0495109** (collection code: BLF08147, 2w, CAS): Prov. Toamasina, Montagne d'Anjanaharibe, 18.0 km 21° NNE Ambinanitelo, N -15.18833, E 49.615, alt 470 m, Fisher, Griswold et al., 3_8_2003; **CASENT0498718** (collection code: BLF10016, 2w, CAS), **CASENT0498721** (collection code: BLF10016, 2w, CAS): Prov. Antsiranana, Forêt d'Ampondrabe, 26.3 km 10° NNE Daraina, N -12.97, E 49.7, alt 175 m, B.L. Fisher, 12_10_2003.

Description of workers. Body color: yellow. Body color pattern: Body concolorous. Absolute cephalic size: 496 [460, 574]. Cephalic length vs. maximum width of head capsule (CL/CWb): 1.23 [1.16, 1.35]. Postocular distance vs. cephalic length (PoOc/CL): 0.48 [0.46, 0.50]. Postocular sides of cranium contour frontal view orientation: converging posteriorly. Postocular sides of cranium contour frontal view shape: convex. Vertex contour line in frontal view shape: straight; slightly concave. Vertex sculpture: main sculpture inconspicuous, ground sculpture smooth. Gena contour line in frontal view shape: convex. Genae contour from anterior view orientation: converging. Gena sculpture: rugoso-reticulate with feeble areolate ground sculpture. Concentric carinae laterally surrounding antennal foramen: present. Eye length vs. absolute cephalic size (EL/CS): 0.26 [0.23, 0.27]. Frontal carina distance vs. absolute cephalic

size (FRS/CS): 0.31 [0.29, 0.33]. Longitudinal carinae on median region of frons: absent. Smooth median region on frons: present. Antennomere count: 12. Scape length vs. absolute cephalic size (SL/CS): 0.74 [0.69, 0.78]. Median clypeal notch: variable. Ground sculpture of submedian area of clypeus: smooth; present. Median carina of clypeus: variable. Lateral carinae of clypeus count: present. Metanotal depression: variable. Dorsal region of mesosoma sculpture: areolate ground sculpture, superimposed by dispersed rugae. Lateral region of pronotum sculpture: ground sculpture areolate, main sculpture absent. Mesopleuron sculpture: ground sculpture areolate, main sculpture absent. Metapleuron sculpture: ground sculpture areolate, main sculpture absent. Petiole width vs. absolute cephalic size (PEW/CS): 0.22 [0.19, 0.24]. Anterior profile of petiolar node contour line in lateral view shape: concave. Dorso-caudal petiolar profile contour line in lateral view shape: convex. Dorsal region of petiole sculpture: ground sculpture smooth, main sculpture absent. Postpetiole width vs. absolute cephalic size (PPW/CS): 0.33 [0.30, 0.36]. Dorsal region of postpetiole sculpture: ground sculpture smooth, main sculpture dispersed rugose.

Diagnosis. Workers of *N. nitidus* cannot be confused with *N. gibber* because the conspicuous mesothoracic hump that is a diagnostic character of the latter species is absent in *N. nitidus* workers. This species also can be easily separated from dark phenotypes of *N. madecassus* based on color: the dark madecassus phenotypes are dark brown but the workers of *N. nitidus* are light yellow. Morphometric ratio (PoOC/CW) and discriminant D4 function helps to separate *N. nitidus* from other *madecassus* phenotypes; further details are given in Diagnosis under *N. madecassus*.

The workers of this species are the most similar to that of *N. flavus*. The broadly overlapping elevational distribution as well as qualitative and quantitative traits of *N. flavus* and *N. nitidus* workers hamper easy separation. A simplified discriminant D2 function with a greatly reduced character set for safe separation is provided in the diagnosis section of *N. flavus*.

Biology and distribution. This species typically occurs in Madagascar's rain forests at lower altitudes between 10 and 1550 meter, mean: 383 m (Fig. 3). This species is known to forage in low vegetation, nests can often be found in dead twigs, stems above ground or rarely in rotten logs at higher elevations.

Acknowledgements

First, we would like to thank Michele Esposito, from CASC, for her enduring support with databasing, imaging processing, proofreading, and her overall support in the lab. We also want to thank Dr. Phil S. Ward from the University of California Davis, U.S.A., for providing additional material collected in Madagascar. Moreover, the fieldwork on which this study is based could not have been completed without the gracious support of the Malagasy people and the Arthropod Inventory Team (Balsama Rajemison, Jean-Claude Rakotonirina, Jean-Jacques Rafanomezantsoa, Chrislain Ranaivo, Hanitriniana Rasoazanamavo, Nicole Rasoamanana, Clavier Randrianan-

drasana, Dimby Raharinjanahary). Special thanks due to Flavia Esteves for helping in R. This study was supported by the National Science Foundation under Grant No. DEB-0072713, DEB-0344731, and DEB-0842395. Finally, SC was supported by the Schlinger Fellowship at the California Academy of Sciences and an Ernst Mayr Travel Grants to the MCZ.

Reference

- Beleites C, Sergio V (2015) hyperSpec: a package to handle hyperspectral data sets in R (R package version 0.98-20150304). <http://hyperspec.r-forge.r-project.org>
- Blaimer BB, Fisher BL (2013) How much variation can one ant species hold? Species delimitation in the *Crematogaster kelleri*-group in Madagascar. Public Library of Science ONE 8: e68082. doi: 10.1371/journal.pone.0068082
- Bolton B (1994) Identification Guide to the Ant Genera of the World. Harvard University Press, Cambridge, MA, 222 pp.
- Csősz S, Fisher BL (2015) Diagnostic survey of Malagasy *Nesomyrmex* species-groups and revision of *hafahafa* group species via morphology based cluster delimitation protocol. ZooKeys 526: 19–59. doi: 10.3897/zookeys.526.6037
- Csősz S, Fisher BL (2016a) Toward objective, morphology-based taxonomy: a case study on the Malagasy *Nesomyrmex sikorai* species group (Hymenoptera: Formicidae). PLoS ONE 11(4): e0152454. doi: 10.1371/journal.pone.0152454
- Csősz S, Fisher BL (2016b) Taxonomic revision of the Malagasy members of the *Nesomyrmex angulatus* species group using the automated morphological species delineation protocol NC-PART-clustering. PeerJ 4: e1796. doi: 10.7717/peerj.1796
- Csősz S, Heinze J, Mikó I (2015) Taxonomic Synopsis of the Ponto-Mediterranean Ants of *Temnothorax nylanderi* Species-Group. PLoS ONE 10(11): e0140000. doi: 10.1371/journal.pone.0140000
- Csősz S, Seifert B, Müller B, Trindl A, Schulz A, Heinze J (2014) Cryptic diversity in the Mediterranean *Temnothorax lichtensteini* species complex (Hymenoptera: Formicidae). Organisms Diversity & Evolution 14(1): 75–88. doi: 10.1007/s13127-013-0153-3
- Evenhuis NL (2013) The insect and spider collections of the world website. <http://hbs.bishop-museum.org/codens/> [accessed: 3 Mar 2014]
- Fisher BL (2009) Two new dolichoderine ant genera from Madagascar: *Aptinoma* gen. n. and *Ravavy* gen. n. (Hymenoptera: Formicidae). Zootaxa 2118: 37–52.
- Harris RA (1979) A glossary of surface sculpturing. California Department of Food and Agriculture, Bureau of Entomology 28: 1–31.
- Hita Garcia F, Fisher BL (2014) The hyper-diverse ant genus *Tetramorium* Mayr (Hymenoptera, Formicidae) in the Malagasy region taxonomic revision of the *T. naganum*, *T. ple-siarum*, *T. schaufussii*, and *T. severini* species groups. ZooKeys 413: 1–170. doi: 10.3897/zookeys.413.7172
- Maechler M, Rousseeuw P, Struyf A, Hubert M, Hornik K (2014) cluster: Cluster Analysis Basics and Extensions. R package version 1.15.3.

- Nilsen G, Borgan O, Liestøl K, Lingjærde OC (2013) Identifying clusters in genomics data by recursive partitioning. *Statistical Applications in Genetics and Molecular Biology* 12: 637–652. doi: 10.1515/sagmb-2013-0016
- Nilsen G, Lingjaerde OC (2013) clusterGenomics: Identifying clusters in genomics data by recursive partitioning. R package version 1.0. <http://CRAN.R-project.org/package=cluster-Genomics>
- R Core Team (2015) R: A language and environment for statistical computing. R Foundation for Statistical Computing, Vienna, Austria. <http://www.R-project.org/> [accessed: 20 January 2015]
- Rakotonirina JC, Csősz S, Fisher BL (2016) Revision of the Malagasy *Camponotus edmondi* species group (Hymenoptera, Formicidae, Formicinae): integrating qualitative morphology and multivariate morphometric analysis. *ZooKeys* 572: 81–154. doi: 10.3897/zookeys.572.7177
- Revell LJ (2012) phytools: an R package for phylogenetic comparative biology (and other things). *Methods in Ecology and Evolution* 3.2 (2012): 217–223. doi: 10.1111/j.2041-210X.2011.00169.x
- Seifert B, Ritz M, Csősz S (2014) Application of exploratory data analyses opens a new perspective in morphology-based alpha-taxonomy of eusocial organisms. *Myrmecological News* 19: 1–15.
- Tibshirani R, Walther G, Hastie T (2001) Estimating the number of clusters in a data set via the gap statistic. *Journal of the Royal Statistical Society: Series B (Statistical Methodology)* 63(2): 411–423. doi: 10.1111/1467-9868.00293
- Venables WN, Ripley BD (2002) *Modern Applied Statistics with S*. (4th ed.) Springer, New York. doi: 10.1007/978-0-387-21706-2
- Yoshimura M, Fisher BL (2012) A revision of male ants of the Malagasy Amblyoponinae, with resurrections of the genera *Stigmatomma* and *Xymmer*. *Public Library of Science ONE* 7(3): e33325.

New Brazilian Cerambycidae from the Amazonian region (Coleoptera)

Antonio Santos-Silva¹, Maria Helena M. Galileo²

1 Museu de Zoologia, Universidade de São Paulo, São Paulo, SP, Brazil **2** PPG Biologia Animal, Departamento de Zoologia, Universidade Federal do Rio Grande do Sul, Porto Alegre, RS, Brazil. (Fellow of the Conselho Nacional de Desenvolvimento Científico e Tecnológico)

Corresponding author: Antonio Santos-Silva (toncriss@uol.com.br)

Academic editor: Ann Ray | Received 27 November 2015 | Accepted 16 June 2016 | Published 6 July 2016

<http://zoobank.org/4CA15222-99F3-420D-8626-71908479BB8A>

Citation: Santos-Silva A, Galileo MHM (2016) New Brazilian Cerambycidae from the Amazonian region (Coleoptera). ZooKeys 603: 131–140. doi: 10.3897/zookeys.603.7335

Abstract

Three new species of Cerambycidae are described from the Brazilian Amazonian region: *Psapharochrus bezarki* (Lamiinae, Acanthoderini); *Xenofrea ayri* (Lamiinae, Xenofreini); and *Mecometopus wappesi* (Cerambycinae, Clytini). *Mecometopus wappesi* is added to a previous key.

Keywords

Neotropical region, taxonomy

Introduction

Psapharochrus Thomson, 1864 is a large genus of Acanthoderini from the American continent, currently with 92 species. Monné (2015b) recorded 90 species, not including *P. wappesi* Galileo et al., 2015, and *P. langeri* Martins et al., 2015. However, this catalogue includes *Psapharochrus quadrigibbus* (Say, 1831), a species currently belonging to *Acanthoderes* (*Acanthoderes*) Audinet-Serville, 1835 (e.g. Audureau 2010), and does not include *P. lengii* (Wickham, 1914), from the U.S.A, a species described in *Acanthoderes* and transferred to *Psapharochrus* by Linsley (1961), without explanation. Twenty one species are currently recorded from the Brazilian Amazonian region.

Xenofrea Bates, 1885 is an exclusively American genus, occurring from Mexico (Chiapas) to Central and South America. According to Monné (2015b), the genus encompasses 52 species. With the recent description of *X. wappesi* Galileo et al., 2015, currently *Xenofrea* includes 53 species. Sixteen species are recorded from the Brazilian Amazonian region.

Mecometopus Thomson, 1861 encompasses 14 species, occurring from Mexico to Southern South America (Monné 2015a). Currently eight species are recorded from the Brazilian Amazonian region.

Material and methods

Photographs were taken with a Canon EOS Rebel T3i DSLR camera, Canon MP-E 65mm f/2.8 1–5× macro lens, controlled by Zerene Stacker AutoMontage software. Measurements were taken in “mm” using a micrometer ocular Hensoldt/Wetzlar - Mess 10 in the Leica MZ6 stereomicroscope, also used in the study of the specimens.

The collection acronyms used in this study are as follows:

INPA Coleção Sistemática de Entomologia, Instituto Nacional de Pesquisas da Amazônia, Manaus, Amazonas, Brazil;

MZSP Museu de Zoologia, Universidade de São Paulo, São Paulo, Brazil.

Systematics

Acanthoderini Thomson, 1860

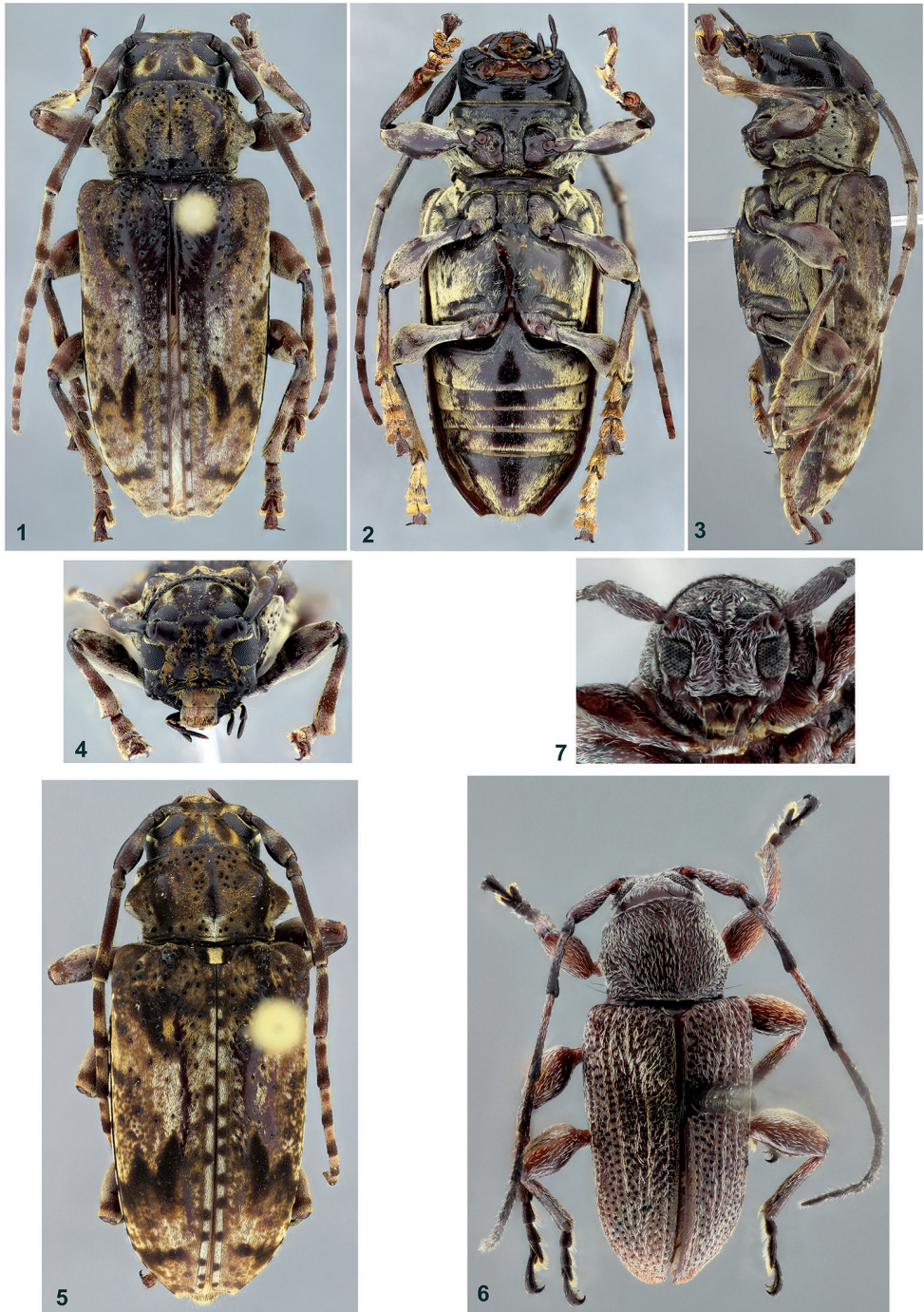
Psapharochrus bezarki sp. n.

<http://zoobank.org/C131C15F-145C-4412-B6DA-4A1BB126D4CA>

Figs 1–5

Description. Holotype female. Integument dark-brown; mouthparts reddish-brown, except for palpi mostly dark-brown.

Head. Frons moderately coarsely, sparsely punctate; with ochraceous pubescence on wide band on each side of longitudinal sulcus, longitudinal lateral wide band connected to transverse band below antennal tubercles and narrow band around eyes; remaining surface glabrous or nearly so. Area between antennal tubercles moderately, coarsely punctate laterally, smooth centrally; with ochraceous pubescence close to antennal tubercles, glabrous centrally. Vertex moderately, coarsely punctate between upper eye lobes, impunctate on remaining surface; on each side with large, elliptical macula with brown pubescence, surrounded laterally and posteriorly with dense, yellowish pubescence (becoming wider behind upper eye lobe); remaining surface with slightly



Figures 1–7. 1–5 *Psapharochrus bezarki*, female: 1 dorsal habitus, holotype 2 ventral habitus, holotype 3 lateral habitus, holotype 4 head, frontal view, holotype 5 dorsal habitus, paratype 6–7 *Xenofrea ayri*, holotype male: 6 dorsal habitus 7 head, frontal view.

conspicuous brownish pubescence. Area behind eyes microsculptured on wide band close to eye, moderately, finely, abundantly punctate on remaining surface; glabrous, except for narrow pubescent band close to eye. Genae transversely striate laterally, very finely striate and punctate toward frons; with short, ochraceous, sparse setae, except for narrow band close to eye. Submentum with transverse, narrow central carina; microsculptured, with short, ochraceous pubescence. Antennal tubercles mostly glabrous, impunctate. Longitudinal sulcus distinct from clypeus to anterior margin of prothorax. Distance between upper eye lobes 0.55 times length of scape; distance between lower eye lobes in front equal to length of scape. Antennae 1.4 times elytral length; reaching elytral apex; scape with brownish pubescence, maculate with ochraceous pubescence; antennomeres III–IV with yellowish-white pubescence on base and transverse band before apex, remaining surface with brownish pubescence; antennomeres V–X with yellowish-white pubescence on basal third, brown on distal third (gradually widening toward X); antennomere XI with yellowish-white pubescence; antennal formula based on antennomere III: scape = 0.70; pedicel = 0.18; IV = 0.71; V = 0.51; VI = 0.41; VII = 0.37; VIII = 0.32; IX = 0.31; X = 0.26; XI = 0.26.

Thorax. Prothorax 1.8 times wider than long (including lateral tubercles); lateral tubercles, large, conical, with blunt apex. Pronotum coarsely, deeply, sparsely punctate, finer, denser on each side of central tubercle; with three distinct tubercles: one on each side, very large, reniform; another centrally, triangular at base, carina-shaped toward apex; with ochraceous pubescence, denser on some regions, absent or nearly so on others. Sides of prothorax coarsely, moderately abundantly punctate; with yellowish-white, dense pubescence, less so near anterior margin. Prosternum impunctate; with yellowish-white pubescence laterally and close to coxal cavities. Prosternal process wide, centrally distinctly wider than base of peduncle of profemora; with yellowish-white pubescence, not obscuring integument. Mesosternum microsculptured, except for smooth, transverse anterior band; with short, moderately sparse, ochraceous pubescence, but glabrous on smooth region. Mesepisterna, mesepimera, and metepisterna with dense yellowish-white pubescence. Metasternum with dense yellowish-white pubescence; centrally rubbed in the holotype. Scutellum centrally depressed distally; distal lateral sides distinctly elevated; with brown pubescence, except for narrow yellowish band at apex.

Elytra. Sides slightly convergent toward distal third, then gradually curved toward apex; with distinct tubercle on each side of scutellum; without distinct carinae; coarsely, sparsely punctate; central area of disc on basal third mostly glabrous; remaining surface of basal 2/3 with ochraceous pubescence, mixed with brown and white pubescence (laterally, on center of this region, with distinct, oblique band of brown pubescence); with zig-zag, transverse band of brown pubescence about beginning of distal third (not reaching suture); with transverse band of brown pubescence on distal quarter; along suture, with rounded spots of brown pubescence; remaining surface of distal third with ochraceous pubescence mixed with brown and white pubescence; apex truncate, with outer angle slightly projected and sutural angle rounded.

Legs. Femora and tibiae with yellowish-white pubescence, except for golden pubescence on dorsal sulcus of mesotibiae and ventral apex of meso- and metatibiae.

Abdomen. Ventrites microsulptured; with yellowish-white pubescence (partially rubbed in the holotype); ventrite V with longitudinal, narrow, central sulcus on basal 3/4.

Variation. Frons totally pubescent, but with glabrous area on holotype covered with short, yellowish-brown pubescence; pubescence on frons ochraceous, almost covering entire surface (except for elliptical brown macula); antennal tubercles mostly with ochraceous pubescence; scutellum centrally with wide, yellowish band of pubescence; elytral without glabrous area on basal third; pubescence on ventral side of body more ochraceous.

Dimensions in mm (female). Total length (from mandibular apex to abdominal apex), 16.4–17.8; prothorax: length, 2.9–3.4; anterior width, 4.3–4.8; posterior width, 4.3–4.8; largest width, 5.4–6.1; humeral width, 6.3–6.9; elytral length, 11.5–12.7. The largest dimensions are those of the holotype.

Type material. Holotype female from BRAZIL, *Amazonas*: Manaus (ZF2, km 14, Torre – 40 m high, 02°35'21"S / 60°06'55"W, light trap), 19-22.III.2004, J. A. Rafael, C. S. Motta, F. F. Xavier Filho, A. Silva Filho and J. T. Câmara col. (INPA). Paratypes - BRAZIL, *Amazonas*: Manaus (ZF2, km 14, Torre – 35 m high, 02°35'21"S / 60°06'55"W, light trap), female, 13-16.VIII.2004, J. A. Rafael, F. F. Xavier Filho, A. R. Ururahy, A. Silva Filho and S. Trovisco col. (MZSP); female, 9-12.XI.2004, C. S. Motta, A. S. Filho, S. Trovisco and L. S. Aquino col. (INPA).

Etymology. The new species is named after Larry G. Bezark, for his contribution toward the knowledge of Cerambycidae, his friendship, and constant help.

Remarks. *Psapharochrus bezarki* sp. n. is similar to *P. bimaculatus* (Fuchs, 1959), but differs by the elytra more parallel-sided (distinctly more narrowed toward apex in *P. bimaculatus*), and by the presence of the zig-zag brown macula on the distal half of the elytra (absent in *P. bimaculatus*). It differs from *P. nigropunctatus* (Tippmann, 1960) by the scutellum proportionally larger, longitudinally sulcate posteriorly (smaller and flat in *P. nigropunctatus*), and by the protibiae not laterally flattened (flattened in *P. nigropunctatus*). It can be separated from *P. lanei* (Marinoni & Martins, 1978) by the lateral tubercles of pronotum reniform (subconical in *P. lanei*), by the scutellum larger and longitudinally sulcate posteriorly (smaller and flat in *P. lanei*), and by the lateral tubercles of prothorax with blunt apex (acute in *P. lanei*).

Xenofreini Aurivillius, 1923

Xenofrea ayri sp. n.

<http://zoobank.org/84B64850-D902-4005-A1C9-F24B9D0CEBCA>

Figs 6–9

Description. Holotype male. Integument dark-brown, almost black; base of antennomeres III–V, coxae, femora, and most tibiae dark reddish-brown; abdominal ventrites brown.

Head. Frons, area between eyes and vertex finely, abundantly punctate; with gray pubescence, not entirely obscuring integument. Area behind eyes microsulptured,

mainly toward lower lobe; with wide band of gray pubescence close to eye, glabrous toward prothoracic margin. Genae finely, abundantly punctate close to eye, smooth on apex; with gray, moderately sparse pubescence. Antennal tubercles covered with gray pubescence. Longitudinal sulcus distinct from clypeus to posterior margin of upper eye lobes. Distance between upper eye lobes 0.3 times length of scape; distance between lower eye lobes in frontal view 0.6 times length of scape. Antennae 1.85 times elytral length; reaching elytral apex at middle of antennomere VIII; antennomeres with short, gray pubescence interspersed with short, erect yellowish setae (denser toward distal antennomeres); antennal formula based on antennomere III: scape = 0.91; pedicel = 0.27; IV = 1.24; V = 0.72; VI = 0.69; VII = 0.67; VIII = 0.57; IX = 0.51; X = 0.48; XI = 0.51.

Thorax. Prothorax 1.3 times wider than long (including lateral tubercles); lateral tubercles placed before middle, blunt; anterolateral tubercles slightly distinct. Pronotum finely, abundantly punctate; with moderately thick, decumbent, abundant, gray setae, distinctly not obscuring integument, slightly denser laterally and on narrow, longitudinal, central band on anterior half; basal margin straight; anterior margin, rounded, somewhat projected forward centrally. Sides of prothorax with sculpture and setae as on pronotum (punctures slightly coarser). Prosternum notably narrow, about 1/3 of length of procoxal cavity; finely, densely punctate, with very short, decumbent setae. Prosternal process centrally narrowed, narrowest area as wide as half of base of peduncle of profemora. Mesosternum about as long as prosternum; finely, densely punctate; with short, decumbent, gray setae, not obscuring integument. Mesepisterna and mesepimera finely, abundantly punctate (punctures slightly coarser than on mesosternum); with gray, decumbent setae (longer than on mesosternum), not obscuring integument. Metepisterna with gray, decumbent, dense setae, obscuring integument. Metasternum with gray, dense pubescence. Scutellum with gray, moderately sparse, decumbent setae.

Elytra. Sides slightly convergent from humerus to about distal third, then rounded, narrowed toward sutural angle; coarsely, densely punctate (slightly finer toward apex); with gray, thick, short setae forming longitudinal rows (somewhat less distinctly on anterior quarter).

Legs. Femora notably clavate; with decumbent, gray pubescence, not obscuring integument. Tibiae mostly with gray, decumbent, short setae.

Abdomen. Ventrites finely, abundantly punctate; with decumbent, grayish setae, not obscuring integument.

Dimensions in mm. Total length, 4.40; prothorax: length, 1.00; anterior width, 1.15; posterior width, 1.15; largest width, 1.40; humeral width, 1.75; elytral length, 3.15.

Type material. Holotype male from BRAZIL, *Amazonas*: Novo Airão (02°38'39"S / 60°56'07"W; armadilha luminosa, dossel, 18:00–21:00h), 27.VIII.2011, F. F. Xavier & A. Agudelo col. (INPA).

Etymology. Tupi, *ayrí* = tiny; relating to the small size of the species.

Remarks. *Xenofrea ayri* sp. n. is the smallest known species of the genus, and can be easily recognized by the elytral pubescence forming rows, while in the other species the elytra always have different complex patterns.



Figures 8–13. 8–9 *Xenofrea ayri*, holotype male: 8 ventral habitus 9 lateral habitus 10–13 *Mecometopus wappesi*, holotype male: 10 lateral habitus 11 dorsal habitus 12 ventral habitus 13 head, frontal view.

Clytini Mulsant, 1839

Mecometopus wappesi sp. n.

<http://zoobank.org/C8FCF792-A63C-44D3-AF05-13340F85BD33>

Figs 10–13

Description. Holotype male. Head reddish-brown, more brownish on some areas; mandibles reddish-brown on basal 2/3, dark-brown on apical third; scape, pedicel and antennomeres III–IV reddish-brown; antennomeres V–XI brown, more reddish ventrally on distal antennomeres; prothorax dark-brown, except for reddish-brown anterior region of prosternum; mesosternum dark-brown; remaining ventral surface reddish-brown; elytra dark-brown, except for reddish-brown areas under dense yellow pubescence; pro- and mesofemora mostly reddish-brown (slightly darker on mesofemora), except for yellowish-brown distal area of club; metafemora mostly brown, except for reddish brown region of peduncle and part of club, and apex of club; pro- and mesotibiae yellowish-brown; metatibiae yellowish-brown on basal 2/3, reddish-brown on apical third; tarsi from yellowish-brown to reddish-brown. Pubescence mostly yellow, more whitish on mesosternal process, and yellowish-white on ventral side of meso- and metathorax and abdomen; brown on dark regions of elytra.

Head. Frons finely, densely punctate, except for narrow, longitudinal, central band and triangular area close to clypeus with punctures slightly coarser, distinctly sparser; with wide band of short, decumbent setae on each side (distinctly not obscuring integument). Area between antennal tubercles and upper eye lobes with sculpture and setae as on frons. Vertex microsculptured interspersed with fine, moderately sparse punctures, except for narrow, smooth, longitudinal, central band; with very short, sparse setae, except for longer, denser setae close to basal area. Area behind eyes finely, abundantly punctate (punctures slightly coarser, sparser toward margin of prothorax); with moderately dense, narrow band of pubescence close to eyes (wider toward apex of upper eye lobe); remaining surface glabrous. Area between gena and submentum with long, sparse setae. Genae 1.3 times as long as lower eye lobe; finely, abundantly punctate, except for smooth, narrow area close to apex; with short, sparse setae (sparser toward apex). Submentum smooth, except for some small, very sparse asperites; with short, moderately sparse setae (slightly denser laterally) interspersed with long setae. Antennal tubercles with sculpture and setae as on frons, except for narrow glabrous, smooth area close to apex. Distance between upper eye lobes 1.15 times length of scape; distance between lower eye lobes in frontal view 0.95 times length of scape. Antennae 0.7 times elytral length; reaching about basal quarter of elytra; antennal formula based on antennomere III: scape = 1.03; pedicel = 0.42; IV = 0.64; V = 0.67; VI = 0.53; VII = 0.39; VIII = 0.32; IX = 0.28; X = 0.21; XI = 0.25.

Thorax. Prothorax as long as wide at widest region; sides rounded. Pronotum coarsely, densely punctate; longitudinal carina distinct from basal quarter to near anterior margin, enlarged at middle, with small transverse oblique keels; with three wide, transverse bands of dense pubescence, fused on lateral side of prothorax: one basally, narrowed on

middle; one centrally, interrupted by the longitudinal carina; one close to anterior margin; remaining surface with pubescence sparser, mainly on longitudinal carina. Sides of prothorax with sculpture and pubescence as on pronotum. Prosternum with sculpture as on pronotum, except for transverse band at anterior quarter finely striate and punctate; pubescence dense, obscuring integument, except for subglabrous, transverse band at anterior quarter. Prosternal process moderately narrowed centrally; distal half deeply, widely sulcate centrally; with dense pubescence. Mesosternum finely rugose; with short, sparse setae, except for small region with dense pubescence close to mesocoxal cavities and mesepisterna. Mesepisterna with sparse pubescence on anterior region, notably dense on posterior region. Mesepimera with brown, sparse pubescence. Mesosternal process with dense pubescence. Scutellum densely yellow pubescent. Metepisterna with dense, yellow pubescence, except for narrow anterior band with brown, sparse pubescence. Metasternum densely pubescent, except for transverse, wide band with distinctly sparser pubescence. Elytra. Each elytron with five wide areas with dense, yellow pubescence: one at basal third, oblique, distinctly enlarged from side to anterior margin (not reaching lateral and anterior margin); one longitudinal laterally at basal quarter; one before middle, triangular, narrowed toward side, then projected forward (reaching suture, almost reaching lateral margin); one transverse, about middle of distal half (reaching suture, almost reaching lateral margin); one covering almost entire distal quarter, less dense. Elytral apex obliquely truncate, with small spine at outer and sutural angles.

Legs. Inner and outer apex of metafemora triangularly projected.

Abdomen. Ventrites I–IV densely pubescent distally, distinctly sparser on anteriorly (this latter gradually wider from I to IV). Ventrite V with sparse pubescence throughout.

Dimensions in mm. Total length, 8.7; prothorax: length, 2.1; anterior width, 1.5; posterior width, 1.6; largest width, 2.1; humeral width, 2.1; elytral length, 5.5.

Type material. Holotype male from BRAZIL, *Amazonas*: 60 Km N Manaus (Fazenda Esteio; ZF-3 km 23), 6.XII.1984, B. C. Klein col. (INPA).

Etymology. The new species is named after James E. Wappes, for his contribution toward the knowledge of Cerambycidae, friendship, and constant help.

Remarks. *Mecometopus wappesi* sp. n. is similar to *M. globicollis* (Laporte & Gory, 1841), but differs as follows: body distinctly slender; pronotum covered with yellow pubescence; yellow triangular macula on the elytra reaches the sides and is then projected forward; distal quarter of the elytra with yellow pubescence. In *M. globicollis* (see photograph of the holotype at Bezark 2015) the body is wider, the pronotum is not covered with yellow pubescence, the yellow triangular macula on the elytra does not reach the sides, and the distal quarter of the elytra has no yellow pubescence.

Mecometopus wappesi also resembles *Mirichlytus triangularis* Martins & Galileo, 2008, but differs mainly by the antennae distinctly 11-segmented (antennomeres VIII–XI fused in *Mirichlytus*), by the transverse and oblique bands of yellow pubescence on the elytra being wider (narrow in *M. triangularis*).

Mecometopus wappesi can be included in the alternative of couplet “11”, from Martins and Galileo (2011) (translated; modified):

- 11(10) Sides at middle of elytra without small spot of white pubescence **11'**
 – Sides at middle of elytra with small spot of white pubescence **12**
 11'(11) Pronotum with distinct yellow pubescence; yellow triangular macula of elytra reaching sides; apical quarter of elytra with yellow pubescence. Brazil (Amazonas) ***M. wappesi* sp. n.**
 – Pronotum without yellow pubescence; yellow triangular macula of elytra not reaching sides; apical quarter of elytra without yellow pubescence. French Guiana, Brazil (Amazonas, Pará, Maranhão)
 ***M. globicollis* (Laporte & Gory, 1836)**

Acknowledgements

We thank José Albertino Rafael (INPA), who sent the specimens for study to the late Ubirajara R. Martins. We also express our sincere thanks to James E. Wappes for the information on *Miriclytus triangularis* and to Larry G. Bezark for corrections to the manuscript.

References

- Audureau A (2010) Complément a l'inventaire faunistique des Cerambycidae de la reserve privée forestière de Domitila (Nicaragua) avec description de nouvelles espèces (Coleoptera, Cerambycidae). Les Cahiers Magellanes 110: 1–10.
- Bezark LG (2016) A photographic Catalog of the Cerambycidae of the New World. <https://apps2.cdfa.ca.gov/publicApps/plant/bycidDB/wsearch.asp?w=n> [accessed November 2015]
- Linsley EG (1961) The Cerambycidae of North America. Part I. Introduction. University of California Publications in Entomology 18: 1–97.
- Martins UR, Galileo MHM (2011) Tribo Clytini. In: Martins UR (Eds) Cerambycidae Sul-Americanos (Coleoptera). Taxonomia. Sociedade Brasileira de Entomologia, Curitiba, v. 12, 8–264.
- Monné MA (2015a) Catalogue of the Cerambycidae (Coleoptera) of the Neotropical Region. Part I. Subfamily Cerambycinae. http://www.cerambyxcat.com/Part1_Cerambycinae.pdf [accessed November 2015]
- Monné MA (2015b) Catalogue of the Cerambycidae (Coleoptera) of the Neotropical Region. Part I. Subfamily Lamiinae. http://www.cerambyxcat.com/Part2_Lamiinae.pdf [accessed November 2015]

Morphology and development rate of the immature stages of *Glyphidops (Oncopsia) flavifrons* (Bigot, 1886) (Diptera, Neriidae) under natural conditions

Andrés Felipe Vinasco Mondragón¹, Nancy Soraya Carrejo Gironza¹

¹ Departamento de Biología, Facultad de Ciencias Naturales y Exactas, Universidad del Valle, Santiago de Cali, Colombia

Corresponding author: Andrés Felipe Vinasco Mondragón (andres.vinasco@correounivalle.edu.co)

Academic editor: T. Dikow | Received 2 December 2015 | Accepted 7 June 2016 | Published 6 July 2016

<http://zoobank.org/1F03C899-E62B-4088-BB9E-7A50E1998F76>

Citation: Vinasco AFM, Carrejo NSG (2016) Morphology and development rate of the immature stages of *Glyphidops (Oncopsia) flavifrons* (Bigot, 1886) (Diptera, Neriidae) under natural conditions. ZooKeys 603: 141–159. doi: 10.3897/zookeys.603.7355

Abstract

Of the 116 Neriidae species known to date, 113 species have not been studied in their immature stages. Here, we examine the development of the immature stages of *Glyphidops (Oncopsia) flavifrons* (Bigot, 1886), which has one of the broadest distributions of Neriidae in southern North America, Central America, and South America; offering excellent opportunities for biological studies. A population of this species was monitored over a five month period. The following characteristics were tracked for a population located on the University of Valle campus in Cali, Colombia: oviposition duration, number of eggs per egg mass and lifespan of each immature stage (egg, larva, and puparium) under natural conditions (*in situ*). The external morphology of the egg, larva, and puparium were described; their stages lasted 58 (\pm 4) hours, 10 (\pm 1) days and 13 (\pm 1) days, respectively. The lapse of time for each larval instar was statistically supported by using Tukey comparisons and cluster analysis of hypopharyngeal sclerite length and mandibular area. In addition, it was also sustained throughout the morphological study of structural changes in mouth hook, and anterior and posterior spiracles. Finally, the presence of the labial and epipharyngeal sclerites are reported as new characters of Neriioidea. Natural history data are provided.

Keywords

Cactus flies, cephalopharyngeal skeleton, hypopharyngeal sclerite, immature stage, Neriioidea

Introduction

Neriidae (Diptera: Brachycera) is represented by 116 species grouped in 17 genera (Pape et al. 2011, Sepúlveda et al. 2014). Studies of this family in the Neotropical Region have increased in the past five years, focusing on its adult stage (Sepúlveda et al. 2013a, 2013b, 2014, Mongiardino et al. 2014). However, since 1947, only three species from all around the world have been described in their immature stage (Berg 1947, Olsen and Rickman 1963, Mangan and Baldwin 1986). *Telostylinus lineolatus* (Wiedemann, 1830), an Australo-Oceanic species, whose larvae were described from eight mature larvae and 12 pupae collected on the banks of the Tenaru River in the Solomon Islands and studied by Berg (1947). *Odontoloxozus longicornis* (Coquillett, 1904), distributed from the southwestern United States to Costa Rica (Olsen and Rickman 1963, Mangan and Baldwin 1986), was described based on larvae raised for several generations in necrotic tissue of *Opuntia occidentalis* Engelm. from San Dimas Canyon, California by Olsen and Rickman (1963). *Odontoloxozus pachycericola* Mangan & Baldwin, 1986, was studied from senita cactus (*Lophoceros schottii* (Engelm)) and cactus carbon (*Pachycereus pringlei* (S. Wats.) from the cape region of Baja California, México and bred for several generations by Mangan and Baldwin (1986). The study, however, focused on the adult and only the number of prothoracic spiracular papillae of the 3rd larval instar was determined. Nevertheless, Foote and Teskey (1991) proposed that neriid larvae lack diagnostic distinctive characters that allow them to be properly separated from other muscomorphan saprophagous families like Micropezidae or Cypselosomatidae (McAlpine 1989, Wiegmann et al. 2011).

Regarding their biology, some authors consider neriids as synanthropic or at least opportunistic flies (Barraclough 1993). Eberhard (1998) taped adults of *G. flavifrons* and *Nerius plurivittatus* displaying aggressive behavior, copulation, and oviposition over branches of a fallen tree on a decomposition stage in a mature rainforest in Panama. In the same country, Cresson (1938) observed neriid adults on decomposing flesh of *Cereus* Mill., pumpkin (*Cucurbita* L.) and rotting trunks of papaya (*Carica papaya* L.). In North America, Olsen and Ryckman (1963) found and bred *Odontoloxozus longicornis* (Coquillett) larvae from eggs laid in necrotic tissue of several cactus species and Steyskal (1987) reported it on stems of *C. papaya*. Preston-Mafham (2001) reports males of *Gymnonerius fuscus* and *Telostylinus* sp. guarding rot-holes (beetle larval borings and female oviposition in fallen Mango branches in Sulawesi, Indonesia. Barraclough (1993) reports *Chaetonerius* larvae reared from decaying pumpkin in South Africa and Zimbabwe and also proposed that *C. apicalis* could develop in fruits or flowers of *Strelitzia nicolai* Regel & Koern. Finally, Bezzi (1928) cited by Berg (1947) reported neriid larvae in cotton capsules from Australia.

Glyphidops (Oncopsia) flavifrons (Bigot, 1886) can be found throughout the Neotropical Region, from south-eastern Brazil (Espírito Santo) to the southern United States (Arizona, Florida) in the southern Nearctic Region (Sepúlveda et al. 2014). Its reproductive behavior has been studied by Eberhard (1998), yet their immature stages remain unknown. The present paper will describe the immature stages and life history of *G. (O.) flavifrons* and report development time for each life stage under natural conditions in Cali, Colombia, during May and April (2014). Larvae of *G. (O.) flavifrons* are compared morphologically with those of *O. longicornis*, *O. pachycericola*, and *T. lineolatus*.

Materials and methods

Breeding and immature lifespan

Glyphidops flavifrons was reared *in situ*, between the months of March and May, 2014 on the Melendez campus of the University of Valle located in Santiago de Cali, Colombia (3°22.448'N; 76°32.084'W; 987 masl) found in the tropical dry forest life zone *sensu* Holdridge (1967).

The study area was composed of *C. papaya* trees and *Tradescantia zebrina*, with vegetation coverage varying between 58% and 70%.

For the breeding process, fresh *C. papaya* stems were cut into 30 cm long pieces and placed at the study site in a plastic container to protect them from other organism during decomposition (2–3 days). Afterwards the stems were exposed to adults of *G. (O.) flavifrons* population (previously identified) for four hours. The time of oviposition was recorded. The egg masses were individualized by one-ounce plastic containers with fragments of *C. papaya* of 8 mm, each container was labeled and covered with fine mesh to allow ventilation and prevent intrusion by other invertebrates. To prevent injury of the eggs, the number of eggs per egg mass was recorded after the maturation of it (24 hours later) (Olsen and Rickman 1963, Craig 1967). After hatching, the larvae were observed daily. The puparia were individualized in plastic containers containing a layer of sifted and sterilized soil.

For the developmental rate assessment, 30 eggs were separated and observed every four hours until hatching. After hatching, ten larvae were sacrificed, following the method proposed by Adams and Hall (2003). Ten larvae were sacrificed daily until pupation occurred. An observation of 15 puparia was made every 12 hours, until emergence.

Humidity and temperature data were compiled daily, at 15 minute intervals with the help of a Dickson Data Logger TP125.

Morphology

Egg

Twenty-six eggs were set on hollow plates with distilled water. Polar diameter and respiratory filament length were measured. Description follows the terminology used by Olsen and Rickman (1963).

Larva

To ensure accuracy, larval body length was measured immediately after sacrifice (Adams and Hall 2003). Micro-preparation of cuticular surface and cephalopharyngeal skeleton was performed following the methodology suggested by Niederegger et al. (2011). Body length (lateral view), hypopharyngeal sclerite length, and mandibular area (mandibular sclerite + mouth hook) measurements were performed daily. Additionally, antennal variations, maxillary palp, antenomaxillary lobe, and spinulose areas were observed. Description follows the terminology used by Foote and Teskey (1991).

Puparium

Total length of puparium was measured and morphology of both anterior spiracles (prothoracic spiracle) and thorny areas were examined. To determine duration of pupariation, photographic records were performed every 15 minutes for 150 minutes after pupation initiated (Bunchu et al. 2012).

Measurements and images

Measurements of egg, larva, and puparium were performed using tpsDig2, version 2.22 (Rohlf 2007).

Photographic records were performed using a Canon EOS Rebel T3i camera, adapted to a Nikon Eclipse E200 microscope. Photographic compilation was done using Helicon Focus software. Diagrams were constructed with Corel DRAW program.

Data analysis

Larval instars were determined by using a one-way ANOVA (confidence level: 95%). Post-ANOVA (Tukey comparisons) was used to calculate the variation of hypopharyngeal sclerite length and mandibular area throughout the observation period. Moreover, a cluster analysis was performed for each measurement (including body length) using Euclidean measures and neighbor-joining as a linkage method for each cluster.

Additionally, scatter plots were graphed for each of the measured variables to monitor their distribution over time. Box-plot graphs were used to compare distribution between the variables for each different larval instar (Ln). Figures and analyses were performed using Microsoft Excel 2013 and Minitab16 software.

Results

Development time

Development time of *Glyphidops (O.) flavifrons* was determined under natural conditions, temperature mean 25.8 °C (maxim. 41.06 °C, minim. 18.6 °C) and relative humidity mean 69.38% (maxim. 82.9%, minim. 44.9%). The eggs hatched 58 ± 4 hours ($n = 30$) after being laid. The total larval development time was 10 ± 1 days ($n = 15$) and the puparium stage had a development time of 13 ± 2 days ($n = 15$).

ANOVA showed significant differences for values of mandibular area versus time ($df = 9.40$; $F = 1829.61$ and $P = 0.000$) and the hypopharyngeal sclerite length versus time ($df = 9.40$; $F = 7870.85$ and $P = 0.000$). Post-ANOVA of mandibular area showed four groups, and post-ANOVA of hypopharyngeal sclerite length showed

Table 1. Size and life span for each *Glyphidops* (*O.*) *flavifrons* larval instar, under natural conditions (25.79 ± 4.11 °C, 69.38 ± 9.23 % H.R.).

Post-hatching days	N° larvae	Body length (mm)	Mand. Area (mm ²)	Post-ANOVA mand. area †	Hypophr. Scl. Length (mm)	Post-ANOVA Hypophr. Scl. length †
L₁						
1	10	1.22–1.75	0.00084	A	0.097	A
2	8	1.88–2.52	0.00085	A	0.1	A
L₂						
3	11	2.95–4.45	0.0045	B	0.13	B
4	11	4.41–6.2	0.0047	B	0.13	B
L₃						
5	6	6–9.56	0.0134	C	0.24	C
6	7	6.58–10.53	0.015	D	0.24	C
7	10	6.35–10	0.015	D	0.24	C
8	10	7.99–10.59	0.015	D	0.24	C
9	11	8.87–11.16	0.015	D	0.24	C
10	7	8.14–10.08	0.015	D	0.23	C
Instar summary						
L ₁	18	1.76 +/- 0.12	0.00084		0.098	
L ₂	22	4.36 +/- 1.14	0.0046		0.13	
L ₃	51	9.17 +/- 1.53	0.015		0.238	

† Post-ANOVA individual confidence level: 99.82%

three groups, thus confirming three distinct larval instars L₁, L₂ and L₃. Life spans of all larval instars are summarized in Table 1.

Scatter plots (Fig. 1a and c) show two distinct jumps in growth for the observed structures: the first between day 2 and 3 and the second between day 4 and 5. Furthermore, box-plot graphs (Fig. 1b and d) graphically support the findings from the Tukey test, by illustrating the variation in each structure's measurements.

Morphology

Egg

Body length 1–1.24 mm ($\bar{x} = 1.16$, $n = 20$); respiratory filament length 3.13–4.01 mm ($\bar{x} = 3.3$; $n = 20$). Body semi-cylindrical, dorsally convex and dorso-ventrally flattened, with a blunt posterior region. Respiratory filament originates from the anterior region, as long as 3.21 times the egg body length (Fig. 2). Two longitudinally lateral hatching lines departing from the respiratory filament attachment point and dim gradually towards the 1/6th posterior region of the egg body. Chorion sculpted with cells varying from pentagonal to octagonal (Fig. 2b), forming a mesh-like pattern that is more conspicuous in the posterior 1/6th. Anterior quarter region of the egg body with a small elliptical tubercle band visible with 10× magnification (Fig. 2c).

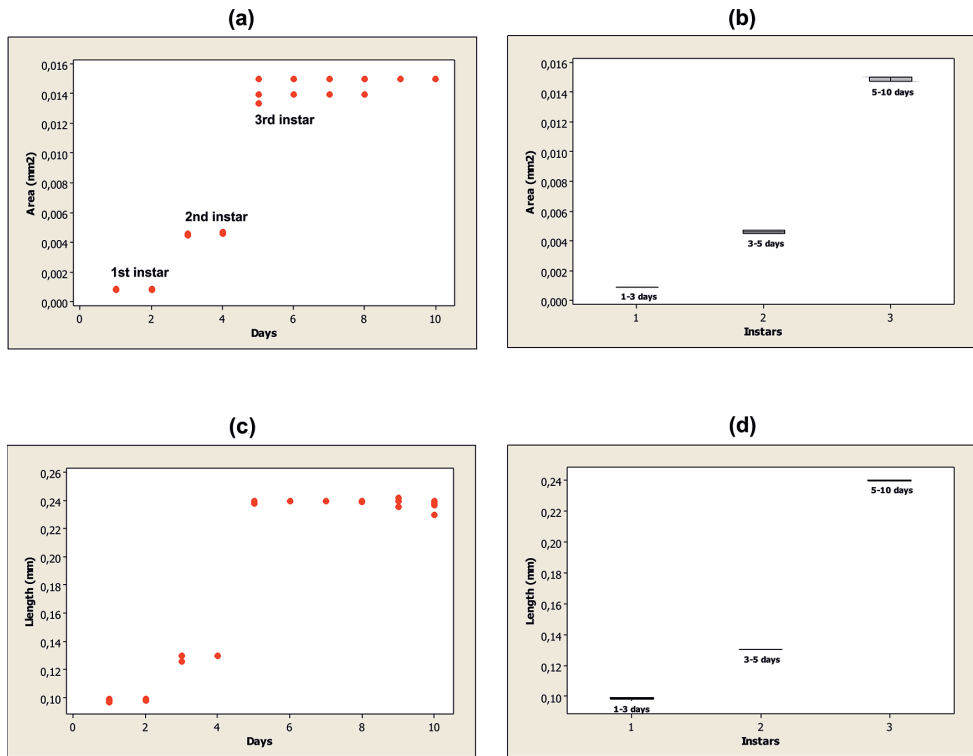


Figure 1. Scatterplot and Box-Plot: **a, b** mandibular area **c, d** hypopharyngeal sclerite length.

Larva

Vermiform body, glabrous, light to semitransparent (Fig. 3a–c). Head: (Fig. 4a–c) retractable, with two pairs of appendages located antero-dorsally; maxillary palpus bulbous, with an apical sensory depression, containing four to five tubercles with bristles over them; antenna reduced, with two to three antennomeres; a pair of ventrally curved mouth hooks, each originating from a mandibular sclerite (Fig. 6a–c.); antennoxillary strongly lobed: lobes with 28–30 oral or pseudo-tracheal bridges, each radiating from the labial lobe; epipharyngeal sclerite (Fig. 4a) U-shaped with projections joining ventro-posteriorly to the back margin of labial sclerite; labial sclerite (Fig. 4b and c), arrow-shaped, directed antero-ventrally; Thorax: Pro-, meso-, and metathorax well-defined. Hypopharyngeal sclerite H-shaped, as long as 5.5 times its width (lateral view), formed by two parallel bars connected by a strong bridge originated in the anterior half of the sclerite, “bridge” concave, forming a canal that links antero-dorsally with epipharyngeal sclerite. Tentoropharyngeal sclerite from before the anterior half of the prothorax to almost the previous anterior half of metathorax, with two pairs of parastomal bars extending dorsally and ventrally along the hypopharyngeal sclerite, dorsal pair as long as 0.8 times the length of hypopharyngeal sclerite and ventral pair as long as 0.3 times the length of hypopharyngeal sclerite; dorsal bridge dorsally dark, extending anteriorly

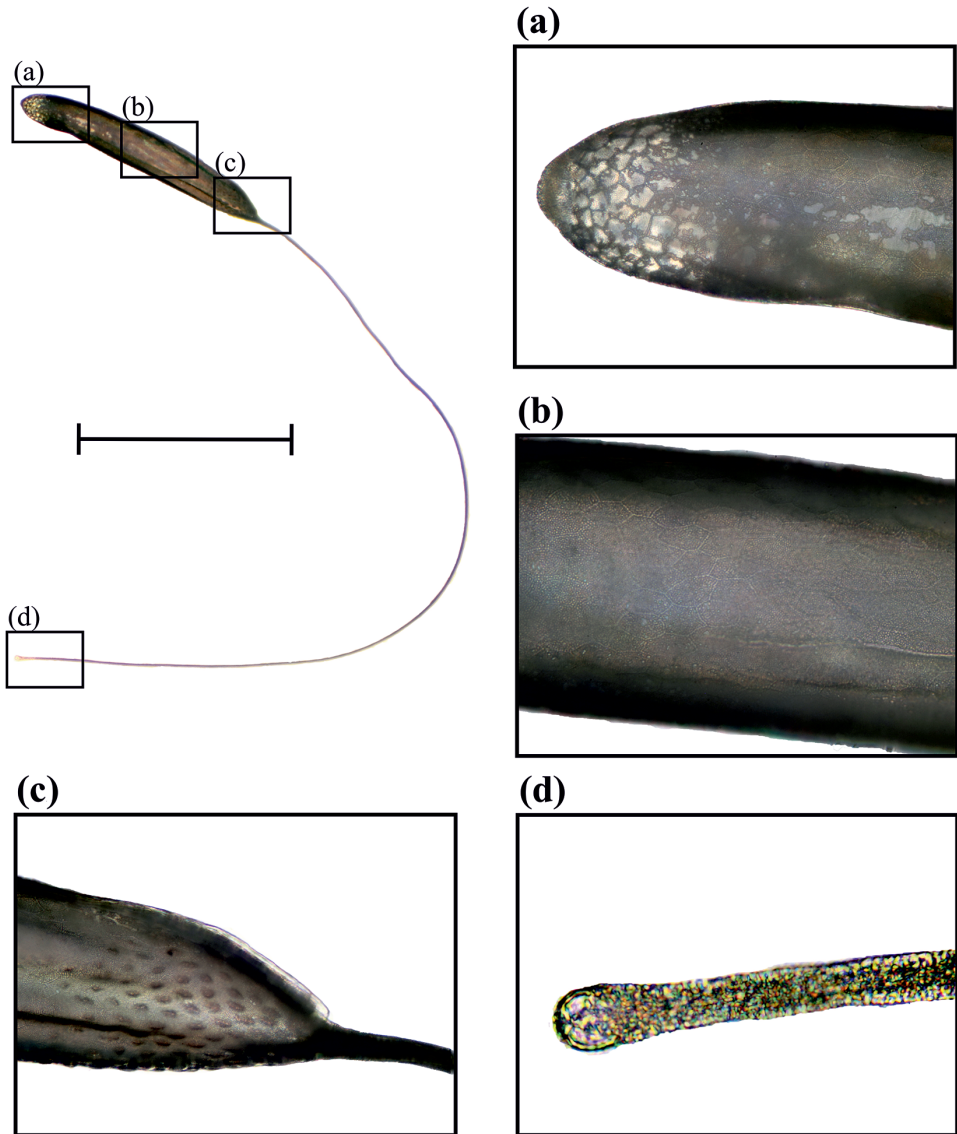


Figure 2. Egg in latero-dorsal view. Details **a** posterior end **b** average area of the egg, note the hexagonal pattern of the corium **c** basal respiratory filament point, note the tubercles over the apical area of the egg body **d** apex of the respiratory filament. Scale bar: 1 mm.

subsequently $\frac{1}{4}$ of hypopharyngeal sclerite; ocular spherical depression conspicuously located below the dorsal bridge; ventral cornu fused to the pharynx, forming a cavity that connects posteriorly with the esophagus and anteriorly with the cibarium; dorsal cornu 0.3 times shorter than the ventral cornu. Anterior spiracles, located dorsally in the latero-posterior half of pro-thorax, palmiform (Fig. 6a and b) variable across instars. Abdomen eight segmented, each (except I and VIII) in ventral view with two spinulose

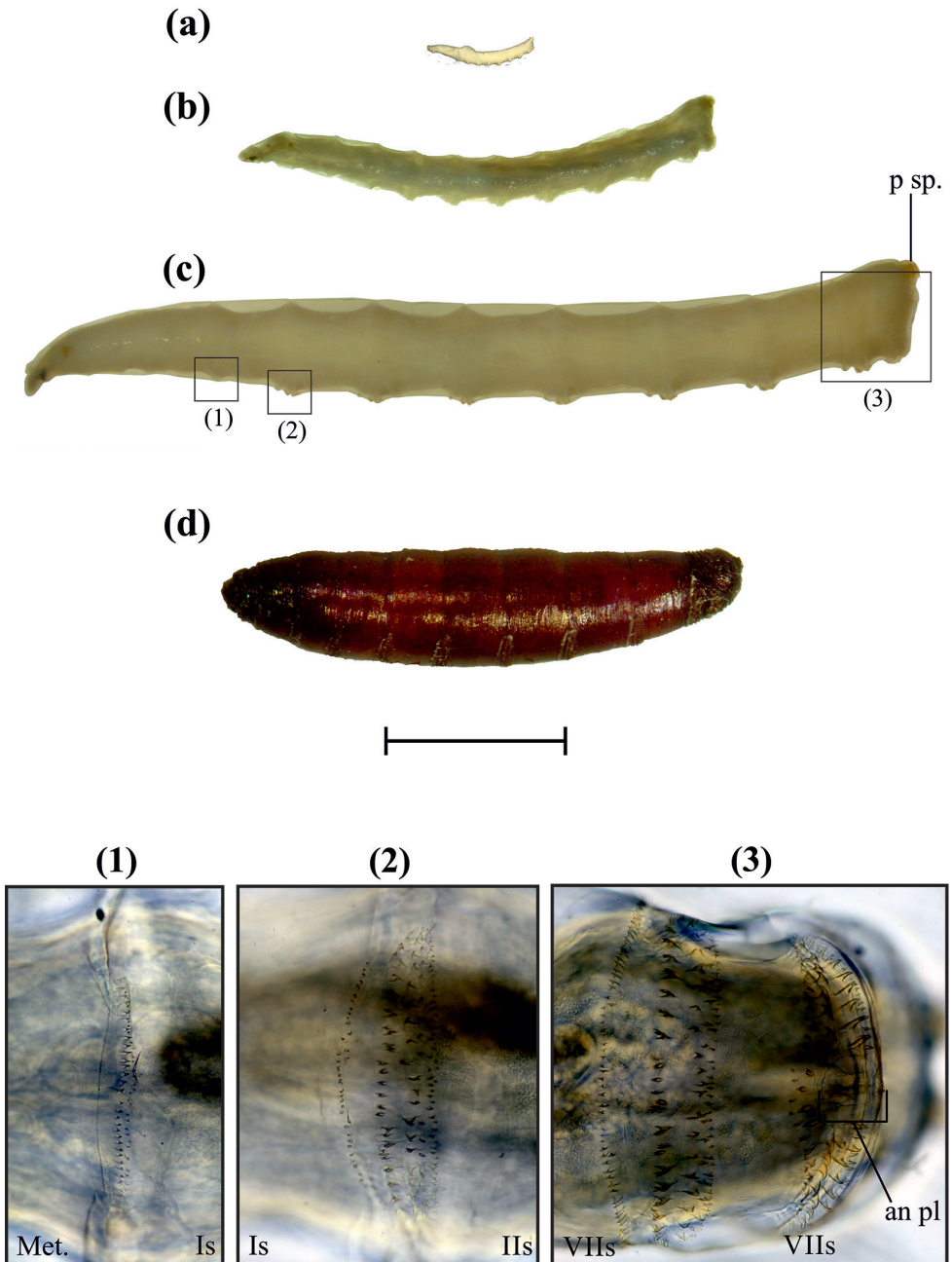


Figure 3. Larvae and puparium in lateral view and approach to the third larval instar spinulose areas. **a** L₁, **b** L₂ and **c** L₃ **d** Puparium. (1) Spinulose area of the first abdominal segment, (2) posterior row of spines on abdominal segment I and anterior spinulose area on abdominal segment II, (3) posterior row of spines on segment VII and spinulose areas on abdominal segment VIII. an. pl., anal plate; p sp., posterior spiracles; Met. metathorax. Scale bar: 2 mm.

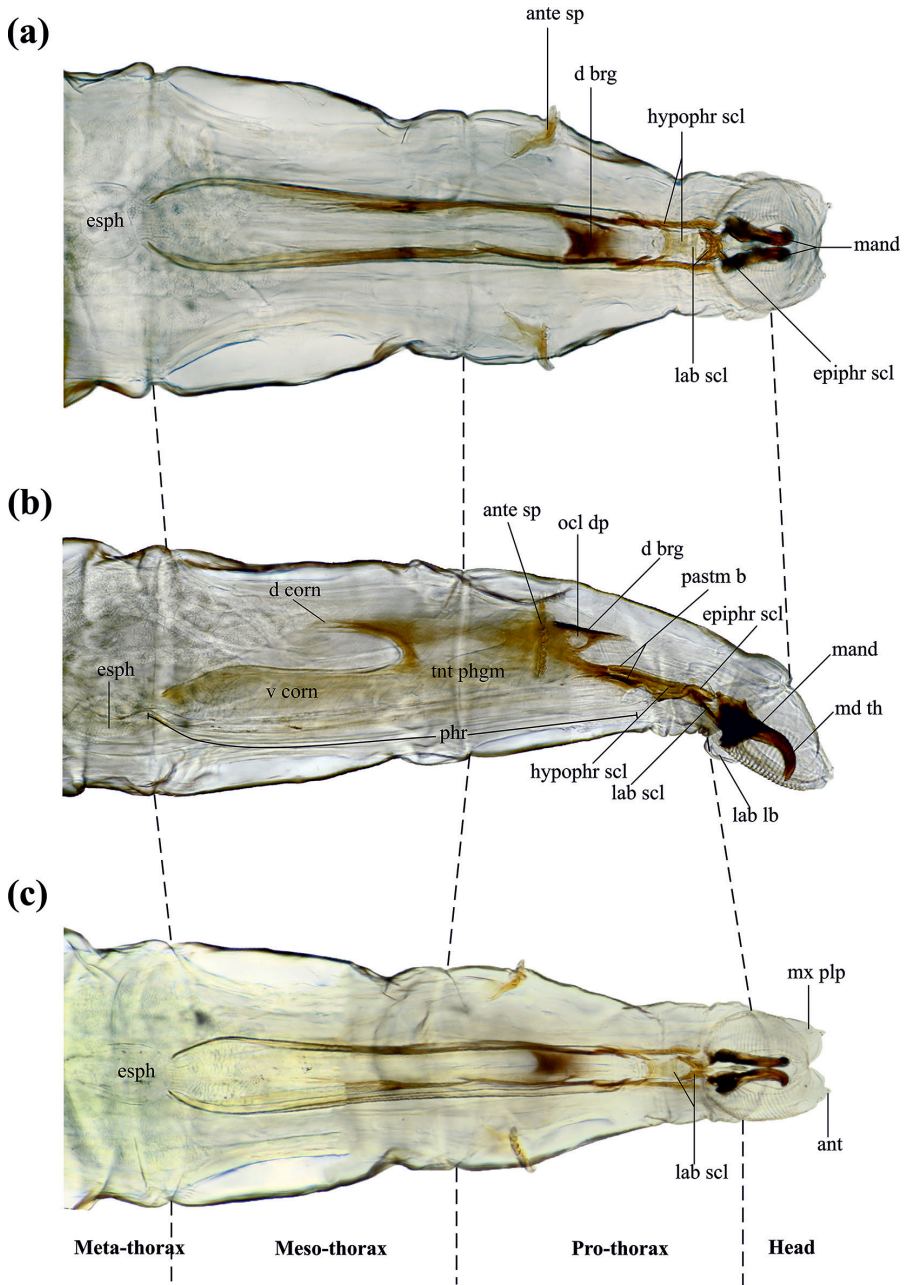


Figure 4. Cephalopharyngeal skeleton. **a** dorsal view **b** side view **c** ventral view. ant, antenna.; ante sp, anterior spiracle; d brg., dorsal bridge; d corn, dorsal corn; epiphr scl, epipharyngeal sclerite; esph, esophagus; hypophr scl, hypopharyngeal sclerite; lab lb, labial lobe; lab scl, labial sclerite; mand, mandible; md th, mandibular tooth; mx plp, maxilar palp; pastm b, parastomal bar; phr, pharynx; ocl dp, ocular depression; tnt phgm, tentorial phragm; v corn, ventral corn. Scale bar: 3 mm.

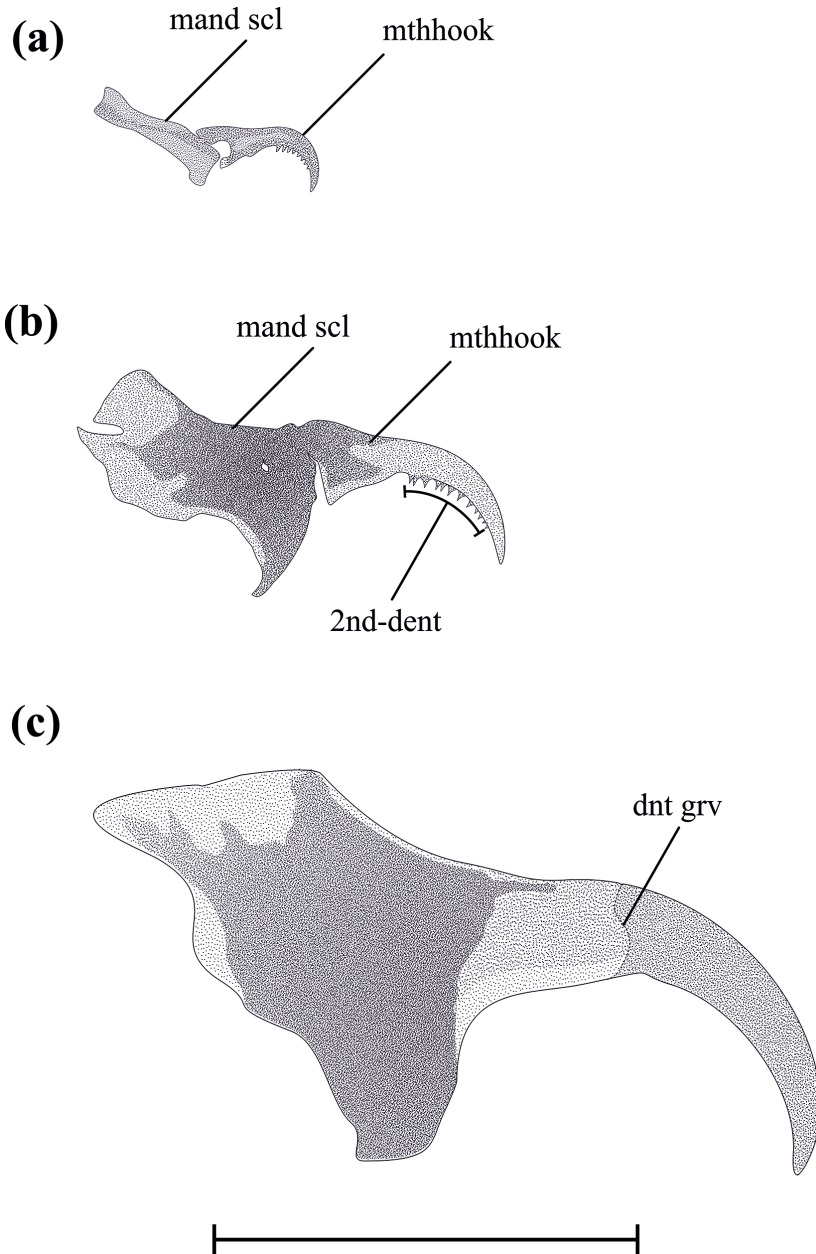


Figure 5. Mandibles of each larval instar. **a** L₁ **b** L₂ and **c** L₃. dnt grv, dental groove; mand scl, mandibular sclerite; mthhook, mouthhook; 2nd-dent., secondary dentition. Scale bar: 1.5 mm.

areas, anterior area with three transverse rows of spines, first anteriorly directed and second and third posteriorly directed, posterior area with only one transverse row of spines anteriorly directed; abdominal segment I, with two posteriorly directed anterior ventral

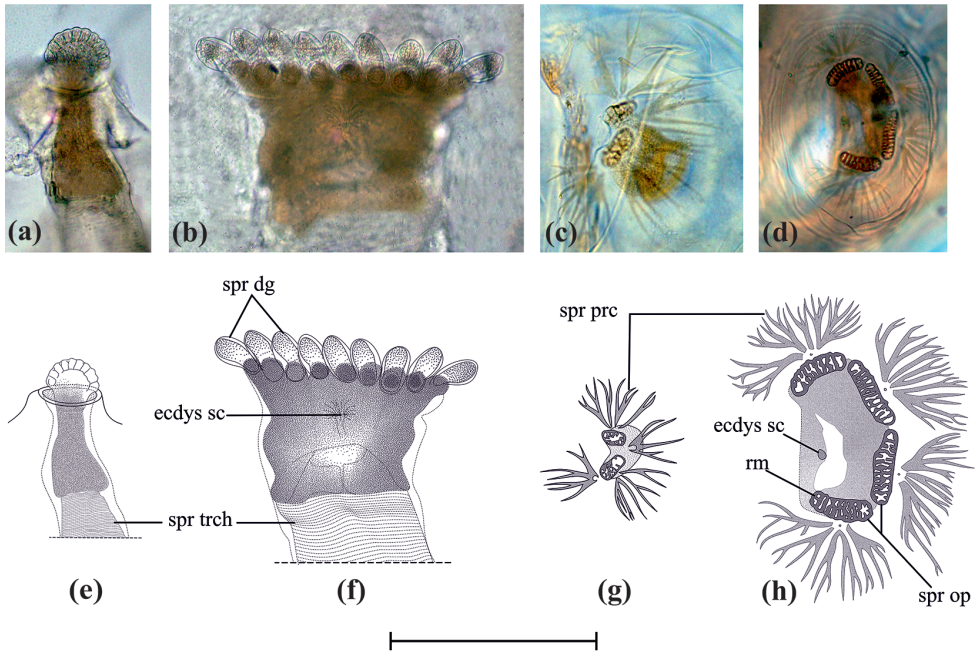


Figure 6. Spiracles of each larval instar. Anterior spiracle on L_2 (a, e) and L_3 (b, f). Posterior spiral on L_1 - L_2 (c, g) and L_3 (d, h). Scale bar of drawings 0.15 mm. ecdys sc, ecdysial scar; spr dg, spiracular digit; spr op, spiracular opening; spr prc, spiracular process; spr trch, spiracular trachea; rm, rime.

rows, first with $36 (\pm 1)$ small spinules and second with $35 (\pm 2)$ papillae as spinules (Fig 4c1), posterior row with $28 (\pm 2)$ spines directed above; abdominal segment VIII with two spinulose areas, anterior area with three transverse arranged rows of spines, first row with $34 (\pm 3)$ spines, anteriorly directed and the following two rows with $29 (\pm 2)$ and $43 (\pm 2)$ spines, posteriorly directed, posterior spinulose area with three transverse rows, the first continuous and the following two discontinuous: first row with $27 (\pm 4)$ spines, anteriorly directed and discontinuous rows with $8 (\pm 2)$ spines on each side, posteriorly directed (Fig. 3c3). Ventro-posterior rounded anal plate with a longitudinal slit in the middle; two dorso-posterior spiracular plates, located on abdominal protrusions, each with four processes as fractals (branchy structure) and spiracular openings that vary in number and shape on each instar (Fig. 6c and d).

Larval instar

L_1 . From 1.22 to 2.52 mm ($\bar{x} = 1.76$, $n = 18$) in length; antenna bi-segmented, apical segment oval; mandibular sclerite slightly sclerotized, elongated, three times longer than wide, dorsally articulated with the mouth hook, the latter with marked sclerotic outside and with 7–8 ventral teeth (Fig. 5a); anterior spiracles not observed (under light microscope); posterior spiracles with two semicircular spiracular openings (Fig. 6c) and four spiracular processes: two of them closely associated with spiracular openings, the other two free.



Figure 7. External coloration of *G. (O.) flavifrons* puparium, up to 3 hours after beginning cuticular excretion. From right to left: top row 0, 15, 30, 45, 60; bottom row 75, 90, 105, 135, and 180 minutes after beginning pupation. Scale bar: 1 mm.

L₂. From 2.95 to 6.2 mm (\bar{x} = 4.36; n = 22) in length; antenna with two antennomeres, distally oval; mandibular sclerite as long as 2.5 times wider, differentially sclerotized, antero-dorsally fused with mouth hook (Fig. 5b); ventral margin of mouth hook with 10 teeth; anterior spiracle 2.5 times longer than its greatest width, apical third visible as a small stump with 8–9 digital radiation and light interdigital recesses (Fig 7e.); posterior spiracle as L₁.

L₃. From 6 to 11.16 mm (\bar{x} = 9.17; n = 51) in length; tri-segmented antenna, second antennomere truncated, with sclerotized apical border, third antennomere reduced 0.3 times length of second like a papilla; mandible uniformly sclerotized, mandibular sclerite completely fused to mouth hook, reddish-brown, without ventral teeth mouth hook, showing a slight groove in basal 1/3 (Fig 6c.); anterior spiracle 0.8 times as long as its greatest width, with 9–11 digits (Fig 7b.), each on average 1.7 times longer than its greatest width, fully everted completely inside out, ecdysial conspicu-

ous scar, mesal to digital projections (Fig 7d); posterior spiracles with defined ecdysial scar, four spiracular openings elongated, mitochondrial-shaped (Fig. 6d), arranged semi-circularly to the scar, each opening with a spiracular process associated medially to the outer margin, each spiracular process radiates in a filamentous way to a small sclerotized point.

Puparium

Coarctate; 5.48–7.49 mm (\bar{x} = 5.93; n = 15) in length, reddish brown (Fig. 3d and Fig. 7) with transverse striations or wrinkles that are more prominent on segments VII and VIII; anterior spiracles situated frontally (side view), with 9–11 sclerotized digits; posterior spiracles with four spiracular openings and a poorly defined spiracular process.

Biology

The body of each egg is buried in the substrate and the filament is spread over the surface. As the female began laying eggs (reaching packages up to 20 eggs, one egg at a time), it was observed that numerous filaments were emerging and radiating from the same point. Along this process, the male remains close to the female and the mating happen continuously between laid eggs. See Suppl. material 2.

Just moments before the hatching, the larva is observed moving the body and the head, rubbing its mandibles against the inner wall of the egg and finally thrusting the corium. The larva emerges from the anterior part of the egg by using one of the two longitudinally lateral hatching lines. See Suppl. material 3.

The pupation took between 150 and 175 minutes (n = 15) (Fig. 7a–k). The emergence of the imago was passed through a circular suture that ran from the anterior spiracles halfway to the first abdominal segment, separating two plates, one ventral and one dorsal, where the latter was completely separated from the puparium.

Species comparison

Table 2 shows the main features found when comparing pre-imaginal stages described to date.

Discussion

According to the Brooks-Dyar rule (Dyar 1890, Crosby 1973, Hutchinson and Tongring 1984) the growth rate of one or more sclerotized structures increases at a geometric rate throughout the larval stages. Over the years this rule has become an indispensable tool for the description and establishment of the larval stages for many holometabolous insect species. For Muscomorpha, research focused on the variation of hypopharyngeal sclerites or mandibles (Petitt 1990) and showed that the cephalic tagma has lost its outer sclerotization and is reduced to a membranous area. As shown in figures 1a and 1c, two

Table 2. Morphological comparison between immature stages of *Glyphidops flavifrons*, *Telostylinus lineolatus*, *Odontoloxozus longicornis* and *Odontoloxozus pachycericola*.

Feature	<i>G. (O.) flavifrons</i>	<i>T. lineolatus</i>	<i>O. longicornis</i>	<i>O. pachycericola</i>
Egg body length	1.0–1.24	-	0.89–1.09	-
Egg respiratory filament length	3.13–4.01	-	2.50–3.70	-
Anterior region of egg body with small elliptical tubercles band	Present	-	Absent	-
No. of antennomeres on L ₃	3	3	3	-
Ventral lobe on dorsal cornu	Absent	Absent	Absent	-
No. papillae on anterior spiracles on L ₃	9–11	8, 9 ‡	16 ‡, 17–19	13–15
No. of posterior spiracle openings on L ₃	4	4	4	4
Mandible composed on L ₁ and L ₂	Yes	-	Yes	-
Labial sclerite	Present	-	-	-
Epipharyngeal sclerite	Present	-	-	-
Hypophr. scl. Length on L ₃ (mm)	0.236–0.242	-	0.27–0.31	-
Body length on L ₃ (mm)	6–11.16	5.9–8.1	8.77–13.28	-
Puparium length (mm)	5.48–7.49	4.8–6.3	5.8–8.75	.

(-) Unknown, (‡) Usually

significant leaps in the individual measurements of each structure were observed, with a growth ratio of 1.31 (L₁ to L₂) and 1.84 (L₂ to L₃) for hypopharyngeal sclerite length, and 5.44 (L₁-L₂) and 3.26 (L₂ to L₃) in the mandibular area. Additionally, it was possible to determine each larval stage through tracking the changes of external morphological features, such as the rise of the anterior spiracles on L₂ and its noticeable modification when entering L₃, as well as the increase of spiracular posterior openings (two to four) when transitioning from L₂ to L₃, and finally the significant changes of the mandibular sclerotization and loss of the mouth hook's ventral teeth, throughout each of the instars. Even though the anterior spiracle was not distinct on L₁ under the microscope light, some authors have found evidence of the presence of this on several Schizophora species using the scanning electron microscope (Kitching 1976, Grzywacz 2012). It is possible that an anterior spiracle exists in *G. (O.) flavifrons* L₁, however additional studies are required.

On the larval descriptions of Diopsoidea's families (sister group of Neriioidea *sensu* McAlpine), only two allusions to the labial and the epipharyngeal sclerite have been done. The first one on *Sphyracephala brevicornis* (Say) says that both features were undeveloped (Lavigne 1962). The second one by Foote (1970), on *Tanypeza longimana* Fallén showed a broadly V-shaped ligulate sclerite (= labial sclerite, Foote and Teskey 1991) immediately anterior to the hypostomal plate (= hypopharyngeal sclerite, Teskey 1981). The shape and position of the "ligulate sclerite" suggests that the labial sclerite found in *G. (O.) flavifrons*, represents a homologous structure.

Foote and Teskey (1991) undertook a morphological review of Diptera larvae, they did not find specific features to differentiate Neriidae larvae from other closely related saprophagous families, but proposed the four elliptical openings surrounding the ecdysial scar in the posterior spiracles as a potentially strong diagnostic feature. Our

study confirms their proposal and additionally reports two new features for the family: the presence of the epipharyngeal sclerite and the labial sclerite. These two novel features are also new at the superfamily level since neither of them have been reported in Cypselosomatidae, or Micropezidae larval descriptions (Berg 1947, Bohart and Gressitt 1951, Olsen and Ryckman 1963, McAlpine 1966, Wallace 1969, Teskey 1972, Foote and Teskey 1991, Mangan and Baldwin 1986, Barnes 2015).

The morphological characters observed in *G. (O.) flavifrons* immature stages indicate that both adult and larval stages of nerioid flies retain plesiomorphic features, such as larva with filter apparatus for particle feeding, mandibles separate, parastomal bars present and dorsal cornua with a window. Nevertheless, there are some autapomorphies in Neriidae, such as eggs with longitudinal dorsal hatching seam; these are not in the ground plan of Acalyprata. The monophyletic group Neriidae+Cypselosomatidae was initially proposed by McAlpine (1989) supported by seven synapomorphies of adults flies. Therefore, we propose that the four elliptical openings, surrounding the ecdysial scar in the posterior spiracles of L_3 , serve as a synapomorphy of the larval stage, since this condition is only found within these two families of Neriodea and it is not known to appear in any other Acalyprate taxon (Teskey 1981, Foote and Teskey 1991, Borkent and Rotheray 2009).

Olsen and Ryckman (1963) stated that *Odontoloxoxus longicornis* could be differentiated from *Telostylinus lineolatus* by the number of anterior spiracle digits. Likewise, Mangan and Baldwin (1986) found that the same feature allowed the separation of *O. longicornis* from *O. pachyericola*. *Glyphidops (O.) flavifrons* supports the use of the number of anterior spiracle digits as a consistent feature to separate the four species (Table 2). Nonetheless, the overlap between number of digits may generate difficulties in the future, thereby a further morphometric study (of gradual growth of the hypopharyngeal sclerite and mandibles) is recommended to determine its potential usefulness as a diagnostic character to differentiate larval neriids.

Acknowledgments

A special thanks goes to the laboratory of Grupo de Investigaciones Entomológicas (GIE), for providing access to all the required laboratory equipment. To James Montoya and Carmen Elisa Posso for loaning the field equipment and thanks to the University of Valle biology laboratory technicians for providing the necessary chemicals. We also thank two anonymous reviewers for their helpful comments on an earlier version of the manuscript.

References

- Açzél ML (1961) A Revision of American Neriidae (Diptera, Acalypratae). *Studia Entomologica* 4(1-4): 257–346.

- Adams ZJO, Hall MJR (2003) Methods used for the killing and preservation of blowfly larvae, and their effect on post-mortem larval length. *Forensic Science International* 138: 50–61. doi: 10.1016/j.forsciint.2003.08.010
- Barnes JK (2015) Biology and immature stages of *Comptosia univitta* (Walker, 1849) (Diptera: Micropezidae: Calobatinae). *Proceedings of the Entomological Society of Washington* 117(4): 421–434. doi: 10.4289/0013-8797.117.4.421
- Barracough DA (1993) The southern African species of Neriidae (Diptera). *Annual Natal Museum* 34 (1): 1–17.
- Berg CO (1947) Biology and metamorphosis of some Solomon Islands Diptera. Part I: Micropezidae and Neriidae. *Occasional papers of the museum of Zoology* 503(1-20): 9–12.
- Bohart GF, Gressitt JL (1951) Filth-Inhabiting flies of Guam. *Bernice P. Bishops Museum Bulletin* 204: 1–152.
- Bunchu N, Thaipakdee C, Vitta A, Sanit S, Sukontason K, Sukontason KL (2012) Morphology and developmental rate of the blow fly, *Hemipyrellia ligurriens* (Diptera: Calliphoridae): Forensic Entomology Applications. *Journal of Parasitology Research* 2012(3712): 1–10. doi: 10.1155/2012/371243
- Craig DA (1967) The eggs and Embriology of Some New Zealan Blepharoceridae (Diptera, Nematocera) with Reference to the Embryology of Other Nematocera. *Zoology* 8(18): 191–206.
- Cresson Jr ET (1938) The Neriidae and Micropezidae of America North of Mexico (Diptera). *Transactions of the American Entomological Society* 64(4): 293–366.
- Crosby TK (1973) Dyar's rule predated by Brooks' rule. *The New Zealand Entomologist* 5: 175–176. doi: 10.1080/00779962.1973.9722993
- Dyar HG (1890) The number of molts of Lepidopterous larvae. *Psyche* 5: 420–422. doi: 10.1155/1890/23871
- Eberhard WG (1998) Reproductive Behavior of *Glyphidops flavifrons* and *Nerius plurivitatus* (Diptera, Neriidae). *Journal of Kansas Entomological Society* 71(2): 89–107.
- Grzywacz A, Pape T, Szpila K (2012) Larval morphology of the lesser housefly, *Fannia canicularis*. *Medical and Veterinary Entomology* 26(1): 70–82. doi: 10.1111/j.1365-2915.2011.00968.x
- Foote BA (1970) The Larvae of *Tanypeza longimana* (Diptera: Tanypezidae). *Annals of the Entomological Society of America* 63(1): 235–238. doi: 10.1093/aesa/63.1.235
- Foote BA, Teskey HJ (1991) Order Diptera. In: Stehr FW (Ed.) *Immature Insects Volume 2*. Kendall/Hunt Publishing Co. Dubuque, Iowa, 690–800.
- Holdridge LR (1967) *Life Zone Ecology*. Tropical Science Center. San José, Costa Rica.
- Hutchinson GE, Tongring N (1984) The possible adaptive significance of the Brooks-Dyar rule. *Journal of Theoretical Biology* 106: 437–439. doi: 10.1016/0022-5193(84)90040-7
- Kitching RL (1976) On the prothoracic spiracles of the first instar larvae of Calyptrate Cyclorapha (Diptera). *Journal of Australian Entomological Society* 15: 233–235. doi: 10.1111/j.1440-6055.1976.tb01698.x
- Lavigne RJ (1962) Immature stages of the stalk-eyed fly, *Sphyracephala brevicornis* (Say) (Diptera: Diopsidae), with observations on its biology. *Bulletin Brooklyn Entomology Society* 107: 5–14.

- Mangan RL, Baldwin D (1986) A new cryptic species of *Odontotoxozus* (Neriidae: Diptera) from the Cape Region of Baja California Sur (Mexico). *Proceedings of the Entomological Society of Washington* 88(1): 110–121.
- McAlpine DK (1966) Description and biology of an Australian species of Cypselosomatidae (Diptera), with a discussion of family relationships. *Australian Journal of Zoology* 14(4): 673–685. doi: 10.1071/ZO9660673
- McAlpine JF (1989) Phylogeny and Classification of the Muscomorpha. In: Peterson BV, Shewell GE, Teskey HJ, Vockeroth JR, Wood DM, McAlpine JF (Eds) *Manual of Nearctic Diptera, Volume 1. Biosystematics Research Centre, Ottawa, Ontario, Monograph No 28, 1397–1502.*
- Mongiardino NK, Soto IM, Ramírez MJ (2014) First phylogenetic analysis of the family Neriidae (Diptera), with a study on the issue of scaling continuous characters. *Cladistics*, 1–24. doi: 10.1111/cla.12084
- Niederegger S, Wartenberg N, Spieß R, Mall G (2011) Simple clearing technique as species determination tool in blowfly larvae. *Forensic Science International* 206: e96–e98. doi: 10.1016/j.forsciint.2011.01.012.
- Olsen LE, Ryckman R (1963) Studies on *Odontotoxozus longicornis* (Diptera - Neriidae). Part I. Life History and Description of Immature Stages. *Annals of the Entomological Society of America* 56: 454–469. doi: 10.1093/aesa/56.4.454
- Petitt FL (1990) Distinguishing larval instars of the Vegetable Leafminer, *Liriomyza sativae* (Diptera: Agromyzidae). *The Florida Entomologist* 73(2): 280–286.
- Preston KM (2001) Resource defence mating system in two flies from Sulawesi: *Gymnonerius fuscus* Wiedemann and *Telostylinus* sp. near *duplicatus* Wiedemann (Diptera: Neriidae). *Journal of Natural History* 35: 149–156. doi: 10.1080/002229301447916
- Rohlf FJ (2007) TPSDig software series, digitize landmarks & outlines from image files, scanner, or video, version 2.22. Stony Brook, Department of Ecology and Evolution, State University of New York. <http://life.bio.sunysb.edu/morph/index.html> [Accessed 13 August 2014]
- Sepúlveda TA, Pereira-Colavite A, de Carvalho CJB (2013a) Revision of the Neotropical genus *Cerantichir* (Diptera: Neriidae) with new records and a key to species. *Revista Colombiana de Entomología* 39(1): 125–131.
- Sepúlveda TA, Wolf MI, de Carvalho CJB (2013b) Revision of the Neotropical genus *Eoneiria* (Diptera: Neriidae) with description of a new species from Colombia. *Zootaxa* 3636: 245–256. doi: 10.11646/zootaxa.3636.2.2.
- Sepúlveda TA, Wolff MI, de Carvalho CJB (2014) Revision of the New World genus *Glyphidops* Enderlein (Diptera: Neriidae). *Zootaxa* 3785(2): 139–174. doi: 10.11646/zootaxa.3785.2.2
- Steyskal GC (1987) Neriidae. In: Peterson BV, Shewell GE, Teskey HJ, Vockeroth JR, Wood DM, McAlpine JF (Ed.) *Manual of Nearctic Diptera, Volume 2. Biosystematics Research Centre, Ottawa, Ontario, Monograph No 28: 769–771.*
- Teskey HJ (1972) The mature larva and pupa of *Compsobata univitta* (Diptera: Micropezidae). *The Canadian Entomologist* 104: 295–298. doi: 10.4039/Ent104295-3
- Teskey HJ (1981) Morphology and Terminology-Larvae. In: Peterson BV, Shewell GE, Teskey HJ, Vockeroth JR, Wood DM, McAlpine JF (Eds) *Manual of Nearctic Diptera, Volume 1. Biosystematics Research Centre, Ottawa, Ontario, Monograph No 28: 65–88.*

Wallace JB (1969) The mature larva and pupa of *Calobatina geometroides* (Cresson) (Diptera: Micropezidae). Entomological News 80: 317–321.

Wiegmann BM, Trautwein MD, Winkler IS, Barra NB, Kim JO, Lambkin C, Bertone MA, Cassel BK, Bayless KM, Heimberg AM, Wheeler BM, Peterson KJ, Pape T, Sinclair BJ, Skevington JH, Blagoderov V, Caravas J, Kutty SN, Schmidt-Ott U, Kampmeier GE, Thompson FC, Grimaldi DA, Beckenbach AT, Courtney GW, Friedrich M, Meier R, Yeates DK (2011) Episodic radiations in the fly tree of life. PNAS 108(14): 5690–5695. doi: 10.1073/pnas.1012675108

Supplementary material 1

Cluster analysis of mandibular area and hypopharyngeal sclerite

Authors: Andrés Felipe Vinasco Mondragón, Nancy Soraya Carrejo Gironza

Data type: TIF file

Explanation note: Cluster analysis of mandibular area and hypopharyngeal sclerite length across time supports the concept of three larval instar (similarity indexes between 95% and 100%). (a) body length of the larva, (b) mandibular area and (c) length of hypopharyngeal sclerite. Each color represents a larval instar (Ln).

Copyright notice: This dataset is made available under the Open Database License (<http://opendatacommons.org/licenses/odbl/1.0/>). The Open Database License (ODbL) is a license agreement intended to allow users to freely share, modify, and use this Dataset while maintaining this same freedom for others, provided that the original source and author(s) are credited.

Supplementary material 2

Mating and oviposition process of *Glyphidops (Oncopsia) flavifrons*

Authors: Andrés Felipe Vinasco Mondragón, Nancy Soraya Carrejo Gironza

Data type: Video mp4 file

Explanation note: The body of each egg is buried in the substrate and the filament is spread over the surface. As the female began laying eggs (reaching packages up to 20 eggs, one egg at a time), it was observed that numerous filaments were emerging and radiating from the same point. Along this process, the male remains close to the female and the mating happen continuously between laid eggs.

Copyright notice: This dataset is made available under the Open Database License (<http://opendatacommons.org/licenses/odbl/1.0/>). The Open Database License (ODbL) is a license agreement intended to allow users to freely share, modify, and use this Dataset while maintaining this same freedom for others, provided that the original source and author(s) are credited.

Supplementary material 3

Egg hatching of *Glyphidops (Oncopsia) flavifrons*

Authors: Andrés Felipe Vinasco Mondragón, Nancy Soraya Carrejo Gironza

Data type: Video mp4 file

Explanation note: Moments before the hatching, the larva is observed moving the body and the head, rubbing its mandibles against the inner wall of the egg and finally thrusting the corium. The larva emerges from the anterior part of the egg by using one of the two longitudinally lateral hatching lines.

Copyright notice: This dataset is made available under the Open Database License (<http://opendatacommons.org/licenses/odbl/1.0/>). The Open Database License (ODbL) is a license agreement intended to allow users to freely share, modify, and use this Dataset while maintaining this same freedom for others, provided that the original source and author(s) are credited.

Psallops niedzwiedzki, a new species from Ghana with a key to African species (Heteroptera, Miridae, Psallopinae)

Aleksander Herczek¹, Yuri A. Popov², Jacek Gorczyca¹

1 Silesian University, Department of Zoology, 40-Katowice, Bankowa 9, Poland **2** Borissiak Paleontological Institute, Russian Academy of Sciences, Profsoyuznaya Str. 123, 117997 Moscow

Corresponding author: Aleksander Herczek (aleksander.herczek@us.edu.pl)

Academic editor: Pavel Štys | Received 27 October 2015 | Accepted 29 February 2016 | Published 7 July 2016

<http://zoobank.org/D3E12271-BE51-47D2-A48E-103FA21E44E1>

Citation: Herczek A, Popov YA, Gorczyca J (2016) *Psallops niedzwiedzki*, a new species from Ghana with a key to African species (Heteroptera, Miridae, Psallopinae). ZooKeys 603: 161–169. doi: 10.3897/zookeys.603.6978

Abstract

A new species from Ghana, *Psallops niedzwiedzki* Herczek & Popov, **sp. n.** is described. The dorsal habitus, head and male genitalia are presented and some morphological features are discussed. A key, short descriptions and map of the distribution of the African species of the genus are also provided.

Keywords

Heteroptera, Miridae, Psallopinae, *Psallops*, new species, Africa

Introduction

The small plant bug subfamily Psallopinae is most probably a relict group that is closely related to the subfamily Isometopinae. Schuh and Schwarz (1984) and Cassis and Schuh (2012) believed that Isometopinae, Psallopinae and Cylapinae should constitute a single clade. Currently, these subfamilies are considered to be the primitive groups among the other Miridae. The geographical distribution and life history of Psallopinae is still poorly known, although eight species from Asia

were recently added (Lin 2004, Yasunaga 1999, Yasunaga et al. 2010). Bionomical data are known for 11 species in the subfamily: seven were caught using a light trap, three were found on plants, two were caught with a sweep net and two by using Malaise traps. Details about their habitats and habits are also poorly known. Usinger (1946) reported *Psallops oculatus* Usinger, 1946 on *Asplenium nidus* Linne, 1753 (Polypodiales: Aspleniaceae). Some psallopineous bugs from Thailand have been found under half-detached bark fragments of fabaceous broadleaf plants (Yasunaga et al. 2010). Only *Psallops myiocephalus* Yasunaga, 1999 from Japan is known from the oak *Quercus acutissima* Carruth, 1862 (Fagaceae) in the Nagasaki Prefecture of Kyushu (Yasunaga 1999). These insects probably have nocturnal habits. They all have a small body size, i.e. 1.73–3.5 mm. All of the species that have recently been described have been placed in the genus *Psallops* Usinger, 1946.

To date, only two species that belong to the subfamily Psallopinae have been described from Africa, *Psallops webbii* Herczek & Popov, 2014 (Herczek and Popov 2014) and *Psallops linnavuorii* Herczek, Popov & Gorczyca, 2016 (Herczek et al. 2016). *Psallops webbii* was collected by R. E. Linnavuori in Igboho-Kiohi (the northern part of Oyo province in western Nigeria) in July 1973 (the second specimen of *P. webbii* comes from Equatoria (south Sudan) and was collected by R.E. Linnavuori in April 1963). *Psallops linnavuorii* was collected by Leston in Ghana in November 1965 (Fig. 8).

Material and methods

The species was encountered in the collection of the Museum in Copenhagen. *Psallops niedzwiedzki* sp. n. was collected from a forest habitat in October 1965 by L. R. Cole. It belongs to D. Leston's collection (coll. 1976-5093). The abdomen and aedeagus had already been dissected and placed in a separate vial under the specimen. When describing the species, the genitalic structures were transferred to KOH, chloroaldehyde and finally to chloralphenol. After the examination, the structures were immersed in a drop of Berlese liquid on a celluloid board and attached underneath the specimen. The original vial did not contain the right paramere. Colour photographs and drawings were obtained using a Nikon Eclipse E 600 microscope and the computer program NIS Elements, Ver. 4.10. Measurements were taken with a micrometer and are presented in millimetres (mm). The proportions of the selected body parts are presented in Table 1. The terminology used for the male genitalia follows Konstantinov (2003).

Taxonomy

Genus *Psallops* Usinger, 1946: 86.

Type species by original designation *Psallops oculatus* Usinger, 1946: 87.

***Psallops niedzwiedzki* Herczek & Popov, sp. n.**

<http://zoobank.org/459FFE5F-85C3-4AD9-9FAB-57282F3F7DC8>

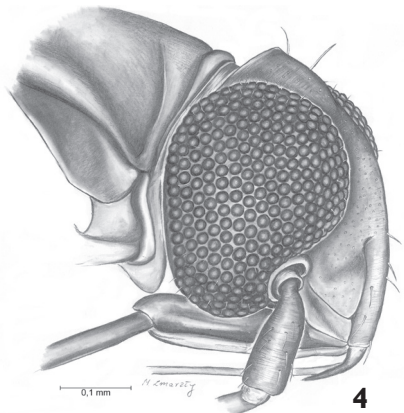
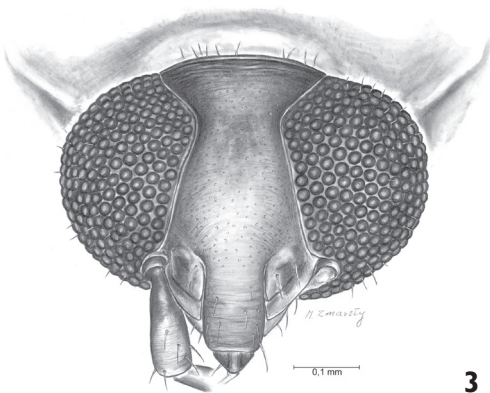
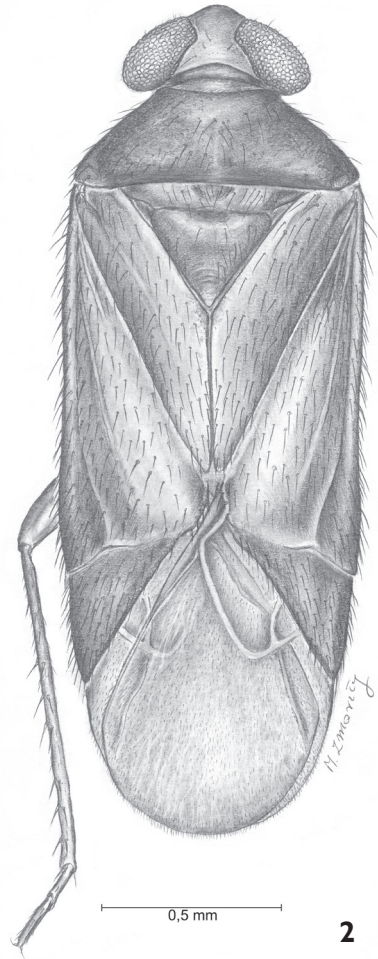
Material examined. Holotype: male. X. 65, Forest, Ghana, 2°28'W, 5°25'N, L. R. Cole. D. Leston coll. BM. 1976-509.

Diagnosis. Recognized by the following combination of characters: yellow brown frons and clypeus, a pale reddish-brown, semihyaline corium with a darker embolium, a dark brown cuneus with a lighter apex, metatibiae ferruginous with yellowish apical part. *Psallops niedzwiedzki* sp. n. is unique due to the ratio (3.78) of its antennae I and II segments, head width to length ratio (2.7), pronotum width to length ratio (2.47), hind tibia to hind femur length ratio (1.12), hind tibia length to pronotum width ratio (1.16) and others. The species is also defined by the distinctive structure of the aedeagus and left paramere (Figs 5, 6, 7).

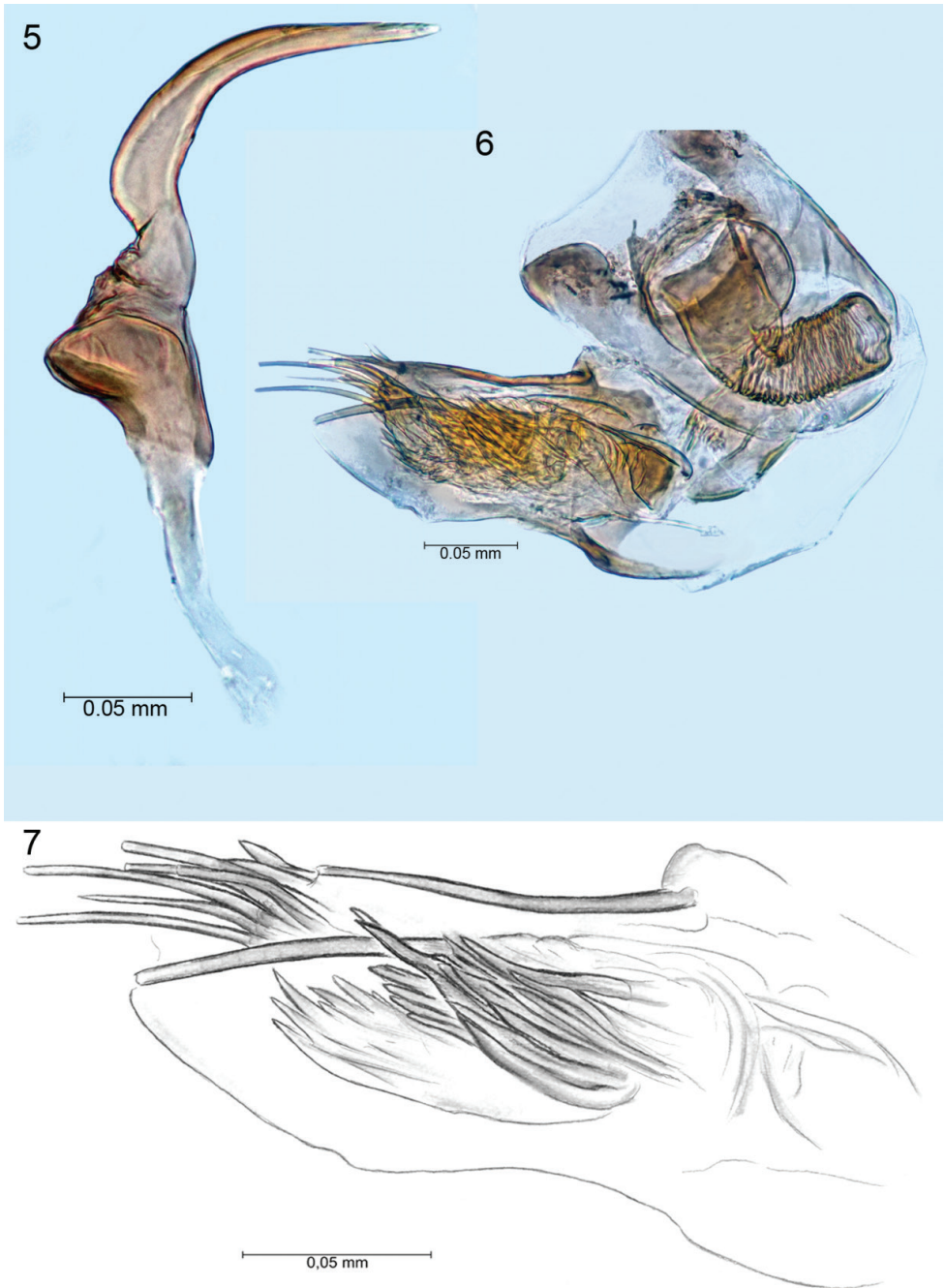
Description. Male. *Coloration and vestiture:* body generally brownish ferruginous, elongate with brown, semi-erect setae; setae sparsely distributed on pronotum. Dorsal surface weakly smooth, pronotum shagreened. Head, eyes, antennal segments II, rostrum, pronotum, scutellum, cuneus and femora dark brown. Anterior portion of hemelytron and mesoscutum reddish brown. Antennal segment I, frons, clypeus, mandibular and maxillary plates and coxae yellowish brown. Protibiae yellow, mesotibiae brown. Distal 2/3 of metatibiae ferruginous, apical 1/3 yellowish. External tibiae with two rows of brown spines. Membrane slightly smoky, grey.

Structure: body elongated, 2.67× longer than wide. Head 2.7× wider than long at plane of vertex. Eyes not dissociate at curvatures of vertex (Figs 1, 3). Vertex wide – at narrowest 0.5× as wide as eye. Clypeus relatively short and almost half height of eye, smoothly fused to frons. Mandibular plate wide and short; maxillary plate narrower than buccula. Fovea antennalis situated low, eyes deeply indented. Labium reaches middle coxa. Antennal segments I and II equally thick; segment I 3.78× shorter than II. Pronotum 1.6× longer than head and 2.47× wider than long. Collar clearly visible, but calli weakly marked. Scutellum shorter than pronotum; cumulative length of mesoscutum and scutellum equal to length of claval commissure (1.03). PCu on clavus weakly marked. Corium 3.27× longer than cuneus. Hemelytral membrane with large cell well-developed, with length 2.22× width; smaller cell strongly reduced; vein M forming obvious long process, somewhat shorter than length of large cell (Figs 1, 2). Metafemora, slightly thickened, approximately 3.73× longer than maximum width. Tibiae 2.71× longer than length of tarsus. Tarsi two-segmented, with hind second tarsal segment 2.60× as long as first. Aedeagus delicate and membranous; apical portion of endosoma with eight sublinear strip-like blunt spines with different lengths; medial portion of endosoma with one bunch of sharp tipped spicules (Figs 6, 7). Left paramere scythe-shaped, with sensory lobe with inverted bowl shape; apical process narrow, elongated and subtly serrate. Paramere body stoutly adjoins apical process (Fig. 5). Right paramere missing.

Female. Unknown.



Figures 1–4. 1, 2 *Psallops niedzwiedzki* sp. n. dorsal view 3, 4 Front of head, side of head.



Figures 5–7. Left paramere, aedeagus, endosoma.

Table 1. Proportions of the selected male body parts of African species.

	<i>P. niedzwiedzki</i>	<i>P. linnavuorii</i>	<i>P. webbii</i>
Body length / width	2.67	2.70	2.74
Head width / length	2.7	2.48	2.79
Eye dorsal width / vertex width	2.0	2.0	1.12
Head width / vertex width	4.5	5.18	2.79
Head width / pronotum width	0.68	0.76	0.62
Antennal segments II: I	3.78	4	-
II antennal segment length / pronotum width	0.67	0.91	-
Pronotum width / head width	1.46	1.32	1.62
Pronotum length / head length	1.6	1.35	1.58
Pronotum posterior / anterior length	2.26	1.53	2.0
Pronotum width / length	2.47	3.08	2.87
Pronotum length / commissurae claval length	0.76	0.72	0.83
Mesoscutum + scutellum length / pronotum length	1.03	1.19	1.37
Scutellum length / Mesoscutum length	3.12	3.44	3.1
Commissurae claval length / mesoscutum + scutellum length	1.27	1.16	0.88
Corium length / cuneus length	3.27	3.53	3.17
Hind femur length / width	3.73	3.04	3.0
Hind tibia length / femur length	1.12	1.62	1.47
Hind tibia length / pronotum width	1.16	1.64	1.33
Tibia length / tarsus length	2.71	3.97	4.60
Hind tarsus II: I	2.6	2.08	1.90
Cell length / width	2.22	2.59	2.39

Measurements. male: body length – 2.30; width – 0.86; head: length – 0.20; width – 0.54; height – 0.45; dorsal width of eye – 0.24; width of vertex – 0.12; antennal segments: I – 0.14; II – 0.53; III and IV – missing; rostral segments: I – 0.28; II – 0.26; III – 0.11, IV – 0.13; length of pronotum – 0.32; anterior width – 0.35; posterior width – 0.79; length of mesoscutum – 0.081; length of scutellum – 0.25; length of claval commissurae – 0.42; length of hind femur – 0.82; width – 0.22; hind tibia – 0.92; length of tarsus – 0.34 (I- 0.10; II- 0.26); length of hemelytron – 1,79; length of corium – 1.08; length of cuneus – 0.33.

Etymology. Named in honour of our friend Jacek Niedzwiedzki.

Remarks. *Psallops niedzwiedzki*, sp. n. is distinguished from other species of *Psallops* primarily by the ratios of the head, antenna, pronotum and legs (see Table 1). The new species also shares certain characters with a few widely distributed species: *P. linnavuorii*, *P. myiocephalus* Yasunaga, 1999, *P. sakarat* Yasunaga, 2010, and *P. webbii*. The new species resembles *P. sakarat* in the head to vertex width ratio (4.5), head to pronotum width ratio (0.68 and 0.69, respectively) and pronotum to head width ratio (1.46 and 1.44, respectively). The second and third ratios are also typical



Figure 8. The distribution of African species: **1** *Psallops linnavuorii* **2** *P. niedzwiedzki*, sp. n. **3** *P. webbii* **4** *Psallops*, undescribed species

of *P. miocephalus* (the former 0.69 and the latter 1.44). The head width to length ratio and the scutellum to mesoscutum length ratio are similar to those in *P. webbii* (2.79 and 3.1, respectively).

The structure of the aedeagus approximates that in *P. linnavuorii* although the number of apical spines, shape and arrangement of the bunched medial spicules are different. In *P. linnavuorii* the endosoma has two dense bunches of medial sclerotized spicules and four long, blunt tipped spines apically. Moreover, the shape of the left paramere in *P. linnavuorii* is similar to *P. niedzwiedzki*; both species are not thickened at the area adjoining the apical process.

Key to African species

- 1 Dorsal part of body brownish to brownish ferruginous, weakly smooth or shagreened. Cuneus brown to dark brown, without yellowish brown distally. Head width to length ratio 2.4–2.7 **2**
- Dorsal part of body dark brown, slightly crumpled; cuneus dark brown, terminal part yellowish brown. Head width to length ratio 2.79
..... ***Psallops webbii* Herczek & Popov, 2014**
- 2 Body brownish ferruginous, cuneus dark brown with paler apex. Metafemora dark brown, metatibiae / 3 ferruginous, apical 1/3 yellowish. Head width to length ratio 2.7 ***Psallops niedzwiedzki* sp. n.**
- Body brownish, cuneus brown, near cuneal fracture whitish and ½ apical part tinged with red. Metafemora brown, metatibiae pale yellow. Head width to length ratio 2.48 ... ***Psallops linnavuorii* Herczek, Popov & Gorczyca, 2016**

***Psallops webbii* Herczek & Popov, 2015**

Diagnosis. Male. General colouration of head, pronotum, prosternum, mesosternum, metasternum, first segment of labium, cuneus and anterior margin of hemelytron uniformly dark brown. Mandibular plates, clypeus, antennal segment I, fore and middle legs, tibiae and tarsi of hind legs and labium (except segment I) pale yellow. Eyes reddish-brown with paler edges. Mesoscutum, scutellum and metafemora reddish brown. Corium yellowish brown with anterior portion paler. Corium with small red patches adjoining cuneus. Membrane grey-brown, weakly creased and covered with very fine setae. Body surface slightly crumpled and semi-dull. Mesoscutum and scutellum glossy basally. . Labium long, almost reaching apex of hind coxae; labial segment I reaching middle of mesofemur. Tibiae with sparsely distributed pale spines on external surface; length of spines slightly longer than diameter tibia.

***Psallops linnavuorii* Herczek, Popov & Gorczyca, 2016**

Diagnosis. Male. Body generally brownish and elongated. Dorsal surface weakly shagreened with pale, uniformly distributed depressed setae. Head and pronotum dark brown. Frons and clypeus brown. Eyes, antennae and labium infuscate. Mesoscutum, scutellum, clavus, corium, cuneus, coxae and femora brown. Basal part of hemelytron tinged with red, inner apical part and femora pale brown. Cuneus near cuneal fracture whitish and ½ apical part of cuneus tinged with red. Tibiae and tarsi pale yellow. Tibiae with two rows of pale brown spines on external surface; length of spines longer than diameter of tibia.

Acknowledgements

We are greatly indebted to Prof. Henrik Enghoff from the Zoological Museum, University of Copenhagen, who loaned us *Psallops* specimens for our study. We also thank Marzena Zmarly (Katowice, Poland) for the excellent drawings.

References

- Carvalho JCM, Sailer RI (1954) A remarkable new genus and species of isometopid from Panama (Hemiptera, Isometopidae). *Entomological News* 4: 85–88.
- Cassis G, Schuh RT (2012) Systematics, biodiversity, biogeography and host associations of the Miridae (Insecta: Hemiptera: Heteroptera: Cimicomorpha). *Annual Review of Entomology* 57: 377–404.
- Herczek A, Popov YA (2014) New psallopineous plant bugs (Hemiptera: Heteroptera, Miridae, Psallopinae) from the New Hebrides and Nigeria. *Zootaxa* 3878(4): 366–378.
- Herczek A, Popov YA, Gorczyca J (2016) A new psallopineous plant bug (Heteroptera, Miridae, Psallopinae) from Ghana. *Entomologica Americana* 122(1/2): 164–168.
- Konstantinov FV (2003) Male genitalia in Miridae (Heteroptera) and their significance for suprageneric classification of the family. Part I: general review, *Isometopinae* and *Psallopinae*. *Belgian Journal of Entomology* 5: 3–36.
- Lin CS (2004) First record of the plant bug subfamily Psallopinae (Heteroptera: Miridae) from Taiwan and China, with descriptions of three new species of the genus *Psallops* Usinger. *Formosan Entomologist* 24: 273–279.
- Schuh RT, Schwartz MD (1984) *Carvalhoma* (Hemiptera: Miridae): revised subfamily placement. *Journal of the New York Entomological Society* 92: 48–52.
- Usinger RL (1946) Hemiptera, Heteroptera of Guam. *Insects of Guam (II)*. *Bulletin of the Bishop Museum* 189: 11–103.
- Yasunaga T (1999) First record of the plant bug subfamily Psallopinae (Heteroptera: Miridae) from Japan, with descriptions of three new species of the genus *Psallops* Usinger. *Proceedings of the Entomological Society of Washington* 101: 737–741.
- Yasunaga T, Yamada K, Artchawakom T (2010) First record of the plant bug subfamily Psallopinae (Heteroptera: Miridae) from Thailand, with descriptions of new species and immature forms. *Tijdschrift voor Entomologie* 153: 91–98.

